ADVANCES
IN BIOCHEMICAL ENGINEERING
BIOTECHNOLOGY

Managing Editor
T. Scheper

75

History and Trends in Bioprocessing and Biotransformation

Springer

VISIT…

History of Modern Genetics in Germany

Friederike Hammar

Institute for Physiological Chemistry, Johannes-Gutenberg-University, 55099 Mainz, Germany,
e-mail: hammar@mail.uni-mainz.de

The history of modern genetics in Germany during the 20th century is a story of missed chances. In the USA the genetic revolution opened a fascinating new field for ambitious scientists and created a rapidly growing new industry. Meanwhile Germany stood aside, combating with political and social restrictions. Promising young scientists who wanted to work in the field left Germany for the US, and big companies moved their facilities out of the country. Up until the middle of the 1990s molecular biology in Germany remained a "sleeping beauty" even though many brilliant scientists did their jobs very well. Then a somewhat funny idea changed everything: the German minister for education and science proclaimed the BioRegio contest in order to award the most powerful biotechnology region in Germany concerning academia and especially industry. Since then Germany's biotechnology industry has grown constantly and rapidly due to the foundation of a number of small biotech companies; big companies have returned their interests and their investments to Germany, paralleled by an improvement in academic research because of more funding and better support especially for younger scientists. In respect to biotechnology and molecular biology, Germany is still a developing country, but it has started to move and to take its chances in an exciting global competition.

Keywords. History, Molecular genetics, Biotech industry, Genomics, Proteomics

1 Introduction 2

1.1 The Birth of Modern Genetics 2
1.2 Molecular Genetics Grows Up 4
1.3 Sequencing the Human Genome 5
1.4 The Max Planck Society 6

2 The 1970s: The 'First Genetic Revolution' – and Germany? 8

2.1 The Max Delbrück Center in Berlin-Buch 9
2.2 The German Center for Cancer Research in Heidelberg 10
2.3 The European Molecular Biology Laboratory in Heidelberg 10

3 The 1980s: Molecular Genetics Struggling Against Political Forces 11

3.1 Hoechst and Insulin – A Never-Ending Story 12

4 The 1990s: A New Beginning – 'The Second Genetic Revolution' . . 13

4.1 Developing a German Biotech Industry 14
4.1.1 Qiagen – The Pioneer 14
4.1.2 Rhein-Biotech – Becoming a Global Player 14

Advances in Biochemical Engineering/
Biotechnology, Vol. 75
Managing Editor: Th. Scheper
© Springer-Verlag Berlin Heidelberg 2002

4.1.3 MWG-Biotech – An Instrumentation Supplier Develops into a Genomics Company . . . 15
4.1.4 Evotec – Molecular Evolution for Drug Screening . . . 15
4.2 The BioRegio Contest – Gambling for Success . . . 15
4.3 Germany's Contribution to the Human Genome Project and Other Genome Projects . . . 16
4.3.1 DHGP – German Human Genome Project . . . 17
4.3.1.1 Milestones . . . 21
4.3.2 Microbial Genomes . . . 22

5 After 2000: Starting the Biological Age . . . 23

5.1 Beyond the Genome – Functional Genomics and Proteomics . . . 23
5.2 Ethical, Legal and Social Implications of Genomic Research . . . 25
5.2.1 Patents . . . 26

6 Further Perspectives: 'Green' Biotechnology . . . 27

References . . . 28

Abbreviations

BMBF	Federal Ministry of Education and Research
DFG	German Research Association
DGHP	German Human Genome Project
DKFZ	German Center for Cancer Research
EMBL	European Molecular Biology Laboratory
GBF	Gesellschaft für Biologische Forschung – Society for Biological Research
GDR	German Democratic Republic
IMB	Institute of Molecular Biology
KWS	Kaiser Wilhelm Institute
MDC	Max Delbrück Center
MPI	Max Planck Institute
MPS	Max Planck Society
PCR	polymerase chain reaction
SAGE	serial analysis of gene expression
TIGR	The Institute of Genomic Research

1 Introduction

1.1 The Birth of Modern Genetics

From a biologist's point of view, the 20th century can be named the 'century of genetics': starting with the rediscovery of the Mendelian laws by Carl Erich

Correns (Berlin), Erich von Tschermak (Vienna) and Hugo de Vries (Amsterdam) in 1900 [1]. Mendel's rules, originally formulated in 1866, postulate that different genetic traits are inherited independently. In 1902 Walter Stanborough Sutton observed chromosomal movements during meiosis and developed the chromosomal theory of heredity. He stated that the chromosomes are the carriers of Mendel's 'factors' of heredity. Sutton gave these factors the name we still use today: he called them 'genes'. In 1903 Sutton and Theodor Boveri working independently suggested that each germ cell contains only one half of each chromosome pair. In 1905, Edmund Wilson and Nellie Stevens proposed the idea that separate X and Y chromosomes determine sex. Thomas Hunt Morgan started experiments with the fruit fly *Drosophila melanogaster* in 1910 and proved that certain genes are linked to each other and that linked genes can be exchanged by a mechanism called crossing over [2, 3]. Based on these results, Alfred Sturtevant was able to draft the first genetic maps to locate the genes on the chromosomes in 1913 [4]. Herman Müller, who also worked in Morgan's laboratory, performed the first experiments to produce mutations by radioactive radiation. In 1927 he was able to demonstrate that X-rays cause a high rate of mutations [5]. These experiments, A. E. Garrod's observation of inherited diseases like phenylketonuria [6] and later the work of George Beadle and Edward Tatum on the fungus *Neurospora crassa*, showed the relationship between genes and enzymes and led to the formulation of the 'one-gene-one-enzyme' hypothesis in 1941 [7, 8].

However, until 1944, nothing was known about the nature of the substance building the genes. Then Oswald Avery was able to show that nucleic acids are the molecules that constitute the genes [9] – a result that was regarded with suspicion by the greater part of the scientific community who favored proteins because of their greater complexity. They doubted that a molecule as simple as DNA could perform the complex tasks of processing genetic information. But Avery's experiments had an enormous influence on the work of Erwin Chargaff, an Austrian scientist who had emigrated to the USA in 1934. He demonstrated that in every nucleic acid the numbers of the nucleo-bases adenine and thymine are equal as well as the numbers of the bases guanine and cytosine [10]. This was the first hint to elucidate the base-pairing in a DNA molecule and it determined the work of James Watson and Francis Crick. In 1953 they were able to deduce a model for the structure of DNA from the crystallographic pictures provided by Rosalind Franklin [11–13].

Two other scientific personalities greatly influenced the early steps of molecular genetics: Max Delbrück, a German physicist who went to the USA in 1937 and the chemist Linus Pauling. Together they developed a theory to explain the complementary interaction of biological molecules using weak binding forces like hydrogen bonds [14]. Max Delbrück was one of the pioneers of bacterial genetics. He and his co-worker Salvador Luria developed the first quantitative test to study mutations in bacteria [15]. They also invented a simple model system using phage to study how genetic information is transferred to host bacterial cells. Moreover they organized courses on phage genetics that attracted many scientists to Cold Spring Harbor, which soon became an interesting and exciting center for new ideas about explaining heredity at the molecular and cellular level.

1.2 Molecular Genetics Grows Up

As the field of molecular genetics grew, the DNA molecule became the focus of many research efforts. Francis Crick and George Gamov developed the 'sequence hypothesis' to explain how DNA makes protein. They stated that the DNA sequence specifies the amino acid sequence of a protein and postulated the central dogma of molecular genetics: the flow of genetic information is a one-way road, it always takes the direction from DNA to RNA to protein [16]. In the same year, 1957, Mathew Meselson and Frank Stahl demonstrated the replication mechanism of DNA [17]. In 1958, DNA polymerase became the first enzyme used to make DNA in a test tube.

The work of Marshal Nirenberg and Heinrich Matthaei between 1961 and 1966 resulted in the cracking of the genetic code [18]. They demonstrated that a codon consisting of three nucleotide bases determines each of the 20 amino acids.

In 1967, the enzyme DNA ligase was isolated. DNA ligase binds together strands of DNA. Its discovery, together with the isolation of the first restriction enzyme in 1970, paved the way for the first recombinant DNA molecules to be created by Paul Berg in 1972. In doing so, he created the field of genetic engineering. However, upon realizing the dangers of his experiment, he terminated it before it could be taken any further. He immediately, in what is now called the 'Berg Letter', proposed a 1-year moratorium on recombinant DNA research, in order for safety concerns to be worked out. These safety concerns were later discussed by molecular biologists at a conference in Asilomar in 1975 – a unique event in the history of the sciences. This concern of the scientific community reflects the attitude of the general public: until today, molecular biology and genetic engineering are at least in part regarded with suspicion and mistrust by a large part of the population not only in Germany but also in Great Britain and other countries.

In 1973 Cohen and Boyer combined their research efforts to produce the first recombinant DNA organisms: cells of the bacterium *E. coli*. Cohen and Boyer's implementation of the technique laid the foundations for today's modern genetic engineering industry. As a logical consequence, Herbert Boyer together with Robert Swanson, a young visionary venture capitalist, established the first Biotechnology Company: Genentech was founded in 1976. As soon as 1977 Genentech reported the production of the first human protein – Somatostatin – manufactured in a bacteria [19]. In the USA the 'Age of Biotechnology' had begun.

In the following 20 years most of the major inventions in molecular genetics were not made in Germany. In 1977, Walter Gilbert and Allan Maxam devised a method for chemically sequencing DNA [20, 21]. In 1983 Kary Mullis developed the polymerase chain reaction (PCR) [22, 23]. This technique allows for the rapid synthesis of DNA fragments. In about an hour, over 1 million copies of a DNA strand can be made. The technique has been invaluable to the development of biotechnology and genetic engineering.

The first transgenic animals were produced in 1981 at Ohio University [24] and the technical developments towards powerful and efficient automated DNA

sequencing machines took place in the USA. In 1996 Ian Wilmut and Keith Campbell, researchers at the Roslin Institute in Scotland, created Dolly, the first organism ever to be cloned from adult cells [25–27]. A consolation for German scientists may be the fact that one of the pioneers of cloning was a German embryologist: In 1928 Hans Spemann performed the first nuclear transfer experiment with salamander embryo cells.

1.3 Sequencing the Humane Genome

About 10 years ago the scientific community felt that automation techniques for sequencing genes and the supporting computers and software were at a state to start one of the most challenging scientific projects: In October of 1990, the National Institutes of Health officially began the Human Genome Project, a massive international collaborative effort to locate the estimated 30,000 to 100,000 genes and sequence the 3 billion nucleotides making up the entire human genome. By determining the complete genetic sequence, scientists hope to begin correlating human traits with specific genes. With this information, medical researchers have begun to determine the intricacies of human gene function, including the source of genetic disorders and diseases that have plagued medical researchers for years. To date more than 200 genes predisposing for diseases have been analyzed, e.g. Parkinson's disease [28], breast cancer [29], prostrate cancer [30] and Alzheimer's disease [31].

In planning the project, research was divided among various American universities. The $3-billion project was scheduled for completion in 2005, but there were doubts whether this deadline would be made. After 5 years of considering the pros and the cons Germany finally joined the Human Genome Project in 1995. The German Ministry for Research and Education is supporting the German Human Genome Project (DGHP) until 2003 with 200 million German Marks.

In January of 1998, the biotechnology firm Perkin-Elmer Corp. announced that it was teaming up with gene-sequencing expert J. Craig Venter to privately map the human genome. Perkin-Elmer plans to use brand new gene-sequencing technology to completely map all human DNA by the year 2001 for an estimated cost of $150–200 million dollars. Venter had proposed a new approach for sequencing the human genome with shotgun techniques, an idea regarded with skepticism by his colleagues. As he was not able to raise public funding for his idea, he offered it to Perkin-Elmer who was soon convinced to give him a try and supported the foundation of Celera Genomics to perform the task.

The competition among the private and the public initiatives accelerated the human genome project dramatically. Already in June 2000, 5 years ahead of the public prospect and even 1 year in advance of his own proposal, Craig Venter announced the completion of the human genome sequence. One of the most important milestones of genetic research had been achieved.

Even though German scientists had much influence on the emerging discipline of 'molecular genetics', the greatest part of the development took place in America and not in Germany. Max Delbrück, for example, one of the 'fathers' of

Table 1. Curriculum vitae of Max Delbrück

– 1906 born in Berlin
– 1930 Ph.D. Göttingen, theoretical physics (quantum mechanics) in the group of Max Born
– 1930 – 1932 postdoctoral years in England, Switzerland and Denmark, contact with Wolfgang Pauli and Niels Bohr
– 1932 Berlin, to work with Otto Hahn and Lise Meitner
– 1937 fellowship of the Rockefeller Foundation to Caltech, work with Emory Ellis
– 1940 instructor of physics, Vanderbilt University
– 1947 Caltech, cooperation with Salvador Luria, establishment of the 'Phage Group'
– from 1950 work on *Phycomyces*
– 1956 helps to set up the Institute of Molecular Genetics at the University of Cologne
– 1969 Nobel Prize in Physiology and Medicine
– 1981 died in the USA

molecular biology, started his career at the former Kaiser Wilhelm Institute in Berlin (see Table 1). In 1932 he – like many other German scientists – left Germany for well-known political reasons and did not return after World War II was over; with one exception: when he helped to establish the Max Planck Institute for molecular genetics at the university of Cologne, which was opened in1962.

In the 1970s and 1980s German scientists were also working at the cutting edge of modern molecular biology. But similar to Axel Ulrich or Peter Seeburg – both now directors of Max Planck Institutes in Munich and Heidelberg, respectively – who were researchers at Genentech in the early years of the company, many of them had left their home country because political restrictions and unfriendly public opinion limited the possibilities for researchers especially in the biological sciences in Germany.

What were the reasons for the hesitant progress of modern genetics in Germany after World War II? The reconstruction of the Max Planck Society (MPS) on the ruins of the former Kaiser Wilhelm Institutes reflects the development of research and technology in general and of molecular genetics in particular, in relation to public and political support.

1.4 The Max Planck Society

The Max Planck Society for the Advancement of the Sciences (MPS) is an independent, non-profit research organization. It was established on February 26, 1948, as the successor organization of the former Kaiser Wilhelm Society. Max Planck Institutes conduct basic research in service to the general public in the areas of natural science, social science and the arts and humanities.

Following the collapse of the Third Reich, for German science, as for many sectors of public life, the need for a new start was essential. The state of Germany's institutions at the end of the war corresponded to the general chaos accompanying the defeat. The various institutes of the Kaiser Wilhelm Society (KWS) originally founded in 1911, the predecessor of the Max Planck Society, were damaged or housed provisionally at different evacuation sites. The years of

the National Socialist dictatorship had left doubts as to the moral integrity of the internationally renowned scientific organization. Several KWS institutes had been pressed into service for military research tasks during the war and individual scientists had broken the fundamental ethical rules of science. The organization of the KWS had during the years of National Socialist government lost its independence and its moral reputation. Therefore, many scientists of the destructed KWS thought that a new beginning was absolutely necessary. Parallel to the construction of the federal government, the MPS emerged from the ruins of the KWS due to the initiatives of individual institutes and their scientists. The months of struggle for survival as a research organization after the end of World War II were followed by years of striving to ensure a financial basis for the MPS. The MPS was, from the very beginning, dependent on public funding. In accordance with the federal structure, the responsibility of providing the MPS with basic financial means fell at first solely to the individual German states, with respect to their sovereignty in cultural matters. Since the MPS spoke with one voice for the entirety of its institutes, the states were obliged to coordinate their efforts to ensure financial backing. On March 24, 1949, even before the establishment of the Federal Republic itself, the cultural and finance ministers of 11 states and West Berlin agreed upon a 'National Act for the Funding of Scientific Research Facilities', the so-called 'Königstein Act', a financial arrangement which codified the common and sole responsibility of the individual states concerning the financial furthering of research and recognized the necessity of a permanent institutional funding for research facilities such as the Max Planck Society as a national obligation.

The 1950s were years in which the first steps towards a limited scientific restructuring could be undertaken. For instance, the MPS addressed itself to new research topics, such as behavioral psychology, chemistry of cells, aeromony and astrophysics, nuclear or plasma physics, or concentrated on issues already being pursued such as virus research or physical chemistry. Scientific cooperation beyond Germany's borders was extended step by step. Particularly high expectations accompanied the establishment of contacts between scientists of the MPS and those of Israel's Weizmann Institute in 1959.

The 1960s meant an unparalleled phase of upswing and further scientific development for the MPS. Within 6 years the number of research installations rose to 52. At the beginning of the 1970s the MPS had 8000 employees, of whom 2000 were scientists. With the number of new establishments and the extension of sectional structures in the institutes, the number of directorial staff doubled. These years witnessed the rise of new large research centers of international dimensions in biochemistry, biophysical chemistry, molecular genetics, immune biology, biological cybernetics and cellular biology. New, elaborate research endeavors in physics and chemistry of interdisciplinary character were launched. The decision to establish new institutes in the 1960s was still making a profound effect at the beginning of the 1970s. From the middle of the 1970s, however, the MPS suddenly found itself staggering under the burden of stagnating budgets. Even if previous new research topics were taken up in these years, this was only possible through shifting of internal priorities and reshuffling. The Society could no longer count on further expansion. The founding of new institutes was

only possible through the renaming or shutting down of entire institutes in other locations. The restructuring and thematic shift of emphasis affecting whole institutes on the occasion of a director taking his leave assumed major importance. Sustaining research under conditions of stagnating budget became the first great challenge. In the interim between 1972 and 1984, 20 institutes and/or sections were shut down. New forms of research promotion, such as temporary research groups, especially in the area of clinical research, as well as project groups, were introduced; participation in large-scale research projects increased. Eleven institutes, in part emerging from project groups, were founded. In the Biology-Medicine section the sectors endocrinology, neurology, psychology and psycholinguistics came to the fore, while labor physiology and virus research received a new orientation towards system physiology or developmental biology. In the 1970s the Max Planck Society expanded its international activities even further.

Only towards the end of the 1980s was a breakthrough achieved in the finance question. In December, 1989, the governing parties at the federal and state levels gave an unmistakable demonstration of their support for a preferred promotion of scientific excellence and financial security of future planning for that leading organization in the area of pure research. Even though no new posts were assigned, it was again possible to provide every German state with at least one Max Planck Institute. In the 1990s the unification of the two German states appeared on the horizon. At the same time the accelerated process of European unification placed German research configurations under pressure to adapt. For the MPS, German unification meant both challenge and opportunity [32]. The MPS aimed to construct 20 institutes, whose quality as international centers of excellence had to be ensured both in personnel and with respect to overall conception. The Society resolved to adopt, alongside its long-term program of institute establishment, an immediate package of measures. It conceived of and financed 27 workshops for 5 years and thus alleviated the integration in institutes of higher learning through additional project promotion. In addition, it set up two temporary branches of Max Planck Institutes and took seven temporary focal points of research in humanities into its care. Parallel to these immediate steps, the MPS continued with the founding of new institutes. The qualitative and temporal dimensions of the establishment program became a test of stress and strain for the scientific committees. With the simultaneous construction and deconstruction that took place in the 1990s, the Max Planck Society underwent a development that is also characteristic for a Germany that has enlarged its own borders. The willingness of the federal government and the states to finance the Society's establishment program in full will result in enhanced research opportunities for the MPS.

2
The 1970s: The 'First Genetic Revolution' – and Germany?

The "age of biotechnology" started in the USA with the foundation of the first biotech company. Genentech was founded by the renowned biochemist Herbert Boyer and the young visionary venture capitalist Robert Swanson. (Of the

people who worked there from the very beginning two were German scientists: Axel Ulrich, now director at the Max Planck Institute for Biochemistry in Martinsried, and Peter Seeburg, at present director at the Max Planck Institute for Medical Research in Heidelberg.)

However, in Germany, everything progressed more slowly. Many scientists in Germany regarded the field of recombinant DNA technology with skepticism and did not foresee its potential. As a consequence, they concentrated on traditional techniques to study the basic mechanisms in genetics, cell and molecular biology.

An example to the contrary, a researcher who worked at the forefront of molecular biology is Hartmut Hoffmann-Berling who in 1966 was appointed director of the first Department of Molecular Biology at the Max Planck Institute for Medical Research in Heidelberg. Hoffmann-Berling had performed pioneering studies on ATP-driven cell motility during the 1950s, but switched to molecular biology at the beginning of the 1960s after he discovered two new bacterial viruses. Hoffmann-Berling concentrated initially on the characterization of these bacteriophages, one of which was the first example of a rod-shaped, nonlethal bacteriophage [33]. Between 1966 and 1974, he moved from the examination of viral self-assembly to the general processes of DNA replication. By the mid-1970s, he had immersed himself into the search for individual components of the multienzyme complex that is responsible for DNA synthesis. In 1976, he discovered the first example of a DNA helicase [34–36]. Until his retirement in 1988, Hoffmann-Berling concentrated on unraveling the mechanisms by which these ATP-driven motor proteins unwind the double helix during DNA synthesis, repair damaged DNA and other related processes.

During the late 1960s and 1970s several other centers of excellence in the field of molecular biology were established in Germany.

2.1 The Max Delbrück Center in Berlin-Buch

Berlin-Buch has a long tradition as a place for medical science, starting with the foundation of the center at the turn of the century which temporarily comprised hospitals with over 5000 beds. In 1928 the former Kaiser Wilhelm Society established an Institute for Brain Research on what nowadays forms the Max Delbrück Center's (MDC) campus.

Later, the Academy of Sciences of the German Democratic Republic (GDR) founded three research institutes in Berlin-Buch: one for Cancer Research, another for Cardiovascular Research and a third one for Molecular Biology. In 1992, due to the German reunification, a new institution was developed from these three institutes – the Max Delbrück Center. It is named after the Berlin-born scientist Max Delbrück who strongly influenced the development of molecular biology.

Scientists of the MDC cooperate closely with clinicians of two specialized hospitals in the vicinity: the Robert Rössle Cancer Clinic and the Franz Volhard Clinic for Cardiovascular Disease. Both clinics form part of the Virchow University Clinic, the Medical Faculty Charité of the Humboldt University of

Berlin. The close integration between basic and clinical research is aimed at making new scientific findings available for patients as quickly as possible. The MDC is a national research foundation. It obtains 90% of its funding from the Federal Ministry of Education and Science, with the remaining 10% coming from the state of Berlin.

2.2 The German Center for Cancer Research in Heidelberg

The German Center for Cancer Research (DKFZ – Deutsches Krebsforschungszentrum) was founded in Heidelberg in 1964. As a non-profit organization it is mainly funded by the Federal Ministry for Research and Education (90%) and by the Ministry for Research and Sciences of the state of Baden-Württemberg (10%). Additional funding is obtained from other public and private sources, e.g. the German Science Organization (DFG – Deutsche Forschungsgemeinschaft), special projects of the European Union (EU), of Federal and State ministries as well as cooperations with industry and private donations to the foundation. Since 1975, it has been a National Research Center. Today, multidisciplinary cancer research is performed by more than 50 divisions and working groups with and without tenure. The majority of the division heads are appointed jointly with the University of Heidelberg. The Center's research programs concentrate on cell differentiation and carcinogenesis, tumor cell regulation, risk factors for cancer and prevention, diagnostics and experimental therapy, radiological diagnostics and therapy, applied tumor virology, tumor immunology, genome research and bioinformatics.

2.3 The European Molecular Biology Laboratory in Heidelberg

The European Molecular Biology Laboratory (EMBL) was established in 1974. Fifteen countries from Western Europe and Israel support the Institution. It consists of five facilities: the main laboratory in Heidelberg, and subsidiaries in Hamburg (Germany), Grenoble (France), Hinxton (Great Britain) and Monterontondo (Italy). The outstations provide European scientists access to large instruments for studying protein structure, some of the world's oldest and largest DNA and protein sequence databases and a broad range of services offered by skilled biologists simultaneously working for their own research projects.

For most of them EMBL is a station en route. The scientific network created by the people who once worked at EMBL and have now taken positions in other countries has strongly contributed to the development of an international scientific community throughout Europe.

In the late 1970s two young scientists took over their first independent research positions at EMBL: Christiane Nüsslein-Volhard and Eric Wieschaus joined their forces in order to identify the genes which control the early phase of embryonic development in the fruit fly *Drosophila melanogaster*. They treated the flies with mutagenic agents to produce random mutations in the *Drosophila* genes. With a microscope they analyzed the embryos and classified a large num-

ber of malformations due to mutations in genes controlling early embryonic development. They were able to identify 15 different genes that caused defects in segmentation if mutated. In 1980 they published their results in Nature and received much attention from their colleagues [37]. In the years that followed developmental biologists were able to demonstrate that similar genes exist in higher organisms and man, where they perform similar functions.

The pioneering work of Nüsslein-Volhard and Wieschaus and the studies on the genetic basis of homeotic transformations in Drosophila performed by Edward Lewis at the California Institute of Technology, Los Angeles, during the 1970s were honored with the Nobel Price in Physiology and Medicine in 1995.

Nüsslein-Volhard has dedicated a great part of her scientific life to the genes of Drosophila. However, in her laboratory, molecular analysis was begun rather late – in1986 – when she had been appointed director of an independent division at the MPS for developmental biology in Tübingen. The first gap gene, *Krüppel*, was cloned in the group of one of her colleagues, Herbert Jäckle [38].

3
The 1980s: Molecular Genetics Struggling Against Political Forces

During the 1980s natural sciences and technology faced a period of stagnation in Germany. At this time in Germany it was not possible to establish a culture of small companies, which are more flexible than large research institutions or big companies and have a strong interest in the application of their results. One reason was the attitude of many university researchers, who thought that science had to be 'pure' and independent from financial considerations. A scientist who directed his or her research interests according to economic benefit or the needs of a customer – especially when this customer came from the powerful pharmaceutical or chemical industry – was regarded with suspicion.

On the other hand, the environment for possible entrepreneurs was not very friendly. Venture capitalists did not exist, public funding was oriented towards academic research, and banks were not willing to finance these high-risk projects, often basing 'only' on an idea, the vision of the founding scientists. There was a jungle of laws and regulations that had to be respected if one wanted to establish a new or enlarge an existing company.

As a result the first German biotechnology company Qiagen – now a world-leading provider of technologies for separating and purifying nucleic acids – had to move from Germany to the neighboring Netherlands to restructure the company in preparation for the IPO.

Public opinion in Germany was adverse to science and technology; the anti-nuclear movement and the emergence of the Green Party created a climate of suspicion and fear towards applied scientific research and the related industries. In particular, genetic engineering and molecular genetics were regarded as damnable. The nightmare of genetically modified microorganisms escaping from laboratories and killing half of the world population, or the awful vision of an army of cloned super-soldiers, frightened many people in Germany. Of course the technique was new and nobody was able to foresee all of its consequences and possible risks, but a great part of the fear was due to a lack of in-

formation about the real risks and chances of the new technologies. The discussion between opponents and supporters of gene technology was emotional and demagogic instead of being objective and did not clear up the situation. With the growing influence of the Green Party, the regulations for establishing a laboratory for molecular biology or a facility to work with recombinant technologies became so strict that it was almost impossible for research institutions or industrial departments to expand further. A university institute that wanted to apply recombinant techniques had – for sensible reasons – to establish special high-security laboratories. That was not only an expensive but also a time-consuming process due to the sluggish process of approval by regulatory authorities. As a consequence, academic research had only limited possibilities to make use of the novel methodologies, the development of the departments stagnated and a whole generation of promising scientists left Germany to work abroad, mostly in the USA, where they had better conditions to pursue their scientific interests and the possibility to earn their living.

Industrial companies went the same way; they established new subsidiaries in the USA and other parts of the world, and some even closed their research departments in Germany. Instead of funding academic research in Germany, German companies supported American universities. Hoechst, for example, a West German chemical company, gave Massachusetts General Hospital, a teaching facility of Harvard Medical School, 70 million $ to establish a new department of molecular biology in return for exclusive rights to any patent licenses that might emerge from the facility. Even today a deal of this kind would be extremely difficult to manage in Germany but in 1981 it was absolutely impossible.

3.1 Hoechst and Insulin – A Never-Ending Story

The company Hoechst provides another example of the difficulties a company or institution encountered if it wanted to apply recombinant technologies in Germany during the 1980s [39]. The controversy surrounding the official approval by the government of the German state Hessen has become a symbol for the conflict between the German public, politics and gene technology.

Hoechst wanted to establish a plant for the production of recombinant insulin on the company's grounds in Hoechst near Frankfurt/Main. Hoechst was already experienced in the production of insulin by isolating the hormone from animal pancreas and now the company wanted to invent the recombinant process to produce the human hormone, which is better tolerated by many patients than insulin from animals and acts in a more efficient way. The new plant was to consist of three buildings: Fermtec for the fermentation, Chemtec for isolating the crude product from bacteria and Insultec for the chromatographic purification of the hormone. In 1984 Hoechst asked the local governmental authority, the Regierungspräsidium in Darmstadt, for permission to build a plant for the production of recombinant insulin. The request met unexpectedly vehement opposition from the local public. People were afraid of genetically engineered bacteria evading their fermenters and polluting the local environment.

In spite of the protest the Regierungspräsidium gave the approval for the first part of the plant, Fermtec, in 1985. Hoechst started the construction immediately. In 1986 the company applied for permission to construct the second part, the Chemtec plant. In the meantime the Ministry for the Environment abolished the license for the Fermtec plant. Nevertheless, the Chemtec plant was approved in 1987. Local activist groups – arguing that there was no legal basis for the manufacture of genetically engineered products – raised an objection to the construction of both plants. In November 1987 both approvals were withdrawn and Hoechst reacted by applying for immediate execution. In July 1989 the company's petition was granted but 3 months later the opponents filed an application to stop the immediate execution. The application was rejected in the first court case but, in 1989, the opponents were successful with a second appeal. The administrative court of the state of Hessen repealed the immediate execution. Meanwhile the chief administrator in Darmstadt gave the permission to construct the Insultec plant, the last phase of the construction. In spite of their objections the opponents were not able to stop the construction. On the first of July, 1990, the German Gentechnikgesetz (law regulating genetic engineering) came into force. Although there were now legal rules for genetic engineering the opponents managed to stop the production of insulin again. But this time it was the company's own fault. By deleting an unnecessary step of heat-inactivation Hoechst changed the approved manufacturing protocol – without asking for the permission of the approving authorities. The protest of a local citizens' initiative was successful and Hoechst had to make an application to change the license in 1991. In 1994 the chief administrators in Darmstadt and Giessen finally approved the inauguration of the complete plant. However, during the years of waiting, the scientists working at Hoechst had improved their methods. A novel strain of *E. coli* was able to fold the protein correctly, a new plasmid had increased the efficiency of the production process and environmentally beneficial enzymatic steps replaced chemical ones. In 1996 Hoechst received approval for the new procedure. Finally, in 1998, on the 16 March, the complete plant was working for the first time. This date marks the endpoint of a frustrating quarrel that, without doubt, set back Germany's biotech and pharmaceutical industry.

4
The 1990s: A New Beginning – 'The Second Genetic Revolution'

However, in spite of all the obstacles, German scientists at universities, medical hospitals and research institutions were working with recombinant technologies. Many biochemistry departments completed their classical methodological repertoire with cloning and sequencing techniques. Because DNA molecules are relatively easy to handle – due to the simpler structure of nucleic acids compared to the structure of proteins – kits for the different steps of DNA/RNA purification, for cloning and sequencing genes of interest were soon commercially available. PCR became a standard method for medical diagnostics and biological analysis.

Twenty years of gene technology without a serious accident have shown the safety of the techniques if they are handled with care and sense of responsibil-

ity. Former opponents have grown older and regard the future perspectives of molecular medicine from a different point of view. Genetic diagnosis has become a standard tool: in Germany, for example, every pregnant woman over the age of 35 can have an amniocentesis with subsequent chromosomal screen, unborn infants from parents with inheritable disorders like cystic fibrosis can be tested for the mutated gene in-utero and the first drugs and therapies developed on the basis of molecular genetics research are available.

4.1 Developing a German Biotech Industry

Biotechnology for medical applications had become widely accepted and recombinant methods were familiar to most scientists working in the field. The first German biotech companies, the pioneers of the biotech industry in Germany, Qiagen (established 1984), Rhein Biotech (established 1986), MWG-Biotech (established 1990)and Evotec (established 1993), were struggling along.

4.1.1 *Qiagen – The Pioneer*

During his doctoral thesis Metin Colpan, later cofounder and CEO of Qiagen, had developed a new material based on anionic exchange for the isolation of nucleic acids. He offered the new technology to several companies in the life science industry, but nobody saw the necessity to use it. That was the reason for him to found his own company in 1984. With the first Qiagen kit for purification of plasmid DNA the time for preparing a plasmid could be reduced from 3 days to 2 hours. No wonder that the kit and its successors were eagerly accepted by industrial and academic researchers. Today Qiagen has become a market leader in the field of isolation, purification and amplification of nucleic acids. By acquiring a manufacturer of liquid-handling instruments, Qiagen has also entered into the production of equipment. In addition the company offers services around the purification of DNA on the industrial scale and acts as a partner in several large genome-sequencing projects.

4.1.2 *Rhein-Biotech – Becoming a Global Player*

Rhein Biotech was founded in 1985 by Cornelis Hollenberg, head of the Institute of Microbiology at the University of Düsseldorf, as he was no longer able to manage his extensive contract research projects in his university institute. The young company used a patented expression system in yeast for the production of recombinant proteins. Today Rhein-Biotech has become a global player with subsidiaries in South America, Portugal, Africa, India and Korea and is the third largest among the major manufacturers of vaccines for hepatitis B. Other products include proteins for the therapy of infectious diseases and cancer [40–43].

4.1.3
MWG-Biotech – An Instrumentation Supplier Develops into a Genomics Company

MWG started 1990 as a supplier of instrumentation and chemicals for molecular biology applications. Two years later they offered an additional service for custom DNA synthesis and again one year later DNA sequencing completed their services. Soon afterwards MWG started to develop instrumentation and technologies on its own. The strategic concept to finance technological development with the earnings of the services and the selling of instrumentation soon turned out to be profitable. In 1999 MWG took measures to become a fully integrated genomics company, able to address large genomics research projects [44], and invested in the establishment of its own research department.

4.1.4
Evotec – Molecular Evolution for Drug Screening

Nobel laureate Manfred Eigen's interest focused on the technological utilization of ideas concerning evolution. By employing so-called evolution machines that utilize the principles of biological evolution, new compounds can become optimally adapted for particular functions. In the late 1980s/early 1990s, scientists in Eigen's laboratory developed methods to evolve not only self-replicating molecules like RNA and DNA [45–47], but also proteins, particularly enzymes [48, 49]. During a seminar, these results were discussed with Karsten Henco, who had gained substantial experience in the biotech industry as a co-founder and Managing Director of Qiagen. During this gathering the idea was born to start a biotech company that would develop and commercialize products based on the application of evolutionary technology. It was soon recognized that the selection technologies developed for molecular evolution in the laboratory would also be a perfect means to search for and select new potential pharmaceutical drug compounds. Soon, Evotec evolved into what it is today: a drug discovery company. It uses fluorescence correlation spectroscopy and related single-molecule detection technologies and develops liquid-handling instrumentation and high-density assay formats for automated miniaturized ultra-high performance screening.

4.2
The BioRegio Contest – Gambling for Success

Despite the activities of this handful of companies, Germany in the early 1990s was still a wasteland for life science entrepreneurs. Oppressive regulations, a traditionally chemistry-driven pharmaceutical industry and lack of venture capital made Germany a tough place to start a biotech company. American and other international investors were skeptical about providing capital for the founding of a German biotech company. This situation changed abruptly when a politician had a somewhat strange idea: in 1996 Jürgen Rüttgers, then minister for research and education, announced that he intended Germany to become the number one in biotech in Europe by the year 2000. As a means to achieve this goal he proclaimed the BioRegio contest. BioRegio should funnel money to the

three most promising biotechnology regions to support the growth of biotech companies there. The three top regions were Munich, the Rhine-Neckar-Triangle around Heidelberg and the area around Cologne. The former East-German region Jena received a special acknowledgement. But even though only three regions were awarded there were at least 17 winners because the contest released unexpected amounts of energy. All over the country, from Wilhelmshaven in the north to Munich in the south, 17 Bioregions formed – even frontiers between the separate German states were no longer regarded as an obstacle. The regions established networks to support prospective entrepreneurs with experienced consultants, patent attorneys, and money. They established 'incubators', buildings mostly located in the neighborhood of universities or research institutions, where young companies could rent laboratory space at fair prices and get additional administrative support. Among life scientists at the universities – from the youngest Ph.D. student up to the most venerable professor – it felt like a 'gold rush'. Even well-established industrial managers left their positions to join the adventure – like Peter Stadler who had managed Bayer's biotechnology operations in Germany until he founded Artemis Pharmaceuticals, a target discovery and validation company. The scientists at Artemis discover and explore the function of individual genes in multiple experimental animals: due to the scientific background of their co-founders, Christiane Nüsslein-Volhard, Tübingen, and Klaus Rajewski, Cologne, they have access to zebrafish and mice; their co-investor and collaboration partner Exilixis Pharmaceuticals in San Francisco provides them with material from fruit flies and the worm *C. elegans*.

Money has flowed in from governmental funding programs, private funds of the bioregions and venture capital companies became attracted by the emerging biotech scene in Germany. Big companies who had formerly left Germany returned and installed new departments or invested in cooperations with promising start-up companies. Jürgen Rüttger's prophecy turned out to be right: in 1997 when Ernst & Young published the first German Biotech Report they counted 23 big companies, 270 companies of medium size (more than 500 employees) and 123 small biotech companies [50]. In 1998, when the fifth European Life Science Report was published [51], this number had risen to 222 elevating Germany to number two position behind Great Britain and in the seventh annual European Life Sciences Report (2000) Germany has taken over pole position with 279 biotech companies [52]. This is both a great success and also an enormous challenge: now it has to be proved if the German model of encouraging the formation of start-up companies will lead to a sustainable industry. As the Report states: 'Germany can now claim to be Europe's most densely populated biotech kindergarten.' It will certainly take some time to see if that intensely nutured child finally reaches maturity.

4.3
Germany's Contribution to the Human Genome Project and Other Genome Projects

Due to the further development of methodologies and technical equipment, the focus of molecular genetics shifted from single genes to whole genomes. The systematic analysis of complete genomes – the Human Genome Project – as well

as initiatives to determine the total DNA sequence of several model organisms like yeast [53], *E. coli* [54], the plant *Arabidopsis thaliana* [44, 55], the nematode *Caenorhabditis elegans* [56] or the fruit fly *Drosophila* [57] and pathogenic microorganisms, e. g. *Plasmodium falciparum* [58, 59], the cause of malaria, should provide new insights into the various aspects of the biology, pathology and evolution of various organisms. The advancement of the instrumentation alone was necessary but not sufficient for handling such large genome projects. Endeavors of that scale demand the cooperative effort of many research groups and German scientists were able to take their place in these international initiatives.

4.3.1 *DHGP – German Human Genome Project*

In June 1995, Germany joined the international efforts of the Human Genome Project. The German Human Genome Project (DHGP) is funded by the German Federal Ministry of Education and Research (BMBF) and the German Research Organization (Deutsche Forschungsgemeinschaft – DFG). The initiative aims to systematically identify and characterize the structure, function and regulation of human genes, in particular those with medical relevance.

The comprehensive analysis of the human genome will give rise to a basic understanding of the function of the human organism. Due to the more detailed knowledge about the molecular mechanisms, physicians will be able to improve diagnostics and therapy. Between 1990 and 1998 more than 200 genes, that, if mutated, are responsible for serious symptoms of disease, were identified. Of special interest is the analysis of oncogenes and tumor suppressor genes; moreover, genes which predispose a patient for developing diabetes, heart diseases or Morbus Alzheimer are worthy of study. The significance of the Human Genome Project goes far beyond the field of genetic diseases. The knowledge of all the molecular elements of the human body will help the pharmaceutical industry to find new targets for more effective substances and create the opportunity for an individualized drug development. In addition it will make possible fundamentally new approaches for therapy and diagnostics and, in many aspects, will change our view of life. Therefore, special attention is also given to the ethical aspects of human genome studies.

The Resource Center at the Max Planck Institute for Molecular Genetics, Berlin, and the German Cancer Research Center, Heidelberg, constitute the central structural unit of the DGHP [60]. It generates, collects and files standardized reference materials and distributes them among all groups participating in the DHGP [60]. The extensive services of the center can also be accessed by other researchers. Several research centers, 34 research projects and 15 associated working groups spread all over the country are integrated parts of the initiative. The high degree of integration, effective utilization of common resources and tightly organized coordination is achieved by a scientific coordinating committee, consisting of three elected members: Rudi Balling, Munich; Hans Lehrach, Berlin; and Jens Reich, Berlin.

Research topics of the DGHP are bioinformatics, evolution, expression/gene regulation, mapping/cytogenetics, model organisms and sequencing. Table 2

Table 2. Research topics related to the German Human Genome Project. Source: http://www.dghp.de

Research topic	Group leader/coordinator
Bioinformatics	
Bioinformatics of the human genome: from ESTs to genes	W. Mewes, MPI for Biochemistry, Martinsried
Computer-assisted editing of genomic sequences	S. Suhai, DKFZ, Heidelberg P. Levi, Stuttgart University J. Reich, MDC, Berlin A. Rosenthal, IMB, Jena B. E. Wingender, GBF, Braunschweig
A new method for database searching and clustering	M. Vingron, DKFZ, Heidelberg
The Genome Computing Resource within DHGP	S. Suhai, DKFZ, Heidelberg
MEDSEQ: Development of a service for analysis of disease genes	J. Reich, MDC, Berlin
Evolution	
DNA-sequence evolution; mutation and variation in the human genome	S. Pääbo, MPI for Evolutionary Anthropology, Leipzig
Computer-assisted phylogenetic analysis large genomic regions	A. von Haeseler, MPI for Evolutionary of Anthropology, Leipzig M. Vingron, DKFZ, Heidelberg
A comparative map of mouse, rat and Chinese hamster genomes by interspecies chromosome painting; cross-species color segmenting – a novel tool in human karyotype analysis	J. Wienberg, National Cancer Institute, Frederick, MD, USA
Comparative (Zoo-FISH) genome mapping and positional cloning of evolutionary chromosome breakpoints in important mammal and vertebral genomes	T. Haaf, MPI for Molecular Genetics, Berlin
Expression/gene regulation	
Analysis of the transcription apparatus: from sequence to function	I. Grummt, DKFZ, Heidelberg E. Bautz, Heidelberg University G. Peterson, Heidelberg University
DNA replication in large genomes: function of the human homologue of the MCM gene family	G. Feger, Serono Pharmaceutical Research Institute S.A., Plans. Les-Ouates, Switzerland W. Hemmer, GATC GmbH, Konstanz
Expressed RNA sequence tags (ERNs) in mouse brain	J. Brosius, Münster University
Functional analysis of independently regulated transcription units: the human type I interferon gene cluster as a paradigm	J. Bode, GBF, Braunschweig
Generation of comprehensive libraries enriched for full-length cDNAs in the course of the German Genome Project	A. Poustka, DKFZ, Heidelberg S. Wiemann, DKFZ, Heidelberg
Genomic sequencing of human zinc finger gene clusters	H.-J. Thiesen, Rostock University

Table 2 (continued)

Research topic	Group leader/coordinator
Cloning and analysis of large genomic fragments of pre-determined structure	T. Boehm, MPI for Immunobiology, Freiburg
Alternative mRNA splicing: detection and analysis of human exonic enhancer sequences using genomic SELEX	A. Bindereif, Giessen University
Structural and functional characterization of apoptosis induced genes	H. von Melchner, Frankfurt/Main University
Systematic characterization of protein-protein interactions in man	M. Meisterernst, E.-L. Winnacker, LMU Munich
Mapping/cytogenetics	
Central Genotyping Service (GSU) at the Max Delbrück Center	F. Luft, Franz-Volhard-Klinik, Berlin E. Reis, MDC, Berlin H. Schuster, Franz-Volhard-Klinik, Berlin J. Reich, MDC, Berlin K. Rohde, MDC, Berlin T. Wienker, Bonn University
Theoretical and experimental analysis of chromatin three-dimensional structure and internal motions	J. Langowski, DKFZ, Heidelberg T. Cremer, LMU, Munich P. Lichter, DKFZ, Heidelberg E. Cremer, Heidelberg University W. Jäger, Heidelberg University
Exon map in proximal Yq11	P. Vogt, Heidelberg University
Generation of sequence-ready maps of human chromosome 17p	A. Poustka, DKFZ, Heidelberg
Production and application of functional defined DNA probes that can be amplified by PCR for three-dimensional structural analysis of chromosome territories	T. Cremer, LMU, Munich
Nibrin, a novel DNA double-strand break repair protein, is mutated in Nijmegen breakage syndrome	K. Sperling, Virchow-Klinikum, Berlin
Sequencing analysis of a 1.5-Mb contig in the human Xp11.23 region	A. Meindl, LMU, München A. Rosenthal, IMB, Jena
Cloning and characterization of the gene for hypertension and brachydactyly on the short arm of chromosome 12	S. Bähring, Franz-Volhard-Klinik, Berlin A. Reis, MDC, Berlin F. Luft, Franz-Volhard-Klinik, Berlin
Comparative physical and transcriptional mapping of human chromosome 20q13 segment as candidate for imprinting	I. Hangman, Halle University R. Lilly, Marburg University T. Meeting, LMU, Munich
MITOP – the mitochondria project	
Molecular analysis of the vertebrate genome	H. Lehrach, MPI for Molecular Genetics, Berlin R. Setback, MPI for Molecular Genetics, Berlin M.-L. Yaps, MPI for Molecular Genetics, Berlin

Table 2 (continued)

Research topic	Group leader/coordinator
Molecular characterization of the coding capacity of the MHS4 region on chromosome 3q13.1	M. Roche, Jena University T. Duffel, Jena University
Systematic FISH mapping of disease-associated balanced chromosome rearrangements (Debars)	H.-H. Ropers, MPI for Molecular Genetics, Berlin
Multiplex-FISH (M-FISH): a multicolor method for the screening of the integrity of a genome	M. Speeches, LUM, Munich
Model organisms The synapsis associated protein of 47 kD (SAP47): cloning and characterization of the human gene and the function analysis in the model system Drosophila	E. Buchner, Würzburg University
The immunoglobulin κ locus of the mouse in comparison to the human κ locus	H.-G. Zachau, LMU, Munich
Use of yeast artificial chromosomes (YACs) for transgenesis	G. Schütz, DKFZ, Heidelberg
Rat genome resource development and characterization	D. Ganten, MDC, Berlin M. Knoblauch, MPI for Molecular Genetics, Berlin H. Lehrach, MPI for Molecular Genetics, Berlin
The ENU-mouse mutagenesis screen	R. Balling, GSF, Oberschleissheim M. Hrabe de Angelis, GSF, Oberschleissheim E. Wolf, LMU, München
From phenotype to gene: mapping of mutations in the zebrafish	R. Geisler, MPI for Developmental Biology, Tübingen
Isolation and characterization of monosomal mouse cell lines and interspecific hybrid cells with single mouse chromosomes	H. Neitzel, Humboldt-University, Berlin J. Klose, Humboldt-University, Berlin M. Digweed, Humboldt-University, Berlin F. Theuring, Humboldt-University, Berlin
Systematic screen for novel genes required in pattern formation, organogenesis and differentiation processes of the mouse embryo	B. Herrmann, MPI for Immunobiology, Freiburg
The zebrafish molecular anatomy project (ZMAP): towards the systematic analysis of cell-specific gene expression in the zebrafish, *Danio rerio*	F. Bonhoeffer, MPI for Developmental Biology, Tübingen
Functional analysis of mammalian genes by a large-scale gene trap approach in mouse embryonic stem cells	W. Wurst, GSF, Oberschleissheim H.-H. Arnold, Braunschweig University E.-M. Füchtbauer, Aarhus University, Danmark H. von Melchner, Frankfurt University Hospital P. Ruiz, MPI for Molecular Genetics, Berlin

Table 2 (continued)

Research topic	Group leader/coordinator
Systematic functional analysis and mapping of X-chromosomal genes in *Drosophila melanogaster*	H. Jäckle, MPI for Biophysical Chemistry, Göttingen
Sequencing	
Sequencing of full-length cDNAs in the course of the German Genome Project	S. Wiemann, DKFZ, Heidelberg W. Ansorge, EMBL, Heidelberg H. Blöckler, GBF, Braunschweig H. Blum, LMU, Munich A, Düsterhöft, Qiagen GmbH, Hilden K. Köhrer, Düsseldorf University W. Mewes, MPI for Biochemistry, Martinsried B, Obermaier, Medigenomix GmbH, Martinsried A. Poustka, DKFZ, Heidelberg
Towards sequencing of chromosome 21: sequencing and automated annotation of 3 Mb between AML-D21S17 and ETS-D12S349	Rosenthal, IMB, Jena H. H. Blöckler, GBF, Braunschweig H. Lehrach, MPI for Molecular Genetics, Berlin J. Ramser, MPI for Molecular Genetics, Berlin R. Reinhardt, MPI for Molecular Genetics, Berlin
"Multiplex PCR sequencing": an efficient way to analyze candidate gene variation	M. Hoehe, MPI for Molecular Genetics, Berlin
Comparative sequencing of a 1-Mb region in man (chromosome 11p15) and mouse (chromosome 7)	B. Zabel, University Hospital, Mainz A. Winterpacht, University Hospital, Mainz T. Hankeln, Mainz University E. Schmidt, Mainz University

not only shows the various aspects of research related to the human genome project, it is also a small 'who's-who' compendium of molecular genetics in Germany to date.

4.3.1.1 Milestones

In May 2000, The Chromosome 21 Mapping and Sequencing Consortium, consisting of researchers from Japan, Germany, England, France Switzerland and the USA, reported a huge success: the completion of the sequence of chromosome 21 [61], the second finished human chromosome after chromosome 22 [62]. However, only one month later, they were overtaken by US researcher Craig Venter who announced that he had sequenced the whole human genome thereby stepping into the post-genome age.

4.3.2 *Microbial Genomes*

Besides the Human Genome Project, Germany has taken part in several other – especially microbial – genome projects. Since the reporting of the first complete microbial sequence, the genome of the pathogen *Haemophilus influenza* in 1995 [63], by a group from The Institute of Genomic Research (TIGR), 36 microbial genomes have been completely deciphered. These range from yeast and *E. coli* to *C. elegans* and *Drosophila*, the most beloved pets of molecular biologists. Figure 1 gives an overview of microbial genomes already sequenced.

These intensively studied organisms provide an invaluable possibility to correlate genomic data to well-known biological functions. Genomes of pathogenic microorganisms are also under investigation. Knowledge about their biology and especially the mechanisms of their pathogenicity is necessary for developing therapeutic strategies to defeat them. German researchers from academic institutions or biotech companies have participated in sequencing *Bacillus subtillis*, *Mycoplasma pneumonia*, and *Thermoplasma acidophilum* [64–66].

Currently under investigation by German groups are *Clostridium tetani*, *Methanosarcina mazei*, *Thermus thermophilus* (Göttingen Genomics Laboratory), *Corneybacterium glutamicum, Pasteurella haemolytica*, *Ustilago maydis* (LION Bioscience), and *Halobacterium salinarium* (MPI for Biochemistry, Martinsried).

The 6.1-Mb large genome of *Pseudomonas putida* is currently being studied in a joint effort by a team of researchers from the USA and Germany. The US

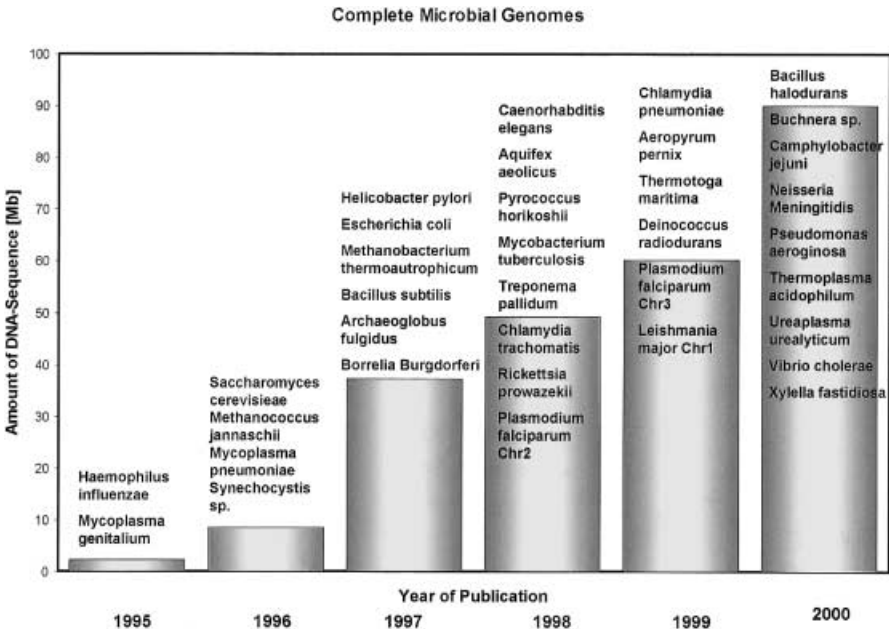

Fig. 1. Completely deciphered microbial genomes as of October 2000. Source: TIGR Microbial Database, http://www.tigr.org/tdb/mdb/mdbcomplete.html

partner is The Institute for Genomics Research (TIGR) in Rockville, MD. The German consortium consists of groups from Hannover Medical School, DKFZ Heidelberg, The Society for Biological Research (GBF), Braunschweig, and Qiagen GmbH, Hilden. While the sequencing work is equally divided between TIGR and Qiagen, the other groups carry out genome wide mapping and functional analysis. Assembly and annotation are performed at TIGR.

The sequencing and the analysis of *Dictyostelium discoideum*, a soil-living amoeba, is an international collaboration between the University of Cologne, the Institute of Molecular Biology (IMB) in Jena, Baylor College of Medicine in Houston, USA, the Pasteur Institute in Paris, France, and the Sanger Center in Hinxton, England. *Dictyostelium* is an excellent organism for the study of the molecular mechanisms of cell motility, signal transduction, cell-type differentiation and developmental processes. Genes involved in any of these processes can be knocked-out rapidly by targeted homologous recombination. The determination of the entire information content of the *Dictyostelium* genome will be of great value to those working with this organism directly, as well as to those who would like to determine the functions of homologous genes from other species. The hereditary information is carried on six chromosomes with sizes ranging from 4 to 7 Mb resulting in a total of about 34 Mb of DNA, a multicopy 90-kb extrachromosomal element that harbors the rRNA genes, and the 55-kb mitochondrial genome. The estimated number of genes in the genome is 8000 to 10,000 and many of the known genes show a high degree of sequence similarity to homologues in vertebrate species.

5
After 2000: Starting the Biological Age

One of the major goals in life sciences is now achieved: the complete sequence of the human genome – for some people the 'holy grail' of molecular genetics – is now available. The findings that were made during the 10 years of sequencing the human genome as well as the results of other genome projects, including model organisms and pathogenic microorganisms, are already revolutionizing biology. Genome research provides a vital thrust to the increasing productivity and persuasiveness of the life sciences.

However, some of the most challenging questions still remain. The sequence of the genome is a static quantity: it provides a list of all the genes in a cell, but it contains no information about their activity. Every single cell contains the complete building plan for the whole organism, but it converts only a part of it and differentiates into a skin, muscle or nerve cell. How are these complex processes regulated and why does a cell develop in a distinctive way? These are questions that cannot be settled by means of a genome analysis.

5.1
Beyond the Genome – Functional Genomics and Proteomics

Regulation of genetic activity and gene function are now the central points of interest. Genetic diseases are rarely caused by the damage of one single gene.

Interactions between different genes – possibly located in spatial distance to each other – can hardly be detected by analyzing the genome.

To test many of the approaches required for a comprehensive analysis of the entire human genome, to systematically identify and analyze all human genes, and to identify the medically interesting genes located there, a detailed investigation of certain regions on specific genes can be of great advantage. The X chromosome is particularly interesting due to the large number of diseases that have been associated with it. (Just remember the 'classical' inherited disorders like hemophilia or color-blindness.) The telomeric part of the X chromosome, Xq27.3-Xqter, is of interest due to the high gene density and the many diseases that have been linked to this region. The systematic generation of physical and transcription maps has facilitated the identification of many of the genes. Together with extensive large-scale genomic sequencing this has led to the establishment of a region-specific gene map with a very high resolution. The knowledge of the methodologies and resources that was accumulated during this work has made distal Xq into one of the best analyzed regions of the human genome. This region can therefore be viewed as a model for the development and testing of strategies for the large-scale identification of genes in the human genome and can now be extended to the systematic functional and evolutionary analysis of genes.

Another focus which has become increasingly important with the progress in technology has been directed at the identification and analysis of genes involved in human cancer. It is obvious that the application of genome analysis techniques is particularly important for cancer, since formation and progression of tumors inherently involve large numbers of genes.

Understanding the molecular basis of psychiatric diseases is also a challenging task. The identification of genes responsible for such diseases can be a step towards the comprehension of these complex disorders.

Only an analysis of the expression of mRNA molecules – which pass genomic information on to the protein-synthesizing machinery – shows which genes are really active in a certain cell of the body. Therefore, development of new automated techniques for displaying gene expression patterns and functional genomics, e. g. DNA chips and serial analysis of gene expression (SAGE), methods for the introduction of macromolecules into living cells, the evaluation of gene expression and their localization, through image acquisition and processing become increasingly important.

High-throughput analysis of differential gene expression is becoming a powerful tool with applications in molecular biology, cell biology, development, differentiation and molecular medicine. The techniques that can be used to address these questions are comparative expressed sequenced tag (EST) analyzing, full-length cDNA sequencing, and SAGE and mRNA hybridization to cDNA or oligonucleotide arrays on miniaturized DNA chips. These methods will help to identify genes that are critical for a developmental process, genes that mediate cellular responses to chemical or physical stimuli or to understand the molecular events affected by mutations in a gene of interest. In molecular medicine they will serve for the identification of molecular markers for various disorders, and in pharmacogenomics for the identification and characterization of drug targets and of the molecular events associated with drug treatment.

Building up expertise in this field, EMBL with its data library is well positioned to play an important European role in establishing a reference DNA array and SAGE database. In the future, the micro-array technology will be developed also for proteins, applying miniaturization, nanotechnology, micro-fabricated devices and reaction chambers.

Genes are the archives that contain the hereditary information, RNA molecules form the 'working copy' of the archive and direct the orders of the genes to protein synthesis. Finally, proteins connect the instructions of the genes to cellular functions. The proteome (= **prote**in complement expressed by the gen**ome**), of a cell – in contrast to its genome – is constantly dynamically changing. It depends on the current status of a cell: a tumor cell differs from a normal cell, a growing cell from a resting one. The proteins of a cell may even vary from one minute to the next.

Analyzing thousands of proteins concurrently opens enormous opportunities both for fundamental research and for commercial developments. At present the technology has been demonstrated, and there will certainly be further developments towards the critical ability to identify and/or verify hundreds of proteins per day in the very near future, thus accelerating the search for clinical markers. By means of analyzing signal transduction pathways, multi-protein-complexes and the dynamic changes of protein expression, the effects of candidate drugs can be determined, including comprehensive studies concerning their molecular toxicology. The new techniques of proteomics – two-dimensional gel electrophoresis fused to high resolution mass spectrometry – based on modern robotics and high end equipment integrated in a special database system will be crucial for target identification and validation connected with biological function.

Genomics, functional genomics and proteomics, with their enabling technologies (biological and biochemical methods, instrumentation, automation techniques and databases), are revolutionizing research in biology and pharmaceutical and medical fields.

A special remark should be made to the emerging discipline bioinformatics. Due to the huge amounts of data that are increasing exponentially from day to day, tools for storage, retrieval and comparison of data are needed. Bioinformatics has exceeded beyond assigning functions to unknown genes based on the degree of homology. Experiments 'in silico' add to experiments 'in vitro' or 'in vivo'.

A nice example to demonstrate this can be found in a paper from a group associated to the DGHP [67]: The authors discovered a cDNA sequence for a novel protein of the globin family in databases of mice. Gene expression analyses showed that the novel protein was predominantly expressed in the brain – therefore the researchers called it Neuroglobin. They isolated Neuroglobin from mouse brain, cloned the respective cDNA and – also characteristic for the new biotech age – they filed a patent for Neuroglobin.

5.2 Ethical, Legal and Social Implications of Genomic Research

Ethical research of the implications of human genome science is an integral part of the German Human Genome Project. The results of the Human Genome

Project will reveal a growing number of diseases that are genetically determined. It will thereby create an extremely broad range of possible uses for predictive genetic tests in the future. These tests will induce a process of hitherto unknown innovative possibilities in the practice of modern medicine. But, along with the new diagnostic potentials, new risks and potential harms will be created. Considering the risks and potentials of predictive genetic testing, the question then arises, which criteria and categorizations would be adequate to ensure both a responsible use of predictive genetic testing and, at the same time, avoid the inherent possibilities of misuse. Such a limitation of tests which are predictive of genetic diseases is being attempted on a worldwide scale by tying them to definite purposes like 'health' or 'medical teleology' – as expressed in the Convention for the Protection of Human Rights and Dignity of the Human Being with regard to the application of biology and medicine of the Council of Europe.

The potential for generating an ever-increasing swell of genetic information about individuals in medical care raises crucial questions regarding the circumstances under which genetic tests should be used, how the tests should be implemented and what uses are made of their results. The main issues concerned among others are: voluntariness of services, freedom of choice, patient autonomy, informed consent, confidentiality of genetic information, privacy, testing of minors, social discrimination and stigmatization.

There is consensus evident in Europe and the USA that the appropriateness, responsiveness and competence of clinical and preventive genetic services in regard to these issues need to be assessed, that genetic technologies, genetic practices and procedures should not be left to the vagaries of economic forces, personal and/or professional interests, fears or vulnerabilities. There is growing agreement that genetic service provision and the implementation process of new genetic testing procedures should be safeguarded by providing general principles and recommendations that are based on solid facts and at the same time recognize and respect the multifaceted aspects of a pluralistic society.

5.2.1 *Patents*

Rapid and broad access to the ever-expanding results of genomic research will undoubtedly result in new and improved therapies for a wide range of disease states. The issue of patents covering genomic inventions and access to these inventions for research purposes is the subject of intense debate both in the US and Europe. Strong patent laws encourage the innovation necessary for the development of new and enhanced therapies.

Reasonable access to appropriately patented genomic inventions should be provided for research purposes and exclusive positions maintained for commercial uses. This will promote rapid access to genomic information and fundamental technologies while optimizing the discovery and disclosure of basic advances in biomedical research. The primary question behind the decision whether to patent a finding from genomic research is: Will patent protection for this invention promote its development? For a potential therapeutic protein, the

question is easy to answer in the affirmative, since, without such protection, no pharmaceutical company will develop the product, given the cost of developing a therapeutic product. This is equally true for many diagnostics, even more so if the potential market is relatively small. For research tools like receptors or DNA sequences, the answer may depend on whether the tool needs significant investment in development before it can be widely used, and whether its useful life will be longer than the time it takes for the patent to be issued.

A step in the right direction was the acceptance of the European Parliament's guideline for patenting of biotechnological inventions by the European Patent Office in 1999. The guideline coordinates the different national patent laws and takes into account ethical aspects, e.g. the cloning of human beings or interventions into the germ line. Pure genomic sequence data without additional information about the function of the respective gene are excluded from being patented. Appropriate protection by a patent is the key to turning the results of genomic research into biomedical applications and last but not least into economic value.

6 Further Perspectives: 'Green' Biotechnology

There is still one issue which has not yet been mentioned in this article: the so-called 'Green' biotechnology which applies genetic engineering to plant and food production in order to produce herbicide resistant plants, crops which can grow productively even under extreme conditions like heat, dry soil, etc., or functional food which is enriched in vitamins or other useful components. Of course German researchers from industry and academia are integrated parts of plant genome projects, e. g. sequencing of the model plant *Arabidopsis thaliana*. Many experts see a great potential in plant biotechnology for solving future food problems due to the growing world population. But, while genetic engineering for health and medical purposes is widely accepted, people, especially in the developed countries, regard the production of recombinant plants with great suspicion. They fear unforeseeable ecological risks and hitherto unknown effects of genetically modified nutrients. This opens a large sphere of activities to molecular biologists working on plants and related scientists. On the one hand there is a strong need for investigating especially the ecological consequences in order to weigh up the possible risks and chances. On the other hand the general public has to be well informed and instructed to be able to consider the pros and cons of Green biotechnology in an objective and unemotional way. This is still a demanding task as long as even well-educated people do not know that every leaf of 'normal' salad contains as many 'foreign' (= non-human) genes as any genetically modified soy bean and that genes are not a poisonous material created by thoughtless scientists but essential constituents of every living being including man. An informed and predominantly consenting public (the later customers of genetically engineered products!) provides the basis for benefiting from the advantages of molecular biology for plant and food production and to establish a sustainable industry in this area of business.

References

1. Fincham JRS (1990) Nature 343:208
2. Morgan TH (1910) Science 32:120
3. Morgan TH (1911) Science 33:496
4. Morgan TH, Sturtevant A, Muller HJ, Bridges C (1923) The mechanism of Mendelian heredity. Holt, New York
5. Muller HJ (1927) Science 66:84
6. Garrod AE (1909) Lancet 2:73
7. Beadle GW, Tatum EL (1941) Proc Natl Acad Sci USA 499
8. Beadle GW (1974) Ann Rev Biochem 43:1
9. Avery OT, McLeod CM, McCarthy M (1944) J Exp Med 79:137
10. Chargaff E (1950) Experientia 6:201
11. Watson JD, Crick F (1953) Nature 171:737
12. Watson JD, Crick F (1953) Nature 171:964
13. Klug A (1968) Nature 219:808
14. Pauling L, Delbrück M (1940) Science 92:77
15. Luria SE, Delbrück M (1943) Genetics 28:491
16. Crick F (1970) Nature 227:561
17. Meselson M, Stahl FW (1958) Proc Natl Acad Sci USA 44:671
18. Nirenberg M, Matthaei JH (1961) Proc Natl Acad Sci USA 47:1588
19. Itakura K, Hirose T, Crea R, Riggs AD et al. (1977) Science 198:1056
20. Maxam AM, Gilbert W (1980) Methods Enzymol 65:499
21. Maxam AM (1980) Fed Proc 39:2830
22. Mullis KB (1990) Ann Biol Clin (Paris) 48:579
23. Mullis KB (1990) Sci Am 262:56
24. Palmiter RD, Brinster RL, Hammer RE, Trumbauer ME et al. (1982) Nature 300:611
25. Campbell KH, McWhir J, Ritchie WA, Wilmut I (1996) Nature 380:64
26. Wilmut I, Schnieke AE, McWhir J, Kind AJ et al. (1997) Nature 385:810
27. Wilmut I, Young L, Campbell KH (1998) Reprod Fertil Dev 10:639
28. Polymeropoulos MH, Higgins JJ, Golbe LI, Johnson WG et al. (1996) Science 274:1197
29. Tavtigian SV, Simard J, Rommens J, Couch F et al. (1996) Nat.Genet. 12:333
30. Smith JR, Freije D, Carpten JD, Gronberg H et al. (1996) Science 274:1371
31. Hutton M, Busfield F, Wragg M, Crook R et al. (1996) Neuroreport 7:801
32. Abbott A (1992) Nature 357:268
33. Hoffmann-Berling H, Kaerner HC, Knippers R (1966) Adv Virus Res 12:329
34. Kuhn B, Abdel-Monem M, Hoffmann-Berling H (1979) Cold Spring Harb Symp Quant Biol 43 Pt 1:63
35. Geider K, Hoffmann-Berling H (1981) Annu Rev Biochem 50:233
36. Hoffmann-Berling H (1982) Prog Clin Biol Res 102 Pt C:89
37. Nusslein-Volhard C, Wieschaus E (1980) Nature 287:795
38. Jackle H, Rosenberg UB, Preiss A, Seifert E et al. (1985) Cold Spring Harb Symp Quant Biol 50:465
39. Peerenboom E (1998) Laborjournal 5:27
40. Hollenberg CP, Gellissen G (1997) Curr Opin Biotechnol 8:554
41. Gellissen G, Hollenberg CP (1997) Gene 190:87
42. Gellissen G, Janowicz ZA, Merckelbach A, Piontek M et al. (1991) Biotechnology (NY) 9:291
43. Janowicz ZA, Melber K, Merckelbach A, Jacobs E et al. (1991) Yeast 7:431
44. Mayer K, Schuller C, Wambutt R, Murphy G et al. (1999) Nature 402:769
45. Biebricher CK, Eigen M, Gardiner WCJ (1985) Biochemistry 24:6550
46. Biebricher CK, Eigen M, Gardiner WCJ (1984) Biochemistry 23:3186
47. Biebricher CK, Eigen M, Luce R (1986) Nature 321:89
48. Eigen M, Rigler R (1994) Proc Natl Acad Sci USA 91:5740

49. Schober A, Walter NG, Tangen U, Strunk G et al. (1995) Biotechniques 18:652
50. Müller A, Kremoser C, Rodewyck BRT (1998) Aufbruchstimmung 98 – 1. Deutscher Biotechnologie Report, Stuttgart
51. Müller A, Lucas P, MacCabe B, Mendoza-Vega O et al. (1998) European Life Sciences 98 – Continental Shift, Ernst & Young International, London
52. Müller A, Powlett Smith W, Mendoza-Vega O, MacCabe B et al. (2000) Evolution – Ernst & Young's Seventh Annual European Life Sciences Report 2000, Ernst & Young International, London
53. Goffeau A, Barrell BG, Bussey H, Davis RW et al. (1996) Science 274:546, 563
54. Blattner FR, Plunkett G, Bloch CA, Perna NT et al. (1997) Science 277:1453
55. Lin X, Kaul S, Rounsley S, Shea TP et al. (1999) Nature 402:761
56. *C. elegans* Sequencing Consortium (1998) Science 282:2012 [published errata appear in Science (1999) 283:35, (1999) 283:2103 and (1999) 285:1493]
57. Adams MD, Celniker SE, Holt RA, Evans CA et al. 287:2185
58. Bowman S, Lawson D, Basham D, Brown D et al. (1999) Nature 400:532
59. Gardner MJ, Tettelin H, Carucci DJ, Cummings LM et al. (1998) Science 282:1126
60. Zehetner G, Lehrach H (1994) Nature 367:489
61. Hattori M, Fujiyama A, Taylor TD, Watanabe H et al. (2000) Nature 405:311
62. Dunham I, Shimizu N, Roe BA, Chissoe S et al. (1999) Nature 402:489
63. Fleischmann RD, Adams MD, White O, Clayton RA et al. (1995) Science 269:496
64. Kunst F, Ogasawara N, Moszer I, Albertini AM et al. (1997) Nature 390:249
65. Himmelreich R, Hilbert H, Plagens H, Pirkl E et al. (1996) Nucleic Acids Res 24:4420
66. Hilbert H, Himmelreich R, Plagens H, Herrmann R (1996) Nucleic Acids Res 24:628
67. Burmeester T, Weich B, Reis B, Reinhardt S et al. (2000) Nature 407:520

Received: January 2001

Biosynthesis of Triterpenoid Saponins in Plants

Kosmas Haralampidis, Miranda Trojanowska and Anne E. Osbourn

Sainsbury Laboratory, John Innes Centre, Colney Lane, Norwich NR4 7UH, UK,
e-mail: annie.osbourn@bbsrc.ac.uk

Many different plant species synthesise triterpenoid saponins as part of their normal programme of growth and development. Examples include plants that are exploited as sources of drugs, such as liquorice and ginseng, and also crop plants such as legumes and oats. Interest in these molecules stems from their medicinal properties, antimicrobial activity, and their likely role as determinants of plant disease resistance. Triterpenoid saponins are synthesised via the isoprenoid pathway by cyclization of 2,3-oxidosqualene to give primarily oleanane (β-amyrin) or dammarane triterpenoid skeletons. The triterpenoid backbone then undergoes various modifications (oxidation, substitution and glycosylation), mediated by cytochrome P450-dependent monooxygenases, glycosyltransferases and other enzymes. In general very little is known about the enzymes and biochemical pathways involved in saponin biosynthesis. The genetic machinery required for the elaboration of this important family of plant secondary metabolites is as yet largely uncharacterised, despite the considerable commercial interest in this important group of natural products. This is likely to be due in part to the complexity of the molecules and the lack of pathway intermediates for biochemical studies. Considerable advances have recently been made, however, in the area of 2,3-oxidosqualene cyclisation, and a number of genes encoding the enzymes that give rise to the diverse array of plant triterpenoid skeletons have been cloned. Progress has also been made in the characterisation of saponin glucosyltransferases. This review outlines these developments, with particular emphasis on triterpenoid saponins.

Keywords. Saponins, Triterpenoids, Sterols, 2,3-Oxidosqualene cyclases, Glycosyltransferases

1 Introduction 32

2 Cyclization of 2,3-Oxidosqualene – The First Committed Step in Triterpenoid Biosynthesis 34

2.1 Resolution of Cyclase Activities Required for Sterol and Triterpenoid Biosynthesis 36
2.2 Cloning of 2,3-Oxidosqualene Cyclases 37
2.2.1 OSCs Required for Sterol Biosynthesis 37
2.2.2 Triterpenoid Cyclases 37
2.2.3 OSC Gene Families 38
2.3 The Relationship Between Structure and Function 38
2.3.1 Conserved Features 39
2.3.2 Processing and Post-Translational Modifications 41
2.3.3 Product Determination 41
2.4 Manipulation of Flux Through the Sterol and Triterpenoid Biosynthetic Pathways 44

Advances in Biochemical Engineering/
Biotechnology, Vol. 75
Managing Editor: Th. Scheper
© Springer-Verlag Berlin Heidelberg 2002

3 Elaboration of the Aglycone 44
3.1 Saponin Glycosyltransferases 45
4 Conclusions 46
5 References 47

List of Abbreviations

αAS α-Amyrin synthase
βAS β-Amyrin synthase
CS Cycloartenol synthase
DS Dammarenediol synthase
EST Expressed sequence tag
LS Lanosterol synthase
LuP Lupeol synthase
OSC Oxidosqualene cyclase
PCR Polymerase chain reaction
SC Squalene-hopene cyclase

1 Introduction

Collectively plants synthesise a diverse array of secondary metabolites, either as part of normal growth and development or in response to pathogen attack or stress. By definition, secondary metabolites are regarded as "luxury items" that are not required for growth and reproduction of the plant, at least under defined conditions. Since the ability to synthesise particular classes of secondary metabolites is restricted to certain plant groups, these compounds are clearly not essential for survival. However they may be important in conferring selective advantages, for example by suppressing the growth of neighbouring plants or by protecting against pests, pathogens and stress [1–5]. They may also have subtle physiological roles in plants, which are as yet uncharacterised. In addition to their natural roles plant secondary metabolites also represent a vast resource of complex molecules that are valued and exploited by man for their pharmacological and other properties [1].

Saponins are an important group of plant secondary metabolites that are widespread throughout the Plant Kingdom [4, 6–9]. The name saponin is derived from *sapo*, the Latin word for soap, since these molecules have surfactant properties and give stable, soap-like foams in aqueous solution. Chemically, the term saponin has become accepted to define a group of structurally diverse molecules that consists of glycosylated steroids, steroidal alkaloids and triterpenoids (Fig. 1). These secondary metabolites often occur in plants as complex mixtures, and saponin content and composition may vary markedly depending on the genetic background of the plant material, the tissue type, the age and physiological state of the plant and environmental factors [6–10].

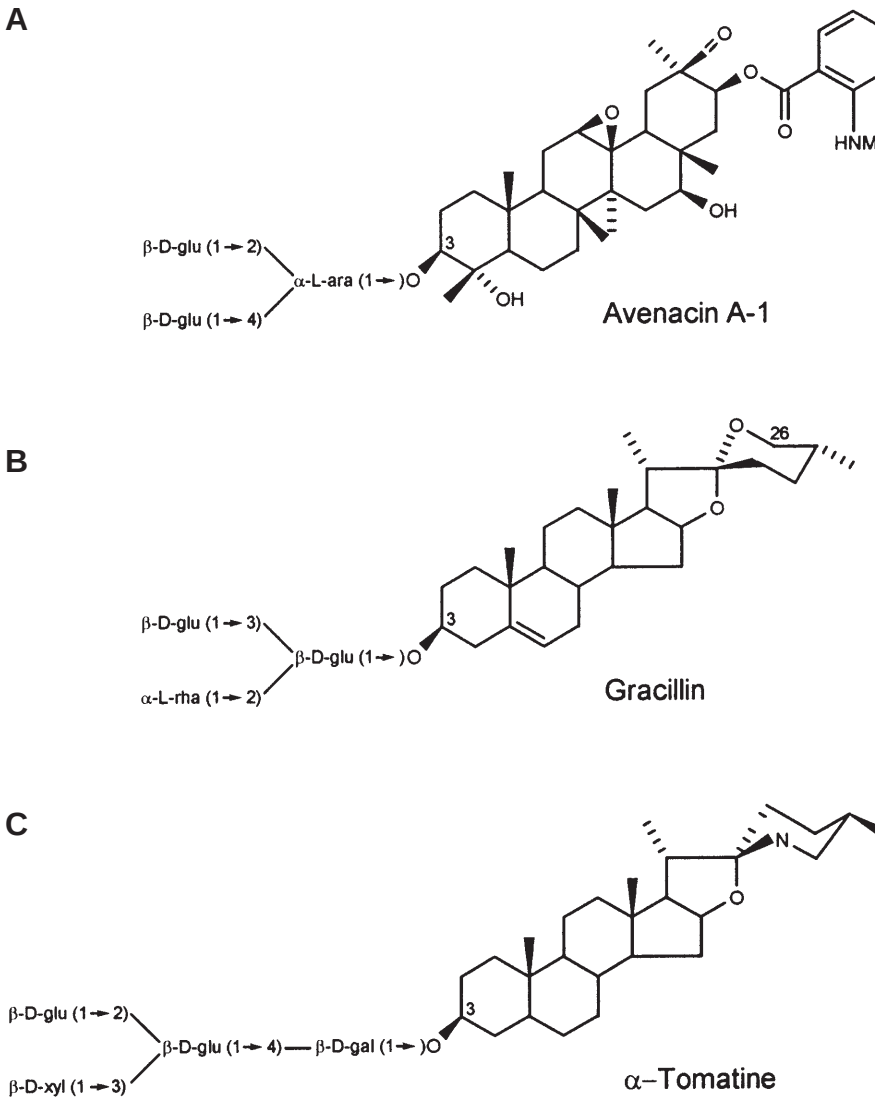

Fig. 1 A–C. Examples of different classes of saponins: **A** the triterpenoid saponin avenacin A-1 from roots of *Avena* spp; **B** the steroidal saponin gracillin, from *Costus speciosus*; **C** the steroidal glycoalkaloid α-tomatine from tomato (*Lycopersicon* spp.)

Saponins have been variously attributed with a diverse range of properties, some of which include both beneficial and detrimental effects on human health, piscidical, insecticidal and molluscicidal activity, allelopathic action, antinutritional effects, sweetness and bitterness, and as phytoprotectants that defend plants against attack by microbes and herbivores [2–11]. A more detailed understanding of the biochemical pathways and enzymes involved in saponin

biosynthesis will facilitate the development of plants with altered saponin content. In some cases enhanced levels of saponins or the synthesis of novel saponins may be desirable (for example, for drug production [9, 12–15] or improved disease resistance [4, 6, 10, 16]) while for other plants reduction in the content of undesirable saponins would be beneficial (for example, for legume saponins that are associated with antifeedant properties in animal feed [8]). This review is concerned with recent progress that has been made in the characterisation of the enzymes and genes involved in the synthesis of these complex molecules, and focuses on triterpenoid saponins.

2 Cyclization of 2,3-Oxidosqualene – The First Committed Step in Triterpenoid Biosynthesis

The first committed step in the synthesis of triterpenoid saponins involves the cyclisation of 2,3-oxidosqualene to give one of a number of different potential products [9]. Most plant triterpenoid saponins are derived from oleanane or dammarane skeletons, although lupanes are also common [9]. This cyclisation event forms a branchpoint with the sterol biosynthetic pathway, in which 2,3-oxidosqualene is cyclised to lanosterol (in animals and fungi) or to cycloartenol (in plants) (Fig. 2). Sterols are important membrane constituents and also serve as precursors for hormone biosynthesis.

The cyclisation, rearrangement and deprotonation reactions leading to the different products shown in Fig. 2 (originally proposed by the "biogenetic isoprene rule") are well established [17–20]. Enzymatic cyclisation of 2,3-oxidosqualene into sterols proceeds in the "chair-boat-chair" conformation to yield the C-20 protosteryl cation, which is then converted to cycloartenol or lanosterol. These cyclisation events are catalysed by the 2,3-oxidosqualene cyclases (OSCs) cycloartenol synthase (CS) and lanosterol synthase (LS), respectively. Triterpenoid synthesis, on the other hand, involves cyclisation of the "chair-chair-chair" conformation of the substrate to give the tetracyclic dammarenyl cation. This cation may then be converted to dammarene-like triterpenoids by the OSC dammarenediol synthase (DS), or may undergo further rearrangements leading to the formation of pentacyclic triterpenoids derived from lupeol, β-amyrin and α-amyrin (Fig. 2). The 2,3-oxidosqualene cyclases (OSCs) that mediate these different cyclisation events are listed in Table 1.

Table 1. 2,3-Oxidosqualene cyclases

Enzyme	Abbreviation	EC Number	Organism
Lanosterol synthase	LS	EC 5.4.99.7	Animals, Fungi
Cycloartenol synthase	CS	EC 5.4.99.8	Plants
Dammarenediol synthase	DS	–	Plants
α-Amyrin synthase	αAS	EC 5.4.99	Plants
β-Amyrin synthase	βAS	EC 5.4.99	Plants
Lupeol synthase	LuS	EC 5.4.99	Plants

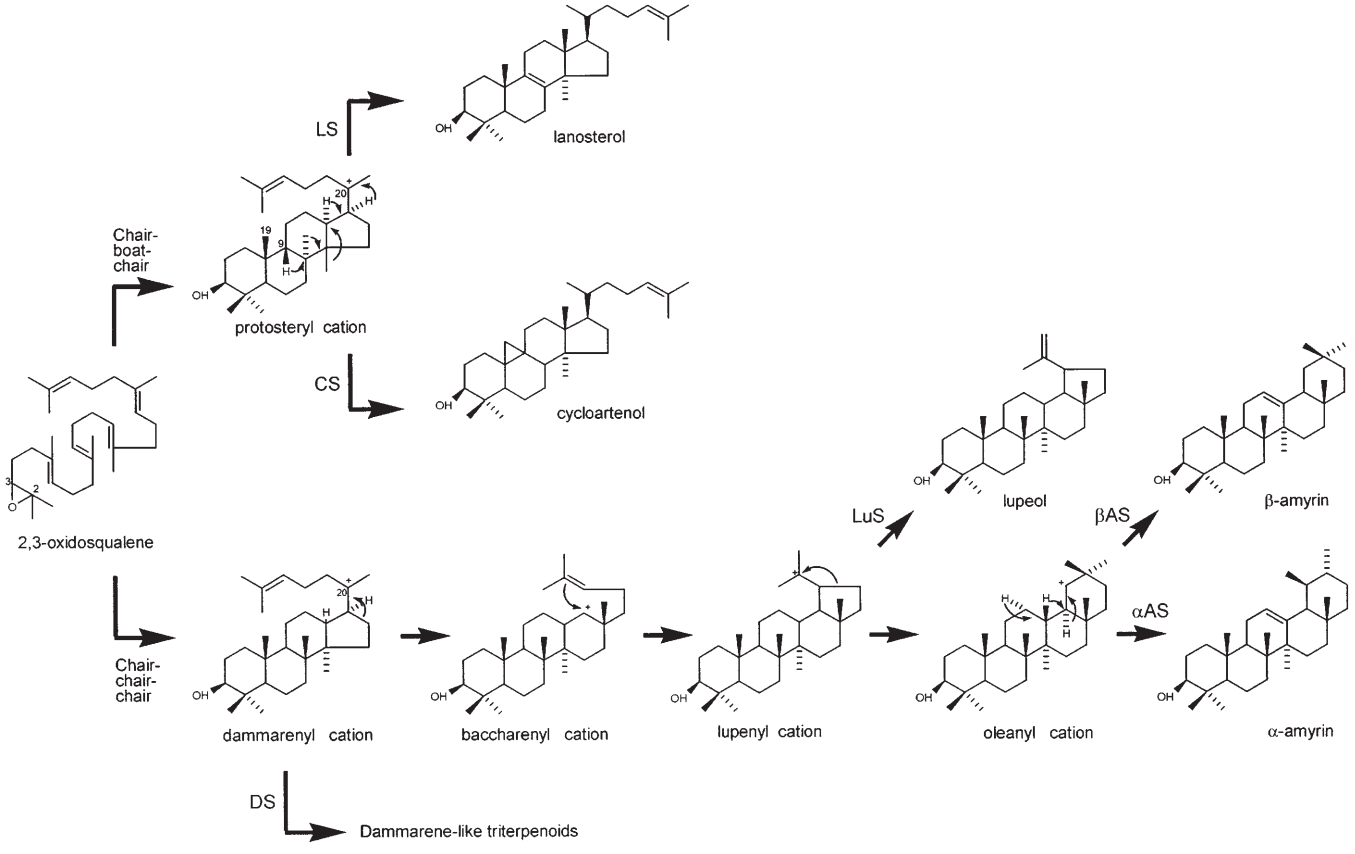

Fig. 2. Cyclization of 2,3-oxidosqualene to sterols and triterpenoids. The 2,3-oxidosqualene cyclase enzymes that catalyse the formation of the different products are indicated: LS, lanosterol synthase; CS, cycloartenol synthase; DS, dammarenediol synthase; LuS, lupeol synthase; βAS, β-amyrin synthase; αAS, α-amyrin synthase

The mechanisms by which 2,3-oxidosqualene is cyclised to a diverse range of products has been a source of intrigue for nearly half a century, and the enzymes that catalyse these reactions are of great interest both to biochemists and to industry. LS enzymes have commercial importance as targets for the development of antifungal [21] and cholesteremic drugs [21, 22]. Since the cyclisation of 2,3-oxidosqualene to sterols and triterpenoids represents a branchpoint between primary and secondary metabolism, plant OSCs are also attractive tools for investigating the regulation of synthesis and the physiological role of triterpenoids, and potentially for manipulation of sterol and triterpenoid content [23–26]. Recent progress in the purification of OSCs and in the cloning and analysis of the corresponding genes has given us substantial insight into the relationship between the nature of the cyclisation event and enzyme structure, and distinct subgroups of enzymes that mediate the conversion of 2,3-oxidosqualene to different cyclisation products are now emerging. Advances in this area are summarised below.

2.1
Resolution of Cyclase Activities Required for Sterol and Triterpenoid Biosynthesis

A key question in understanding triterpenoid biosynthesis has centred around whether the generation of different cyclisation products from 2,3-oxidosqualene involves distinct oxidosqualene cyclase enzymes, or whether these reactions may be mediated by a single enzyme, the product specificity of which may be determined by protein modification or by factors such as electrolyte concentration [23, 27, 28]. In pea (*Pisum sativum*), β-amyrin production is very active during development and just after germination, while sterol biosynthesis increases several days after germination [23]. Similar changes in triterpenoid and steroid biosynthesis in developing seed have been reported for the monocot *Sorghum bicolor* suggesting that this may be a common phenomenon in different plant species [29], although the significance of this dramatic switch between sterol and triterpenoid synthesis is unclear. The levels of β-amyrin synthase (βAS) and cycloartenol synthase (CS) activities in germinating pea seedlings alter during development in parallel with the changes in sterol and triterpenoid content, suggesting that the two enzymes are likely to be distinct proteins [27].

CS and βAS enzymes have been fully purified from seedlings of pea [27, 30, 31] and also from microsomes of cell suspension cultures of another plant species, *Rabdosia japonica* [32]. The purified pea CS and βAS enzymes were identified as 55-kDa and 35-kDa proteins, respectively [27, 30, 31]. Similarly CS and βAS enzymes purified from *R. japonica* were also found to be distinct protein species with molecular masses of 54 kDa and 28 kDa, respectively [32]. The two classes of OSC also show differences in sensitivity to inhibitors and detergents [27, 32]. Taken together, this information suggested that the two cyclisation reactions were carried out by different enzymes. However, in the absence of amino acid sequence information the possibility remained that the enzymes represented different forms of a single gene product. The cloning and characterisation of genes encoding OSCs was required to resolve this.

2.2
Cloning of 2,3-Oxidosqualene Cyclases

2.2.1
OSCs Required for Sterol Biosynthesis

In general, purification of OSCs in sufficient quantity for amino acid sequence determination or antibody production has proved to be difficult due to the small amounts of protein and the problems of obtaining the solubilised enzyme in an active state [20, 27, 33, 34], and so attempts to isolate cDNA clones or genes encoding OSCs by these routes have met with only limited success. However, amino acid sequence information from purified OSCs has been used successfully in reverse genetics approaches to isolate cloned cDNAs for LS from animals and fungi. For example, the cDNA encoding rat LS was cloned in this way [34, 35]. The LS genes from *Candida albicans* and *Saccharomyces cerevisiae* have both been cloned using a different strategy that involved genetic complementation of an LS-deficient (*erg7*) mutant of *S. cerevisiae* [36–38].

Yeast does not synthesise cycloartenol or triterpenes, and so approaches to clone plant OSCs by complementation in *S. cerevisiae* are not feasible because of the lack of appropriate mutants. However, LS-deficient yeast mutants accumulate high levels of 2,3-oxidosqualene, favouring the synthesis of novel cyclisation products generated by heterologous expression of OSCs. The absence of lanosterol also facilitates analysis of the reaction products. Corey and co-workers isolated a cDNA encoding *Arabidopsis thaliana* CS by transforming a plant cDNA expression library into such a yeast mutant and screening protein preparations derived from pools of transformants for the ability to synthesise cycloartenol by TLC [39].

The availability of an increasing amount of DNA sequence information for LS and CS enzymes enabled regions of highly conserved amino acids to be identified in their predicted amino acid sequences. The cDNAs encoding LS from yeast, humans and rat have been cloned by polymerase chain reaction (PCR) amplification using degenerate oligonucleotide primers corresponding to such regions [40, 41]. The *P. sativum* CS cDNA was also isolated in this way [42]. The functions of cDNAs that are predicted to encode OSCs have generally been confirmed by expression in LS-deficient yeast strains. Cycloartenol does not normally accumulate in sufficient amounts to be detected by TLC or HPLC in yeast extracts (probably due to metabolic conversion of cycloartenol by the yeast strain [12, 43]) and so assays for cycloartenol synthase activity are usually carried out in vitro using [^{3}H]oxidosqualene as the substrate.

2.2.2
Triterpenoid Cyclases

An important step was made when the conservation between the predicted amino acid sequences of cloned and characterised LS and CS enzymes was used to isolate two cDNA clones that were predicted to encode OSCs from *Panax ginseng* [12]. Expression of the full-length cDNAs in yeast indicated that one of the

clones encoded CS, while the other encoded βAS. Triterpenoid products generated by heterologous expression of OSCs in yeast are not readily metabolised, and so can be detected by analysis of cell extracts by TLC or reverse-phase HPLC. The deduced amino acid sequence of the *P. ginseng* βAS is 60% identical to that of the CS enzyme, suggesting that the enzymes may share a common ancestral origin. A second βAS has also been cloned from *P. ginseng* [14]. The subsequent cloning of cDNAs encoding α-/β-amyrin cyclase enzymes from pea [44], LuS enzymes from *Olea europaea* and *Taraxacum officinale* [45], and multifunctional triterpene synthases from *Arabidopsis thaliana* [46–48], confirmed that there is overall structural relatedness between the LS and CS enzymes of sterol biosynthesis and the OSCs that mediate the cyclisation of 2,3-oxidosqualene to triterpenoids. However, the triterpenoid cyclases are clearly distinct from LS and CS enzymes, and form discrete subgroups within the OSC superfamily.

2.2.3
OSC Gene Families

Benveniste et al. have carried out the first comprehensive analysis of OSCs in a single plant species by screening *A. thaliana* EST databases and cDNA libraries and have identified 3 cDNAs encoding OSCs [47]. The function of these has been investigated by expression in yeast. One (ATLUP1) was identical to an LuS isolated from *A. thaliana* by Matsuda and co-workers [46], which synthesises primarily lupeol in yeast [46, 47]. ATLUP1 also forms other minor triterpene products including β-amyrin in yeast [46, 47, 49] and because it is more closely related to the *P. ginseng* βAS enzymes than to the LuS enzymes from *Olea europaea* and *Taraxacum officinalis* it has been suggested that in the plant the primary product of ATLUP1 may be β- or α-amyrin or other triterpenoids [47, 49]. The second cDNA (ATLUP2) encoded a multifunctional enzyme that catalysed the production of lupeol, β- and α-amyrin in the ratio 15:55:30 [47, 48]. A third predicted OSC (ATPEN1) was also introduced into yeast but no triterpenoid products were detected. A survey of *Arabidopsis* genomic sequence information identified five genes belonging to the subfamily of OSCs that contained ATLUP1 and ATLUP2, and seven genes that were closely related to ATPEN1. The functions of these triterpenoid cyclases in *A. thaliana* are as yet unknown. *A. thaliana* does not appear to synthesise saponins, but α- and β-amyrin and lupeol are present in extracts of leaves and callus of the plant [47]. It is possible that triterpenoids and their derivatives may play important roles in plant growth and development.

2.3
The Relationship Between Structure and Function

OSCs that have been functionally characterised by expression in yeast are listed in Table 2, and the relatedness between the amino acid sequences of these enzymes is illustrated in Fig. 3. The conserved features of this OSC superfamily and the differences between them that may confer product specificity are considered below.

Table 2. 2,3-Oxidosqualene cyclases that have been cloned and their function confirmed by expression in yeast

Organism	Enzyme	Abbreviation	EMBL/Gene Bank AC	Ref.
Rattus norvegicus	Lanosterol synthase	OSC	U31352	34
Saccharomyces cerevisiae	Lanosterol synthase	ERG7	U04841	40
Candida albicans	Lanosterol synthase	ERG7	L04305	38
Arabidopsis thaliana	Cycloartenol synthase	CAS1	U02555	39
Pisum sativum	Cycloartenol synthase	PSX	D89619	42
Panax ginseng	Cycloartenol synthase	PNX	AB009029	12
Panax ginseng	β-Amyrin synthase	PNY	AB009030	12
Panax ginseng	β-Amyrin synthase	PNY2	AB014057	14
Pisum sativum	β-Amyrin synthase	PSY	AB034802	44
Pisum sativum	Mixed amyrin synthase[a]	PSM	AB034803	44
Olea europaea	Lupeol synthase	OEW	AB025343	45
Taraxacum officinale	Lupeol synthase	TRW	AB025345	45
Arabidopsis thaliana	Lupeol synthase[b]	ATLUP1	U49919	46
Arabidopsis thaliana	Multifunctional[c]	ATLUP2	AF003472	47, 48

[a] Primary products α- and β-amyrin (60%:40%) and also other minor triterpenes [44].
[b] Synthesises mainly lupeol but also produces at least five other minor triterpenoids [46, 47, 49].
[c] Primary products β-amyrin, α-amyrin and lupeol (55%:30%:15%) [47, 48].

2.3.1 *Conserved Features*

Currently there is no experimentally determined three-dimensional structural information available for OSCs, although studies with a related enzyme, squalene-hopene cyclase (SC; EC 5.4.99.7) have proved informative. SCs are involved in the direct cyclisation of squalene to pentacyclic triterpenoids known as hopanoids, which play an integral role in membrane structure in prokaryotes [51]. A number of SC genes have been cloned from bacteria [52–54]. The SC and OSC enzymes have related predicted amino acid sequences, and so should have similar spatial structures [55]. The crystal structure of recombinant SC from the Gram-positive bacterium *Alicyclobacillus acidocaldarius* has established that the enzyme is dimeric [55]. Each subunit consists of two α-α barrel domains that assemble to form a central hydrophobic cavity [55, 56].

The activity of 2,3-oxidosqualene cyclases is associated with microsomes, indicating their membrane-bound nature. However, the predicted amino acid sequences of these enzymes generally lack signal sequences and obvious transmembrane domains. Addition of hydrophobic membrane-localising regions to OSCs during evolution may have removed selection pressures that maintained alternate mechanisms for membrane localisation [33]. Consistent with this, there is a non-polar plateau on the surface of the *A. acidocaldarius* SC enzyme which is believed to be immersed in the centre of the membrane. The squalene substrate for SC is likely to diffuse from the membrane interior into the central cavity of the enzyme via this contact region [55, 56].

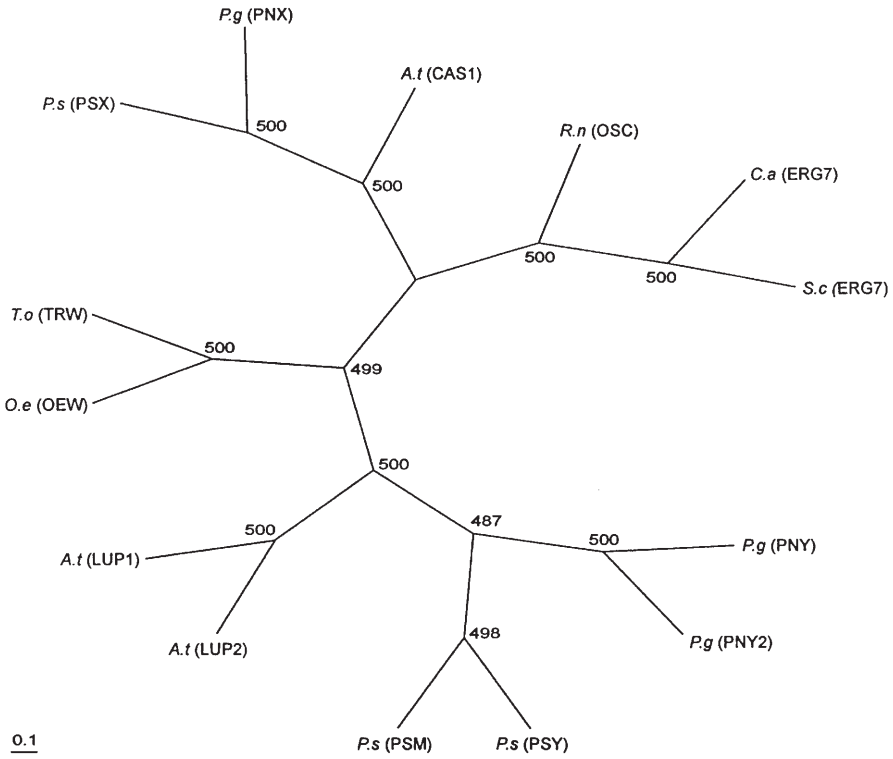

Fig. 3. Relatedness between deduced amino acid sequences of members of the OSC superfamily. *P.s* (PSX), *Pisum sativum* cycloartenol synthase (D89619); *P.g* (PNX), *Panax ginseng* cycloartenol synthase (AB009029); *A.t* (CAS1), *Arabidopsis thaliana* cycloartenol synthase (U02555); *R.n* (OSC), *Rattus norvegicus* lanosterol synthase (U31352); *C.a* (ERG7), *Candida albicans* lanosterol synthase (L04305); *S.c* (ERG7), *Saccharomyces cerevisiae* lanosterol synthase (U04841); *P.g* (PNY), *Panax ginseng* β-amyrin synthase (AB009030); *P.g* (PNY2), *Panax ginseng* β-amyrin synthase (AB014057); *P.s* (PSY), *Pisum sativum* β-amyrin synthase (AB034802); *P.s* (PSM), *Pisum sativum* mixed amyrin synthase (AB034803); *A.t* (LUP2), *Arabidopsis thaliana* multifunctional synthase (AF003472); *A.t* (LUP1), *Arabidopsis thaliana* lupeol synthase (U49919); *O.e* (OEW), *Olea europaea* lupeol synthase (AB025343); *T.o* (TRW), *Taraxacum officinale* lupeol synthase (AB025345). The phylogenetic tree was constructed by using the UPGMA method as implemented in the "Neighbor" program of the PHYLIP package (Version 3.5c) [50]. Amino acid distances were calculated using the Dayhoff PAM matrix method of the "Protdist" program of PHYLIP. The numbers indicate the numbers of bootstrap replications (out of 500) in which the given branching was observed. The protein parsimony method (the "Protpars" program of PHYLIP) produced trees with essentially identical topologies

Mechanism-based irreversible inhibitors and mutational analysis with OSCs have shown that the highly conserved amino acid motif DCTAE is required for substrate binding [27, 46, 57 – 59] (Table 3), and the conserved aspartate residue within this motif (D456) has been implicated as the likely electrophilic activator in the generation of the protosteryl cation for LS [57, 58, 60]. Similar experiments indicate that two aspartate residues at the homologous position of the

Alicyclobacillus acidocaldarius SC amino acid sequence (amino acids 376 and 377 of the DDTAV motif) are also essential for enzyme activity [59]. These residues are located in the large central cavity of the dimeric enzyme [55]. Interestingly, targeted mutations that convert the DDTAV motif of SC to DCTAE (the corresponding OSC motif) result in a change in substrate specificity from squalene to 2,3-oxidosqualene [61].

In addition to the DCTAE/DDTAV motifs, a highly conserved repetitive β-strand turn motif rich in aromatic amino acids (the QW motif) occurs in all OSCs and SCs and is repeated four to eight times (Table 3). These repeats are likely to be important for protein structure and stability and also for catalytic activity [55, 62–64]. The aromatic amino acids of the QW motif have been proposed to constitute sites of negative point charge that may interact with the intermediate cations during the cyclisation process [62].

2.3.2 *Processing and Post-Translational Modifications*

The predicted size for OSCs based on gene sequences is generally around 85 kDa. However, protein characterisation has indicated that the purified enzymes are often smaller than this. For example, the CS and βAS proteins are 55-kDa and 35-kDa respectively in pea [27, 30, 31], and 54-kDa and 28-kDa in *R. japonica* [32], while purified yeast LS has a molecular mass of 26 kDa [65]. These differences may be due to proteolysis associated with post-translational modification or to degradation during purification [38]. It is unlikely that the discrepancy between predicted and actual molecular mass is due to mRNA splicing, since Northern blot analysis of OSC gene expression normally gives a signal in the region of 2–3 kb, which is in the expected size range for the full length sequence [35, 38, 66]. There is evidence to indicate that OSCs are glycosylated, although incubation of rat LS with *N*-glycosidase did not affect activity [34].

2.3.3 *Product Determination*

Comparison of the amino acid sequences of OSCs that generate sterols and triterpenoids reveals a number of residues in addition to the DCTAE and QW motifs that are highly conserved in all classes. These residues may be required to open up the epoxide ring of 2,3-oxidosqualene, a catalytic step that is common to all of these enzymes [46]. Amino acid residues that are conserved exclusively in sterol OSCs or in triterpenoid OSCs may be required for formation of the protosteryl or dammarenyl cations, respectively.

Point mutations that give altered sterol profiles have been generated in *A. thaliana* and *S. cerevisiae* LSs. Matsuda and co-workers used a yeast expression system to select for spontaneous mutations in *A. thaliana* CS that restored sterol-independent growth to an LS-deficient mutant of yeast [67]. In this way they were able to identify a mutation from isoleucine to valine (at Ile481) that allowed synthesis of the sterols lanosterol and parkeol. Further studies have identified a number of other amino acid residues in *A. thaliana* CS and

Table 3. Conserved amino acid motifs of 2,3-oxidosqualene cyclases

Organism	Enzyme	QW motif	QW motif	Substrate binding motif	QW motif	QW motif
Alicyclobacillus acidocaldarius	Squalene-hopene cyclase (SC)	..RAVEYLLSCQKDEGYW..	..MEKIRRYLLHEQREDGTW..	..YPDVCDTAVVVWA..	..RRAVEYLKREQKPDGSW..	..KALDWVEQHQNPDGGW..
Rattus norvegicus	Lanosterol synthase (LS)	..NGVTFYAKLQAEDGHW..	..REEMVRYLRSVQLPNGGW..	..WIVADCTAEALKA..	..NQGLDFCRKKQRADGSW..	..QACHFLLSRQMADGGW..
Homo sapiens	Lanosterol synthase (LS)	..NGMTFYVGLQAEDGHW..	..REEIVRYLRSVQLPDGGW..	..WIVSDCTAEALKA..	..TQGLEFCRRQQRADGSW..	..RACDFLLSRQMADGGW..
Panax ginseng	Cycloartenol synthase (PNX)	..RAMSFYSTLQAHDGHW..	..KREICRYLYNHQNRDGGW..	..WPISDCTAEGFKA..	..EKAALFIEKIQSSDGSW..	..KACDFLLSKQVASGGW..
Panax ginseng	β-Amyrin synthase (PNY)	..RAVHFFSALQASDGHW..	..RKEILRYIYCHQNEDGGW..	..WQVSDCTAEGLKC..	..TNAVRYLEDTQMPDGSW..	..KAVEFLLKSQMDDGGW..
Taraxacum officinale	Lupeol synthase (TRW)	..RAISFYSTIQAHDGHW..	..QLEIKRYIYNHQNEDGGW..	..WQVSDCTAEGLKV..	..SRAVKYVEDTQESDGSW..	..KACKFLLSKQLPDGGW..

Database accession numbers and the regions of amino acid sequences shown for each of the five motifs are as follows: *Alicyclobacillus acidocaldarius* SC (AB007002): amino acids 17–32, 61–78, 372–384, 469–485, 518–533; *Rattus norvegicus* LS (U31352): amino acids 80–95, 125–142, 452–464, 562–578, 615–630; *Homo sapiens* LS (HS225261): amino acids 79–94, 124–141, 451–463, 561–577, 614–629; *Panax ginseng* PNX (AB009029); amino acids 99–114, 147–164, 479–491, 590–606, 640–655; *Panax ginseng* PNY (AB009030): amino acids 102–117, 150–167, 481–493, 593–609, 643–658; *Taraxacum officinale* TRW (AB025345): amino acids 100–115, 148–165, 481–493, 592–608, 642–657.

also in yeast LS that when mutated result in altered ratios of sterol products [68, 69].

The OSCs that give rise to triterpenoids are clearly distinct from LS and CS enzymes (Fig. 3). The LuS enzymes from *O. europaea* (OEW) and *T. officinale* (TRW) both produce lupeol as the sole product when expressed in yeast [45]. Despite their disparate taxonomic origins, these enzymes share 78 % amino acid identity [45, 70]. The ATLUP1 LuS from *A. thaliana* [46] is less closely related to these two enzymes, and differs from them in its deprotonation mechanism [15, 70]. ATLUP1 is also less specific in the products that it generates, and produces β-amyrin and other minor triterpenoids in addition to lupeol [46, 47]. This has led to the suggestion that two groups of LuS genes have arisen during the evolution of higher plants [45]. However the triterpene cyclase ATLUP2, which shares high amino acid sequence relatedness to ATLUP1 (Fig. 3), synthesises β-amyrin and α-amyrin as major products in addition to lupeol [47, 48]. Thus the subgroup of OSCs that consists of ATLUP1 and ATLUP2 are multifunctional enzymes that are capable of generating a number of different triterpenoid products.

The *P. ginseng* βAS (PNY) and the *A. thaliana* LS (ATLUP1) cDNAs have been used to construct a series of chimeric proteins in order to investigate the regions of the enzymes that are important for product specificity [15]. The properties of the chimeric proteins were assessed following expression in yeast. These experiments identified an internal portion of the enzyme extending from approximately 25 – 50 % of the predicted amino acid sequence that was critical for β-amyrin formation. Interestingly, all of the chimeric enzymes were multifunctional, producing mainly β-amyrin and lupeol and also some other minor triterpenoids [15, 71]. Site-directed mutagenesis of the *P. ginseng* βAS PNY and the *O. europaea* LuS OEW has identified single amino acid residues that when mutated give interchanged product specificity [71]. Trp 259 of βAS is believed to control β-amyrin formation through stablization of the oleanyl cation, while the absence of cation stabilization with Leu in the equivalent position in LuS may result in termination of the reaction at the lupenyl cation stage. Mutation of a neighbouring tyrosine residue (Tyr261) that is conserved in all OSCs that produce pentacyclic triterpenoids to histidine, the corresponding residue in OSCs that produce tetracyclic carbon skeletons, resulted in synthesis of dammarenetype triterpenoids. Thus Tyr261 is proposed to play an important role in synthesis of pentacyclic triterpenoids by stabilising one of the cation intermediates generated after the dammarenyl cation [71].

It is clear that while some triterpenoid OSCs are highly specific in the products that they generate (such as the *P. ginseng* βAS enzymes [12, 14] and the LuS enzymes from *O. europaea* and *T. officinale* [45]), others are multifunctional and form a number of different products, at least in yeast [44, 46, 48, 49]. Although oleanane, lupane and dammarane skeletons are the most common triterpenoid structures associated with saponin biosynthesis, over 80 different oxidosqualene cyclase products are likely to be produced by plants [72]. The multifunctional properties of some triterpenoid OSCs and the fact that single amino acid changes can alter the nature of the product suggest that the structural diversity in nature may be generated by a core set of "flexible" enzymes. It is interesting to

note that, although DS enzymes have not yet been cloned from plants, mutations giving rise to a single amino acid change in other triterpenoid OSCs can confer the ability to synthesis dammarane-type triterpenoids [71].

2.4 Manipulation of Flux Through the Sterol and Triterpenoid Biosynthetic Pathways

Since OSCs are implicated in regulation of flux through the isoprenoid pathway leading to sterols and triterpenoids, manipulation of these enzyme activities may be expected to change the metabolic flow towards these two pathways [23, 24]. Several lines of evidence indicate that this is indeed the case. A number of studies have been carried out to investigate the effects of inhibitors of 2,3-oxidosqualene cyclases on sterol and triterpenoid synthesis. 8-Azadecalines bearing an isoprenoid-like N-substituent are excellent inhibitors of LS and CS, but do not inhibit βAS [73–76]. These inhibitors cause blocking of sterol biosynthesis at the level of CS, resulting in accumulation of β-amyrin at the expense of cycloartenol and methylene-24-cycloartenol.

Cell suspension cultures of *Gypsophila paniculata* and *Saponaria officinalis* produce very closely related triterpenoid saponins. Pretreatment of cell suspension cultures of *G. paniculata* with gypsogenin 3,*O*-glucuronide (a triterpenoid saponin precursor in *G. paniculata*) followed by administration of [^{14}C] acetate resulted in a marked reduction in incorporation of radioactivity into saponins and their precursors, but not into sterols and steryl glycosides [26]. Measurements of OSC activities revealed that there was no effect of elicitor treatment on CS levels in either species, but in *G. paniculata* βAS levels went down while in *S. officinalis* they increased. This suggests that in these two species OSCs are regulating steps in the isoprenoid pathway and control the flux to sterols and triterpenes.

In *Tabernaemontana divaricata* treatment of plant cell suspension cultures with an elicitor cause inhibition of CS activity [24, 25]. This response is accompanied by stimulation of activity of constitutive enzyme activities of the isoprenoid pathway leading to 2,3-oxidosqualene (squalene synthase and squalene oxidase), and induction of enzymes required for biosynthesis of pentacyclic triterpenoid phytoalexins (βAS and αAS). Thus inhibition of the branchpoint enzyme CS results in increased flux through the triterpenoid pathway.

Now that a number of cloned CS, LuS and βAS genes are available it will be possible to generate transgenic plants in which the levels of these enzymes have been manipulated. The effects of altering the levels of these different OSCs on sterol and triterpenoid synthesis can then be assessed.

3 Elaboration of the Aglycone

The synthesis of saponins from the cyclisation product of 2,3-oxidosqualene involves a series of additional modifications. These may include a variety of oxidation and substitution events, and the addition of sugars at different positions on the skeleton [9]. Very little is known about the enzymes required for these

elaborations. However, one common feature shared by all saponins is the presence of a sugar chain attached to the aglycone at the C-3 hydroxyl position. The sugar chains differ substantially between saponins but are often branched, and may consist of up to five sugar molecules (usually glucose, arabinose, glucuronic acid, xylose or rhamnose) [9]. An understanding of the glycosylation process (which is believed to be the terminal stage in saponin biosynthesis) is important, since the presence of the C-3 sugar chain is critical for the biological activity of many saponins [2–11]. Substantial progress has been made in the characterisation of saponin glycosyl transferases, and evidence has emerged to indicate that the oligosaccharide chains are likely to be synthesised by sequential addition of single sugar molecules to the aglycone [77–79]. The majority of this work has involved steroidal glycoalkaloids and steroids, and there has been relatively little emphasis on triterpenoid glycosylation by comparison. However these studies are likely to have implications for analysis of triterpenoid glycosylation, and so merit inclusion in this review. The developments in this general area are summarised below.

3.1 Saponin Glycosyltransferases

All plants contain membrane-bound uridine 5′-diphosphate (UDP)-glucose: sterol glucosyltransferases that are required for synthesis of steroidal glycosides. Steroidal glycosides are common components of cell membranes and may play important roles in the regulation of membrane structures. In addition to these sterol glycosyltransferases, a number of plants have also been shown to have glycosyltransferase activities that catalyse the addition of monosaccharides to saponin aglycone substrates ("sapogenins") (Table 4). These enzymes differ from the sterol glycosyltransferases in that they are soluble, their activity is inhibited by Triton X-100, and they are more sensitive to heavy metals such as Zn^{2+} and Hg^{2+} than their membrane-bound counterparts [77, 80–94].

Two sugar transferases that glycosylate steroidal alkaloid aglycones have been purified to homogeneity. These are a UDP-galactose:tomatidine galactosyltransferase from tomato [93] and a UDP-glucose:solanidine glucosyltransferase

Table 4. Saponin glycosyltransferase activities in plants

	Sapogenin	Sugar	Plant	References
Steroid	Nuatigenin	D-Glu	*Avena sativa*	81–83
	Sarsasapogenin	D-Glu	*Asparagus officinalis*	84
	Yamogenin	D-Glu	*Asparagus plumosus*	85
	Diosgenin	D-Glu	*Solanum melongena*	77, 86, 87
Steroidal alkaloid	Solasodine	D-Glu	*Solanum melongena*	86, 87
	Tomatidine	D-Gal	*Lycopersicon esculentum*	91–93
	Solanidine	D-Glu	*Solanum tuberosum*	80, 88–90
	Solanidine	D-Gal	*Solanum tuberosum*	80, 89, 90
Triterpenoid	Oleanolic acid	D-Glu	*Calendula officinalis*	78, 79

from potato [88], which are believed to initiate sugar chain formation during the synthesis of the steroidal glycoalkaloids α-tomatine and α-solanine, respectively. The cDNA encoding the UDP-glucose:solanidine glucosyltransferase (StSGT) has been isolated by expression in yeast [95]. StSGT is the first saponin glycosyltransferase to be cloned from plants. The predicted amino acid sequence of this enzyme contains a conserved UDP-binding domain in common with other plant UDP-glucosyltransferases [95, 96], and also a domain that shares similarity with steroid-specific UDP-glucuronosyltransferases from mammals [95].

Clearly enzymes that are capable of catalysing the addition of single sugars to sapogenins are common in plants (Table 4), although the relatedness between these various enzymes will not become clear until more glycosyltransferases have been purified and/or the relevant genes cloned. The challenge will then be to characterise the other sugar transferase enzymes required for the subsequent glycosylation steps that give rise to the oligosaccharide chains that are typical of saponins. Although enzyme activities that transfer single sugars can be assayed in vitro, the possibility that in plants the oligosaccharide chains may be transferred intact to the aglycone should also be considered.

4 Conclusions

This review has addressed recent advances in two key areas of saponin biosynthesis, namely the cyclisation of 2,3-oxidosqualene and the glycosylation of sapogenins. Good progress has been made in cloning and characterising OSCs and in the elucidation of amino acids that are important for enzyme activity and product specificity; OSCs with altered properties have been generated by construction of chimeric enzymes [15], by targeted mutation of critical amino acid residues [27, 46, 57 – 64, 71] and also by the selection of spontaneous mutants in yeast [67]. Further advances in this area will give a comprehensive insight into the mechanistic enzymology and evolution of this fascinating superfamily of enzymes, and will enable the development of new enzymes that generate novel products by "accelerated evolution". Furthermore, the cloned sterol and triterpenoid OSCs can now be used to generate transgenic plants with altered levels of these cyclase activities (by overexpression or gene silencing). This will establish whether cyclisation of 2,3-oxidosqualene is a rate-limiting step for sterol and triterpenoid biosynthesis, and will enable the effects of manipulation of the different cyclase levels on the flux through these pathways to be investigated.

The synthesis of triterpenoid saponins from the skeletons shown in Fig. 2 involves a series of further modifications that may include a variety of different oxidation and substitution events [9]. Very little is known about the enzymes and genes involved in the elaboration of the triterpenoid skeleton, although genetic and biochemical analysis of saponin-deficient mutants of plants is likely to accelerate the dissection of these processes [16]. Progress has been made in the characterisation of saponin glucosyltransferases (primarily for steroidal and steroidal alkaloid saponins), and the first of these enzymes (StSGT from potato) has been cloned. Since glycosylation at the C-3 hydroxyl position confers am-

phipathic properties on the molecule and is normally critical for biological activity [2–11], this is clearly an important area in which to invest effort in the future.

Acknowledgement. The Sainsbury Laboratory is supported by the Gatbsy Charitable Foundation, and the support of Dupont is also gratefully acknowledged.

References

1. Wink M (1999) Functions of plant secondary metabolites and their exploitation in biotechnology, Sheffield Academic Press, Sheffield
2. Tschesche R (1971) Advances in the chemistry of antibiotic substances from higher plants. In: Wagner H, Hörhammer L (eds) Pharmacognosy and phytochemistry. Springer, Berlin Heidelberg New York, p 274
3. Schönbeck F, Schlösser E (1976) Preformed substances as potential phytoprotectants. In: Heitefuss R, Williams PH (eds) Physiological plant pathology. Springer, Berlin Heidelberg New York, p 653
4. Osbourn AE (1996) Plant Cell 8:1821
5. Morrissey JP, Osbourn AE (1999) Microbiol Mol Biol Revs 63:708
6. Price KR, Johnson IT, Fenwick GR (1987) CRC Crit Rev Food Sci Nutr 26:27
7. Hostettmann K, Hostettmann M, Marston M (1991) Methods Plant Biochem 7:434
8. Fenwick GR, Price KR, Tsukamota C, Okubo K (1992) Saponins. In: D'Mello JP, Duffus CM, Duffus JH (eds) Toxic substances in crop plants. The Royal Society of Chemistry, Cambridge, UK, p 284
9. Hostettmann KA, Marston A (1995) Saponins. Chemistry and pharmacology of natural products. Cambridge University Press, Cambridge, UK
10. Roddick JG (1974) Phytochemistry 13:9
11. Osbourn AE (1996) Trends Plant Sci 1:4
12. Kushiro T, Shibuya M, Ebizuka Y (1998) Eur J Biochem 256:238
13. Kushiro T, Ohno Y, Shibuya M, Ebizuka Y (1997) Biol Pharm Bull 20:292
14. Kushiro T, Shibuya M, Ebizuka Y (1998) Molecular cloning of oxidosqualene cyclase cDNA from *Panax ginseng*: the isogene that encodes β-amyrin synthase. In: Ageta H, Aimi N, Ebizuka Y, Fujita T, Honda G (eds) Towards natural medicine research in the 21st century. Elsevier Science, Amsterdam, p 421
15. Kushiro T, Shibuya M, Ebizuka Y (1999) J Am Chem Soc 121:1208
16. Papadopoulou K, Melton RE, Leggett M, Daniels MJ, Osbourn AE (1999) Proc Natl Acad Sci USA 96:12,923
17. Ruzicka L, Eschenmoser A, Heusser H (1953) Experientia 357
18. Eschenmoser A, Ruzicka L, Jeger O, Arigoni D (1955) Helv Chem Acta 38:1890
19. Nes WR, McKean ML (1977) Biochemistry of steroids and other isoprenoids. University Park Press, Baltimore
20. Abe I, Rohmer M, Prestwich GD (1993) Chem Rev 93:2189
21. Jolidon S, Polak AM, Guerry P, Hartmann PG (1990) Biochem Soc Trans 18:47
22. Cattel L, Ceruti M, Viola F, Delprino L, Balliano G, Duriatti A, Bouvier-Navé P (1986) Lipids 21:31
23. Baisted DJ (1971) Biochem J 124:375
24. Threlfall DR, Whitehead IM (1990) Redirection of terpenoid biosynthesis in elicitor-treated plant cell suspension cultures. In: Quinn PJ, Harwood JL (eds) Plant lipid biochemistry. Portland Press, London, p 344
25. Van der Deijden R, Threlfall DR, Verpoorte R, Whitehead IM (1989) Phytochemistry 28:2981
26. Henry M, Rahier A, Taton M (1992) Phytochemistry 31:3855
27. Abe I, Sankawa U, Ebizuka Y (1992) Chem Pharm Bull 40:1755

28. Goad LJ (1983) Biochem Soc Trans 548
29. Palmer MA, Bowden BN (1977) Phytochemistry 16:459
30. Abe I, Ebizuka Y, Sankawa U (1988) Chem Pharm Bull 36:5031
31. Abe I, Sankawa U, Ebizuka Y (1989) Chem Pharm Bull 37:536
32. Abe I, Ebizuka Y, Seo S, Sankawa U (1989) FEBS Letts 249:100
33. Buntel CJ, Griffin JH (1994) ACS Sym Ser 562:44
34. Abe I, Prestwich GD (1995) Proc Natl Acad Sci 92:9274
35. Kusano M, Shibuya M, Sankawa U, Ebizuka Y (1995) Biol Pharm Bull 18:195
36. Shi Z, Buntel CJ, Griffin JH (1994) Proc Natl Acad Sci 91:7370
37. Kelly R, Miller SM, Lai MH, Kirsch DR (1990) Gene 87:177
38. Roessner CA, Min C, Hardin SH, Harris-Haller LW, McCollum JC, Scott AL (1993) Gene 127:149
39. Corey EJ, Matsuda SPT, Bartel B (1993) Proc Natl Acad Sci 90:11,628
40. Sung CK, Shibuya M, Sankawa U, Ebizuka Y (1995) Biol Pharm Bull 18:1459
41. Corey EJ, Matsuda SPT, Bartel B (1994) Proc Natl Acad Sci USA 91:2211
42. Morita M, Shibuya M, Lee M-S, Sankawa U, Ebizuka Y (1997) Biol Pharm Bull 20:770
43. Venkatramesh M, Nes WD (1995) Arch Biochem Biophys 324:189
44. Morita M, Shibuya M, Kushiro T, Masuda K, Ebizuka Y (2000) Eur J Biochem 267:3453
45. Shibuya M, Zhang H, Endo A, Shishikura K, Kushiro T, Ebizuka Y (1999) Eur J Biochem 266:302
46. Herrera JBR, Bartel B, Wilson WK, Matsuda SPT (1998) Phytochemistry 49:1905
47. Husselstein-Muller T, Schaller H, Benveniste P (2001) Plant Mol Biol 45:63
48. Kushiro T, Shibuya M, Masuda K, Ebizuka Y (2000) Tetrahedron Letts 41:7705
49. Segura MJR, Meyer MM, Matsuda SPT (2000) Org Letts 2:2257
50. Felsenstein J (1996) Methods Enzymol 266:418
51. Ourisson G, Rohmer M, Poralla K (1987) Ann Rev Microbiol 41:301
52. Perzl M, Müller P, Poralla K, Kannenberg EL (1997) Microbiology 143:1235
53. Reipen IG, Poralla K, Sahm H, Sprenger GA (1995) Microbiology 141:155
54. Ochs D, Kaletta C, Entian K-D, Beck-Sickinger A, Poralla K (1992) J Bact 174:298
55. Wendt KU, Poralla K, Schultz GE (1997) Science 277:1811
56. Wendt KU, Lenhart A, Schulz GE (1999) J Mol Biol 286:175
57. Abe I, Prestwich GD (1994) J Biol Chem 269:802
58. Abe I, Prestwich GD (1995) Lipids 30:231
59. Feil C, Sussmuth R, Jung G, Poralla K (1996) Eur J Biochem 242:51
60. Corey EJ, Cheng H, Baker H, Matsuda SPT, Li D, Song X (1997) J Am Chem Soc 119:1277
61. Dang T, Prestwich GD (2000) Chem Biol 7:643
62. Poralla K, Hewelt A, Prestwich GD, Abe I, Reipen I, Sprenger G (1994) TIBS 19:157
63. Sato T, Kanai Y, Hoshino T (1998) Biosci Biotech Biochem 62:407
64. Poralla K (1994) Bioorg Med Chem Lett 4:285
65. Corey EJ, Matsuda SPT (1991) J Am Chem Soc 113:8172
66. Hayashi H, Hiraoka N, Ikeshiro Y, Kushiro T, Morita M, Shibuya M, Ebizuka Y (2000) Biol Pharm Bull 23:231
67. Hart EA, Hua L, Darr LB, Wilson WK, Pang J, Matsuda SPT (1999) J Am Chem Soc 121:9887
68. Herrera JBR, Wilson WK, Matsuda SPT (2000) J Am Chem Soc 122:6765
69. Meyer MM, Segura MJR, Wilson WK, Matsuda SPT (2000) Angew Chem Int Ed 39:4090
70. Kushiro T, Shibuya M, Ebizuka Y (1999) Tet Lett 40:5553
71. Kushiro T, Shibuya M, Masuda K, Ebizuka Y (2000) J Am Chem Soc 122:6816
72. Matsuda SPT (1998) In: Steinbüchel A (ed) Biochemical principles and mechanisms of biosynthesis and degradation of polymers. Wiley-VCH, Weinheim, p 300
73. Taton M, Benveniste P, Rahier A (1992) Biochemistry 31:7892
74. Taton M, Benveniste P, Rahier A (1986) Biochem Biophys Res Comm 138:764
75. Cattel L, Ceruti M (1992) 2,3-Oxidosqualene cyclase and squalene epoxidase: enzymology, mechanism and inhibitors. In: Patterson GW, Nes WD (eds) Physiology and biochemistry of sterols. American Oil Chemists' Society, Champaign, p 50
76. Taton M, Ceruti M, Cattel L, Rahier A (1996) Phytochemistry 43:75

77. Paczkowski C, Wojciechowski ZA (1994) Phytochemistry 35:1429
78. Kintia PK, Wojciechowski Z, Kasprzyk Z (1974) Bulletin de L'Académie Polonaise des Sciences 22:73
79. Wojciechowski ZA (1975) Phytochemistry 14:1749
80. Bergenstråhle A, Tillberg E, Jonsson L (1992) Plant Sci 84:35
81. Kalinowska M, Wojciechowski ZA (1986) Phytochemistry 25:2525
82. Kalinowska M, Wojciechowski ZA (1987) Phytochemistry 26:353
83. Kalinowska M, Wojciechowski ZA (1988) Plant Science 55:239
84. Paczkowski C, Wojciechowski ZA (1988) Phytochemistry 27:2743
85. Paczkowski C, Zimowski J, Krawczyk D, Wojciechowski ZA (1990) Phytochemistry 29:63
86. Paczkowski C, Kalinowska M, Wojciechowski ZA (1997) Acta Biochimica Polonica 44:43
87. Paczkowski C, Kalinowska M, Wojciechowski ZA (1998) Phytochemistry 48:1151
88. Stapleton A, Allen PV, Friedman M, Belknap WR (1991) J Agric Food Chem 39:1187
89. Zimowski J (1991) Phytochemistry 30:1827
90. Zimowski J (1992) Phytochemistry 31:2977
91. Zimowski J (1996) Enzymatic glycosylation of tomatidine in tomato plants. In: Waller GR, Yamasaki K (eds) Saponins used in traditional and modern medicine. Plenum Press, New York, p 71
92. Kalinowska M (1994) Phytochemistry 36:617
93. Zimowski J (1994) Acta Biochimica Polonica 41:202
94. Zimowski J (1998) Plant Sci 136:139
95. Moehs CP, Allen PV, Friedman M, Belknap WR (1997) Plant J 11:227
96. Vogt T, Jones P (2000) Trends Plant Sci 5:380

Received: June 2001

Three-Phase Oxygen Absorption and its Effect on Fermentation

E. Nagy

Kaposvar University, Research Institute of Chemical and Process Engineering, Veszprém, Egyetem ut 2. 8200, Hungary, e-mail: nagy@mukki.richem.hu

The absorption rate of oxygen in the presence of a second, dispersed, organic phase can be significantly increased due to the higher solubility and diffusivity of oxygen in the organic phase. The oxygen supply of micro-organisms, which is very often a limiting factor during fermentation, can be improved, and the critical level of oxygen in the fermentation broth can be avoided by using dispersed organic phase. This paper reviews the models of the enhanced absorption rates and their integration into mass balance equations of fermentation. Several calculations were carried out to illustrate the effect of the dispersed organic phase and kinetic parameters on the absorption rates and on fermentation with double-substrate-limitation kinetics applying batch and continuous operation modes. Using software taking from the literature, the effect of the organic phase on the baker's yeast production is also presented in fed-batch mode.

Keywords. Oxygen absorption, Three-phase mass transfer, Dispersed phase, Heterogeneous model, Fermentation, Bulk oxygen concentration

1 Introduction 53

2 Oxygen Absorption Rate – The Effect of a Dispersed Organic Phase 54

2.1 Heterogeneous Mass Transfer Models 55
2.1.1 One Cubic Particle in the Diffusion Path 56
2.1.1.1 Zero-Order Chemical Reaction 58
2.1.1.2 First-Order Chemical Reaction 59
2.1.2 Number of Cubic Particles in the Diffusion Path 59
2.1.3 Spherical Particles in the Diffusion Path 60
2.1.4 Effect of the Kinetic Parameters 62
2.1.5 Effect of Chemical Reactions 65
2.1.6 Verification of the Model Results 66
2.2 Fermentation with an Enhanced Absorption Rate of Oxygen . . . 67
2.2.1 Integrated Model of Fermentation 69
2.2.1.1 Simulation of a Batch Stirred Tank Reactor 70
2.2.1.2 Simulation of a Continuous Stirred Tank Reactor 74
2.3 Baker's Yeast Production 75

3 Concluding Remarks 78

References 79

Advances in Biochemical Engineering/
Biotechnology, Vol. 75
Managing Editor: Th. Scheper
© Springer-Verlag Berlin Heidelberg 2002

List of Symbols and Abbreviations

a	specific interfacial area, $m^2\,m^{-3}$
d	size of cubic particles, m
d_p	size of spherical droplets, m
D	diffusion coefficient, $m^2\,s^{-1}$
D_r	$= D/D_d$
$\overline{D}$	dilution rate ($= F_L/V$), h^{-1}
E	enhancement factor due to presence of droplets defined by Eq. 7.
E_{loc}	local enhancement of the absorption rate
F	volumetric flow rate, $m^3\,h^{-1}$
H	solubility (partition) coefficient of oxygen between continuous phase and dispersed one ($= O_d/O$)
i	i-th number of particle in the diffusion path of the boundary layer
j	mass transfer rate for the heterogeneous part of interface, $mol\,m^{-2}\,s^{-1}$
J	mass transfer rate without dispersed phase, $mol\,m^{-2}\,s^{-1}$
J_{het}	absorption rate related to the total interface obtained by heterogeneous model, $mol\,m^{-2}\,s^{-1}$
J^*_{het}	average absorption rate related to the total interface, $mol\,m^{-2}\,s^{-1}$ (Eq. 24, 25)
k^o	physical mass transfer coefficient without dispersed phase, $m\,s^{-1}$
k_1	first-order external reaction rate constant, s^{-1}
k_0	zero-order reaction rate constant, $mol\,m^{-3}\,s^{-1}$
K_O	saturation constant in Monod-type kinetics for oxygen, $kg\,m^{-3}$
K_S	Michaelis-Menten coefficient, $kg\,m^{-3}$
M	reaction-diffusion modulus for zero- and first-order reactions (see Eq. 11, 13)
N	total number of particles in the boundary layer perpendicular to the gas-liquid interface
$\underline{O}$	concentration of oxygen in liquid boundary layer, $mol\,m^{-3}$
$\overline{O}$	Laplace transform of concentration O, $mol\,s\,m^{-3}$
O*	concentration of oxygen at gas-liquid interface in the liquid phase, at $x = 0$, $mol\,m^{-3}$
O_L	oxygen concentration in the bulk of liquid phase, $mol\,m^{-3}$
O_L % sat	$= 100\,O_L O^{*-1}$, % sat
$O_{L,in}$	inlet concentration of oxygen, $mol\,m^{-3}$
p	dimensionless parameter defined after Eq. 13
Q	source term, $mol\,m^{-3}s^{-1}$
R	particle radius, m
R*	radius as space coordinate (see Fig. 2), m
R′*	$= R^*/R$
s	surface renewal frequency, s^{-1}
s_0	dimensionless time for the boundary layer at the gas-liquid interface (see Eq. 11)
s_d	dimensionless time for particles in the boundary layer (see Eq. 11)
S	substrate concentration, $kg\,m^{-3}$

t	time, s
T_Δ	differential surface element at the gas-liquid interface, m^2
V	reactor volume, m^3
x	space co-ordinate perpendicular to the gas-liquid interface, m
X	biomass concentration, kg m^{-3}
y	space co-ordinate, m
$Y_{X/S}$	yield coefficient for S → X, kg kg^{-1}
$Y_{X/O}$	yield coefficient for O → X, kg kg^{-1}
z	space co-ordinate, m
β^o	physical mass transfer coefficient in the presence of droplets, m s^{-1}
$\beta^{o,ave}$	averaged value of β^o over the spherical interface using Eq. 23, m s^{-1}
β	mass transfer coefficient with chemical reaction in presence of particles, m s^{-1}
β^{ave}	averaged value of β over spherical interface obtained by Eq. 23, m s^{-1}
$\beta(R^*)$	mass transfer coefficient at a T_Δ surface element, m s^{-1}
δ	penetration depth of oxygen or thickness of the boundary layer, m
δ_0	distance of the first particle from the gas-liquid interface, m
δ_p	distance between two spheres, m
ε	dispersed phase holdup
κ	the change of diffusion distance due to curvature, m
λ	dimensionless parameter given according to Eq. 13
λ_p	dimensionless parameter according to Eqs. 15 – 18., -
μ	specific growth rate, h^{-1}
g	gas
L	liquid
d	dispersed phase
in	inlet

1 Introduction

In industrial fermentation processes, increases in productivity are frequently limited by the transport of a substrate or byproduct. Oxygen is a sparingly soluble substrate whose transport can be a critical factor in aerobic cultures. As long as the oxygen transfer rate to the broth exceeds the rate of oxygen utilization by the cells, cell growth continues at an exponential rate when other nutrients are not limiting. At a certain critical cell concentration, oxygen can no longer be supplied to the broth fast enough to meet the oxygen demand. Under these conditions, oxygen becomes the limiting nutrient for cell growth. This fact often results in reduced growth and culture productivity [1 – 3].

Various techniques used in conventional bioreactors to improve the rate of oxygen transfer from the gas phase include increasing the agitation or aeration rates, modifying the vessel design [2, 4, 5] or raising the partial pressure of oxygen in the gas phase [6, 7]. For a specific fermenter operating pressure, these latter remedies can provide up to a five-fold increase in the concentration driving force. However, the high levels of mixing often create disadvantageous environments for cells sensitive to mechanical stress.

Non-conventional methods reported for improving oxygen supply include oxygen generation in situ with hydrogen peroxide/catalase system [8, 9] or adding hydrogen peroxide to the medium and using an organism with a high natural catalase activity [10]. A biological approach to in situ oxygen generation would be to co-immobilize oxygen-consuming organisms with oxygen-producing organisms such as the alga *Chlorella pyrenoidosa* [11]. Dihydroxiacetone productivity was enhanced 4–5-fold compared with a pure culture. However, the oxygen production is limited and co-immobilization may cause inhibition or competition for the substrate.

Another way of increasing the oxygen supply would be to modify the medium so that it could carry more oxygen. This new aeration strategy consists of the addition to the growth medium of a compound or a second, water-immiscible phase in which oxygen has a high solubility [1, 12–20]. Examples of this phase include hydrocarbons [12, 17–18, 23, 26], hemoglobin [15], perfluorocarbons [1, 13, 14, 19, 25], soybean oil [20], olive oil [24] and silicone oils [16, 21]. The organic phase is usually simply emulsified in the fermentation broth by mechanical agitation (or ultrasonic treatment) and stabilized with surfactants. Depending on the mass transfer kinetic parameters – diffusivity, solubility, surface renewal frequency, droplet size, dispersed phase hold-up, etc. – the oxygen uptake rate can substantially be increased: the enhancements were 3.5-fold using *n*-dodecane [17], 3–4-fold using perfluorocarbon [1] and 4–5-fold using silicone oil [21]. This supplementary oxygen supply can increase the oxygen concentration far above its critical value in the fermentation broth and, as a consequence, it can improve the bioreactor productivity. However, the second dispersed phase can cause additional effects, for example, toxicity, which must not be left out of consideration.

The purpose of the present paper is to review the results of the oxygen absorption enhancement in the presence of a second, dispersed organic phase and to analyze the effect of enhancement on the bulk oxygen concentration, and its effect on fermentation processes.

2
Oxygen Absorption Rate – The Effect of a Dispersed Organic Phase

The presence of fine solid particles or a finely dispersed second liquid phase in the continuous absorbent phase can have a very strong effect on the mass transfer rate between the gas and the continuous phases. The mass transport into the solid particles or liquid drops can essentially alter the concentration gradient and, consequently, the absorption rate [27–36]. The qualitative explanation of this phenomenon is that the particle absorbs oxygen in the oxygen-rich hydrodynamic mass transfer film, after which, desorption of oxygen takes place in the oxygen-poor bulk of the liquid.

In order to estimate the real effect of a dispersed organic phase on the productivity of fermentation, the oxygen absorption rate has to be defined. Knowing its mathematical expression, the rate equation can then be incorporated into the differential mass balance equations of fermentation and, after solving these equations, the concentration of components in a fermentation

broth can be predicted. For describing the phenomenon of gas absorption in the presence of dispersed phase particles in the mass transfer zone, several approximation models have been developed. The first models developed were the homogeneous models using the penetration theory [37–39] or the film-penetration theory [40]. The most important assumption of these models is that the particle size of the discontinuous phase must be much smaller than the so-called liquid film thickness at the gas-liquid interface. For gas absorption in aqueous media in an intensely agitated contactor, a typical value for the „film" thickness is ≈ 10 – 25 µm. This is the case when a micellar microphase is the dispersed phase [38]. This assumption can also be fulfilled when solid particles are the discontinuous phase [27, 30 – 34]. However, the droplet size of a simple emulsified phase, that is the case in fermentation when a simply dispersed organic phase is used, is mostly larger than 10 – 15 µm, thus the assumption for the homogeneous model is no longer fulfilled. Namely, in this case, the particle size can be somewhat less than, equal to, or even larger than the film thickness. For that particle size range ($d_p \approx > 5 – 7$ µm), the mass transport at the gas-liquid interface can only be described by heterogeneous models.

2.1 Heterogeneous Mass Transfer Models

The essential difference between the homogeneous model and the heterogeneous one is that the latter model takes into account the fact that the diffusion of the absorbed component alternately occurs through continuous- and dispersed phases in the liquid boundary layer at the gas-liquid interface. The mass transport through this heterogeneous phase is a nonlinear process, one can get explicit mathematical expression for the absorption rate only after its simplification.

Pioneering work in developing heterogeneous, 3-dimensional models was done by Holstvoogd et al. [30] and Karve and Juvekar [41]. Both developed steady-state models for the description of gas absorption in slurry systems with fast, irreversible chemical reaction at the solid surface. These models are, however, not very suitable for absorption in liquid-liquid systems because they do not allow for diffusion through the dispersed phase. Recently Brilman [42] and Brilman et al. [43] developed a one-dimensional instationary, multiparticle mass transfer model for gas absorption in multiphase systems. The one-dimensional model takes into account the diffusion perpendicular to the gas-liquid interface. With this model the influence of several system parameters was studied. It was found that only those particles located close to the gas-liquid interface determine the mass transfer rate. For these particles the distance of the first particle to the gas-liquid interface and the particle capacity turned out to be the most important parameters. Lin et al. [44] proposed a new axisymmetrical two-dimensional heterogeneous mass transfer model. The model accounts for droplet–droplet and droplet–film interaction. The finite-difference technique was used to solve the model equations. The effects of dispersed holdup, droplet size, partition coefficient and chemical reactions on mass transfer enhancement have been discussed. Very recently, Brilman et al. [54] published simulation data

using both two- and three-dimensional mass transfer models. They investigated the concentration distribution inside and around the particles. It was also shown how the particles alter the enhancement of the neighboring particles using different configurations.

The non-linear models above have numerical solutions only. In order to get an analytical solution to this problem, the mass transport process must be simplified. Unsteady, one-dimensional, heterogeneous, one-particle models (only one particle is located in the diffusion path, perpendicular to the interface, in the boundary layer at the gas-liquid interface) were developed by Junker et al. [45] and Nagy [46]. Junker et al. [45] studied the oxygen transfer rate in aqueous/perfluorocarbon fermentation solutions and suggested a semi-infinite composite model for the case when the droplet size is larger than the laminar boundary layer thickness. For geometric convenience, the spherical, uniform size droplets are modeled as cubic ones of identical volume, thus $d = d_p(\pi/6)^{1/3}$ (Fig. 1). The boundary layer at the gas-liquid interface was assumed to consist of both the continuous and discontinuous phases. In regions were the droplets are located in the boundary layer, oxygen passes first from the gas phase to the continuous phase and thereafter through the discontinuous phase. The one-dimensional composite model using the penetration theory can be regarded as a first approach to getting an analytical solution for the enhancement, where the particle size is larger than the thickness of the boundary layer. Nagy [46] developed a more general, one-particle, heterogeneous model that can be used for the whole particles size range, where the homogeneous model is no longer valid (i. e. when the particle size is somewhat less than or equal to δ, or even when $d_p > \delta$). The mass transfer may be accompanied by a zero- or first-order chemical reaction in both the continuous and the dispersed liquid phases.

2.1.1
One Cubic Particle in the Diffusion Path

Figure 1 illustrates the physical mass transfer model for this situation (see the upper cubic particle where $d<\delta$. There are two parts of the gas-liquid interface:

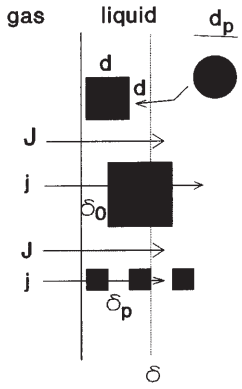

Fig. 1. Physical model of the gas-liquid boundary layer with cubic particles

heterogeneous- and the homogeneous parts. In the former case the absorbed component diffuses through a particle into the bulk phase. This heterogeneous part of the boundary layer consists of three segments, namely, two continuous phase segments (segments between 0 and δ_0 as well between δ_0+d and the inner edge of the boundary layer, that is δ in Fig. 1) and a dispersed phase one, i. e. distance between δ_0 and d. The differential mass balance equations have to be given for every three segment in order to get the absorption rate.

The following assumptions were made for modeling the mass transport:

- the diffusion path is perpendicular to the gas-liquid interface;
- the particles are similar in size, and their distribution in the bulk phase is regular with respect to spacing and arrangement; the distance between them is the same in each space variable and this can be calculated from their size and dispersed volume fraction ε, using Eq. 1.

$$\delta_p = d\left(\frac{1}{\varepsilon^{1/3}} - 1\right) \tag{1}$$

- the distance of the particle from the interface in the x-direction, δ_0 -this space coordinate is perpendicular to the gas-liquid interface-, can, in principle, be varied between 0 and δ_p;
- the surface renewal theory is used to describe the mass transport;
- the absorption rate for the homogeneous part of the interface, J – where there is no particle in the diffusion path (see Fig. 1) – can be given by the well known mass transfer theories [60];
- the mass transport can be accompanied by a zero- or first-order chemical reactions in the continuous phase.

The set of differential mass balance equations for the heterogeneous part of the boundary layer can be given by Eq. 2 and 3 [46]:

For the continuous phase, i. e. for $0 \le x \le \delta_0$ and for $\delta_0 + d \le x < \infty$

$$D\frac{\partial^2 O}{\partial x^2} - Q = \frac{\partial O}{\partial t} \tag{2}$$

For the dispersed phase, i. e. for $\delta_0 \le x \le \delta_0 + d$:

$$D_d\frac{\partial^2 O_d}{\partial x^2} = \frac{\partial O_d}{\partial t} \tag{3}$$

The initial and boundary conditions at the gas liquid interface ($x = 0$), at the liquid-liquid interfaces ($x = \delta_0$ and $x = \delta_0 + d$) and $x \to \infty$ are the following:

$$\begin{aligned}
&\text{if } t = 0 && x > 0 && \text{then } O = O_L\\
&\text{if } t > 0 && x = 0 && \text{then } O = O^*\\
&\text{if } t > 0 \;\; x = \delta_0 \text{ and } && x = \delta_0 + d && \text{then } O_d = HO\\
&\text{if } t = 0 \;\; x = \delta_0 \text{ and } && x = \delta_0 + d && \text{then } D\frac{\partial O}{\partial x} = D_d\frac{\partial O_d}{\partial x}\\
&\text{if } t > 0 \;\; x \to \infty && && \text{then } O = O_L
\end{aligned} \tag{4}$$

The set of differential Eq. 2 and 3 can be solved analytically by means of Laplace transform in the cases of a zero- and first-order chemical reactions. The time-average value of the mass transfer rate, j, can be obtained by Eq. 5 [47]:

$$j = \int_0^\infty j(t)\, s \exp(-st)\, dt = -Ds \left.\frac{d\overline{O}}{dx}\right|_{x=0} \tag{5}$$

Knowing the absorption rate for the heterogeneous- and the homogeneous part of the interface, the specific absorption rate related to the total interface can be expressed as follows:

$$J_{het} = j\varepsilon^{2/3} + J(1 - \varepsilon^{2/3}) \tag{6}$$

The enhancement of the absorption, related the absorption rate to that obtained without dispersed phase, can then be obtained as follows:

$$E = \frac{J_{het}}{J} = \frac{j}{J}\varepsilon^{2/3} + (1 - \varepsilon^{2/3}) \tag{7}$$

The J value denotes the absorption rate without the dispersed phase where the mass transfer rate can be accompanied by zero- or first-order chemical reactions in the continuous phase. These are well-known equations: $J = k^o(O^* + M^2 - O_L)$ and $J = k^o(1 + M^2)^{1/2}(O^* - O_L/(1 + M^2))$ for zero- and first-order reactions, respectively [60].

2.1.1.1
Zero-Order Chemical Reaction ($Q = k_0$)

Substituting the reaction rate, Q, into Eq. 2, the general solution of the Laplace transformed concentration can be given for each differential equation as follows:

$$\overline{O} = F_i \exp\left(\frac{\lambda x}{\delta_0}\right) + F_{i+1} \exp\left(\frac{\lambda x}{\delta_0}\right) \tag{8}$$

The parameter values F_i and F_{i+1} (i denotes ith differential equation from the above three differential equations; altogether we have 6 parameter) can be obtained by replacing the initial and boundary conditions (Eq. 4) in these equations. The absorption rate for the composite medium can be given by Eq. 9 [46]:

$$j = \beta^o(O^* - O_L + O^*M^2\langle 1 - T\rangle) \tag{9}$$

where

$$\beta^o = k^o \frac{\tanh s_0 \left\langle \frac{H}{\sqrt{D_r}} + \tanh s_d \right\rangle + \frac{H}{\sqrt{D_r}} \left\langle 1 + \frac{H}{\sqrt{D_r}} \tanh s_d \right\rangle}{\tanh s_d + \frac{H}{\sqrt{D_r}} \left\langle 1 + \tanh s_0 + \frac{H}{\sqrt{D_r}} \tanh s_0 \tanh s_d \right\rangle} \tag{10}$$

and

$$T = \frac{\frac{H}{\sqrt{D_r}} \tanh s_d + 1 - \frac{1}{\cosh s_d}}{\cosh s_0 \left\langle \tanh s_0 \left[\frac{H}{\sqrt{D_r}} + \tanh s_d \right] + \frac{H}{\sqrt{D_r}} \left[1 + \frac{H}{\sqrt{D_r}} \tanh s_d \right] \right\rangle} \tag{11}$$

The dimensionless parameters in these equations are:

$$s_d = \sqrt{\frac{sd^2}{D_d}};\ s_0 = \sqrt{\frac{s\delta_0^2}{D}};\ M = \frac{\sqrt{\frac{k_0 D}{O^*}}}{k^\circ};\ D_r = \frac{D}{D_d}$$

2.1.1.2 First-Order Chemical Reaction ($Q = k_1 O$)

Substituting the reaction rate, Q, into Eq. 2 and after Laplace transformation, the equations obtained can be solved again by standard methods. The mass transfer rate for the heterogeneous part of the interface can be given as follows:

$$j = \beta \left(O^* - \frac{O_L}{1 + M^2} \right) \tag{12}$$

where

$$\beta = k^\circ \sqrt{1 + M^2} \frac{\tanh \lambda \langle p + \tanh s_d \rangle + p \langle 1 + p \tanh s_d \rangle}{\tanh s_d + p \langle 1 + \tanh \lambda + p \tanh \lambda \tanh s_d \rangle} \tag{13}$$

with the following dimensionless parameters:

$$\lambda = s_0 \sqrt{1 + M^2};\ p = \frac{H}{\sqrt{D_r (1 + M^2)}};\ M = \frac{\sqrt{k_1 D}}{k^\circ}$$

The mass transfer rates for the case when $d > \delta$ can easily be obtained from Eqs. 9 or 12 (see [48]). Using the surface renewal theory this case is not relevant because the boundary layer thickness is here considered to be infinite.

2.1.2 *Number of Cubic Particles in the Diffusion Path*

Brilman et al. [42] and Lin et al. [44] using a numerical method, Nagy [48] by using an analytical method, investigated the effect of the second, third, etc. particles (perpendicular to the gas-liquid interface) on the absorption rate. They obtained that, in most cases, the first particle determines the absorption rate. However, in special cases, the effect of these particles can also be important. Nagy solved the mass transfer problem analytically for the number of particles in the diffusion path [48]. For the sake of completeness we will give the absorption rate for that case, as well (for details see [48]). The mass transfer is accompanied here by a first-order chemical reaction. This situation is illustrated in Fig. 1 where three particles are located behind each other. The absorption rate

can be given by Eq. 12, where the mass transfer coefficient, β, can be expressed as follows:

$$\beta = k^{\circ} \frac{\sqrt{1 + M^2}}{\cosh \lambda} \frac{n_2^N - n_1^N}{n_0^N} \tag{14}$$

with for $1 \le i \le N-1$

$$n_f^i = n_f^{i-1} \langle 1 + p \tanh \lambda_p \tanh s_d \rangle + m_f^{i-1} \left\langle \tanh \lambda_d + \frac{1}{p} \tanh s_d \right\rangle \quad f = 0,1,2 \tag{15}$$

$$m_f^i = n_f^{i-1} \langle \tanh \lambda_p + p \tanh s_d \rangle + m_f^{i-1} \left\langle 1 + \frac{1}{p} \tanh \lambda_d \tanh s_d \right\rangle \quad f = 0,1,2 \tag{16}$$

and for $i = N$

$$n_f^N = n_f^{N-1} \langle 1 + p \tanh \lambda_p \tanh s_d \rangle + m_f^{N-1} \left\langle 1 + \frac{1}{p} \tanh \lambda_d \tanh s_d \right\rangle \quad f = 0,1,2 \tag{17}$$

$$m_f^N = n_f^{N-1} \langle \tanh \lambda_p + p \tanh s_d \rangle + m_f^{N-1} \left\langle 1 + \frac{1}{p} \tanh \lambda_d \tanh s_d \right\rangle \quad f = 0,1,2 \tag{18}$$

with

$$\lambda_p = \sqrt{\frac{s \delta_p^2}{D} (1 + M^2)}$$

The parameters (s_d, λ, p, M,) are identical with those given after Eqs. 11 and 13. The initial values of n and m, which we need to calculate the values of n_f^i and m_f^i are as follows:

$$n_0^0 = \tanh \lambda; \; m_0^0 = 1; \; n_1^0 = m_1^0 = \exp(-\lambda); \; n_2^0 = m_2^0 = \exp \lambda$$

2.1.3 *Spherical Particles in the Diffusion Path*

The mass transfer rate equations defined by Eqs. 9 and 12 and the mass transfer coefficient given by Eq. 14 refers to cubic particles. Obviously, this simplification can lead to major errors in the predicted values of the mass transfer rates. Brilman et al. [42], Lin et al. [44] and Brilman et al. [54] have taken into account that the droplets are rigid spheres in their one-, two- and three-dimensional models. Van Ede et al. [49] worked out a model taking into account the spherical effect by varying the dispersed phase hold-up with the distance from the gas-liquid interface. This model cannot be applied, generally. Using the mass transfer equations given above for cubic particle the mass transfer rate for sphere can easily be obtained by means of geometric considerations. This is illustrated in Fig. 2 [48]. The mass transfer rates for cubic particle can be considered to be valid for a differential surface element, where the diffusion distances, δ_0, d, δ_p, are constants. At Fig. 2 this surface element, T_Δ is an annulus with radius R*, $T_\Delta = 2\pi R \Delta R^*$. The diffusion distances belonging to T_Δ can be obtained from

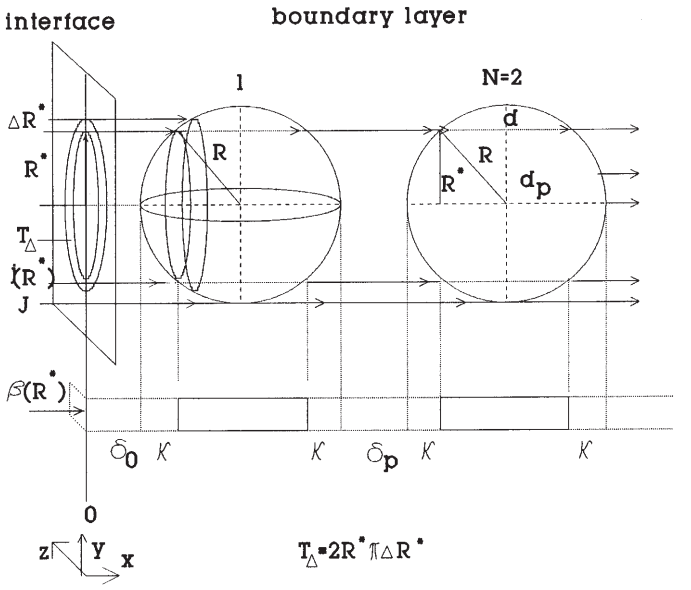

Fig. 2. Geometrical approach to obtain the j^{ave} value for the heterogeneous part of the gas-liquid interface

geometric considerations. For instance, the diffusion distance inside the particle as a function of R* can be given as follows:

$$d = d_p \sqrt{1 - \left(\frac{R^*}{R}\right)^2} \tag{20}$$

The value of κ in Fig. 2 represents the change of the diffusion path in the phase segments, due to the curvature of the particle surface:

$$\kappa = \frac{d_p - d}{2} \tag{21}$$

Knowing the κ value, the diffusion distances belonging to the T_Δ will be $\delta_0 + \kappa$, d, $\delta_p + 2\kappa$ for the three phase segments. Thus, the mass transfer coefficient can be given by the following function:

$$\beta(R^*) = \beta(\delta_0 + \kappa, d, \delta_p + 2\kappa) \tag{22}$$

Now, the average mass transfer coefficient corresponding to the total gas-liquid interface of the heterogeneous part (it is equal to $R^2\pi$) can be obtained after integrating $\beta(R^*)\, T_\Delta$ over the total interface ($R'^* = R^*/R$) and dividing it by the total interface:

$$\beta^{ave} = \frac{1}{R^2\pi} \int_0^R 2R^*\pi\beta(R^*)\, dR^* \tag{23}$$

Knowing the average mass transfer coefficient, the absorption rate referring to the total gas-liquid interface can be given for zero- and first-order reactions, respectively as follows (see also Eq. 7, 9, 12, 14):

$$J^*_{het} = \left\{ \beta^{o,ave}\, 1.2\, \varepsilon^{2/3} \left(1 - \frac{O^*M^2T}{O^* - O_L + O^*M^2} \right) + k^\circ (1 - 1.2e^{2/3}) \right\} \qquad (24)$$

$$(O^* - O_L + O^*M^2)$$

$$J^*_{het} = \left\{ \beta^{ave}\, 1.2\, \varepsilon^{2/3} + k^\circ \sqrt{1 + M^2}\, (1 - 1.2\varepsilon^{2/3}) \right\} \left(O^* - \frac{O_L}{1 + M^2} \right) \qquad (25)$$

The factor of 1.2 in Eqs. 24 and 25 differs for that given in Eq. 6. This follows from the geometrical difference between cubic and sphere.

2.1.4
Effect of the Kinetic Parameters

Both the mass transfer kinetic parameters (diffusion in the phases, D, D_d, surface renewal frequency, s) and chemical reaction rate constants (k_0, k_1) strongly influence enhancement of the absorption rate. The particle size, d_p, the dispersed liquid holdup, ε and the partition coefficient, H can also strongly alter the absorption rate [42–44, 46, 48]. Similarly, the distance of the first particle from the gas-liquid interface, δ_0 is an essential factor. Because the diffusion conditions are much better in the dispersed phase (larger solubility and, in most cases, larger diffusivity, as well) the absorption rate should increase with the decrease of the δ_0 value.

Lin et al. [44] simulated the enhancement using the two-dimensional model, as a function of all important parameters. It is clear from this work that the role of lateral diffusion depends mainly on the particle capacity, that is, on the value of partition coefficient, H. This conclusion was drawn by Brilman et al. [42, 54], as well. The one-dimensional model does not contain the lateral effect and, as a consequence, the absorption rate would be underestimated by this model and the difference of the results obtained by the one- and two-dimensional models would be increased with increasing partition coefficient. The question is in which parameter range this error can be neglected.

First, we compare the enhancement obtained by the model presented to that of obtained by Lin et al. [44] for the case of M = 0 (Fig. 3). The partition coefficient of the organic components ranges between about 10 and 25 (for instance for silicone oil [21], hexadecane [37] octene [49] the H values are equal to about 20, 12, 18, respectively). For the comparison, the partition coefficient was chosen to be 10 because we had obtained numerical data at this value, only. The difference between the results is rather low, it is lower than 10%. Increasing the H value the error will be larger. For H = 100 the difference between the two models can reach 40% in the parameter range given for Fig. 3. This difference for H = 20 might not be higher than 15–20% relating the error to mass transfer rates obtained by our model. From this it can be concluded that the one-dimensional, analytical model (Eqs. 24, 25) can be applied with good accuracy for fer-

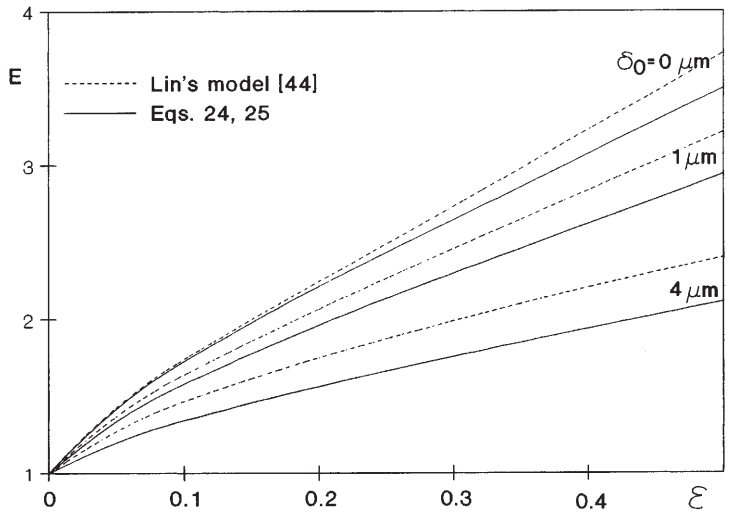

Fig. 3. Comparison the one- (Eq. 24) and the two dimensional model (Lin et al. [44]) results as a function of dispersed phase holdup at different values of particle distance from the interface ($D = 2 \times 10^{-9}$ m^2 s^{-1}, $k^o = 8.5 \times 10^{-5}$ m s^{-1}, $D_r = 1$, $H = 10$, $d_p = 20 \times 10^{-6}$ m, $\varepsilon = 0.1$, $N = 15$, $M = 0$)

mentation in the presence of conventional organic phases with H values up to 20–25.

Another important question is the applicability of the one-particle model, i.e., when only one particle is assumed to be located in the diffusion path perpendicular to the gas-liquid interface. Brilman [42] simulated, using his one-dimensional model, the effect of the particle number in the diffusion path in range of H between 4 and 100 with $d_p = 3$ µm and $k^o = 1 \times 10^{-4}$ m s^{-1} . The increase in the absorption rate due to the second particle ranges from zero to 30%, while that due to the third particle is less than about 8%. Similar results were obtained by Nagy [48]. Generally, it can be stated that the effect of the second and third particles, etc. must not be neglected using the dispersed organic phase with H values up to 25 and under conventional mass transfer conditions. The multiparticle mass transfer rate is illustrated in Fig. 4 and partly in Fig. 5, too. Figure 4 shows the local values of enhancement, E_{loc} at differential radial positions from the particle center. The E_{loc} function was simulated for 1, 2, and 3 particles located next to each other. The distance from the interface, δ_0 was assumed to be equal to zero. Practically, the β^{ave} value can be obtained by averaging the values shown in Fig 4 over the heterogeneous part of the interface. The figure clearly shows that, following from the one-dimensional character of our model, enhancement does not exist at radial positions that are larger than d_p ($d_p = 3$ µm). The E_{loc} strongly decreases with increasing distance from the particle center. The results obtained by Brilman et al. [42] using two- and three-dimensional models for the simulation show that the E_{loc} values is larger than unity in the radial position range of 3 to 5 µm, too, though these values gradually decrease down to unity. This indicates the role of lateral diffusion. It should be noted that the lat-

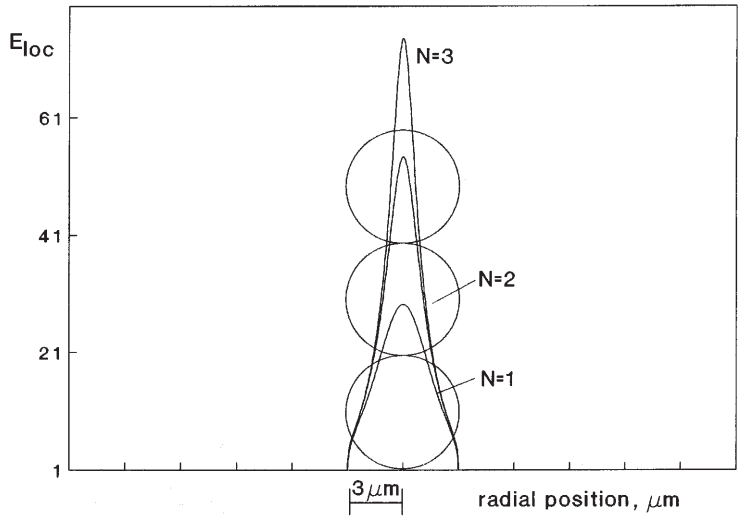

Fig. 4. Local enhancement as a function of radial positions from the particle center using the one-dimensional model presented ($D = 1.24 \times 10^{-9}$ m^2 s^{-1}, $D_r = 0.56$, $H = 103$, $d_p = 3 \times 10^{-6}$ m, $M = 0$)

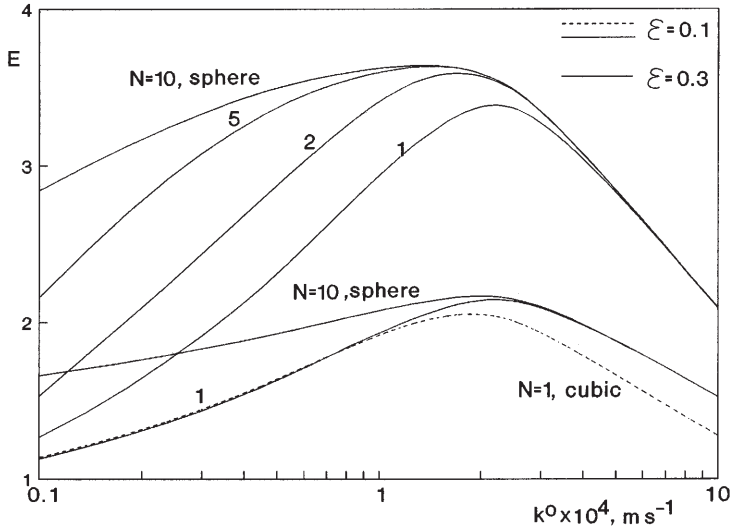

Fig. 5. Enhancement as a function of the physical mass transfer coefficient without dispersed phase at different particle numbers and dispersed phase holdups ($D = 2.3 \times 10^{-9}$ m^2 s^{-1}, $D_r = 0.56$, $H = 18$, $d_p = 10 \times 10^{-6}$ m, $\delta_0 = 0$, $M = 0$)

eral diffusion also has an additional effect, namely, it lowers the values of E_{loc} at every point of the radial position within the particle radius. The E_{loc} values obtained by Brilman et al. [42] are much smaller than that in Fig. 4. That is why the difference in the enhancements obtained by the two models, at lower values of H, is rather low.

The three-phase absorption rate should strongly depend on the physical mass transfer coefficient. In principle, the decrease in the contact time of droplets at the interface should decrease their effect on the mass transfer rate. In reality, the situation is more complex as is shown in Fig. 5. The enhancement has a maximum as a function of the physical mass transfer coefficient, k^o. In the range of k^o where the E value increases to its maximum, the diffusion through the droplets dominates the absorption rate while at higher k^o values, where E decreases monotonously, the diffusion in the continuous phase between the gas-liquid interface and the first particle dominates mostly the E values due to the decreasing diffusion depth of the absorbing component. In this regime the diffusion depth will gradually become smaller than the value of $\delta_0 + d$, and then have the value of δ_0. At lower values of k^o, $k^o <$ about 2×10^{-4} m s^{-1} in Fig. 5, the diffusion depth is much larger than the particle size and, as a consequence, the multiparticle model should be used for this regime. Calculations were carried out at ε values of 0.1 and 0.3 and at different numbers of particles in the diffusion path. At values of $\varepsilon = 0.1$ and $N = 1$, enhancement was also calculated in the case of cubic particles (dotted line) to compare these data to those of spherical ones. Difference between them exists at larger k^o values only, it increases with the increase of k^o but it is less than about 15% in the parameter range investigated.

Droplet diameter is also an important parameter. According to the results obtained by Lin et al. [44] and Nagy [48], the absorption rate increases with the increase of the particle size up to a maximum. When the particle size is larger than the penetration depth, the enhancement decreases with increasing particle size. This conclusion is in contradiction to that of van Ede et al. [49]. According to their model, the absorption rate decreases with the particle diameter. Assuming that the first droplet located at the interface, the dispersed phase holdup increases with the increase of the droplet size and, consequently, the absorption rate should increase in the size range of $d_p < \delta$. Figure 6 illustrates the effect of the droplet size. The absorption rate increases with the size up to $d_p =$ 20 – 30 µm. In this size range the diffusion depth is larger than the droplet diameter, thus, the multiparticle model must be used. With a particle size (d_p) greater than about 30 µm, the size will be larger than the penetration depth, and, due to this fact, the absorption rate gradually decreases with the droplet diameter.

2.1.5
Effect of Chemical Reactions

One must pay great attention to the role of the continuous phase chemical reaction because the reaction rate may continuously change during fermentation. This will have an effect on the absorption rate which will also change during the process and this has also to be taken into account. In reality, the reaction rate in

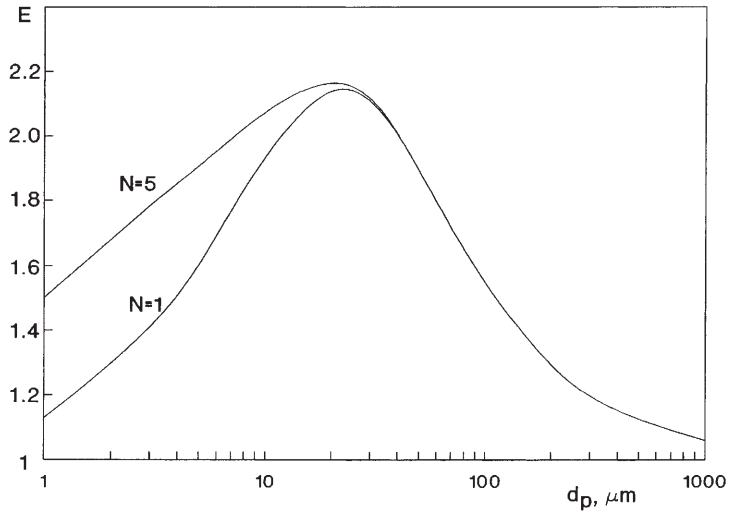

Fig. 6. Enhancement as a function of the particle size ($D = 2.3 \times 10^{-9}$ m^2 s^{-1}, $D_r = 0.56$, $H = 18$, $k^o = 1 \times 10^{-4}$ m s^{-1}, $\delta_0 = 0$, $\varepsilon = 0.1$, $M = 0$)

fermenters is not very high, therefore it might be expected that its effect on the absorption rate can be neglected in most cases. To make a decision you need exact calculations for this problem. To my knowledge, the effect of the continuous phase reactions on the three-phase absorption rate has not been discussed yet. As expected, the absorption rate should decrease with the increase in the reaction rate [60]. Namely, with the increase in the reaction rate, the penetration depth decreases, therefore, the role of the mass transport inside the droplets gradually diminishes. Figure 7 shows the effect of the reaction modulus, M on the enhancement in the cases of both the zero- and first-order reactions. As can be seen, the E value can be regarded to be constant when M is smaller than about 0.4. At larger values of M, enhancement strongly decreases with the increase in the reaction rate. The effect of the zero-order reaction, this is mostly the case during fermentation, is somewhat higher than that of the first-order chemical reaction. It can be stated that the effect of the chemical reaction on the absorption rate in a three-phase system must be considered only when $M > 0.4$.

2.1.6
Verification of the Model Results

Several researchers have measured the absorption rate at the presence of dispersed organic phase [1, 17–18, 37, 39, 49, 51–53]. Bruining et al. [37] measured the oxygen absorption in stirred vessels with plane interface in the presence of small amounts of decane, hexadecane, $\varepsilon = 0.01 - 0.1$ while van Ede et al. [49] applied octene as a dispersed phase. Littel et al.[39] used carbon dioxide for absorption in dispersion of toluene droplets with $\varepsilon = 0 - 0.4$. The theoretical data in the literature were mostly verified by the experimental results of the above

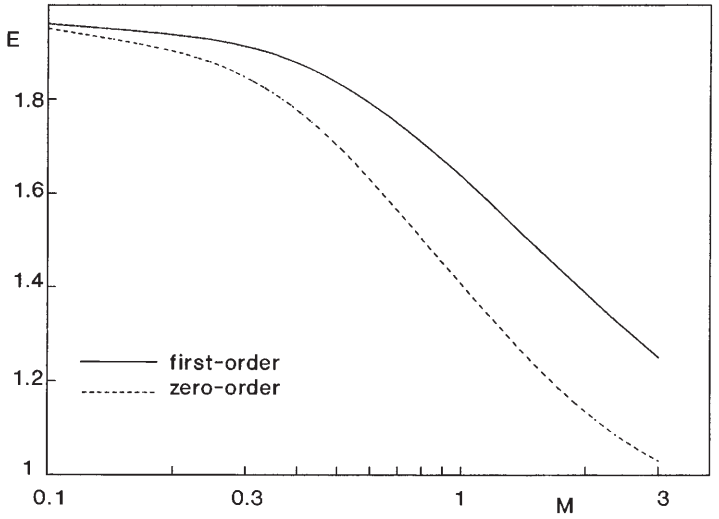

Fig. 7. The effect of the external chemical reactions on enhancement ($D = 2.3 \times 10^{-9}$ m^2 s^{-1}, $D_r = 0.56$, $H = 18$, $d_p = 10 \times 10^{-6}$ m, $k^o = 1 \times 10^{-4}$ m s^{-1}, $\delta_0 = 0$, $\varepsilon = 0.1$)

authors because the gas-liquid interface is known in those cases [43, 44, 46, 49] . The gas-liquid interfacial area in the case of intensive mixing, when the gas-liquid interface is no longer flat, can strongly change with the dispersed phase holdup [52, 53]. Enhancement is affected by the interfacial area, as well, in those cases. Because its values are mostly not known the real value of enhancement is difficult to determine. Generally, the verifications of model data are in good agreement with the experimental ones. However, it has to be mentioned that the δ_0 value and the ε in the boundary layer have not been measured yet, therefore the verification results must be treated carefully. Figure 8 shows an example for the verification of the theoretical data. The experimental data of van Ede et al. [49] are compared to the calculated data using the presented multiparticle model . The calculated data are somewhat higher than the measured ones for the case of $\delta_0 = 0$. At somewhat higher values of δ_0, not shown in Fig. 8, the theoretical model gives the same results as the measured ones. To get more exact verification, among other values, the δ_0 must be estimated or measured. Comparing the theoretical data to other experimental ones [42, 44, 46, 48], one can conclude that the models agree with the experimental results. Thus, it can be concluded that the analytical mass transfer models [46, 48] are accurate enough to be used for the prediction of the mass transfer rates in chemical- or biochemical technologies.

2.2
Fermentation with an Enhanced Absorption Rate of Oxygen

As previously discussed, the oxygen absorption rate can essentially be increased using a dispersed organic phase with higher solubility and/or diffusivity. The

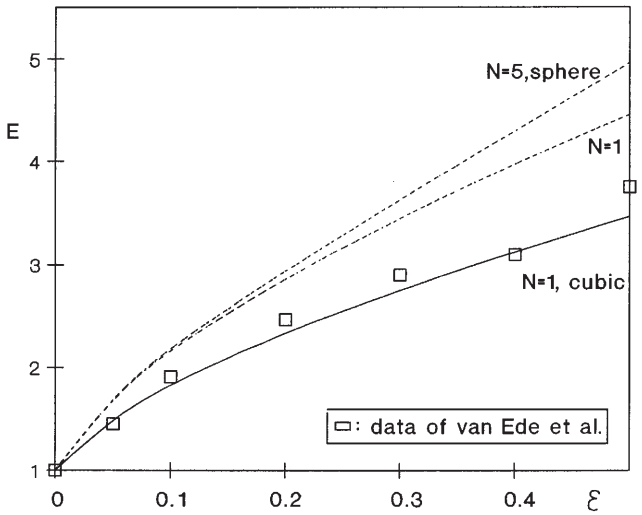

Fig. 8. Verification of the experimental and theoretical data ($D = 2.3 \times 10^{-9}$ m^2 s^{-1}, $D_r = 0.56$, $H = 18$, $d_p = 22 \times 10^{-6}$ m, $k^o = 0.92 \times 10^{-4}$ m s^{-1}, $\delta_0 = 0$)

use of an organic phase in a fermentation broth can have several negative effects as well. The most important one is its potential influence on the microorganisms. The question is how the microorganisms can tolerate the organic phase. There are numerous reports of cell growth reduction in the presence of a dispersed phase. For example, Lowe et al. [55] showed that some perfluorocarbons led to inhibition of growth and other negative effects on mammalian cells. Chandler et al. [56] showed that growth of *Escherichia coli* was inhibited by perfluorocarbon. Electron microscopy showed vacuoles and other structural perturbations of the microorganisms after prolonged contact. Silicon oil also causes loss of activity of the microbial cells [57]. The use of an oxygen acceptor selector such as *p*-benzoquinone, after longer contact, however, can also reduce the activity of microorganism over a longer period of time [58]. An alternative method for avoiding the negative effects of the organic phase might be to encapsulate the oxygen carrier within an ultra-thin, oxygen-permeable membrane, providing an inert barrier between the organic droplets and the cells [21, 22, 59]. With this method, the direct contact between the cells and liquid medium can be eliminated, and thus, the toxicity problems related to direct contact can also be avoided.

Junker et al. [1] investigated the cell mass productivity in a wide range of perfluorocarbon volume fractions using a variety of organisms such as Baker's yeast, *Candida lipolytica*, *Acetobacter pasteurianus* and *Gluconobacter oxydans*. All cells grew adequately in the presence of perfluocarbon, the experimental growth rates, lag times, and cell yields were unaffected by the organic phase. Due to the longer exponential growth periods and higher cell densities, the oxygen uptake rate was increased drastically. For instance, for *Candida lipolytica*, the maximum oxygen uptake rate was six times higher in the presence of a 75% or-

ganic phase, compared to that without an organic phase. While, the maximum cell density was increased from 30 kg dry cell wt m^{-3} at 0% to 145 kg dry cell wt m^{-3} at 75% perfluorocarbon. The exponential growth phase of *Acetobacter pasteurianus* more than doubled in length with the maximum cell density increasing from 5 to 43 kg dry cell wt m^{-3}. For these fermentations, the oxygen uptake rate increased by a factor of 6.5 on an aqueous volume basis. Overall, the observed increases in oxygen uptake rate were found to be linearly related to cell mass productivity, substrate uptake, and product formation rate for a variety of microorganisms. Silicon oil was successfully applied as an oxygen carrier for the production of dihydroxyaceton from glycerol with *Gluconobacter oxydans* [21, 22, 59]. Silicon oils were microencapsulated within polyamide (nylon) membranes cross-linked with polyethylenimine. The addition of 20% encapsulated silicone oil will increase the oxygen availability by a factor of 6.5, in comparison to the reference culture without silicon oils. In batch fermentation, improved oxygen transfer capacity and the removal of oxygen limitation raised the productivity by a factor of five. A toxic effect or inhibition was not observed in the course of fermentation. Therefore, the microencapsulation technique avoids the toxic effects as well as maintaining the high oxygen transfer capacity [21].

2.2.1 *Integrated Model of Fermentation*

During fermentation, the enhanced absorption rate of oxygen increases the bulk concentration and, as a consequence, the production rate of cells can be increased as well. To predict this effect, the enhanced transfer rate has to be incorporated into the differential mass balance equations of fermentation processes studied. If you know the mathematical expression of the biochemical reactions and their dependence on oxygen concentration as well as the enhanced absorption rates due to the dispersed organic phase, you can calculate the fermentation exactly after solving the equation system obtained.

The kinetic modeling of the external transport limitation is successful with aid of a double-substrate-limitation function [61–63]:

$$\mu = \mu_{max} \frac{S}{K_s + S} \frac{O_L}{K_O + O_L} \tag{26}$$

The above equation can be used as a formal kinetic approach without assuming a mechanism. This equation should be incorporated into the mass balance equations for oxygen in which the enhanced oxygen transfer rate due to the dispersed phase should also be considered.

Let us consider an ideal continuously stirred tank reactor with constant broth volume. The mass balance equation for substrate as a carbon source (Eq. 27), biomass (Eq. 28) and oxygen in the fermentation broth (Eq. 29) can be given for the liquid phase, as follows [65, 66]:

$$\frac{dS}{dt} = -\frac{\mu X}{Y_{X/S}} + \overline{D}\,(S_{in} - S) \tag{27}$$

$$\frac{dX}{dt} = \mu X - \overline{D}X \tag{28}$$

$$\frac{dO_L}{dt} = 3600\, J^*_{het} - \frac{\mu X}{Y_{X/O}} + \overline{D}(O_{L,in} - O_L) \tag{29}$$

The absorption rates, J^*_{het} are given in Eqs. 24 and 25. It was assumed that the biomass concentration in the inlet liquid is equal to zero and that the oxygen concentration in the gas phase is constant and, as a consequence, the O* value will also be constant during our simulation. The gas concentration can practically be kept as a constant if the volumetric gas flow rate is high enough. Its change during absorption can easily be taken into account [65, 66]. The above equation system (Eqs. 26 – 29) can only be solved by numerical methods. For the solution, the Runge-Kutta-Feldberg method was used [64].

2.2.1.1
Simulation of a Batch Stirred Tank Reactor

For a batch process, the dilution rate is zero. Typical results are shown in Figs. 9 and 10 where the substrate, oxygen and biomass concentrations in the fermentation broth, as well as the growth rate, are plotted as a function of time. The parameter values used for simulations are given in Table 1. These are practical values that are close to that of bio-chemical processes [61]. Data of the organic phase in the Table corresponds to octene [49]. The values of parameters that are different from that of Table 1 are given separately in the figure legends. Time courses of oxygen concentrations in Fig. 9 are very interesting. Their values gradually decrease as a function of time, reaching a minimum and, when the substrate consumption is practically finished, it starts to increase again. The effect of the dispersed phase holdup is significant. The oxygen concentration is shifted to the right-hand side with the increase of the value of ε and the minimum of curves for oxygen also increases. When the parameter regime is investigated, the initial value of enhancement changes between 1 to 3.9 due to change of ε value. This large increase in the absorption rate causes significant change in the time course of fermentation. Namely, the higher bulk oxygen concentration causes a higher growth rate and, thus, a faster rate of substrate consumption as well as higher production rate. Time for the complete fermentation decreases to

Table 1. Data of parameters used for simulation of fermentation in bacth and continuous fermenters shown in Fig. 9 – 12

$S_{in} = 100$ kg m^{-3}	$X_{in} = 0.05$ kg m^{-3}	$O^* = 9 \times 10^{-3}$ kg m^{-3}
$\mu_{max} = 0.5$ h^{-1}	$K_S = 6$ kg m^{-3}	$K_O = 0.016 \times 10^{-3}$ kg m^{-3}
$D = 0$ or 0.2 h^{-1}	$Y_{X/S} = 0.3$ kg kg^{-1}	$Y_{X/O} = 1.9$ kg kg^{-1}
$k^oa = 200$ h^{-1}		
dispresed phase:	$D = 2.3 \times 10^{-9}$ m^2 s^{-1}	$D_r = 0.56$
$H = 18$	$k^o = 1 \times 10^{-4}$ m s^{-1}	$\delta_0 = 0$ m
$d_p = 20 \times 10^{-6}$ m	$\varepsilon = 0.1$	

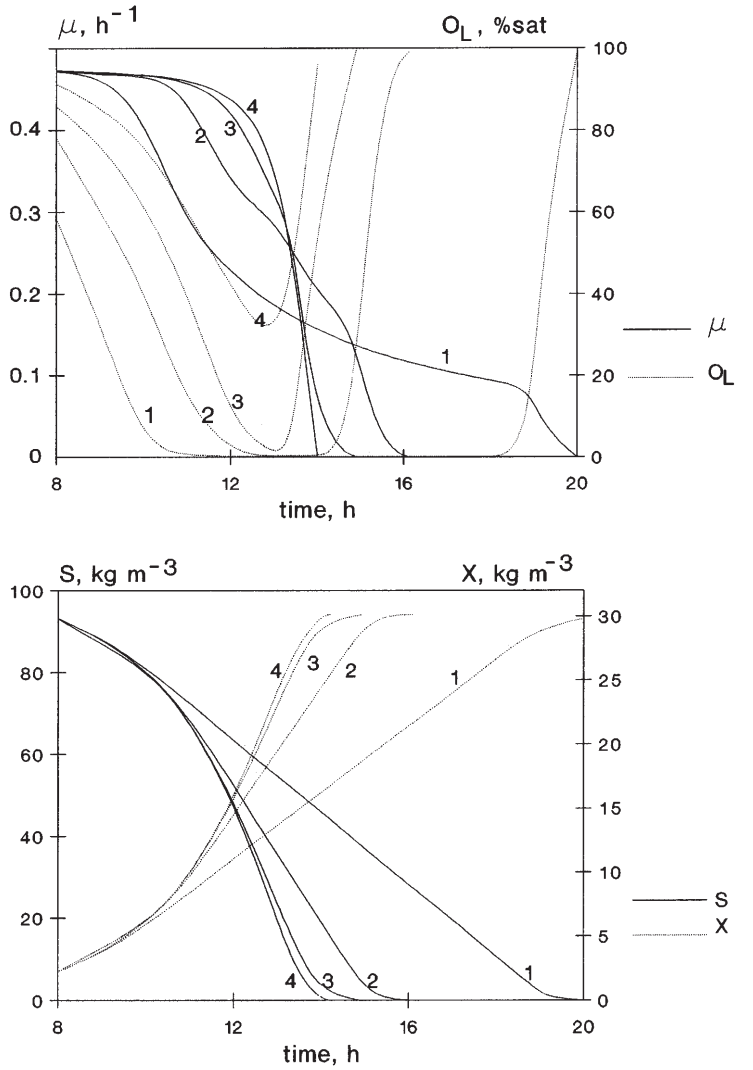

Fig. 9. Time course of concentrations, S, O, X and the μ value; simulated data without (curve 1) and with dispersed phase (1 – $\varepsilon = 0$; 2 – $\varepsilon = 0.07$; 3 – $\varepsilon = 0.2$; 4 – $\varepsilon = 0.39$; enhancement for M = 0 are 1, 1.9, 2.9, 3.9, respectively)

about 30 %, it is lowered from about 20 h down to 14 h due to the enhanced absorption rate.

The K_O saturation coefficient of oxygen in the Monod-type kinetic equation is an important parameter, too. Its value strongly influences the specific growth rate, especially when the value of oxygen concentration is of the same order of magnitude as or lower than the K_O value. Its effect is illustrated in Fig. 10 in the presence of a dispersed organic phase, $\varepsilon = 0.2$. The increasing value of K_O (K_O was chosen to be equal to 0.64×10^{-3}, 0.16×10^{-3} and 0.016×10^{-3} kg m^{-3}) has a

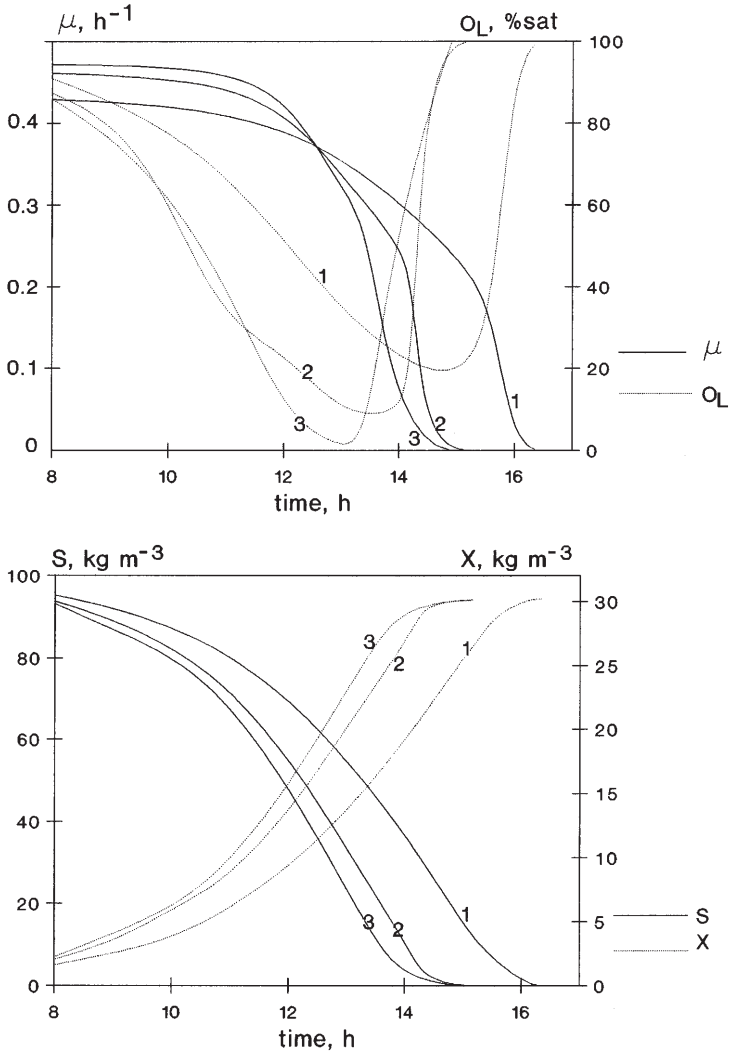

Fig. 10. Time course of concentrations, S, O_L, X and the μ value at different values of K_O, using dispersed organic phase ($\varepsilon = 0.2$, thus E = 2.9 if M = 0); for curves 1, 2 and 3 the values of K_O are equal to 0.64×10^{-3} kg m^{-3}, 0.16×10^{-3} kg m^{-3} and 0.016×10^{-3} kg m^{-3}, respectively;

complex effect on the growth rate, μ. At the beginning it lowers the μ value which then affects the concentrations of reagents and, accordingly, the change of μ, as well. This is responsible for the oxygen curves being shifted towards the higher concentrations. Its minimum will also be increased. The greater values of K_O need lower enhancement of the absorption rate in order to avoid the potential, critical oxygen concentration level.

An important question is how the reaction rate modulus for the continuous phase, M changes during fermentation process. It is well known when $O_L \gg K_O$

then Monod kinetics is a zero-order reaction, while in the case of $O_L \ll K_O$ it is a first-order reaction. There exists an intermediate reaction range where the reaction order lies between unit and zero. The reaction rate constants can be obtained from Eq. 26 as limiting cases above mentioned, for zero- (Eq. 30) and for first-order reaction (Eq. 31).

$$k_0 = \mu_{max} \frac{S}{K_s + S} \frac{X}{Y_{X/O}} \tag{30}$$

$$k_1 = \mu_{max} \frac{S}{K_s + S} \frac{1}{K_O} \frac{X}{Y_{X/O}} \tag{31}$$

The rate constants, k_0, k_1 differ from each other by a factor of K_O, namely $k_0 = k_1 K_O$. During our simulation we calculated the M value in the following manner: when $O_L > K_O$ then Eq. 30 was assumed to be valid, and when $O_L < K_O$ then Eq. 31. With these assumptions, the M value could be calculated continuously during the whole fermentation process. Then, the M value obtained was used to estimate enhancement of the absorption rate during the fermentation. It was obtained that the E value practically does not change in the course of fermentation. As can be seen in Fig. 11, M has rather low values, namely $M < 0.3$, as a function of the oxygen concentration during the fermentation. If we take into account the curves in Fig. 7, where enhancements are shown as a function of M, it can be stated that the effect of the chemical reaction in the continuous phase, under the conditions investigated, can be neglected. This may be true in most cases during bio-chemical processes. However, at higher values of biomass concentration and/or maximum growth rates (μ_{max}), the M value can be higher, as well. In these cases, the effect of the continuous phase reaction on the absorption rate can no

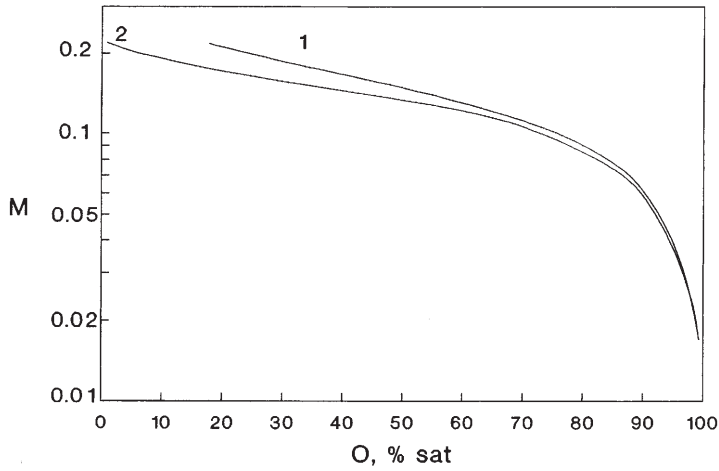

Fig. 11. The change of the reaction-diffusion modulus as a function of the oxygen concentration during the fermentation (parameters are same as in Fig. 10; curve 1: $K_O = 0.64 \times 10^{-3}$ kg m^{-3}; curve 2: $K_O = 0.016 \times 10^{-3}$ kg m^{-3})

longer be neglected. This can be estimated exactly from the rate equations given in this paper.

2.2.1.2 Simulation of Continuous Stirred Tank Reactor

Many reviews and several books [61, 62] have appeared on the theoretical and experimental aspects of the continuous, stirred tank reactor – the so-called chemostat. Properties of the chemostat are not discussed here. The concentrations of the reagents and products can not be calculated by the algebraic equations obtained for steady-state conditions, when $\mu = \overline{D}$ (the left-hand sides of Eqs. 27 – 29 are equal to zero), because of the double-substrate-limitation model (Eq. 26) used. These values were obtained from the time course of the concentrations obtained by simulation of the fermentation. It was assumed that the dispersed organic phase remains in the reactor and the dispersed phase holdup does not change during the process. The inlet liquid phase does not contain either organic phase or biomass.

Figure 12 shows typical values of concentrations as a function of time, without (curves 1) and with a dispersed organic phase (curves 2). The difference between the two cases is significant. The oxygen concentration rapidly decreases down to zero when there is no dispersed phase in the fermentation broth. In contrast, when you use a dispersed phase, the oxygen level remains rather high during the whole process. Even at the minimum, it reaches about 40 % of its saturation concentration. After a short period of time, the oxygen concentration, after its minimum, starts to increase up to its stationary value, that is, up to 70 % of its

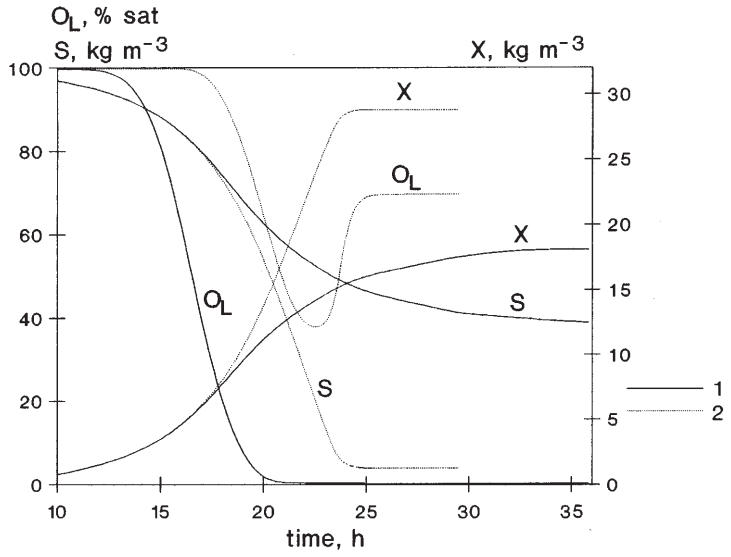

Fig. 12. Simulation of chemostat without (curves 1) and with ($\varepsilon = 0.2$, thus, E = 2.9 if M = 0) dispersed organic phase (curves 2; $\overline{D} = 0.2\ h^{-1}$)

saturation concentration. According to the different oxygen levels of the two cases, substrate- and biomass concentrations also show great differences. The stationary outlet concentration of substrate is practically close to zero, it is about 4 kg m^{-3} using an organic phase while its value is about 37 kg m^{-3} without organic phase. The change of biomass concentration follows from these values.

The effect of the dilution rate is shown in Fig. 13. The stationary outlet concentrations were obtained from the time course data of concentrations. The time needed to reach the steady-state conditions (not plotted here) depends very strongly on the dilution rate and enhancement. Figure 13 shows data with and without organic phases. The oxygen concentration rapidly decreases as a function of the dilution rate when the fermentation takes place without a dispersed organic phase (curves 1). While, with an organic phase, it has relatively high level even at high values of the dilution rate. In the latter case, the substrate concentration is also low. That should mean that the fermentation process can be carried out at a much higher dilution rate using a suitable organic phase. Consequently, the productivity of the fermentation process should be much higher with a dispersed phase. Obviously, the use of an organic phase means additional costs during the process but these costs should be much less than the financial advantage caused by the increase in production.

2.3 Baker's Yeast Production

Though baker's yeast production is a rather complex process, its kinetics are well known [67, 68]. Software developed by Kristiansen [68] for simulation of this

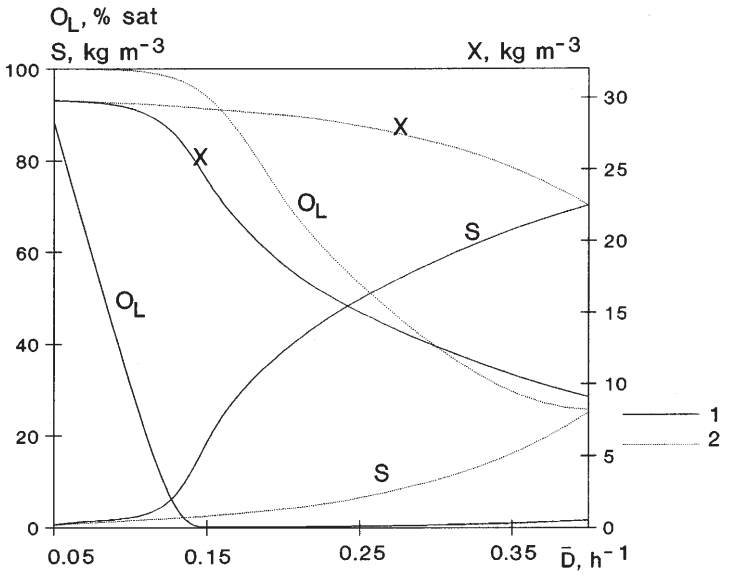

Fig. 13. The change of the steady-state concentrations as a function of the dilution rate without (curves 1) and with ($\varepsilon = 0.2$, thus, E = 2.9 if M = 0) dispersed organic phase (curves 2)

fermentation offered us an excellent opportunity to apply it for the estimation of the effect of a dispersed organic phase on this process as an example. The specific growth rate of baker's yeast consists of three partial specific rates according to three routes: aerobic and anaerobic degradation of sugar, and aerobic degradation of ethanol. Both the sugar- and ethanol concentration as well as the oxygen concentration affect the specific growth rate. According to the Monod model, the rate of glycolysis increases with increasing sugar concentration up to a maximum value. When the rate of glucose consumption exceeds a critical value, a considerable part of the sugar may be converted into carbon-dioxide and ethanol even if there is no oxygen limitation. When the oxygen uptake rate is, or can be, greater than the rate of sugar consumption, aerobic growth on ethanol occurs. Anaerobic ethanol production takes place under oxygen limitation or oxygen starvation. It is important to operate at maximum oxygen transfer capacity of the production vessels. In large bioreactors as used in baker's yeast production, oxygen limitation can occur very often. If this is the case, reduction in yield may be experienced. Details about this process can be found in the literature [67, 68]. We want only to show how the dispersed organic phase can enhance the oxygen concentration in the fermentation broth during the fermentation and, consequently, the production of baker's yeast. Figure 14 shows the calculated concentrations of sugar, S, oxygen, O_L, biomass, X and ethanol without and with organic phases. The oxygen concentration was related to that of its saturation value. That was assumed to be equal to 0.28 mol m^{-3} [22]. The reactor data and other parameter values are listed in Table 2. The kinetic data of the baker's yeast production used for the simulation are the same as given by Kristiansen [69]. The effect of organic phase was taken into account in such a manner that the real mass transfer coefficient of the fermenter obtained with data of Table 2 was multiplied by factor of 2.9. This value corresponds to enhancement of the absorption rate caused by the organic phase with properties given in Table 1 in the case of $\varepsilon = 0.2$. It has to be noted that the same increase of the mass transfer coefficient can be achieved by the increase of the stirrer speed by a factor of 2.4. As can be seen in Fig. 14, the oxygen concentration is significantly higher due to its enhanced absorption rate. This causes the ethanol production to decrease and the productivity increases. The biomass production during the enhanced absorption rate increases 18% more than that obtained without an organic

Table 2. Data of parameters used for simulation of baker's yeast fermentation in fed-bacth fermenter shown in Fig. 14 – 15

	fermenter:	
stirrer speed: 30 rpm	fermenter diameter: 4.7 m	stirrer diameter: 1.5 m
$Power_{number}$: 6	$F_g = 3600\ m^3\ h^{-1}$	$F_L = 10\ m^3\ h^{-1}$
	initial values:	
$V = 11\ m^3$	$S = 2500\ Cmol\ m^{-3}$	$X = 300\ Cmol\ m^{-3}$
ethanol: 0 Cmol m^{-3}	$O_L = 0.15\ mol\ m^{-3}$	$CO_2 = 0.1\ mol\ m^{-3}$
	inlet liquid:	
$S_{in} = 1750\ Cmol\ m^{-3}$	$X_{in} = 0\ Cmol\ m^{-3}$	ethanol: 0 Cmol m^{-3}
$O_{L,in} = 0.15\ mol\ m^{-3}$	$CO_2 = 0.05\ mol\ m^{-3}$	

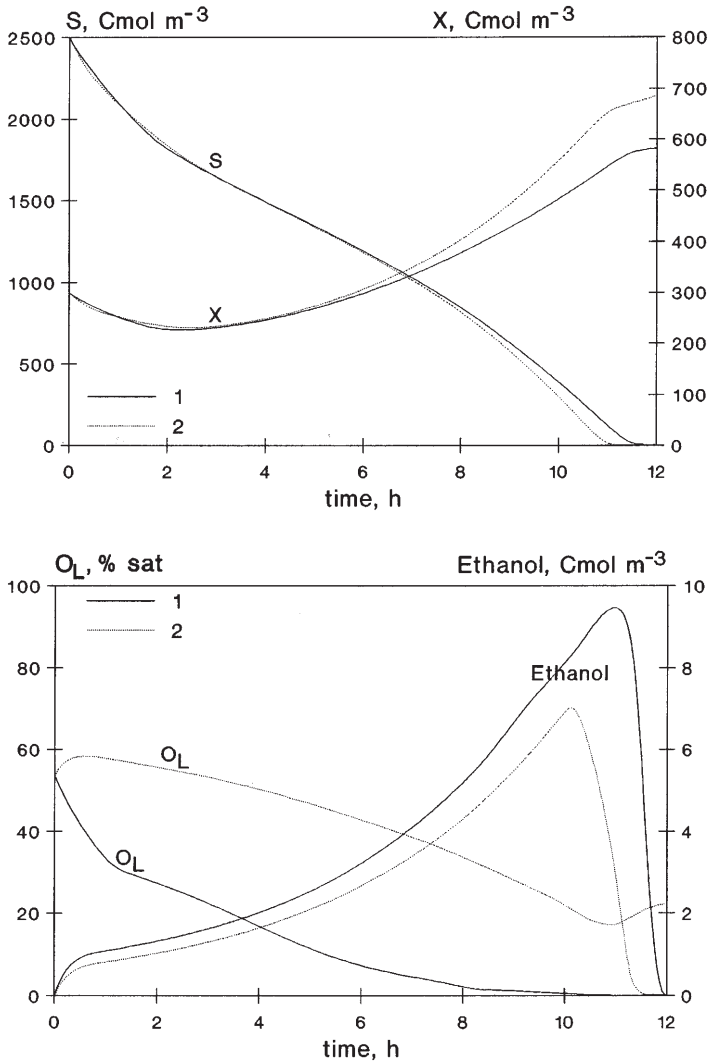

Fig. 14. Time course of baker's yeast fermentation without (curves 1) and with (E = 2.9) dispersed organic phase (curves 2); simulation of fed-batch fermenter with constant liquid feed rate using data of Table 2

phase (the end concentrations of biomass are equal to 581 and 685 Cmol m^{-3} without and with enhanced absorption rates, respectively). Taking into account that the reactor volume is about 130 m^3 at the end of the fermentation this difference means a large amount of biomass. Figure 15 is also typical representation of the time course for the case when the fed liquid rate is gradually increased during the fermentation. Here oxygen- and biomass concentrations are plotted as functions of time. Changes in concentration are similar to those ob-

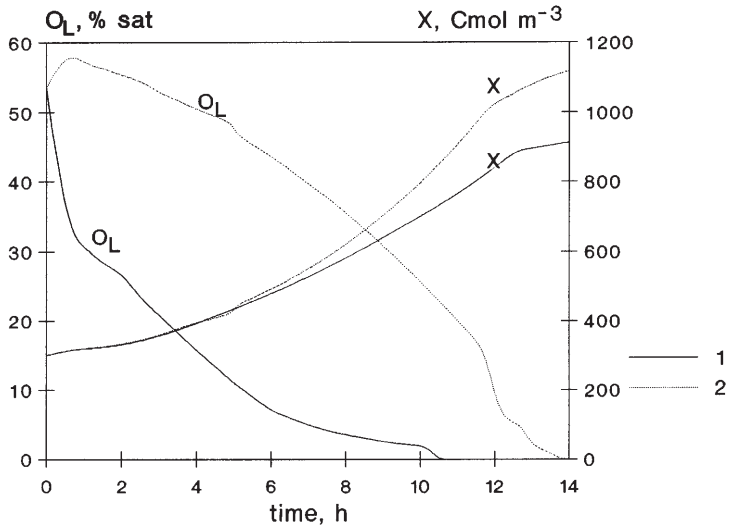

Fig. 15. Time course of baker's yeast fermentation without (curves 1) and with (E = 2.9) organic phase (curves 2) with stepwise increasing, in every hour 1 $m^3\ h^{-1}$ from the 5th hour, of the liquid feed rate from 5 up to 12 $m^3\ h^{-1}$ (the inlet sugar concentration was here: 3000 Cmol h^{-1}, other data as in Table 2)

tained in Fig. 14. The oxygen concentration decreases to zero at the end of fermentation, only, in the case of an enhanced absorption rate. Its value is much higher in the whole fermentation time. The increase of biomass production is also significant, it is equal to about 20%.

Generally, it is clear from the results given above that baker's yeast production, in principle, can essentially be increased by a dispersed organic phase. The same effect obtained by increased stirrer speed needs additional energy and this can be disadvantageous in systems with shear-sensitive cells. This mechanical stress can be avoided using an organic phase instead of higher stirring rates. Obviously, circumspect analysis is needed to consider each important effect, either negative or positive, caused by the presence of an organic phase.

3 Concluding Remarks

Using a dispersed organic phase in the fermentation broth, with higher oxygen capacity and diffusivity than that of the aqueous phase, can significantly enhance the oxygen absorption rate. As has been shown these enhancements are directly translatable into enhancements in fermenter productivity. The production can increase by factor of 3–6 or even more in the presence of an organic phase. Knowing the enhanced absorption rate equation and by coupling it with the mass balance equations of fermentation, the effect of dispersed phase on the production can be predicted exactly. The examples discussed show significant effects of the dispersed organic phase on the oxygen supply of microorganisms

and on the production rate. The main problem caused by the dispersed organic phase might be its potential toxic or inhibitory effects which may be observed using living cells. A promising method to avoid this problem is to produce an oxygen-permeable polymeric membrane for coating the dispersed organic phase [21]. The results obtained by the authors in this respect can be regarded as the first steps. Further research is needed in order to improve the properties of the polymeric membrane, its mechanical resistance, etc., and to check its behavior during fermentation with various fermentation solutions, living cells and operation conditions.

Acknowledgements. The author would like to thank the Hungarian Research Foundation under Grant No. OTKA T 15864 for the financial support of this work.

References

1. Junker B, Hatton TA, . Wang DIC (1990) Biotechnology Bioengineering 35:578
2. Ghommidh C, Cutayer JM, Navarro JM (1986) Biotechnol Lett 8:13
3. Yamada S, Wada M, Chibata J (1978) J Environ Ferment Technol 56:29
4. Jansen NB, Flickinger M, Tsao GT (1984) Biotechnology Bioengineering 26:362
5. Sablayrolles JM, Goma G (1984) Biotechnology Bioengineering 26:148
6. Fuchs R, Wang DIC (1974) Biotechnology Bioengineering 16:1529
7. Liu YC, Chang WM, Lee CY (1999) Bioprocess Engineering 21:227
8. Sriram G, Rao YM, Suresh AK, Sureshkumar GK (1998) Biotechnol Bioeng 59:715
9. Schlegel HG, Ibraim HG (1980) Biotechnology Bioengineering 22:1877
10. Holst O, Enfors SO, Mattiasson (1982) Eur J Appl Microbiol Biotechnol 14:64
11. Adlercreutz P, Holst O, Mattiasson B (1982) Enzyme Microb Technol 4:395
12. Mimura A, Takeda I, Wakasa R (1973) Biotechnol Bioeng Symp 4:467
13. Ho CS, Ju LK, Baddour RF (1990) Biotechnol Bioeng 36:1110
14. Ju LK, Lee JF. Armiger WB (1991) Biotechnol Prog 7:323
15. Adlercreutz P, Mattiasson B (1985) Appl Microbiol Biotech 16:165
16. Leonhardt A, Szwajcer E, Mosbach K (1985) Appl Microbiol Biotech 21:162
17. Rols JL, Goma G (1989) Biotech Adv 7:1
18. Rols JL, Conderet JS, Fonade C, Goma G (1990) Biotechnology Bioengineering 35:427
19. Ju LK, Lee JF, Armiger WB (1991) Biotechnol Prog 7:323
20. Rols JL, Goma G (1991) Biotechnol Lett 13:7
21. Leung R, Poncelet D, Neufeld RJ (1997) J Chem Tech Biotechnol 68:37
22. Poncelet D, Leung R, Centomo L, Neufeld RJ (1993) J Chem Tech Biotechnol 57:253
23. Jia S, Li P, Park YS, Okabe M, (1993) J Ferment Bioeng 19:661
24. Liu HS, Chiung WC, Wang YC (1994) Biotechn Techn 8X:17
25. McMillan JD, Wang DIC (1990) Ann. N.Y. Acad. Sci. p 289
26. Yoshida F, YamaneT, Miyamoto Y (1970) Ind Eng Chem Proc Des Dev 9:570
27. Alper E, Deckwer WD (1981) Chem Engng Sci 36:1097
28. Nagy E, Blickle T, Ujhidy A (1986) Chem Engng Sci 41:2193
29 Janakirman B, Sharma MM (1985) Chem Engng Sci 40:235
30. Holstvoogd RD, van Swaaij WPM, van Dierendonck LL (1988) Chem Engng Sci 43:2181
31. Wimmers OJ, Paulussen R, Vermeulen DP, Fortuin JMH (1984) Chem Engng Sci 39:1415
32. Demmink JF, Mehra A, Beenackers AACM (1998) Chem Engng Sci 53:2885
33. Holsvoogd RD, Ptasinski KJ, van Swaaij WPM (1986) 41:867
34. Zarzycky R, Chacuk A (1993) Absorption: Fundamentals and Application, Pergamon Press, Oxford
35. Mehra A, Pandit A, Sharma MM (1988) Chem Engng Sci 43:913
36. Vinke H, Hamersma PJ, Fortuin JMH (1992) Chem Engng Sci 48:2197

37. Bruining WJ, Joosten GEH, Beenackers AACM, Hofman H (1986) Chem Engng Sci 41:1873
38. Mehra A (1988) Chem Engng Sci 43:899
39. Littel RJ, Versteeg GF, van Swaaij WPM (1994) AIChE J 40-1629
40. Nagy E, Moser A (1995) AIChE J 41:23
41. Karve S, Juvekar VA (1990) 45:587
42. Brilman DWF, van Swaaij WPM, Versteeg GF (1998) Chemical Engineering and Processing 37:471
43. Brilman DWF (1998) Mass transfer and chemical reaction in gas-liquid-liquid Systems, Thesis Twente
44. Lin C, Zhou M, Xu CJ (1999) Chem Engng Sci 54:389
45. Junker BH, Wang DIC, Hatton TA (1990) Biotechnology Bioengineering 35:586
46. Nagy E (1995) Chem Engng Sci 50:827
47. Froment GF, Bischoff KB (1979) Chemical Reactor Analysis and Design, Wiley, New York
48. Nagy E (1998) Hung J Ind Chemistry 26:229
49. van Ede CJ, van Houten R, Beenackers AACM (1995) Chem Engng Sci 50:2911
50. Brilman DWF (1998) Mass transfer and chemical reaction in gas-liquid-liquid Systems, Thesis Twente, p 143
51. Mehra A, Sharma MM (1985) Chem Engng Sci 40:2382
52. Lekhal A, Chaudhari RV, Wilhelm AM, Delmas H (1997) Chem Engng Sci 52:4069
53. Chaudhary RV, Jayasree P, Gupte SP, Delmas H (1997) Chem Engng Sci 52:4197
54. Brilman DWF, Goldschmidt MJV, Versteeg GF, van Swaaij WPM (2000) Chem Engng Sci 55:2793
55. Lowe KC, King AT, Mulligan BJ (1989) Biotechnol 7:1037
56. Chandler D, Davey MR, Lowe KC, Mulligan B (1987) Biotechnol Letters 9:195
57. Chibata I, Yamada S, Wada M, Izuo N, Yamaguchi T (1974) US Patent 3 850 783
58. Adlercreutz P, Holst O, Mattiasson B (1984) Appl. Microbiol. Bitechnol 20:296
59. Munaretto F (1997) Evaluation of microencapsulated silicone oils as oxygen carriers in the production of dihydroxyacetone by *Gluconobacter oxydans*, Thesis, McGill University, Montreal
60. Danckwerts PV (1970) Gas-Liquid Reactions, McGraw-Hill, New York
61. Moser A (1981) Bioprocess Technology. Springer, Berlin Heidelberg New York
62. Schügerl K (1985) Bioreaktionstechnik Band 1. Salle+Sauerlaender, Frankfurt am Main
63. Sinclair CG, Ryder DN, (1975) Biotechnol Bioeng 17:375
64. Burden RL, Faires JD (1985) Numerical Analysis 3ed, Academic Press, Boston p.226
65. Nagy E (1996) 5th Word Congress of Chemical Engineering, San Diego Vol. III. p 711
66. Nagy E (1997) 11th Forum for Applied Biotechnology, Gent Vol. II. p 1573
67. Enfors SO, Hedenberg J, Olsson K (1990) Bioproc Eng 5:191
68. Kristiansen B (1994) Integrated design of a fermentation plant, the production of baker's yeast, VCH, Basel
69. Kristiansen B (1994) Integrated design of a fermentation plant, the production of baker's yeast, VCH, Basel, p 44

Received: July 2000

Microbial Sensors on a Respiratory Basis for Wastewater Monitoring

Klaus Riedel[1], Gotthard Kunze[2], Andreas König[3]

[1] Leobschützer Strasse 28, 13125 Berlin, Germany
[2] Institut für Pflanzengenetik und Kulturpflanzenforschung, Corrensstrasse 3, 06466 Gatersleben, Germany, e-mail: kunze@ipk-gatersleben.de
[3] Universität Stuttgart, Institut für Siedlungswasserbau, Wassergüte- und Abfallwirtschaft, Bandtäle 2, 70569 Stuttgart, Germany, e-mail: koenig@iswa.uni-stuttgart.de

In respect of their rapidity, their online capabilities, and their moderate costs, biosensing systems generally offer an attractive alternative to the existing methods of water analysis. Additionally, one particular advantage of microbial biosensors is the ability to measure direct effects on living cells, e.g., their respiratory activity and its alteration caused by environmental pollutants. It is true that microbial sensors, often do not provide the optimum solution for the determination of individual analytes when compared to established physico-chemical analysis methods. However, these biosensing devices are predestined for the summary determination of environmentally relevant compounds and their complex effects, respectively. For this reason, microbial sensors allow an integral evaluation of the degree of environmental pollution including the interaction of various compounds. Moreover, in some cases specific metabolic pathways in microorganisms are used, resulting in the development of microbial sensors for the more selective analysis for those compounds or pollutants, which cannot be measured by simple enzyme reactions, e.g., the determination of aromatic compounds and heavy metals.

This chapter gives an overview of microbiological biosensors on respiratory basis for the measurement of the following environmentally relevant compounds: inorganic N-compounds, heavy metals, organic xenobiotics and the estimation of sum parameters or so-called complex parameters such as BOD, ADOC, N-BOD, and the inhibition of nitrification.

Keywords. Microbiological biosensors, Wastewater, BOD, Nitrification, Organic compounds, Heavy metals

1 Introduction 82

2 Structure and Function of a Microbial Sensor 83

2.1 Design of a Microbial Sensor 84
2.2 Function and Specialties of Microbial Sensors 84

3 Applications of Microbial Sensors in Water Monitoring 86

3.1 General Considerations 86
3.2 Determination of Sum Parameters 86
3.2.1 Biochemical Oxygen Demand (BOD) 86
3.2.1.1 BOD-Sensors 86
3.2.1.2 Differences Between SensorBOD and BOD_5 87
3.2.1.3 Improvement of the Coincidence of SensorBOD and BOD_5 by Selection of Suitable Microorganisms 90
3.2.1.4 Improvement of the Coincidence of SensorBOD and BOD_5 by Pre-incubation of the Sensor with Wastewater 93

Advances in Biochemical Engineering/ Biotechnology, Vol. 75
Managing Editor: Th. Scheper
© Springer-Verlag Berlin Heidelberg 2002

3.2.1.5 Improvement of the Coincidence of SensorBOD and BOD_5 by Pretreatment of Wastewater Samples 94
3.2.1.6 Calibration of the BOD-Sensor 96
3.2.1.7 Modifications of Transducers for the Design of BOD-Sensors . . . 96
3.2.2 Determination of Available Dissolved Organic Carbon (ADOC) . 97
3.2.3 Determination of Toxicity 97
3.2.4 Determination of the Activity and the Inhibition of Nitrification . 98
3.3 Determination of Individual Substances 101
3.3.1 Determination of Inorganic Substances 101
3.3.1.1 N-Compounds 101
3.3.1.2 Inorganic S-Compounds 103
3.3.1.3 Heavy Metals 103
3.3.1.4 Cyanide 104
3.3.2 Determination of Organic Compounds 105
3.3.2.1 Phenols and Polycyclic Aromatic Hydrocarbons 105
3.3.2.2 Halogenated Aromatics 109
3.3.2.3 Detergents 111

4 Conclusion 111

References 112

List of Abbreviations

ADOC	Available Dissolved Organic Carbon
AOX	Adsorbate Fraction of Organic Halogenated Compounds
BOD	Biochemical Oxygen Demand
2,4-D	2,4-Dichlorphenoxy acid
LAS	Linear Alkylbenzene Sulfonates
PAH	Polycyclic Aromatic Hydrocarbons
PCB	Polychlorinated Biphenyls

1 Introduction

The increasing pollution of the environment especially with toxic compounds and substances presenting a potential human health risk is a problem of enormous importance. Therefore, a rapid and sensitive analytical control of the environment is necessary. In general, it is beneficial if analytical methods are simple and rapid to perform, if they have a sufficient sensitivity and precision and, finally, if all this is possible at reasonable costs. However, traditional instrumental analysis is very costly and time-consuming. As an example, the average cost of a laboratory analysis for environmental samples is in the range of $130– $200, whereas it is generally agreed that a price of $1 – $15 would be desirable [1].

All these requirements can be met with biosensors. Biosensors are the combination of a biological component consisting of microorganisms, enzymes, an-

tibodies, organelles, or cells from animals or plants in intimate contact with a physico-chemical transducer device, e. g., a kind of electrode. When the biological component reacts to an analyte in the sample, the transducer finally converts the biochemical reaction to a quantifiable electrical response signal.

Because of their high sensitivity, relatively long life, short response time, reasonable price, portability, and easy handling, biosensors particularly offer some distinct advantages for certain applications. For example, microbial sensors are especially suitable for environmental monitoring because of their ability to recognize a group of substances simultaneously, designated as multi-receptor behavior. It is also possible to follow multi-step transformations, which is difficult or even impossible to achieve with enzymatic sensing systems. A further advantage of microbial sensors is their physiological variability, which allows the adaptation to specific milieu conditions as well as the measurement of the response to toxic products. These capabilities are exploited for the determination of complex variables, such as the sum of biodegradable compounds in wastewater, e. g., the BOD and ADOC, as well as the detection of toxic effects in environmental samples.

Furthermore, microbial sensors are distinguished by a simple preparation procedure because extensive enzyme extraction and purification steps are not necessary [2]. Another important advantage of biosensors is their increased stability, because their biological component is a living system and therefore could be fed and kept alive for a long period. The inexhaustible reservoir of microorganisms with their wide spectrum of different metabolic types opens a wide field of applications concerning the use of microbial sensors for environment monitoring. One particular advantage is the ability to measure directly the respiratory activity of microorganisms and its alteration resulting from effects caused by the tested substances. This allows a relatively simple and rapid transduction of the microbial response by an oxygen electrode. About 80 % of all described microbial sensors are based on this principle.

2
Structure and Function of a Microbial Sensor

2.1
Design of a Microbial Sensor

The principal design of a microbial biosensor on respiratory basis is shown in Fig. 1. The main parts of such a biosensor are the microorganisms, acting as the recognition system, and an amperometric oxygen electrode, functioning as the physical transducer monitoring oxygen levels. In addition, it is also possible to determine the respiration activity by an optical principle [3] or by use of redox mediators, such as phenazine ethosulfate [4], ferricyanide [5], ferricyanide coupled with benzoquinone [6], or ferrocene, tetrathiafulvalene, and tetracyanoquinodimethane [7]. However, these mediators have the disadvantage, that they may exhibit a long-term toxicity to microorganisms, which impairs their longevity.

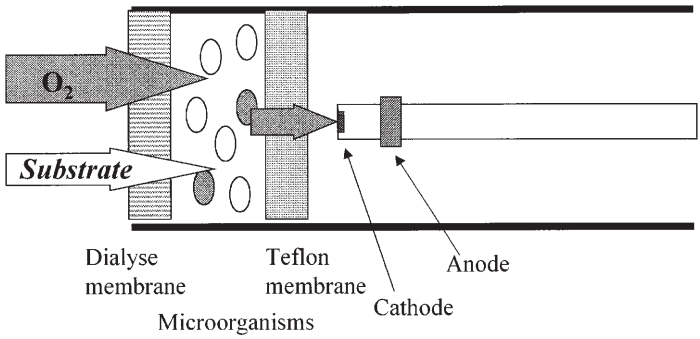

Fig. 1. Design of a respiratory-based microbial sensor

2.2 Function and Specialties of Microbial Sensors

Microbial sensors show important differences to biosensors containing biomolecules as their sensing component, such as enzymes, antibodies, or DNA. The act of sensing by biosensors based on biomolecules happens by selective molecular binding of a chemical analyte to the biocomponent, including an alteration of the analyte. In contrast to that, microbial sensors employ all possible physiological responses of living cells acting as the sensing component.

Basic requirements for such a "measurement" of physiological responses of microorganisms are very low "microbial loadings", suitable immobilization techniques for microorganisms, and the use of thin membranes [8]. Only if all these conditions are fulfilled is the sensitivity of a microbial sensor determined by the "cell activity" and not by diffusional limitation, allowing response times in a comparable order of magnitude to enzyme sensors. (Those biosensors with a relatively high concentration of biomass generally have response times significantly longer than enzyme sensors.) The behavior of microorganisms is a function of their physiological state, which is characterized under biosensor conditions by extreme nutrient limitation. Their metabolism is in a stand-by state to guarantee the survival of the cell [9].

Figure 2 shows a flow scheme of the physiological response, which includes the following steps:

1. Substrate uptake through the cell membrane: Solutes pass into the cells only via specific translocation systems, either by an active transport system or by facilitated diffusion; a passive transport by diffusion is of minor importance. Active transport allows accumulation of substrates against a concentration gradient. This requires high specificity carrier proteins and metabolic energy. The coupling to the cell energy-transducing systems, especially to the respiratory chain, is an important aspect of active transport.
2. The intracellular modification or degradation of the substrate by metabolic sequences of enzymatic systems under aerobic conditions in connection with the respiration processes. These processes result in an increased respiratory rate,

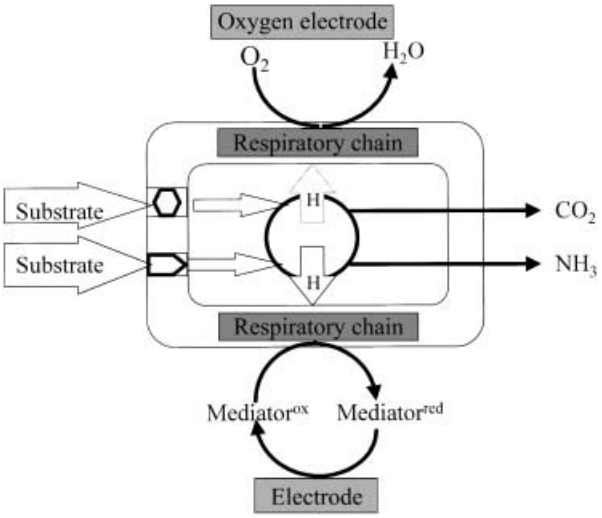

Fig. 2. Physiological responses of a respiratory-based microbial sensor

which subsequently leads either to a decrease of the "dissolved" oxygen concentration or to a reduction of the mediator in the microbial immobilizate.

3. Secretion or separation of metabolic products and by-products: For example, organic acids such as lactate and pyruvate, or other compounds like CO_2, ammonium ions, and H_2S are secreted as by-products.

For a sensor based on the respiration of microorganisms, the formation of the signal can be described as follows. Oxygen molecules diffuse from the air-saturated sample solution through the outer dialysis membrane, through the layer of immobilized microorganisms, and through the inner Teflon membrane, which covers the cathode. Finally, the oxygen molecules reach the cathode, where they get reduced. During this process, a small part of the oxygen molecules is consumed by the microorganisms, reflecting the microbial endogenous respiration. Adding assimilable substrates causes an increase of the respiration rate, resulting in a decrease of the "dissolved" oxygen concentration. This process is designated as "acceleration" of respiration [10].

In principle, there are two possible ways to measure this effect. First, there is the end-point measurement (steady-state mode), where the difference is calculated between the initial current of the endogenous respiration and the resulting current of the altered respiration, which is influenced by the tested substances. Second, by kinetic measurement the decrease or the acceleration, respectively, of the respiration with time is calculated from the first derivative of the current-time curve. The first procedure has been most frequently used in microbial sensors. These biosensors with a relatively high concentration of biomass have a longer response time than that of enzyme sensors. Response times of comparable magnitude to those of enzyme sensors are reached only with kinetically controlled sensors.

3
Application of Microbial Sensors in Water Monitoring

3.1
General Considerations

Micobial sensors have been described for the determination of more than 30 different environmentally relevant compounds, such as nitrite, nitrate, sulfate, phosphate, heavy metals as well as synthetic organic pollutants like aromatics and their halogenated derivatives (see for review [11, 12]). However, in most cases the detection limits obtained by biosensors are obviously too high for the use in monitoring drinking water samples according to maximum permissible concentration allowed by the national and international environmental protection legislations (for example EC Directives for Drinking Water). Moreover, the specificity is in most cases not satisfactory.

For these reasons, microbial sensors are less suitable for the determination of individual analytes. However, some practical applications for biosensors based on enzymes or antibodies for the specific determination of environmentally relevant compounds can be expected soon [11]. Furthermore, in some cases defined specific metabolic pathways in microorganisms are used, leading to microbial sensors for more selective analysis for those environmental pollutants which cannot be measured by the use of simple enzyme reactions, e. g., aromatic compounds and heavy metals. In this context it is also important to mention the aspect of bioavailability, a parameter which is included by the measuring procedure of microbial sensors as an integral effect.

Without doubt, the favored field of application of microbial sensors is the measurement of complex effects like sum parameters. The difficulties involved in analyzing the numerous substances that are present in wastewater samples make sum parameters an indispensable part of the wastewater monitoring systems. Additionally, sum parameters often allow a better evaluation of the status of the environment than the determination of the concentration of individual substances. Examples for complex parameters are the sum of biodegradable or bioavailable compounds and toxicity (BOD, ADOC).

3.2
Determination of Sum Parameters

3.2.1
Biochemical Oxygen Demand (BOD)

3.2.1.1
BOD-Sensors

The Biochemical Oxygen Demand (BOD) is an important parameter for wastewater monitoring. It gives information about the biodegradable organic pollution in wastewater. The main disadvantage of the conventional BOD-method is the required extended investigation time, which for example takes five days for

the measurement of the so-called BOD_5. For this reason, the conventional BOD allows only a subsequent evaluation of the wastewater after approximately one week and is therefore unsuitable for process control.

A more rapid estimation of BOD is possible by using a microbial sensor. The first report of such a microbial BOD sensor was published in 1977 [13]. Meanwhile some BOD-sensor systems are commercially available (see review in [11]). Table 1 gives an overview of the hitherto described BOD sensors including the manufacturers.

The rapid determination of BOD enables new possibilities in process control. Online measuring systems for process control have been developed and marketed by Nisshin Electric ("BOD-1100") and AUCOTEAM ("BODyline P") [11].

3.2.1.2 Differences Between SensorBOD and BOD_5

For the estimation of the suitability of microbial sensors for practical use, a sound evaluation of the applicability and the limitations of the method is necessary. As an example, the correlation to the conventional five-day test has to be investigated carefully. Repeatedly it has been described that the sensorBOD values are not in all cases identical to those of the BOD_5 [11] (see Tables 3 and 4).

Differences between both tests result from the different test principles. Biosensors use either a pure culture of microbes or a defined combination of several species of microorganisms with a fixed metabolic state, whereas for the conventional method an undefined bacterial population derived from activated sludge is used. In Sect. 3.2.1.3 it is shown that this obstacle can at least partly be overcome by the selection of suitable microorganisms for the BOD-sensor design.

It is also plausible that additional differences between the sensor and the five-day test result from the extremely different investigation time. While a measurement with a biosensor represents a short-time test for biological activity which only takes a few minutes, in this way providing a kind of "snapshot", the determination of BOD_5 measures the sum of various biochemical processes during a period of five days. These processes include the adaptation of the biocoenosis to different substrates by induction of those enzymes necessary for the degradation and the enzymatic hydrolysis of polymers. For these reasons, polymers such as starch, proteins, and lipids cannot be estimated by a BOD-sensor directly because the processes of enzyme induction and hydrolysis of these molecules cannot be carried out during the short measuring time. In Sects. 3.2.1.4 and 3.2.1.5, some possible solutions to improve the correlation of sensorBOD and BOD_5 values resulting from the different range of investigation times are listed.

For all these reasons, a microbial BOD-sensor needs to be calibrated before it can be used as a biochemical activity test. Only after a foregoing calibration procedure does a BOD-sensor finally reveal results which are both reliable and comparable to the conventional BOD_5 method. Some consideration concerning the calibration of biosensors are given in Sect. 3.2.1.6.

Table 1. Microbial species used for BOD-sensors based on amperometric oxygen determination and their parameters (it is noted when other transducer are used)

Microorganisms	Annotation (specialties; commercial BOD tools)	Measuring ing range[a] (mg l^{-1} BOD)	Measuring time (min)	Precision (%)	Stability (days)	Reference
Activated sludge		5–22	15	7.5	10	[13]
		3.5–40	0.3	5.6	2	[14]
Magnetic activated sludge	Magnetic oxygen electrode	< 60	30	5	n.d.	[15]
Unidentified strain 1–1		2–10[b]	n.d.	n.d.	30	[16]
Unidentified strain		3–33	6	1.3	48	[17]
Arxula adeninivorans		8–550[c]	1.1	5	30	[18, 19]
	Use of mycel	2–524[c]	1.1	5	60	[20]
Alcaligenes eutrophus	Resistant to heavy metals	0.35–3.66	0.5	4	30	[21]
Bacillus subtilis		2–22[c]	0.1–0.2	5	40	[22]
Bacillus polymyxa		1–45	15	6	60	[23]
Candida parapsilopsis	BSBmodul (Prüfgerätewerk Medingen GmbH Dresden)	2–33	< 1	< 10	30	[24, 25]
	BODpoint (AUCOTEAM GmbH, Berlin)	5–500 (with internal dilution)	<1	<10	30	[26–28]
Clostridium butyricum	Biofuel cells	50–300	30–40	10	30	[29]
Hansenula anomala		1–45	15–20	6–9	7	[30–33]
Photobacterium phosphoreum	Luminescence	5–120	15	7	n.d.	[34]
Pseudomonas putida	Arsenic resistant	1–66	8	n.d.	7	[35]
Pseudomonas sp.		1–45	13–20	6	20	[31]
Serratia marcescens		< 44	n.d.	n.d.	n.d.	[36]
Thermophilic bacteria		1–10	7	n.d.	40	[37]
Torulopsis candida		10–100	0.2	n.d.	45	[38, 39]
Trichosporon cutaneum (beigelii)	BOD-2000 (Nishin Electric & Co, Tokyo)	3–60	20–40	6	40	[40, 41]

Table 1 (continued)

Microorganisms	Annotation (specialties; commercial BOD tools)	Measuring ing range [a] (mg l^{-1} BOD)	Measuring time (min)	Precision (%)	Stability (days)	Reference
	Disposable sensor on silicon chip	0,2–18	20	8	3	[42]
	BODpoint (AUCOTEAM GmbH, Berlin)	5–500 (with internal dilution)	< 1	< 10	30	[22, 26–28, 43]
	BSBmodul (Prüfgerätewerk Medingen GmbH Dresden)	2–33	< 1	< 10	30	[22, 24, 25, 43]
	Optical oxygen determination (fluorescence)	1–110	5–10	5	30	[3]
Bacillus subtilis + B. *licheniformis*		10–300	4–15	5	22	[44]
Citrobacter sp. + *Enterobacter* sp.		6–18	8	< 11	n. d.	[45]
Rhodococcus erythropolis + *Issatchenkia orientalis*	ARAS, ECM Multi plus BSB (Dr. Bruno Lange GmbH Berlin)	2–300 [d]	< 1 (with hydrolysis of sample: 90 min)	< 5	30	[46–48]
	Thick-film Pt electrode	n. d.	5	n. d.	14	[49]
Lipomyces kononenkoae + *β-galactosidase*	Hydrolysis of lactose-containing wastewater	4–90	5	n. d.	n. d.	[50]
Tr. cutaneum (*beigelii*)+ protease +amylase		2–100	3	n. d.	n. d.	[51]
Tr. cutaneum+amylases	Hydrolysis of starch-containing wastewater	30–200	3.75	n. d.	14	[51, 52]

n. d. not determinable; [a] GGA: glucose glutamic acid standard; [b] Artificial wastewater [16]; [c] Glucose standard; [d] glycerol

3.2.1.3
Improvement of the Coincidence of SensorBOD and BOD_5 by Selection of suitable Microorganisms

The selection of appropriate microorganisms is a possible way to improve the correlation between BOD and BOD_5 [16, 53]. The prerequisite for the use of microorganisms for BOD-sensors is a wide substrate spectrum. Therefore several samples of activated sludge from different wastewater plants were investigated [13, 14]. One problem with an activated sludge based biosensor is the variability of sensor response with time. These BOD-sensors with an undefined variety of microbial species revealed no reproducible results. For that reason, BOD-sensors were developed using various types of defined cultures of microorganisms (Table 1).

Yeasts are specially suitable, because they are able to use a wide substrate spectrum combined with a wide measuring range.

Another way to increase the substrate spectrum of BOD-sensors is to combine various types of microorganisms, which exhibit different substrate sensitivities. Such a combined sensor containing *Bacillus subtilis* and *B. licheniformis* [44], *Citrobacter* sp., and *Enterobacter* sp. [45], or the bacterium *Rhodococcus erythropolis* and the yeast *Issatchenkia orientalis* is used in a commercialized BOD-sensor system [11, 46]. In these biosensors, the substrate sensitivities of both species associated, as shown by Riedel and Uthemann [54].

A recently described biosensor consisting of cells of the yeast *Arxula adeninivorans* showed a higher sensitivity to many of the substances listed in Table 2, when compared with BOD-sensors based on other microorganisms [18, 19, 55].

The superiority of the *Arxula adeninivorans*-containing sensor in comparison to the commercial BOD-sensor with *Issatchenkia orientalis* and *Rhodococcus erythropolis* is demonstrated in Table 3, where data of the determination of the BOD of different domestic wastewater are given [19].

Further substantial advantages of the yeast *Arxula adeninivorans* can be seen in its osmotolerance or halotolerance and thermoresistance [56]. These properties offer the possibility to estimate the BOD of wastewaters specifically from coastal and island regions as well as from tropical and subtropical zones. As an example, several investigations already demonstrated that the halotolerance of *A. adeninivorans* allows BOD measurements in salt water [57–60]. It is also worth noting that, depending on temperature, *A. adeninivorans* is able to grow as budding cells as well as in form of a mycelium [61]. The suitability of mycelia as the microbial component of a biosensor was tested by Tag et al. [20]. Their experiments showed that a mycelium-biosensor distinguishes itself by a better correlation between sensorBOD and BOD_5 compared with the cell-based sensor. In Table 4, the BOD-values obtained by the mycelium-sensor agree well with the conventional BOD_5 for 65% of the analyzed samples, if a deviation of 30% is allowed. The cell-biosensor meets this criterion only in 14% of the samples. Moreover, the mycelium-sensor is not influenced by NaCl up to a concentration of 30%, while the cell-based biosensor is able to measure salt water only up to 10% [20, 57, 59]. A further advantage of the mycelium-sensor is its storage sta-

Table 2. Comparison of sensitivity of BOD-sensors consisting of various species of microorganisms in to various substrates in relation to conventional BOD_5 as sensorBOD/BOD_5-ratio (substrate solution equivalent 275 mg l^{-1} BOD_5; calculation of sensorBOD-values with a glucose standard of measuring data according to Riedel and Kunze [55])

Substrate	Sensor BOD/BOD_5-ratio						
	Arxula adeninvorans	Issatchenkia orientalis	Candida lactiscondensi	Rhodococcus erythropolis	Pseudomonas putida	Alcaligenes sp.	Trichosporon cutaneum[b]
Glucose	1.00	1.00	1.0	1.0	1.0	1.0	1.1
Fructose	0.45	0.18	0.36	2.08	0.49	0.13	0.48 – 0.86
Galactose	0.80	0.07	0.02	0	0.33	0.22	n.d.
Ribose	0.01	0	0.01	0	0.06	0.07	n.d.
Xylose	0.41	0.11	0.03	0.03	0.23	0	n.d.
Sorbitol	0	0	0.02	0	0	0.16	n.d.
Sucrose	0.21	0.21	1.18	0.05	0.53	0	0.24 – 0.47
Lactose	0.07	0	0.04	0	0.08	0.67	0.01
Maltose	0.20	0.20	0.17	0.01	0.20	0	n.d.
Glucosamin	0.17	0.16	0	0.11	0.20	0.22	n.d.
Citric acid	0.03	0.07	0	0	0	0	1.0
Acetic acid	3.81	2.04	0.5	8.61	0.12	0.64	2.4
Ethyl alcohol	4.40	3.37	0.48	0.76	2.12	0.02	2.23
Glycerol	0.10	0.01	0.05	1.57	0.23	3.35	1.04
Alanine	1.36	0.47	0.4	0.49	1.36	0.36	0.75
Glycine	1.72	0.39	0.21	0.22	0.45	0.09	0.82
Glutamic acid	0.16	0.85	0.15	0.59	0.25	0.16	1.09
Lysine	0.76	0.11	0.08	0.03	0.61	0	n.d.
Methionine	0.69	0.34	0.09	0.16	0.28	0	n.d.
Tryptophan	0.17	0.10	0.13	0	0.05	0	n.d.
Butyric acid[a]	0.83	0.95	0.07	6.87	5.27	1.31	n.d.
Capron acid[a]	3.10	0.99	0.23	6.81	1.75	1.55	n.d.
Capryl acid[a]	5.01	0.51	0.68	6.9	4.36	2.44	n.d.
Caproic acid[a]	3.65	0.92	0.22	5.72	3.89	0.62	n.d.
Lauryl acid[a]	0.55	0.48	0.07	2.85	2.34	0.95	n.d.
Propionic acid[a]	0.70	0.40	0.05	5.47	0.08	0.07	n.d.
Oil	0.03	0.12	0.05	0.15	0.06	0.13	n.d.
Phenol	0	0.07	0.05	0.03	0.02	0.27	n.d.
Benzoate	0.02	0.07	0.04	0.03	0	0.56	n.d.

n. d. not determinable; [a] Na salt; [b] References: [40, 43]

Table 3. Comparison of BOD-values estimated by microbial sensor containing *Arxula adeninivorans* and a commercial biosensor containing *Issatchenkia orentalis* and *Rhodococcus erythropolis* with BOD determined by the five day method for various domestic wastewater samples [19]

Microbial BOD-Sensor		*Rhodococcus erthropolis* + *Issatchenkia orientalis*		*Arxula adeninivorans*	
Wastewater	BOD_5 [mg l^{-1}]	BOD	Ratio sensorBOD to BOD_5	BOD	Ratio sensorBOD to BOD_5
MW6	131	90	0.69	98	0.75
MW8	123	91	0.76	86	0.70
MW11	180	162	0.96	123	0.68
MW13	112	63	0.58	89	0.79
MW14	53	23	0.49	37	0.70
MW17	108	50	0.46	86	0.80
MW18	153	57	0.37	77	0.50
MW21	114	46	0.40	68	0.60
MW22	166	100	0.60	175	1.05
MW23	169	130	0.77	195	1.15
MW12	3	6	2.00	2	0.67
MW15	1	2	2.00	1	1.00
MW20	0	0		0	
MW24	3	2	0.67	3	1.00

Table 4. Comparison of BOD-values estimated by the cell- and mycelium-based *Arxula adeninivorans* biosensor with BOD_5 for various wastewater samples (i – influent, e – effluent) [20]

Microbial BOD-sensor		Cell-biosensor		Mycelia-biosensor	
Wastewater	BOD_5 (mg l^{-1})	BOD	Ratio sensorBOD to BOD_5	BOD	Ratio sensorBOD to BOD_5
MW2503i	82.6	50.3	0.6	121.2	1.5
MW2503e	43.2	23.8	0.5	34.0	0.8
MW0104i	59.0	42.3	0.7	40.7	0.7
MW0104e	38.6	16.2	0.4	15.0	0.4
MW2907i	116.6	51.8	0.4	124.0	1.1
MW2907e	33.7	16.7	0.5	20.5	0.6
MW0209i	52.3	27.7	0.5	54.2	1.0
MW0209e	46.4	16.8	0.4	27.7	0.6
MW0909i	49.5	32.3	0.6	42.8	0.9
MW0909e	34.3	10.0	0.3	14.0	0.4
MW1609i	19.6	27.0	1.4	22.5	1.2
MW1609e	32.9	9.3	0.3	28.2	0.9
MW2309i	28.2	36.8	1.3	26.3	0.9
MW2309e	30.2	1.0	0.1	29.5	1.0

bility of six months in comparison to cell-biosensors with three months stability only.

A general problem of microbial BOD-sensors could be poisoning of the cells by toxic substances in wastewater. One possibility to reduce or even to eliminate toxic effects on BOD-sensors is achieved by shortening measuring times down to not more than 1 min, in this way preventing toxic effects on the cells because of the short time of exposure to the toxic agents.

Moreover, the use of resistant strains is of interest. Slama et al. [21] described a heavy metal resistant BOD-sensor using *Alcaligenes eutrophus*, which contains plasmids encoding resistance to nickel, copper, cadmium, and zinc. An arsenic resistant BOD-sensor based on *Pseudomonas putida* was developed by Ohki et al. [35]. Another interesting possibility is the elimination of heavy metals by covering the BOD-sensor with a poly(4-vinylpyridine)-coated polycarbonate membrane [36] or poly(sodium styrene sulfonate) [62].

Unidentified microorganisms isolated from activated sludge [16, 17] or thermophile microorganisms from hot springs [37] were also used successfully. A rather unusual BOD-sensor with thermally-killed cells of *Bacillus subtilis* was described by Qian and Tan [63, 64]. The process of killing the bacteria was carried out by exposing the cell to a vacuum at 280 °C for 2.5 min.

3.2.1.4 Improvement of the Coincidence of SensorBOD and BOD_5 by Pre-incubation of the Sensor with Wastewater

The improvement of the correlation of sensorBOD and BOD_5 can also be achieved by incubating the biosensor for some hours in this wastewater sample, which has to be measured [53]. This allows the induction of all of the microorganisms required metabolic degradation systems [65]. As shown in Table 5, preincubated microbial sensors and the conventional BOD_5 method revealed similar results.

Table 5. Increase of sensor activity by adaptation to the appropriate substrate or wastewater incubation [53]

Substrate and wastewater	BOD sensor	BOD_5 (mg l^{-1})	SensorBOD (mg l^{-1})	
			Untreated	Induced
Fructose[a]	*Trichosporon*	0.71	0.44	0.60
Maltose[a]	*cutaneum*	0.49 – 0.76	0.02	0.15
Alanine[a]		0.55	0.19	0.41
OECD model wastewater		18,000	10,640	13,680
Chemical factory		726	470	853
Food factory		8000	4076	8764
Paper factory	*Issatchenkia* +	n.d	91	146
Municipal wastewater	*Rhodococcus*	n.d	15	46
Industrial wastewater		n.d.	14	34

[a] mg BOD/mg substance; n.d. not determinable.

3.2.1.5 Improvement of the Coincidence of SensorBOD and BOD_5 by Pretreatment of Wastewater Samples

Due to their short time of exposure to the sample, microbial sensors are generally not able to detect polymers. The time required for the microbial degradation of proteins, starch, or cellulose normally is considerable longer than the usually applied measuring time. This is one of the main reasons why the sensorBOD value of wastewater is in most cases lower compared to the BOD_5 method.

The pretreatment of wastewater with hydrolases or acids is one of the best ways to overcome this obstacle, because in this way the big polymer molecules can be decomposed to smaller units, which can be measured by the biosensor. The positive effect of an enzymatic pretreatment of wastewater prior to sensorBOD measurement was demonstrated [53, 66]. In these investigations, different types of wastewaters, which contained milk powder, starch, or cellulose, were treated by proteases, α-amylases, and cellulases or a mix of these enzymes, respectively. This pretreatment resulted in a good correlation between sensorBOD and the conventional five-day BOD, while the sensorBOD values for untreated wastewater were significantly lower (see Table 6). As an example, the sensorBOD of a wastewater from a paper factory increased approximately to the fourfold value when treated by a mixture of cellulase and β-glucosidase.

In general, the high specificity of enzymes limits the application of this method, because for the treatment of each wastewater sample it is necessary to use a special consortium of various types of enzymes. Therefore, for practical reasons the acid hydrolysis of wastewater is the preferred laboratory method for the pretreatment of polymers. By the use of acid hydrolysis for one hour at 148 °C with 6 mol/l HCl ("acid hydrolyse" kit from Dr. Lange GmbH Berlin 1996; [48]), the polymers are decomposed to their monomers such as monosaccharides, glycerol, fatty acids, or amino acids, respectively. The hydrolysis of wastewater caused in most cases an increase of the BOD measured (Table 6), resulting in an improved concurrence of sensorBOD and BOD_5 [53, 68].

However, this method also has some disadvantages. These are the relatively high expenditure of time as well as the use of high temperatures in connection with high concentrated aggressive acid. Furthermore, the measured values are partly higher than the data obtained by the conventional method. This effect is probably due to the more or less total decomposition by the polymers due to the crude chemical conditions used for acid hydrolysis. It is unlikely that in most cases BOD_5 samples such a high degree of decomposition occurs by microbial degradation only.

The decomposition of polymer molecules in wastewater samples can also be achieved by a hybrid sensor, which consists of a consortium of microorganisms and hydrolases together. As an example, the BOD of lactose-containing wastewater was determined by a hybrid sensor consisting of cells of the yeast *Lipomyces kononenkoae* and of the enzyme β-galactosidase [50, 69]. It is also possible to use a column containing immobilized enzymes, which is inserted in the measuring device (e.g., an FIA) before the biosensor [52, 70]. Such a combination of an enzyme column, which contains α-amylase and amy-

Table 6. Influence of the pretreatment of wastewater on the measured sensorBOD values

Wastewater	Procedure of pretreatment	BOD_5 ($mg\ l^{-1}$)	SensorBOD ($mg\ l^{-1}$)			Ratio of SensorBOD to BOD_5	Ref.
			Untreated	Treated	Increase		
Paper factory	Cellulase+β-Glucosidase	n.d.	10	29	2.9		[53]
Paper factory	Cellulase+β-Glucosidase	n.d.	44	75	1.8		[53]
Paper factory	Cellulase+β-Glucosidase	n.d.	5	21	4.2		[53]
Domestic	acid Hydrolysis	123	91	103	1.13	0.84	[53]
Domestic	acid Hydrolysis	112	63	103	1.63	0.92	[53]
Domestic	acid Hydrolysis	169	130	175	1.35	1.04	[53]
Artificial[a]	Protease +Amylase +Cellulase	947	173	660	3.82		[66]
River water	Ozonation	1.0	0.57	1.72	3.02	1.72	[67]
River water	Ozonation	5.3	4.86	5.47	1.13	1.03	[67]
River water	Ozonation	2.39	1.41	1.87	1.33	0.78	[67]
River water	Ozonation	8.89	8.98	9.4	1.05	1.05	[67]
River water	Ozonation	10.9	8.7	11.21	1.29	1.02	[67]

[a] Composition of artificial wastewater: starch, cellulose and milk powder [66].

loglucosidase, was used for the BOD determination of starch-containing wastewater.

A new and highly sensitive method for the decomposition of organic compounds based on preozonation is described by Karube and coworkers [67]. Using mild reaction conditions (pH 7) and a short reaction time of 3 min, ozonation of organic polymers in water leads to the formation of biodegradable compounds of lower molecular size. The high sensitivity of this procedure allowed the determination of the BOD of river waters in an order of magnitude down to 1 mg l^{-1}. Furthermore, these sensorBOD values correlated well with those determined by the conventional BOD_5.

3.2.1.6
Calibration of the BOD-Sensor

Another problem is the calibration of BOD-sensor to enable the comparison with the conventional BOD. For calibrating a BOD-sensor, a glucose-glutamic acid standard solution (the so-called GGA-standard), which is also used as standard solution for the BOD_5-method [71], or aqueous solutions of glucose or glycerol with a defined BOD_5 [43, 54] are used.

However, a calibration using one substrate only does not allow the measurement of the total activity of all enzymes provided by the microorganisms of a biosensor. Therefore, Tanaka et al. [16] favored a combination of specific compounds, such as beef extract, peptone, nitrohumic acid, tannic acid, ligninsulfonic acid, sodium lauryl sulfate, gum arabic, and minerals. The disadvantage is that these standards are probably unstable because they can be rapidly altered by microbial degradation. Recently, another way was used in the BOD-sensor measuring system ARAS of the company Dr. Bruno Lange GmbH, Germany [48]. This operation is a pure calculation of the calibration function without the use of a substrate. However, the applicability of this procedure is restricted to exactly defined milieu conditions only.

3.2.1.7
Modifications of Transducers for the Design of BOD-Sensors

The predominantly applied transducer device for BOD-sensors is the amperometric Clark-type oxygen probe [72, 73]. Recently, miniature oxygen electrodes were developed, which are also able to measure BOD [42]. These are the so-called disposable type sensors, due to their generally short operational lifetime of a few days only. The yeast cells of *Trichosporon cutaneum* were immobilized directly on a semiconductor device, which was fabricated on a silicon substrate by the use of micromachining techniques. This miniaturized BOD-sensor distinguishes itself by a high sensitivity with a detection limit of 0.2 mg l^{-1} BOD. Another miniaturized BOD-sensor measuring system was developed by Bilitewski and coworkers [49]. The immobilized microorganisms (*Rhodoccocus erythropolis* and *Issatchenkia orientalis*) were integrated in a flow-through system with a screen-printed electrode as transducer. The use of such flow-through

or flow injection analysis systems (FIA), respectively, has already been described by Riedel et al. 1990 [74] and by Sangeetha et al. 1996 [39].

An interesting modification in the field of transducer systems for BOD determinations is the construction of a magnetic oxygen electrode [21]. This system uses magnetically activated sludge, which is prepared by mixing magnetic powder with acclimated activated sludge.

The application of an optical transducer based on the fluorescence quenching effect of oxygen was described by Preininger et al. [3]. Another interesting technique is represented by the use of the luminous bacterium *Photobacterium phosphoreum* [34]. This device is based on the correlation of the intensity of luminescence to the cellular assimilation of organic compounds from the wastewater.

The use of a biofuel cell type electrode for BOD-determination has been described by Karube et al. [29]. The current generated by the biofuel cell results from the oxidation of hydrogen and formic acid produced from organic compounds by *Clostridia* under anaerobic conditions.

3.2.2
Determination of Available Dissolved Organic Carbon (ADOC)

The concentration of bioavailable organic carbon compounds, which is known as *a*vailable *d*issolved *o*rganic *c*arbon (ADOC), is an important parameter in microbial ecology. This parameter gives information about the state of the microbial metabolism and its regulation in the sediment of a lake and for that reason about the status of the lake itself. Several bioassays were used for determination of ADOC, especially by the growth of standardized pure cultures of heterotrophic microorganisms added to a filtered sample. Recently, a microbial biosensor containing the yeast *Rhodotorula mucilaginosa* was developed for the micro-scale measurement of ADOC [75, 76]. Calibration of this biosensor was achieved in mineral salt medium with glucose and the values of ADOC were declared as $\mu g\ ml^{-1}$ organic C. The use of such microbial sensor for ecological studies has some advantages in comparison to the hitherto used bioassays. It is possible to determine the ADOC directly in the sediment of sea by a response time of 10 s as demonstrated by Neundörfer and Meyer-Reil [75, 76]. Here it is necessary to declare the difference of ADOC and BOD. In principle the assimilable or bioavailable organic compounds are determined with BOD-sensor as well as ADOC-sensor. The difference results from the definition of both parameters in connection to the adequate calibration. ADOC is defines as organic carbon compounds ($\mu g\ ml^{-1}$). The sensorBOD must be in relation to BOD_5, which gives the oxygen demand for the degradation of organic pollutants in wastewater (see Sect. 3.2.1.1).

3.2.3
Determination of Toxicity

Measuring the increased oxygen resulting from the inhibition of respiration allows one to register the toxicity of wastewater. Toxic substances cause a reduction of the metabolic activity of the microorganisms used in the biosensor, resulting in a decrease of respiration.

The respirographic sensor system "RODTOX", marketed by KELMA NV, Belgium, allows the online determination of the toxicity of wastewater as well as of BOD [77, 78]. The biological part of this biosensor system consists of a reactor vessel containing activated sludge. The detection principle is the comparison of the calibration respirograms and respirograms from the wastewater samples showing, respectively, biodegradability or toxic effects. Moreover, the "RODTOX"-system is able to determine the specific activity of the biological sludge.

A further possibility is the use of a mediated amperometric biosensor incorporating activated sludge to provide rapid determination of toxicity [79]. The respiratory activity of this biosensor is determined by using the redox mediator *p*-benzoquinone.

3.2.4
Determination of the Activity and the Inhibition of Nitrification

Nitrification is a vital step in the process of biological elimination of nitrogen in sewage plants. The consortium of microorganisms involved in this process is usually very sensitive to many pollutants from different industrial and agricultural sources. The rapid detection of such pollutants is essential for processing of sewage.

König et al. [80–84] demonstrated that microbial sensors are suitable for the summary quantification of nitrifiable compounds (see also Sect. 3.3.1) as well as for the detection of nitrification inhibiting effects. Such biosensors, which contain a mixed population of the nitrifying bacteria *Nitrosomonas* sp. and *Nitrobacter* sp., exhibit a specific supplementary metabolic capacity. This enables the amperometric determination of ammonia according the following scheme of nitrification:

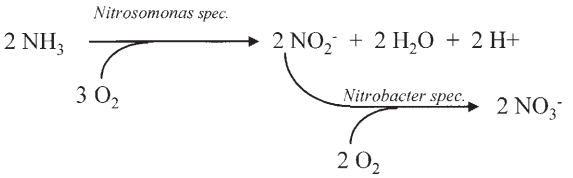

(1)

The oxygen demand by the nitrifying bacteria is therefore a measure of the ammonia concentration in the sample. For this rapid determination method a detection limit for ammonium in the ppb-range was observed. Because this biosensor reacts also to nitrite and urea, but shows only little reaction to other C-compounds (see Table 7), it is further suitable for the summary quantitation of nitrifiable N-compounds, the so-called N-BOD [85, 86]. This parameter can be useful for the control of aerobic wastewater treatment processes, due to the fact that the oxygen demand for nitrifiable N-compounds can make up to 20–40% of the total oxygen demand.

Furthermore, the detection of nitrification inhibitor compounds is possible in wastewater. The principle of detection of nitrification inhibition is shown in Fig. 3. When starting such investigations, the sensor is first exposed to a surplus of substrate (ammonium or urea). The basic current becomes stable at a low

Table 7. Sensibility of the nitrification biosensor to various C-compounds and amino acids [80, 83]

Substrate	Relative response (%)	Substrate	Relative response (%)	Substrate	Relative response (%)
Ammonium-N	100	Serine	15.7	Trypsine	2.7
Urea	98	Threonine	9.8	Glutamate	3.4
Nitrite	112	Glutamine	4.1	Alanine	2.0
Acetate	3.2	Asparagine	11.8	Glycine	1.5
Lactate	1.5	Arginine	3.1	Methionine	1.2
Ethanol	0.6	Leucine	5.0	Phenylalanine	1.8
Glycerol	0.3	Isoleucine	3.9	Proline	6.5
Citrate	0.1	Valine	2.4	Creatinine	0

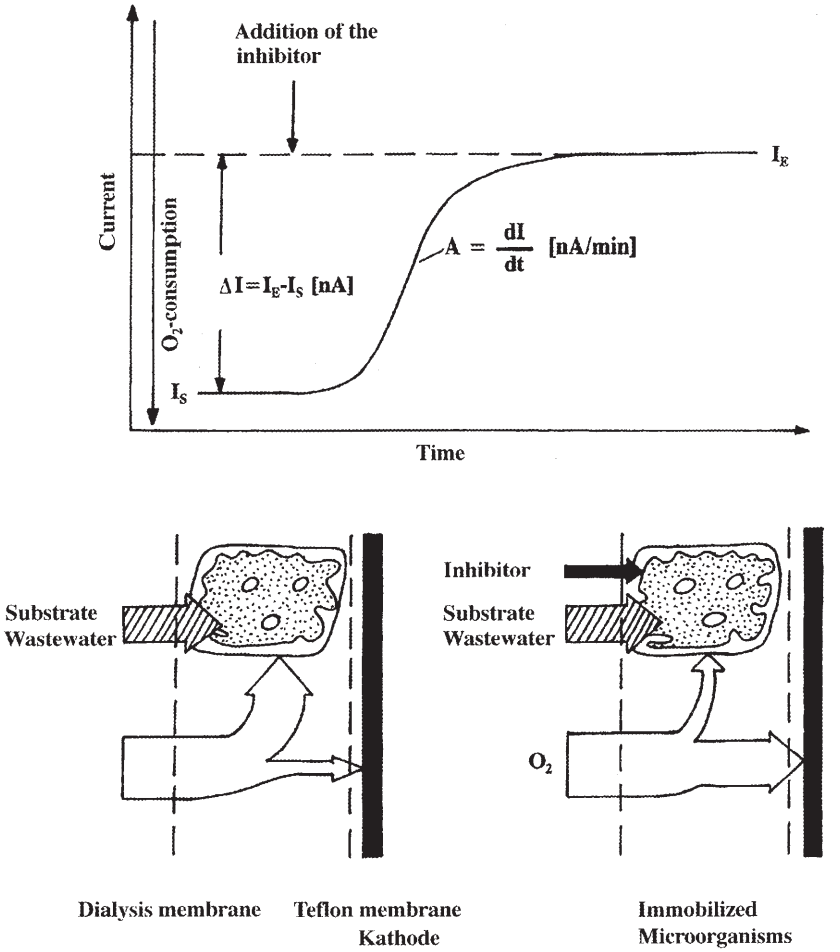

Fig. 3. Principle of detection of nitrification inhibiting effects with the nitrification biosensor

level, because under these conditions the oxygen consumption by the immobilizate increases to the maximum rate, and therefore the oxygen molecules diffuse through the bacterial immobilizate in relatively small amounts. The addition of an inhibitor leads to a rapidly decreased bacterial oxygen consumption. This results in an increased diffusion of oxygen through the bacterial immobilizate to the oxygen probe until a steady-state is registered by the Clark electrode.

Performing investigations with several pure substances which are known to act as nitrification inhibitors as well as investigations with polluted environmental samples demonstrated the suitability of the biosensor to detect nitrification inhibition (see Table 8).

Moreover, a substantial advantage of this microbial sensor over other existing tests for measuring the inhibition of nitrification is the very short measuring

Table 8. Determination of nitrification inhibition of pure substances and wastewater samples with nitrifiers containing biosensor [80, 82, 83]

Sample and annotations	IC_{50} (mg l^{-1})	Maximum inhibitory effect (%)
Allyl thiourea	1.2	100
Thiourea	0.8	100
2-Chlorophenol	0.1	100
p-Cresol	5.9	100
Aniline	8.2	93
Phenol	8.4	100
Styrol	28.9	100
p-Xylol	37.5	85
Benzene	28.4	100
Dimethylsulfoxide	49.0	85
Cu^{2+}-ions	187	100
Methanol	190	85
Acetonitrile	352	100
Cyanoguanidine	350	100
Ethyl acetate	360	100
Potassium chlorate	1400	100
Petrol	0.11	95
Alcohol solution from a fermentation process	0.9	100
Wastewater from a refinery	21	85
Enzymatic washing agent from textile industry	371	75
Vapor condensate from meat processing industry	180	100
Tannery wastewater samples: crude materials from the pretreatment of hides	n.i.	20 – 55 [a]
Various process wastewater samples from a tannery	n.i.	15 – 20 [b]
Effluent of a textile factory	n.i.	100
Deliming agent, used in tanneries	n.d.	Threshold effect: 25 g/l
Water sample from a fish farm	n.d.	Threshold effect: 500 ml/l

n.i. not investigated; n.d. not determinable; [a] Observed inhibitory effect at a dilution of 500 ml l^{-1}; [b] Observed inhibitory effect at a dilution of 20 ml l^{-1}.

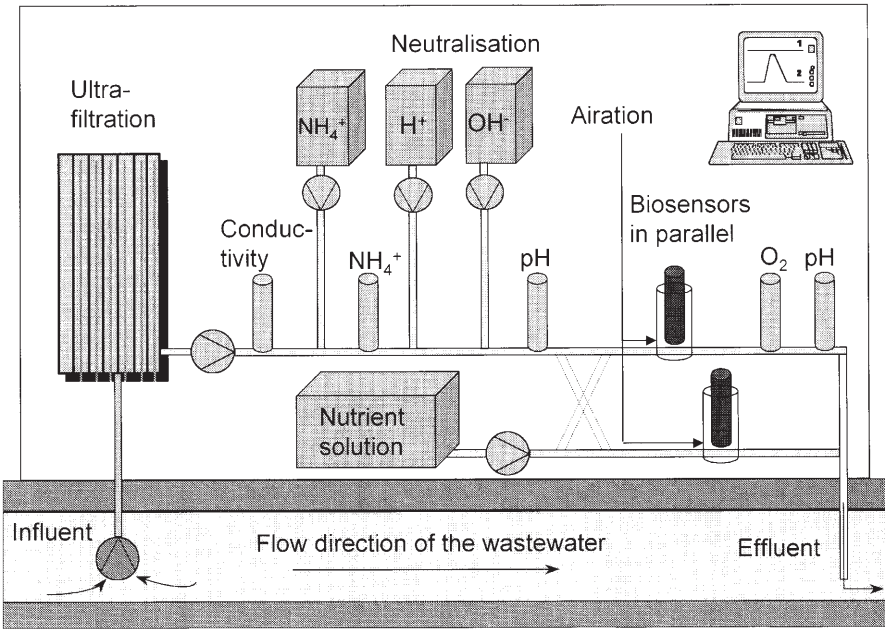

Fig. 4. Principle of function of the field device for online monitoring of inhibitors in sewage systems

time. This is the basis for the integration of this biosensor in a field testing plant for online monitoring of the sewage system directly in the wastewater stream (Fig. 4) [80].

With this testing system a municipal sewage plant influent was monitored for a period of a few months. As shown in Fig. 5, this measuring system allowed directly the rapid registration of toxic pollutants.

3.3 Determination of Individual Substances

3.3.1 *Determination of Inorganic Substances*

3.3.1.1 N-Compounds

In addition to the summary registration of nitrifiable substances, it is also possible to quantify N-compounds selectively by using microbial sensors. Microbial sensors for the monitoring of ammonium ions, ammonia, nitrite, nitrate and urea have been described (see Table 9). Nitrifiers are generally used, but not only (see also Sect. 3.2.4).

It is also possible to determine ammonium ions with microorganisms other than nitrifiers, e.g., with *Bacillus subtilis*, *Pseudomonas aeruginosa*, and

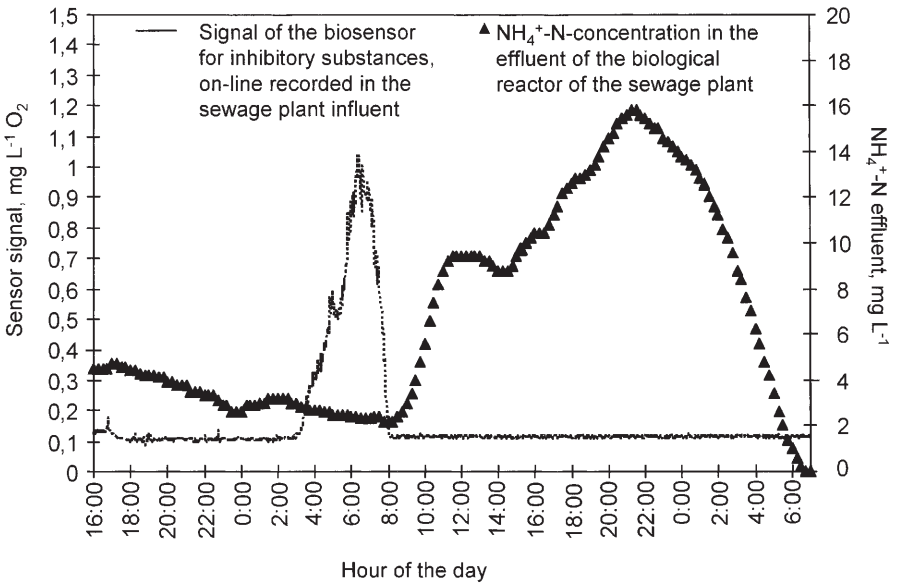

Fig. 5. Online detection of a pollutant in the influent stream of a municipal sewage plant with the nitrification biosensor installed in the testing plant in Fig. 4 (from [82])

Table 9. Determination of ammonium ions, ammonia, nitrite, nitrate, and urea with microbial biosensors on respiratory basis

N-Compounds	Microorganisms	Detection limit (mg l^{-1})	Response time (min)	Ref.
Ammonium ions	*Nitrosomonas europaea*	0.04	8	[87]
	Nitrifying bacteria	8.5	8	[88]
	Bacillus subtilis	0.2	0.1	[89]
	Nitrifying bacteria	0.03	0.5	[80–83]
	Nitrifying bacteria (disposable sensor)	0.05	2	[84]
Ammonia	Nitrifying bacteria	1	10	[90]
Nitrite	*Nitrobacter* sp.	2.3	10	[91]
	Nitrobacter vulgaris	0.5	3	[92]
Urea	Nitrifying bacteria + Urease	125	7	[93]

Trichosporon cutaneum [89]. The principle of this method is based on the measurement of the rapid alteration (or acceleration) of respiration after addition of ammonium ions in the presence of glucose. The physiological background of this principle is probably the uptake of ammonium ions in connection with the respiration process. Finally, the combination of nitrifying bacteria with urease on a hybrid sensor also allows an amperometric determination of urea [93].

3.3.1.2 Inorganic S-Compounds

Sulfor oxidizing bacteria oxidize sulfide and sulfite to sulfate. The decrease of oxygen [94, 95] as well as the alteration of pH [96] can be used as indicators of these reactions. With a *Thiobacillus thioparus*-containing sensor, a detected limit of 4 µmol/l sulfite is reached [94]. The detection limit of a sensor with *Thiobacillus thiooxydans* for sulfide is 0.02 mmol/l only [95].

3.3.1.3 Heavy Metals

Heavy metals are ubiquitously distributed in the environment and have a high potential human health risk because of their toxicity. An indicator of their toxicity is the "bioavailable" form which is more suitable than total heavy metal concentration. The determination of metal bioavailability is quite difficult or not possible, respectively, with chemical or physical methods. To solve this problem, biosensors can be used. Especially suitable are the microorganisms which are able to grow in metal contaminated areas. These microbes are usually adapted to the presence of toxic metal by genetically encoded resistance mechanisms. The regulation of the resistance gene expression has been utilized in the construction of specific sensor microorganisms, in which the strictly regulated promoter is connected to a sensitive reporter gene, such as the *lux* gene encoding for a luminescent protein or genes encoding for enzymes of metabolism and degradation of determined substrates in connection with respiration. Luminescence-based microbial sensors have been developed for the detection of some heavy metal: aluminum, mercury, cadmium, chromate, thallium, nickel, arsenic, aluminum, copper, zinc, and lead ions (see reviews at [97, 98]).

Recently, the amperometric determination of heavy metal with a microbial biosensor based on respiration has been made possible by combination of regulatory genes with structural genes, as demonstrated, for example, for the determination of Cu^{2+} with a *Saccharomyces cervisiae* strain [99, 100]. Moreover, plasmids were constructed containing the *CUP1* promoter of *S. cerevisiae*, which is induced by copper ions, fused to the *LacZ* gene of *E. coli*. Transformants containing such plasmids cannot utilize lactose as a carbon source. The fusion construct is therefore only transcribed and translated in solutions containing Cu^{2+}. When lactose is present in the measuring solution the transformed cells are able to utilize this substance as carbon source only in presence of Cu^{2+}. The function of this measuring principle is shown schematically in Fig. 6.

Therefore changes in oxygen consumption of lactose depend on the concentration of Cu^{2+}. A concentration range of 0.5 – 2 mmol l^{-1} $CuSO_4$ (15 – 60 mg l^{-1} Cu^{2+}) can be measured.

The ability of the chemolithoautotrophic bacteria *Thiobacillus ferrooxidans* to oxidize Fe^{2+} has already been utilized for construction of a microbial sensor for the determination of iron [101]. The limit of determination of this biosensor is 60 µmol l^{-1} with a response time ranging from 30 s to 5 min, depending on the Fe^{2+}-concentration in the sample.

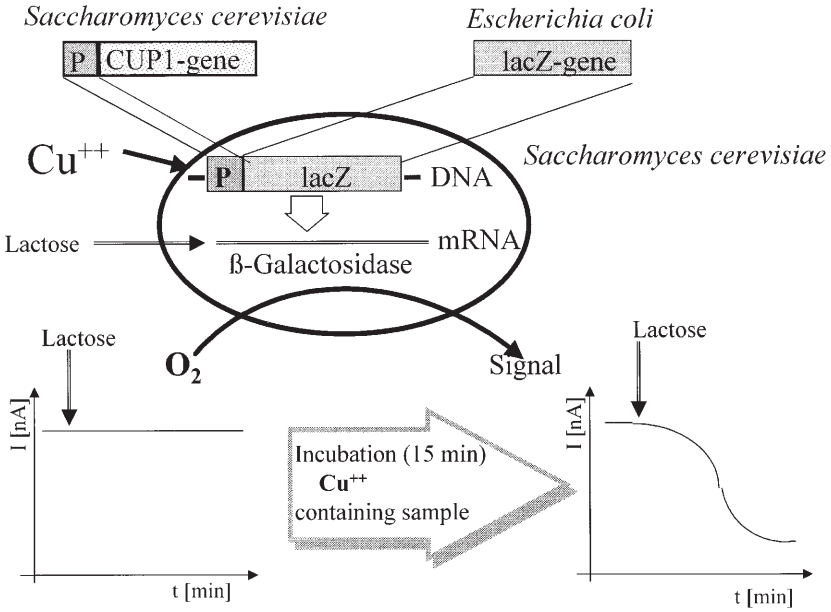

Fig. 6. Schematic design of a microbial sensor containing genetically manipulated yeast cell for detection of Cu^{2+}

3.3.1.4 Cyanide

The monitoring of cyanide with microbial sensor is possible in two ways. The first principle is based on the inhibition of respiration of *Saccharomyces cervisiae* by cyanide [102, 103]. This sensor showed a linear response in the range 0 – 15 µmol l^{-1} by a response time of approximately 10 min and a stability of 9 days. Another method for the determination of cyanide is enabled by the use of cyanide-degrading microorganisms such as *Pseudomonas fluorescens* [104]. This bacterium specifically oxidizes cyanide by consuming oxygen:

$$CN^- \xrightarrow[O_2]{\text{Pseeudomonas fluorescens } NADH_2 \;\; NAD^+} OCN + H_2O \xrightarrow{\text{Pseeudomonas fluorescens}} NH_3 + CO_2 \qquad (2)$$

With this sensor, concentrations between 0.1 ppm and 1 ppm of cyanide can be measured with a response time of less than 2 min. The cyanide-sensor shows a stability of some days only.

3.3.2 *Determination of Organic Compounds*

3.3.2.1 Phenols and Polycyclic Aromatic Hydrocarbons

Many phenols and their substitution products are used as disinfection and preservation agents. Furthermore, phenols also occur in human excretion products in daily amounts of 50 – 150 mg per individual. The appearance of phenols in surface waters and drinking water is undesirable because of their toxicity, their disadvantageous organoleptic properties, and their high potential for bioaccumulation. Polycyclic aromatic hydrocarbons also exhibit a high impact on the environment due to their toxicity, their carcinogenic potential, and their persistence in the biosphere. For these reasons, their monitoring is essential for environmental protection and wastewater management.

Biosensors based on specialized microorganisms are capable of degrading aromatics by oxygen consumption and allow rapid analyses. These microorganisms have adapted their metabolism to these xenobiotic chemicals, so that their metabolic enzymes are able to degrade those substances. In general, the process of aerobic degradation of aromatics shows a high similarity for all microbial species. The aerobic microbial degradation of aromatics is mainly performed by a common mechanism [105]. The initial reactions are the formation of diols (e.g., catechol) by dioxygenases, which are the key intermediates of aerobic degradation of aromatics. The following steps of cleavage via muconic acid and oxidation reactions may lead to complete mineralization. Due to the fact that the aerobic degradation of the various aromatics leads to mutual intermediates, microbial biosensors are relatively unspecific. Therefore, the key metabolite catechol or the corresponding diol of this substance causes a very high signal with all microbial sensors. The first step of degradation is most specific and inducible. However, in the detection of aromatic compounds it is important to register the total pool as sum parameters. Such parameters allow better evidence on the state of environment than the pure substances.

A way to obtain a highly sensitive microbial sensor for estimation of aromatic compounds was described by Priro and Garcia [106]. Such a microbial sensor has been constructed by coupling the transport system of the aromatic compound 4-hydroxyphenylacetate to a regulator circuit that controls the formation of β-galactosidase.

Microbial biosensors associated with respiration have been described for the following aromatics: phenol, benzoate, naphthalene, dibenzofuran, biphenyl, and benzene. Table 10 gives a survey of the characteristic parameters of these microbial sensors along with interfering substances.

It is to be noted that similar compounds and degradation products tend to interfere with the signal of the analyzed compounds. The severest interferences were observed for catechol and resorcinol, whereas cresols and chlorophenols had only little effect. Common substrates, such as glucose and amino acids, produced only low signals. A *Rhodococcus* P1, which has been isolated from sediment of the river Saale, in particular had a very high sensitivity to phenol and

Table 10. Microbial sensors for the detection of aromatic pollutants using oxygen electrodes

Analyte	Microorganisms	Detection limit [mg l^{-1}]	Standard deviation (%)	Response time (min)	Stability (d)	Specificity interferences	Reference
Phenol	*Rhodococcus* sp.	2	5	0.25	5	Chlorophenols	[107, 108]
	Escherichia coli	0.05	n. d.	30	n. d.	Chlorophenols, Pentachlorophenol	[109]
	Rhodotorula sp.	1	2	0.2	12	n.d.	[110]
	Pseudomonas putida	0.1	5	5	30	Nitrophenol, Pyrocatechol, Mesityl oxide, Aniline	[111, 112]
	Pseudomonas putida	0.1	7	0.1	14	Catechol	[113]
	Azotobacter sp.	2	n. d.	4	n.d	Hydroquinone, Catechol, Chinhydrone, 2,4-Dinitrophenol	[114]
Benzoate	*Rhodococcus P1*	2.8	n. d.	0.25	n. d.	Chlorophenols	[108]
	Pseudomonas putida	0.5	n. d.	0.25	n. d.	Chlorobenzoate	[115]
	Pseudomonas putida	0.25	7	0.1	14	Chlorobenzoate	[113]
Benzene	*Pseudomonas putida*	5	2 – 10	n. d.	n. d.	Toluene, o-Xylene, p-Xylene, m-Xylene, Ethylbenzene, Ethyltoluene, Chlorotoluene	[116]
Naphthalene	*Sphingomonas* sp. *Pseudomonas fluorescens*	3	3 – 5	5	20	Salicylate Toluene, o-Xylene, p-Xylene, m-Xylene, Ethylbenzene, Ethyltoluene, Chlorotoluene	[117]
Biphenyl	*Pseudomonas putida*	> 100	n. d.	0.25	n. Xd.	Catechol, 2,3-Dihydroxybiphenyl, Benzoate, Chlorobenzoate, Salicylaldehyde, Acetate	[118 – 121]
	Pseuomonas putida	0.3 – 0.4	n. d.	2.5 – 3	3	Catechol, Benzoate, Ethanol, Salicylate, Phenol, 2-Chlorobenzoate	[122]
	Rhodococcus globerulus (old name: *Coryne-bacterium* MB1)					Catechol, 2,3-Dihydroxybiphenyl, Phenol, Benzoate, Chlorobenzoate, PCB	[119, 121]

Table 10 (continued)

Analyte	Microorganisms	Detection limit [mg l^{-1}]	Standard deviation (%)	Response time (min)	Stability (d)	Specificity interferences	Reference
Dibenzofuran	*Sphingomonas* sp. *RW 1 1 (*old: *Pseudomonas* sp. *RW1)*	n.d.	n.d.	n.d.	n.d.	Phenol, Chlorophenols, Benzoate, Chlorobenzoate, Salicylaldehyde, Dihydroxybiphenyl	[118, 121]
	Pseudomonas sp. HH 693	n.d.	n.d.	n.d.	n.d.	2,3-Dihydroxy-benzofuran, Dihydroxy-biphenyls, Catechol, Phenol, Salicylaldehyde, 2,4-D acetate	[121]
Aniline	*Pseudomonas putida*	0.1	5	5	30	Phenol Pyrocatechol Mesityl oxide	[112]
Nitrophenol	*Pseudomonas putida*	2.4	n.d.	n.d.	n.d.	Phenol, Acetophenone, Cumene hydroperoxide	[111]
2-Ethoxy-phenol	*Rhodococcus rhodochorus*	5.5	n.d.	n.d.	n.d.	2-Methoxyphenol, Catechol, Glucose, Acetate	[123]

n.d. not determinable.

benzoate, but scarcely reacted to glucose. The specificity of this biosensor to phenol or benzoate could further be improved significantly either by cultivation of *Rhodococcus* P1 cells or by direct induction of the biosensor with the desired aromatic compound (see Table 11) [107]. The incubation of a sensor containing phenol-cultivated cells with benzoate also results in an excessive increase of the signal for this compound. Therefore, this *Rhodococcus* species is especially suitable for phenol or benzoate analysis.

Similar results were obtained with a *Pseudomonas putida* biosensor [113]. Phenol-induced cells showed little cross reaction to other compounds. This sensor did not react to benzoate. Detection of benzoate is possible only with cells grown on benzoate.

Pseudomonas putida GFS-8-containing biosensors enable the determination of aniline with a relative activity of 71% compared to phenol [112]. Furthermore, it is possible to determine 2-ethoxyphenol with a *Rhodococus rhodochorus* 116-containing sensor, despite the fact that the chemically similar compound 2-methoxyphenol and the degradation product catechol as well as glucose and acetate also led to a detectable signal [123]. This microbial sensor reacted to 2-ethoxyphenol with a higher signal than with glucose.

An amperometric biosensor consisting of *Pseudomonas putida* ML2 is suitable for the determination of benzene in terms of sensitivity and specificity [116]. The sensitivity of interfering compounds was less than 2.5% in relation to benzene.

Moreover, the sensitivity of biosensors containing *Sphingomonas* sp. or *Pseudomonas fluorescens* allowed the specific determination of the polycyclic aromatic hydrocarbon (PAH) naphthalene, although both biosensors showed relatively high responses to salicylate and acetate [117]. However, the remarkably low limit of detection obtained by these biosensors of 10 $\mu g\ l^{-1}$ naphthalene was not sufficient for the monitoring of drinking water, due to the prescribed upper limit for the concentration of PAH in drinking water of 0.2 $\mu g\ l^{-1}$.

It is also possible to determine other PAH with microbial sensors, as demonstrated for dibenzofuran with *Pseudomonas* sp. HH693 and *Sphingomonas* sp. *RW 1* (old designation: *Pseudomonas* sp. *RW1)* [121] as well as for biphenyl using *Rhodococcus globerulus* (old designation: *Corynebacterium* MB1 and *Pseudomonas putida*) [118–122]. However, the signal for these analytes is very

Table 11. Improvement of specificity and sensitivity of a *Rhodococcus* containing biosensor by cultivation or incubation with phenol or benzoate (substrate concentration: 20 $\mu mol\ l^{-1}$) [107]

Analyte	Signal ($nA\ min^{-1}$)			
	Cultivation with		Incubation of "benzoate"-cells with	
	Phenol	Benzoate	Phenol	Benzoate
Glucose	0	0	36	0
Phenol	166	0	206	0
Benzoate	0	427	560	677

low. The metabolic intermediates of these compounds, like 2,3-dihydroxybenzofuran, 2,3-dihydroxybiphenyl, catechol, and phenol, as well as various similar compounds, led to even higher signals than dibenzofuran and biphenyl by themselves. The relatively poor sensitivity and specificity attained for these sensors has not yet allowed practical applications.

The mean problem when measuring many aromatics and their halogenated derivatives is their hydrophobicity. For that reason it is desirable that these compounds be measured in non-polar organic solvents. It was demonstrated, that the response of a *Rhodococcus globerulus* (old name *Corynebacterium* MB1) containing biosensor to 2,3-dihydroxybiphenyl in decane or octane remained constant for up to 60 min [119]. The use of *n*-hexane in a biosensor system based on *Pseudomonas putida* increased the sensitivity for phenol fivefold, the measurement frequency sixfold, and operational stability was 7 h [113].

3.3.2.2 Halogenated Aromatics

Halogenated hydrocarbons have an extended field of industrial applications, e. g., as solvents and dilutions, as degreasing and extraction agents, for chemical cleaning, as refrigerants, fire extinguishing agents, propellant gases, as disinfectants and preservatives, plastic materials and plasticizers, stabilization agents, wood preservatives, pesticides, detergents, pharmaceuticals, etc. The analytical control of haloaromatic compounds is of substantial significance, because these substances are classified as dangerous to the environment due to their toxicity and persistence.

Fortunately, some microbial species are capable of degrading such chemicals [124–126]. This ability is used for the development of microbial sensors for chloroaromatic compounds (see Table 12).

In general, the observed specificity of these microbial sensors is very poor because of the degradation mechanism and the non-specific degradation enzymes. On the other hand, this low specialty favors the possibility of the determination of sum parameters of the desired halogenated aromatics, analogue to the sum parameter AOX (*a*dsorbable *o*rganic *h*alogen). *Pseudomonas putida* 87 was successfully used to determine 3-chlorobenzoate, although the signal for this compound only was 39% of the signal for the non-chlorinated benzoate [115]. The sensitivity for further mono- and dichlorobenzoates as well as for chlorophenols was comparatively low. *Pseudomonas* a*eruginosa* is specifically suitable for the determination of 2,5-dichlorobenzoate [122].

The determination of chlorinated phenols was possible with biosensors containing *Rhodococcus* sp. P1 [108] or *Trichosporon beigelii (cutaneum)* [127]. The *Rhodococcus*-sensor allowed an overall determination of mono- and dichlorophenols with a sensitivity for mono- and dichlorinated phenols on an average 30–40% in relation to phenol. Moreover, a sensitive determination of chlorophenols was possible with a *Trichosporon beigelii (cutaneum)*-containing sensor [127]. The signals for the mono- and dichlorinated phenols were markedly higher than for phenol itself. Notwithstanding this high specificity, the attained detection limit of 50 μg l^{-1} of chlorophenols means that this sensor is

Table 12. Microbial sensors for the determination of chlorinated phenols and benzoates

Analyte	Chlorobenzoates		Chlorophenols	
Main substrate	3-Monochloro-benzoate	2,5-Dichloro-benzoate	4-Mono-chlorophenol	4-Mono-chlorophenol
Microorganisms	*Pseudomonas putida* 87 [115]	*Pseudomonas aeruginosa* [122]	*Rhodococcus* sp. P1 [108]	*Trichosporon beigelii (cutaneum)* [127]
Detection limit [mg l^{-1}]	50	1.5 – 2.0	0.4	0.2
Standard deviation [%]	5.5	n.d.	5.5	5.5
Sensitivity (%) [a]				
Benzoate	100	100	14	0
3-Monochlorobenzoate	39	n.d	8	42
2-Monochlorobenzoate	9	150	11	0
4-Monochlorobenzoate	24	90	1	0
2,4-Dichlorobenzoate	6	n.d.	2	n.d.
2,5-Dichlorobenzoate	n.d.	270	n.d.	n.d.
Phenol	0	0	100	100
2-Monochlorophenol	n.d.	n.d.	43	373
3-Monochlorophenol	9	n.d.	45	875
4-Monochlorophenol	4	n.d.	53	1167
2,3-Dichlorophenol	n.d.	n.d.	36	538
2,4-Dichlorophenol	4	n.d.	20	725
2,6-Dichlorophenol	n.d.	n.d.	15	1077
3,4-Dichlorophenol	n.d.	n.d.	20	n.d.
2,3,6-Trichlorophenol	n.d.	n.d.	7	Inhibition
2,4,6-Trichlorophenol	n.d.	n.d.	8	Inhibition
2,4,5-Trichlorophenol	n.d.	n.d.	11	Inhibition
Catechol	n.d.	340	n.d.	n.d.
Salicylate	n.d.	300	n.d.	n.d.
Glucose	2	< 50	0	n.d.

n.d. not determinable; [a] In relation to the basic aromatic compounds benzoate or phenol, respectively.

not yet suitable for practical application, because the permissible concentration in drinking water is 0.5 µg l^{-1} phenols (EC Directive for Drinking Water, German Drinking Water Ordinance).

Microorganisms capable of degrading polychlorinated biphenyls (PCB) have been isolated and used in biosensors to determine these important group of xenobiotics. Table 13 shows that the sensors reacted to PCB, but the sensitivity and specificity was not sufficient for the specific determination of PCB for all used microorganisms [119 – 121].

Furthermore, the use of *Ralstonia eutropha* JMP134-containing sensors for the determination of the herbicide 2,4-dichlorophenoxyacetic acid (2,4-D) has been described [118, 121]. This sensor was sensitive to 2,4-D and 2,4,5-T (2,4,5-trichlorophenoxyacetic acid) with a detection limit of 40 mg l^{-1} with a response time of 15 s. Moreover, catechol, benzoic acid, and salicylaldehyde caused higher signals, but no or very little signal was obtained for phenol, biphenyl, and the usual substrates such as glucose, fructose, ethanol, and acetate.

Table 13. Relative PCB-activity of microbial sensors in relation to 3-PCB [119–121]

	Ralstonia eutropha H850 (old name: *Alcaligenes eutrophus)*	*Rhodococus globerulus* (old name: *Corynbacterium* sp. *MB1)*	*Pseudomonas LB400*
3-PCB	100	100	100
2,2′-PCB	50	150	105
2,3-PCB	130	136	100
2,2′,4,4′,5,5′-PCB	205	120	45
3,3′,4,4′-PCB	115	200	140
PCB Mix	24	60	116
Interfering compounds			
Biphenyl	156	308	44
Dibenzofuran	246	85	18
2,3-Dihydroxybiphenyl	1568	1162	318
Catechol	1064	517	164
Phenol	0	600	0
Benzoic acid	61	520	65

3.3.2.3 Detergents

Domestic wastewater contains a large amount of detergents, especially anionic surfactants, such as linear alkylbenzene sulfonates (LAS). A sensitive biosensor containing *Trichosporon cutaneum* has been developed in Japan and used to monitor river water [128, 129]. With this sensor a detection limit of 0.2 mg l^{-1} LAS has been reached.

4 Conclusion

Microbiological biosensors associated with respiration have a high potential for practical analytical applications in environmental protection. The alteration of respiration as a physiological response of sensor-microorganisms is relatively simple to measure and allows the use of the oxygen electrode as a transducer system for many similar applications. The main area of application for this type of biosensor is the determination of complex environmentally relevant compounds or effects that allow an integral evaluation of the environment including the interaction of these chemicals. This refers to the determination of sum parameter such as BOD, ADOC, and N-BOD, the monitoring of nitrification toxicity, as well as the overall sum-values for groups of compounds such as organic pollutants.

Microbial sensors are less suitable for the determination of individual analytes. However, in some cases, specific metabolic pathways are used, allowing microbial sensors to be more selective for those xenobiotic compounds, which are not detectable with simple enzyme reactions, e.g., aromatic compounds and

heavy metals. In this context, the aspect of bioavailability, which can be registered by the integral properties of microbial sensor measurements, plays an important role.

However, up till now there has been a certain discrepancy between research and development of biosensors on the one hand and their practical application on the other. Only very few biosensors are commercially produced and used on a large scale, like the microbial BOD-sensor. This situation is mainly due to the insufficient stability of microorganisms in comparison to chemical and physical methods under conditions of practical applications. In some cases, microbial sensors also suffer from relatively poor selectivity and sensitivity.

As an outlook, the optimization of the efficiency of microorganisms with methods of genetic engineering will result in an increased sensitivity, selectivity, and stability, in connection with the further miniaturization of biosensor systems, especially the development of portable biosensor measuring devices, represents a promising feature for environmental monitoring by microbial sensors.

Acknowledgement. We thank M.W. Leckenby for the careful review of this manuscript and helpful suggestions.

References

1. Rogers KR (1995) Biosensors for environmental application. Biosens Bioelectron 10:533–541
2. Riedel K (1998) Microbial biosensors based on amperometric detection. In: Mulchandani A, Rogers KR (eds) Enzyme and microbial biosensors: technicals and protocols. Humana Press, Totowa, pp 199–223
3. Preininger C, Klimant I, Wolfbeis OS (1994) Optical fiber sensor for biological oxygen demand. Anal Chem 66:1841–1846
4. Turner APF, Ramsay G, Higgin IJ (1983) Application of electron transfer between biological systems and electrodes. Biochem Soc Trans 11:445–448
5. Richardson NJ, Gardner S, Rawson DM (1991) A chemical modified amperometric biosensor for monitoring eubacterial respiration. J Appl Bact 70:422–426
6. Turner APF, Gardosi MF, Ramsay G, Schneider BH, Swain A (1986) Biosensors for use in the food industry: a new rapid bioactive monitor. In: Biotechnology in the food industry. Online Publ, Pinner, UK, pp 97–116
7. Kaláb T, Skládal P (1994) Evaluation of mediators for development of amperometric microbial bioelectrodes. Electroanalysis 6:1004–1008
8. Riedel K, Renneberg R, Liebs P (1988) Biochemical basis of kinetically controlled microbial sensors. Bioelectrochem Bioenerg 19:137–144
9. Riedel K (1991) Biochemical fundamentals and improvement of selectivity of microbial sensors – a minireview. Bioelectrochem Bioenerg 25:19–30
10. Riedel K, Liebs P, Renneberg R (1985) An electrochemical method for determination of cell respiration. J Basic Microbial 25:51–56
11. Riedel K (1998) Application of biosensors to environmental samples. In: Ramsay G (ed) Commercial biosensors: application to clinical, bioprocess and environmental samples. Wiley, New York, pp 267–294
12. Bilitewski U, Turner APF (2000) Biosensors for environmental monitoring. Harwood Academic, Amsterdam
13. Karube I, Mitsuda S, Matsunaga T, Suzuki S (1977) A rapid method for estimation of BOD by using immobilized microbial cells. J Ferm Technol 55:243–248

14. Liu J, Björnsson L, Mattiasson B (2000) Immobilised activated sludge based biosensor for biochemical oxygen demand measurement. Biosens Bioelectron 14:883–893
15. Sakai Y, Abe Y, Takahashi F (1995) BOD sensor using magnetic activated sludge. J Ferment Bioeng 80:300–303
16. Tanaka H, Nakamura E, Minamiyama Y, Toyoda T (1994) BOD biosensor for secondary effluent from wastewater treatment plants. Water Sci Tech 30:215–227
17. An L, Niu H, Zeng H (1998) A new biosensor for rapid oxygen demand measurement. Water Environ Res 70:1070–1074
18. Riedel K, Lehmann M, Adler K, Kunze G (1997) Physiological characterization of a microbial sensor containing the yeast *Arxula adeninvorans* LS3. Anthonie van Leeuwenhoek 71:345–351
19. Riedel K, Lehmann M, Tag K, Renneberg R, Kunze G (1998) *Arxula adeninivorans* based sensor for the estimation of BOD. Anal Lett 3:1–12
20. Tag K, Lehmann M, Chan C, Renneberg R, Riedel K, Kunze G (2000) Measurement of biodegradable substances with a mycelia-sensor based on the salt tolerant yeast *Arxula adeninivorans* LS3. Sensors Actuators B67:142–148
21. Slama M, Zaborosch C, Spener F (1995) Microbial sensor for rapid estimation of Biochemical Oxygen Demand (BOD) in presence of heavy metal ions. In: Wilken R-D, Förster U, Knödel A (eds) Heavy metals in the environment. CEP Consultants, Edinburgh, vol 2, pp 171–174
22. Riedel K, Renneberg R, Kühn M, Scheller F (1988) A fast estimation of biochemical oxygen demand using microbial sensor. Appl Microbial Biotechnol 28:316–318
23. Su YC, Huang JH, Liu ML (1986) A new biosensor for rapid BOD estimation by using immobilized growing cell beads. Proc Natl Sci Counc B ROC 10:105–112
24. Szweda R, Renneberg R (1994) Rapid BOD measurement with the Medingen BOD-module. Biosens Bioelectron 9:IX–X
25. Klinger E, Merten H (1992) Meßsystem für die Abwasserkontrolle. Mikroelektronik 6
26. Merten H, Neumann B (1992) BSB-Kurzzeitmessung mit Biosensor. BioTec 6
27. Merten H, Gehring S (1995) BSB-Kurzzeit-Messung mit Biosensoren in kommunalen Klärwerken.WWT Waserwirtschaft Wassertechnik (Berlin) 3:2–6
28. Merten H, Röding B, Kelm S, Mallon I, Noack J, Titze J (1994) Einsatzerfahrungen mit BSB-Kurzzeit-Meßgeräten bei der Situatuionsanalyse im Betrieb mit einer Fuzzy-Steuerung in einem kommunalen Klärwerk Brandenburgs. In: Kunze PM, Heesen te D, Köhne M, Schwedt G (eds) 3. TAE-Symposium: Erfahrungen mit Analysen- und Prozeßmeßgeräten in Abwasserreinigungsanlagen. Esslingen
29. Karube I, Matsunaga T, Mitsuda S, Suzuki S (1977) Microbial electrode BOD sensor. Biotechn Bioeng 19:1535–1547
30. Kulys J, Kadziauskiene K (1980) Yeast BOD sensor. Biotechn Bioeng 22:221–226
31. Li YR, Chu J (1991) Study of BOD microbial sensors for wastewater treatment control. Appl Biochem Biotechnol 28:855–863
32. Ihn GS, Park KH, Pek UH, Moo Jeong (1992) Microbial sensor of biochemical oxygen demand using *Hansenula anomala*. Bull Korean Chem Soc 13:145–148
33. Sohn M-J, Hong D (1993) Comprehension of the response time in a microbial BOD sensor (II). Bull Korean Chem Soc 14:666–668
34. Hyan C-K, Tamiya E, Takeuchi T, Karube I (1993) A novel BOD sensor based on bacterial luminescence. Biotechnol Bioeng 41:1107–1111
35. Ohki A, Shinohara K, Maeda S (1990) Biological oxygen demand sensor using an arsenic resistant bacterium. Anal Sci 6:905–906
36. Kim M-N, Kwon H-S (1999) Biochemical oxygen demand sensor using *Serratia marcescens* LSY 4. Biosens Bioelectron 14:1–7
37. Karube I, Yokoyama K, Sode K, Tamiya E (1989) Microbial BOD sensor utilizing thermophilic bacteria. Anal Lett 22:791–801
38. Rajasekar S, Madhav VM, Rajasekar R, Jeyakumar D, Rao GP (1992) Biosensor for the estimation of biological oxygen demand based *Torulopsis candida*. Bull Electrochem 8:196–198

39. Sangeetha S, Sugandhi M, Murugesan M, Murali M, Berchmans S, Rajasekar R, Rajasekar S, Jeyakumar D, Prabhakara RG (1996) *Torulopsis candida* based sensor for the estimation of biochemical oxygen demand and its evaluation. Electroanalysis 8:698–701
40. Hikuma M, Suzuki H, Yasuda T, Karube I, Suzuki S (1979) Amperometric estimation of BOD by using living immobilized yeasts. Eur J Appl Microbiol Biotechn 8:289–297
41. Nomura Y, Chee G-J, Karube I (1998). Biosensor technology for determination of BOD. Field Anal Chem Technol 2:333–340
42. Yang Z, Suzuki H, Suzuki S, Karube I (1996) Disposable sensor for biochemical oxygen demand. Appl Microbiol Biotechnol 46:10–14
43. Riedel K, Lange KP, Stein HJ, Kühn M, Ott P, Scheller F (1990) A microbial sensor for BOD. Water Res 24:883–887
44. Tan TC, Li F, Neoh KG, Lee YK (1992) Microbial membrane-modified dissolved oxygen probe for rapid biochemical oxygen demand measurement. Sensors and Actuators B 8:167–172
45. Galindo E, Garcia JL, Torres LG, Quintero R (1992) Characterization of microbial membranes used for the estimation of biochemical oxygen demand with a biosensor. Biotechnol Techniques 6:399–404
46. Riedel K, Kloos R, Uthemann R (1993) Minutenschnelle Bestimmung des BSB. WBL Wasser, Boden und Luft 11/12:35–38
47. Riedel K (1994) Microbial sensors and their application in environment. Exp Technique of Physics 40:63–76
48. Grabert E, Kloos R (1999) Der SensorBSB der zweiten Generation als schnelle und einfache Alternativmethode zur herkömmlichen BSB_5-Bestimmung. Kommunalwirtschaft 1999/4:176–180
49. Heim S, Schmieder I, Binz D, Vogel A, Bilitewski U (1999) Development of an automated microbial sensor system. Biosens Bioelectron 14:187–193
50. Reiss M, Tari A, Hartmeier W (1993) BOD-Biosensor basing on an amperometric oxygen electrode covered by *Lipomyces kononenkoae*. Bioengineering 9:87
51. Riedel K, Renneberg R, Lange K-P, Ott P, Scheller F (1990) Mikrobiologisches Sensorsystem zur Bestimmung des "Biochemischen Sauerstoffbedarfs" (BSB) von komplex zusammengesetzten, höhermolekulare Verbindungen enthaltenden Medien. DD-Pat 275, 379
52. Reiss M, Heibges A, Metzger J, Hartmeier W (1998) Determination of BOD-values of starch-containing wastewater by a BOD-biosensor. Biosens Bioelectron 13:1083–1090
53. Riedel K (1997) Microbial BOD sensors: problems of practical use and comparison of sensorBOD and BOD_5. In: Scheller FW, Schubert F, Fedrowitz J (eds.) Frontiers in biosensorics. Birkhäuser, Basel Boston Berlin 2:99–108
54. Riedel K, Uthemann R (1994). SensorBSB – ein neuer mit Biosensoren gewonnener Summenparameter in der Abwasseranalytik. Wasserwirtsch-Wassertechn 2:35–38
55. Riedel K, Kunze G (1997) Rapid physiological characterization of microorganisms by biosensor technique. Microbiol Res 152:233–237
56. Kunze G, Kunze G (1996) *Arxula adeninivorans*. In: Wolf K (ed.) Nonconventional yeasts. Springer, Berlin Heidelberg New York, pp 389–409
57. Chan C, Lehmann M, Tag K, Lung M, Kunze G, Riedel K, Gründig B, Renneberg R (1999) Measurement of biodegradable substances using the salt-tolerant yeast *Arxula adeninivorans* for a microbial sensor immobilized with poly(carbamoyl)sulfonate (PCS). Part I: Construction and characterization of the microbial sensor. Biosens Bioelectron 14:131–138
58. Lehmann M, Chan C, Lo A, Lung M, Tag K, Kunze G, Riedel K, Gründig B, Renneberg R (1999) Measurement of biodegradable substances using the salt-tolerant yeast *Arxula adeninivorans* for a microbial sensor immobilized with poly(carbamoyl)sulfonate (PCS). Part II: Application of the novel biosensor to real samples from coastal and island regions. Biosens Bioelectron 14:295–302
59. Tag K, Lehmann M, Chan C, Renneberg R, Riedel K, Kunze G (1998) *Arxula adeninivorans* LS3 as suitable biosensor for measurements of biodegradable substances in salt water. J Chem Technol Biotechnol 73:385–388

60. Renneberg R, Kwong WK, Chan C, Kunze G, Riedel K (1999) Rapid measurement of biodegradable substances in water using novel microbial sensors. In: Advances in biosensors, JAS Press, pp 195 – 213
61. Wartmann T, Krüger A, Adler K, Bui MD, Kunze I, Kunze G (1995) Temperature dependent dimorphism of the yeast *Arxula adeninivorans* LS3. Antonie van Leeuwenhoek 68:215 – 223
62. Li F, Tan TC (1994) Monitoring BOD in the presence of heavy metal ions by a poly(4-vinylpyridine) coated microbial sensor. Biosens Bioelectron 9:445 – 455
63. Qian Z, Tan TC (1998) A model for multicomponent biosensing and its application to dead-base BOD biosensor. Chem Engineer Science 53:3281 – 3294
64. Qian Z, Tan TC (1999) BOD measurement in the presence of heavy metal ions using a thermally-killed *Bacillus subtilis* biosensor. Water Res 33:2923 – 2928
65. Riedel K, Renneberg R, Scheller F (1990) Adaptable microbial sensors. Anal Lett 23: 757 – 770
66. Tag K, Kwong AWK, Lehmann M, Chan C, Renneberg R, Riedel K, Kunze G (2000) Fast detection of high-molecular substances in wastewater based on an enzymatic hydrolysis combined with the *Arxula* BOD sensor system. J Appl Chem Biotechnol 75:1080 – 1082
67. Chee GJ, Nomura Y, Ikebukuro K, Karube I (1999) Development of highly sensitive BOD sensor and its evaluation using preozonation. Anal Chim Acta 394:65 – 71
68. Kwong W, Chan C, Renneberg R (1998) Monitoring biodegradable substances with high-molecular content with a microbial sensor. Anal Lett 31:2309 – 2325
69. Hartmeier W, Tari A, Reiss M (1993) BOD-biosensors basing *Lipomyces* cells and β-galactosidase from mold origin. Med Fac Landhouw Univ Gent 59:1799 – 1801
70. Reiss M, Hartmann W (1999) Monitoring of environmental processes with biosensors. In: Winter J (ed) Biotechnology Wiley-VCH-Verlag, Weinheim, vol 11a, pp 125 – 137
71. JIS K 3602 (1990) Japanese Industrial Standard: Apparatus for the estimation of biochemical oxygen demand (BOD_S) with microbial sensor
72. Clark LC Jr (1956) Monitor and control of blood and tissue oxygen tensions. Trans Am Soc Artif Intern Organs 2:41 – 48
73. Clark LC Jr, Lyons C (1962) Electrode systems for continuous monitoring in cardiovascular surgery. Ann NY Acad Sci 102:29
74. Riedel K, Fahrenbruch B, Klimes N, Neumann B, Kopprach W, Scheller F (1990) Determination of BOD using a FIA system with microbial sensor. GBF-Monographs 14: 231 – 246
75. Neudörfer F, Meyer-Reil LA (1997) A microbial biosensor for the microscale measurement of bioavailable organic carbon in oxide sediments. Marine Ecology Progr Ser 147:295 – 309
76. Meyer-Reil LA, Neudörfer F (1998) Biosensors based on immobilized microbial cells. In: Flemming H-C, Szewzyk U (eds) The investigation of biofilms. Springer, Berlin Heidelberg New York, pp 1 – 5
77. Kong Z, Vanrolleghem PA, Verstraete W (1993) An activated sludge-based biosensor for rapid IC_{50} estimation and on-line toxicity monitoring. Biosens Bioelectronics 8:49 – 58
78. Vanrolleghem PA, Kong Z, Rombputs G, Verstraete W (1994) An on-line respirographic biosensor for the characterization of load and toxicity of wastewaters. J Chem Biotechnol 59:321 – 333
79. Evans MR, Jordinson GM, Ralwson DM, Rogerson JG (1998) Biosensors for the measurement of toxicity of wastewaters to activated sludge. Pestic Sci 54:447 – 452
80. König A, Kayser G, Flemming HC, Riedel K (1997) Ein mikrobieller Sensor zur Erfassung nitrifikationshemmender und nitrifizierbarer Verbindungen. Vom Wasser 88:185 – 204
81. König A, Secker J, Riedel K, Metzger JW (1997) A microbial sensor for measuring inhibitors and substrates for nitrification in wastewater. Am Lab (Shelton Conn) 29:12 – 21
82. König A, Riedel K, Metzger JW (1998) A microbial sensor for detecting inhibitors of nitrification in wastewater. Biosens Bioelectronics 13:869 – 874
83. König A (1999) Entwicklung von Nitrifikanten-Biosensoren für die Abwasseranalytik. (Dissertation an der Universität Stuttgart). Stuttgarter Berichte zur Siedlungswasserwirtschaft, Band 152, Oldenbourg Verlag, München

84. König A, Bachmann TT, Metzger JW, Schmid RD (1999) Disposable sensor for measuring N-BOD and inhibition of nitrification in wastewater. Appl Microbiol Biotechnol 15:112–117
85. Wagner R (1990) Glossarium – Biochemischer Saurstoffbedarf (BSB). In: Wagner R (ed) Wasserkalender 1990. Erich Schmidt, Berlin, pp 187–197
86. Deai J, Tang Y, GongY, ZhangJ, Sun Y (1991) Factors affecting the relationship between the N-BOD values and the amounts of nitrogen pollutants: A field study on the Lee river. Water Res 25:485–489
87. Hikuma M, KuboT, Yasuda T, Karube I, Suzuki S (1980) Ammonia electrode with immobilized nitrifying bacteria. Anal Chem 52:1020–1024
88. Okada T, Karube I, Suzuki S (1982) Ammonium ion sensor based on immobilized nitrifying bacteria and a cation exchange membrane. Anal Chim Acta 135:159–165
89. Riedel K, Huth J, Kühn M, Liebs P (1990) Amperometric determination of ammonium ions with a microbial sensor. J Chem Tech Biotechnol 47:109–116
90. Tanaka H, Nakamura E, Hoshikawa H, Tanaka Y (1993) Development of the ammonia biosensor monitoring system. Wat Sci Techn 28:435–445
91. Karube I, Okada T, Suzuki S, Suzuki H, Hikuma M, Yasuda T (1982) Amperometric determination of sodium nitrite by a microbial sensor. Eur J Appl Microbiol Biotechn 15:127–132
92. Reshetelov AN, Iliasov PV, Knackmus HJ, Boronin AM (2000) The nitrite oxidizing activity of *Nitrobacter* strains as a base of microbial biosensor for nitrite detection. Anal Lett 33:29–41
93. Okada T, Karube I, Suzuki S (1982) Hybrid urea sensor using nitrifying bacteria. Eur J Appl Microbiol Biotechn 14:149–154
94. Suzuki M, Lee S, Fujil K, Arikawa Y, Kubo I, Kanagawa T, Mikami E, Karube I (1992) Determination of sulfite by using microbial sensor. Anal Lett 15:973–982
95. Kurosawa M, Hiroano T, Nakamura K, Amano Y (1994) Microbial sensor for selective determination of sulphide. Appl Microbol Biotechnol 41:556–559
96. Nakamura K, Saegusa K, Kurosawa M, Amano Y (1993) Determination of free sulfur dioxide in wine by using a biosensor based on a glass electrode. Biosci Biotechn Biochem 57:379–382
97. Tauriainen S, Karp M, Chang W, Virta M (1998) Luminescent bacterial sensor for cadmium and lead. Biosens Bioelectron 13:931–938
98. Williams G, D'silva C (1994) Field-based heavy metal analyser for the simultaneous determination of multiple cations on-site. Analyst (London) 119:2337–2341
99. Lehmann M, Riedel K, Adler K, Kunze G (1998) Schnellverfahren: Nutzung der Biosensor-Technik für Messungen von Umweltproben. Chemie Technik 27:104–105
100. Lehmann M, Riedel K, Adler K, Kunze G (2000) Amperometric measurement of copper ions with a deputy substrate using a novel *Saccharomyces cerevisiae* sensor. Biosens Bioelectron 15:211–219
101. Mandl M, Macholan L (1990) Membrane biosensor for the determination of iron (II, III) based on immobilized cells of *Thiobacillus ferroxidans*. Folia Microbiol 35:363–367
102. Ikebukuro K, Miyata A, Cho SJ, Nomura Y, Chang SM, Yamauchi Y, Hasebe Y, Uchiyama S, Karube I (1996) Microbial cyanide sensor for monitoring river water. J Biotechnol 48:73–80
104. Lee JM, Karube I (1995) A novel microbial sensor for the determination of cyanide. Anal Chim Acta 313:69–74
105. Dagley S (1987) Microbial metabolism of aromatic compounds. In: Cooney CL, Humphrey AE (eds) Comprehensive biotechnology. Pergamon, pp 483–505
106. Prito MA, Garcia JL (1997) Identification of the 4-hydroxyphenylacetate transport gene of *Escherichia coli* W: construction of a highly sensitive cellular biosensor. FEBS Letters 414:293–297
107. Riedel K, Hensel J, Ebert K (1991) Biosensoren zur Bestimmung von Phenol und Benzoat auf der Basis von *Rhodococcus*–Zellen und Enzymextrakten, Zbl Bakt 146:425–434

108. Riedel K, Hensel J, Rothe S, Neumann B, Scheller F (1993) Microbial sensors for determination of aromatics and their chloroderivatives. Part II: Determination of chlorinated phenols using a *Rhodococcus* containing biosensor. Appl Microbiol Biotechnol 38: 556 – 559
109. Gaisford WC, Richardson NJ, Haggert BGD, Rawson DM (1991) Microbial sensors for environmental monitoring. Biochem Soc Trans 19:15
110. Ciucu A, Mareaur V, Flexhin S, Lucaciu I, David F (1991) Biocatalytic membrane electrode for phenol. Anal Lett 24:567 – 580
111. Ignatov OV, Kozel AB (1995) The determination of aromatic compounds by microbial biosensors. In: Moo-Young M et al. (eds) Environmental biotechnology: principles and application. Kluver Academic Publishers, pp 66 – 74
112. Rainina EI, Badalian IE, Ignatov OV, Federov AY, Simonian AL, Varfolomeyev SD (1996) Cell biosensor for detection of phenol in aqueous solution. Appl Biochem Biotechnol 56:117 – 127
113. Bachmann T, Bilitewski U, Schmid RD (1998) A microbial sensor based on *Pseudomonas putida* for phenol, benzoic acid and their monochlorinated derivatives which can be used in water and *n*-hexane. Anal Lett 32:2361 – 2373
114. Reiss M, Metzger J, Hartmeier W (1995) An amperometric microbial sensor based on *Azotobacter* species for phenolic compounds. Med Fac Landbouw Univ Gent 60/4b: 2227 – 2230
115. Riedel K, Naumov AV, Boronin LA, Golovleva LA, Stein J, Scheller F (1991) Microbial sensors for determination of aromatics and their chloroderivates. Part I: Determination of 3-chlorobenzoate using a *Pseudomonas*-containing biosensors. Appl Microbiol Biotechnol 35:495 – 562
116. Tan HM, Cheong SP, Tan TC (1994) An amperometric benzene sensor using whole cell *Pseudomonas putida ML2*. Biosens Bioelectron 9:1 – 8
117. König A, Zaborosch C, Muscat A, Vorlop KD, Spener F (1996) Microbial sensors for naphthalene using *Spingomonas* sp. *B1* or *Pseudomonas fluorescens* WW4. Appl Microbiol Biotechnol 45:844 – 850
118. Beyersdorf-Radek B, Schmid RD, Riedel K, Neumann B, Scheller F (1991) Microbial sensors for the determination of aromatics and their chloroderivatives. In: Verachtert H, Verstraete WF (eds) Proc Symp Environm Biotechnol Oostende, pp 65 – 68
119. Beyersdorf-Radek B, Riedel K, Neumann B, Scheller F, Schmid RD (1992) Development of microbial sensors for determination of xenobiotics. GBF Monographs 17:55 – 60
120. Beyersdorf-Radek B, Riedel K, Neumann B, Scheller F, Schmid RD (1993) Entwicklung mikrobieller Sensoren zur Bestimmung von Xenobiotika. In: Fachgruppe Wasserchemie in der GDCh (eds) Biochmische Methoden zur Schadstofferfassung im Wasser. VCH Weinheim, New York, Basel, Cambridge, pp 141 – 146
121. Beyersdorf-Radeck B, Riedel K, Karlson U, Bachmann TT, Schmid RD (1998) Screening of xenobiotic compounds degrading microorganisms using biosensor techniques. Microbiol Res 153:1 – 7
122. Reshetelov AN, Iliasov PV, Slepenkin AV, Greschkina GM, Starovoitov II (1999) *Pseudomonas*-based amperometric detection of biphenyl and chlorinated benzoates. Anal Lett 32:11 – 23
123. Beyersdorf-Radeck B, Karlson U, Schmid RD (1994) A microbial sensor for 2-ethoxyphenol. Anal Lett. 27:285 – 298
124. Häggblom M (1990) Mechanisms of bacterial degradation and transformation of chlorinated monoaromatic compounds. J Basic Microbiol 30:115 – 141
125. Neilson AH (1990) The biodegradation of haloaromatics. J Appl Bacteriol 69:445 – 470
126. Chaudhry GR, Chapalamadugu S (1991) Biodegradation of halogenated organic compounds. Microbiol Rev 55:59 – 79
127. Riedel K, Beyersdorf-Radeck B, Neumann B, Scheller F (1995) Microbial sensors for determination of aromatics and their chloroderivatives. Part III: Determination of chlorinated phenols using a biosensor containing *Trichossporon beigelii (cutaneum)*. Appl Microbiol Biotechnol 43:7 – 9

128. Nomura Y, Ikebukuro K, Yokoyama K, Takeuchi T, Arikawa Y, Ohno S, Karube I (1994) A novel microbial sensor for anionic surfactant determination. Anal Lett 27:3095–3108
129. Nomura Y, Ikebukuro K, Yokoyama K, Takeuchi T, Arikawa Y, Ohno S, Karube I (1998) Application of a linear alkylbenzene sulfonate biosensor to river water monitoring. Biosens Bioelectron 13:1047–1053

Received: December 2000

Reverse Micellar Extraction for Downstream Processing of Proteins/Enzymes

S. Hari Krishna [1], N. D. Srinivas [2], K. S. M. S. Raghavarao [2], N. G. Karanth [1]

[1] Department of Fermentation Technology & Bioengineering, Central Food Technological Research Institute, Mysore 570 013, India, e-mail: ferm@cscftri.ren.nic.in
[2] Department of Food Engineering, Central Food Technological Research Institute, Mysore 570 013, India

New developments in the area of downstream processing are, hopefully, to fulfill the promises of modern biotechnology. The traditional separation processes such as chromatography or electrophoresis can become prohibitively expensive unless the product is of high value. Hence, there is a need to develop efficient and cost-effective downstream processing methods. Reverse micellar extraction is one such potential and a promising liquid-liquid extraction technique, which has received immense attention for isolation and purification of proteins/enzymes in the recent times. This technique is easy to scale-up and offers continuous operation. This review, besides briefly considering important physico-chemical and biological aspects, highlights the engineering aspects including mass transfer, mathematical modeling, and technology development. It also discusses recent developments in reverse micellar extraction such as affinity based separations, enzymatic reactions in reverse micelles coupled with membrane processes, reverse micellar extraction in hollow fibers, etc. Special emphasis has been given to some recent applications of this technique.

Keywords. Downstream processing, Reverse micelles, Protein/enzyme extraction, Modeling, Recent developments

1 Introduction 124

2 Reverse Micellar Systems 125

2.1 Surfactants 126
2.2 Solvents 128
2.3 Co-Solvents 128

3 Protein Extraction Using Reverse Micelles 129

3.1 Water Content and Water Pool 134
3.2 Aqueous Phase pH 134
3.3 Ionic Strength 135
3.4 Surfactant Type 136
3.5 Surfactant Concentration 136
3.6 Micelle Size 137
3.7 Miscellaneous Factors 137
3.8 Mechanism and Methods of Protein Solubilization 138
3.9 Back Extraction 140
3.10 Mass Transfer Kinetics 141

Advances in Biochemical Engineering/
Biotechnology, Vol. 75
Managing Editor: Th. Scheper
© Springer-Verlag Berlin Heidelberg 2002

4 Mathematical Modeling of Reverse Micellar Extraction 142

4.1 Model for Protein Inclusion 145
4.2 Model for Protein Extraction Using Hollow Fibers 146
4.3 Enzyme Distribution in Relation to Water Content 148
4.4 Modeling of Forward and Back Extractions 149
4.5 Thermodynamic Model for Protein Partitioning 150
4.6 Thermodynamic Modeling for the Size of RMs 151
4.7 Interfacial Mass Transfer Model 152
4.8 Modeling of Affinity Based RME 154
4.9 Molecular Thermodynamic Model for Osmotic Pressures 155
4.10. Remarks on Modeling 156

5 Technology Development Aspects of Reverse Micellar Extraction . 157

6 Recent Developments in Reverse Micellar Systems 160

6.1 Affinity Based Reverse Micellar Extraction and Separation (ARMES) 160
6.2 Reverse Micellar Extraction in Hollow Fibers 162
6.3 Some New Surfactants for Reverse Micellar Systems 162
6.3.1 Nonionic Surfactants 163
6.3.2 Di(tridecyl) Phosphoric Acids as Surfactants 163
6.3.3 Sugar Ester as Surfactant 164
6.3.4 Sodium Bis(2-ethyl hexyl) Phosphate (NaDEHP) as a Novel Anionic Surfactant 164
6.4 Enzymatic Reactions in RMs Coupled with Membrane Processes . . 164
6.5 Micellar Enhanced Ultrafiltration (MEUF) 165
6.6 Micellar Electrokinetic Capillary Chromatography (MECC) 166
6.7 Cloud-Point Extractions (CPE) 166

7 Some Recent Applications 166

7.1 Protein Refolding 167
7.2 Self Replicating RMs 171
7.3 Antigen-Antibody Interactions 171
7.4 Other Applications of RMs 172

8 Concluding Remarks 174

References 176

List of Abbreviations and Symbols

Notations

A	interfacial area
a	thickness of surfactant head-group region
A_{eff}	effective Hamaker constant
A_{j}	specific surface area in mixer *j*

b	separation distance
C^0	initial solute concentration
c_{aq}	concentration of aqueous phase
C_j	concentration of active enzyme in phase *j*
c_{org}	concentration of organic phase
C_P	solute concentration
C_P^{aq}	concentration of protein in aqueous phase
C_P^{org}	concentration of protein in organic phase
c_{si}	concentration of surfactant forming micelles of type *i*
d	fiber diameter
D	diffusion coefficient in membrane
e	electronic charge
E	electric field between surfaces
$[E]_i$	enzyme concentration in each domain
F_e	electrostatic force between two charged plates separated by an electrolyte solution
G_{el}	contributions from electrostatic interactions both between protein-surfactant and surfactant-surfactant
G_{mix}	contributions from ideal mixing of two classes of RMs into organic medium
G_{tail}	contributions from steric interactions between adjacent surfactant tails
G_{tot}	system's total free energy
ΔG	insertion free energy
H	partition coefficient
J	initial flux
k	Boltzmann constant
k_BT	Boltzmann's energy
K_E^1, K_E^2	enzyme partition coefficients between domains
k_f	mass transfer coefficient for forward transfer
k_{ij}	inactivation rate constant in phase *j*
K_{in}	overall mass transfer coefficient
k_{in}	individual mass transfer coefficients inside fibers
k_{mem}	individual mass transfer coefficients across fiber wall
k_{oj}	individual mass transfer coefficient in mixer *j*
k_{out}	individual mass transfer coefficients outside fibers
k_r	mass transfer coefficient for back transfer
1/K	Debye screening length
l	length of surfactant molecule
ℓ	fiber length
N	Avagadro number
N_e	reference salt concentration in bulk aqueous phase for empty micelles
N_e^s	surfactant aggregation number of empty RMs
N_e^w	water aggregation number of empty RMs
N_F	reference salt concentration in bulk aqueous phase for filled micelles
N_F^s	surfactant aggregation number of filled RMs
N_F^w	water aggregation number of filled RMs

N_s	stirring speed
q^I	interface charge density
Q_{in}	volumetric flow of inner fluid
Q_{out}	volumetric flow of outer fluid
q^P	protein surface charge densities
R_e	radius of the empty RMs including polar heads
R_F	radius of protein filled RMs including polar heads
R_f	total resistance
$R_{f,b}$	bulk resistance
$R_{f,i}$	interfacial resistance to forward transfer
R_P	radii of protein
Δr_i	copartition ratio of species *i*
T	absolute temperature
t	time
v	surfactant packing parameter
V	volume of phase
V_{aq}	volume of aqueous phase
V_i	volume of each domain
V_{in}	reservoir volume of inner fluid
V_{org}	volume of organic phase
V_{out}	reservoir volume of outer fluid
V_p	the protein volume
v_s	velocity
V_{sh}	polar head volume
V_w	water molecule volume
W_0	molar ratio of water and surfactant concentrations
x_i	mole fraction of component *i*
Z	coordination number
Z_i	valence of component *i*

Greek symbols

α	separation factor
α'	prefactor (dependent upon diffusion coefficient of species)
β	empirical model parameter
δ	effective membrane thickness
ε	dielectric constant
ε_j	hold-up of dispersed phase in mixer *j*
σ_m	surface charge density of micelle
σ_P	surface charge density of protein
ϱ	density number
τ_j	residence time in mixer *j*
μ_i	chemical potential of species *i*
λ_c	charging parameter (represents fraction of final charge attained on protein and micellar surfaces at any stage in charging process)
ψ	electrostatic potential at radial position *r* within micelle
Π	osmotic pressure
Π^{i-CS}	repulsion term with droplet deformation

Π^{vdW} van der Waals term
Π^{MSA} long range electrostatic term
Φ volume fraction of droplets
Φ^{eff} effective volume fraction
Φ_{cp} hexagonally close packed volume fraction
$\Delta\phi$ excess osmotic coefficient of charged particles
$\Delta\xi$ reduced quantity utilized in place of ΔG
$\Delta\xi_{Eel}$ reduced form of electrostatic energy contribution to free energy
$\Delta\xi_{id}$ reduced form of counter-ions mixing contribution to free energy
$\Delta\xi_{mix}$ reduced form of RMs partition contribution to free energy
$\Delta\xi_{Sel}$ reduced form of electrostatic entropy contribution to free energy

Abbreviations

ADH alcohol dehydrogenase
AGP α_1-acid glycoprotein
AOT sodium bis(2-ethyl-1-hexyl) sulfosuccinate, aerosol OT
ARMES affinity based reverse micellar extraction and separation
ATPE aqueous two-phase extraction
ATPS aqueous two-phase system
BDBAC *N*-benzyl-*N*-dodecyl-*N*-bis(2-hydroxy ethyl) ammonium chloride
BSA bovine serum albumin
CBF cibacron blue F-3GA
CE capillary electrophoresis
Con A concanavalin A
CPB cetyl pyridinium bromide
CTAB cetyltrimethyl ammonium bromide
CZE capillary zone electrophoresis
DDAB didocyldimethyl ammonium bromide
DOLPA dioleyl phosphoric acid
DSP downstream processing
DTDPA di(tridecyl) phosphoric acid
HLB hydrophilic-lipophilic balance
LLE liquid-liquid extraction
MECC micellar electrokinetic capillary chromatography
MEUF micellar enhanced ultrafiltration
NaDEHP sodium bis(2-ethylhexyl) phosphate
PEG polyethylene glycol
QELS quasi electric light scattering
RME reverse micellar extraction
RMs reverse micelles
SANS small angle neutron scattering
SAXS small angle X-ray scattering
SBP soybean peroxidase
SDS sodium dodecyl sulfate
TOMAC trioctylmethyl ammonium chloride
TTAB tetradecyltrimethyl ammonium bromide

1 Introduction

In recent years there have been tremendous efforts by research and industrial community for the production of biochemicals through application of fermentation technology and cell culture. However, the technology for downstream processing (DSP) of biological products from the media/broth has not kept pace with the advances in upstream operations involving bioreactors, despite the fact that in many cases DSP contributes major share of the final product cost. The separation of many biochemicals from the product stream is still performed by batch mode small-scale processes such as column chromatography, salt and solvent precipitation and electrophoresis for which scale-up poses considerable problems, making them uneconomical unless the product is of high value. Affinity-based chromatographic separations though have excellent selectivity and have been carried out on a large scale; for the most part such systems operate discontinuously and the economy of scale has not often been realized [1]. Therefore, current research in the area of DSP is directed towards efficient and scalable alternative bioseparation processes with potential for continuous operation.

Liquid-liquid extraction (LLE) is a traditional chemical engineering unit operation for which the design and scale-up of both batch as well as continuous processes are already accomplished. Unlike affinity chromatography and precipitation, LLE is well known to operate continuously on a large scale with high throughputs, ease of operation, and high flexibility in its mode of operation [2]. LLE using organic/aqueous phase has been employed in many chemical industries. However, this technique with all its advantages has not gained wide industrial recognition in the field of biotechnology, mainly due to the poor solubility of proteins in organic solvents and the tendency of organic solvents to denature the proteins.

In recent years LLE using the aqueous two-phase systems (ATPS) has been recognized as a superior and versatile technique for DSP of biomolecules [3], and a wealth of information has been reported in the literature on various aspects of aqueous two-phase extraction (ATPE) for the isolation and concentration of proteins, enzymes, and other biological materials [4–7]. The major advantages of ATPE include high capacity, biocompatible environment, low interfacial tension, high yield, lower process time and energy, and high selectivity. Further, it offers ease of scale-up, continuous operation, and, most importantly, allows easy adaptation of the equipment and the methods of conventional organic-aqueous phase extraction used in the chemical industry [8, 9].

Reverse micellar extraction (RME) is another attractive LLE method for DSP of biological products, as many biochemicals including amino acids, proteins, enzymes, and nucleic acids can be solubilized within and recovered from such solutions without loss of native function/activity. In addition, these systems offer low interfacial tension, ease of scale-up, and continuous operation. RME offers a number of unique, desirable features in comparison with ATPE, which has been extensively studied:

1. The partitioning behavior of biomolecules in RME can be regulated by varying the size and shape of the reverse micelles (RMs). This can be easily ac-

complished by the self-assembling and labile nature of RMs as opposed to the unchanging identity and nature of the polymers (which is fixed upon synthesis) used in ATPE.
2. Partitioning selectivity of proteins can be achieved in RME based on the hydrophobic nature of proteins due to the fact that RMs provide both hydrophobic and hydrophilic environments to solutes simultaneously.
3. Recovery of biomolecules from the reverse micellar phase can be easily facilitated by exploiting the de-assembling nature of RMs in aqueous media. Further, the surfactants can be separated from the biomolecules by filtration [10] and can be recycled. In contrast, efficient methods for the recovery and recycling of polymers in ATPE have not yet been developed [8]. For example, although recently Tjernald and coworkers [11] have solved this problem to some extent by employing thermo-separating polymers, a suitable method for the recovery of polyethylene glycol (an extensively studied polymer in ATPE) is not yet developed.

RME shows particular promise in the recovery of proteins/enzymes [12–14]. In the past two decades, the potential of RME in the separation of biological macromolecules has been demonstrated [15–20]. RMs have also been used as media for hosting enzymatic reactions [21–23]. Martinek et al. [24] were the first to demonstrate the catalytic activity of α-chymotrypsin in RMs of bis (2-ethylhexyl) sodium sulfosuccinate (Aerosol-OT or AOT) in octane. Since then, many enzymes have been solubilized and studied for their activity in RMs. Other important applications of RME include tertiary oil recovery [25], extraction of metals from raw ores [26], and in drug delivery [27]. Application of RMs/microemulsions/surfactant emulsions were recognized as a simple and highly effective method for enzyme immobilization for carrying out several enzymatic transformations [28–31]. Recently, Scheper and coworkers have provided a detailed account on the emulsion immobilized enzymes in an exhaustive review [32].

Although a number of research articles and a few review papers have been published in the past relating to various aspects of RME, no comprehensive review encompassing all aspects is available. Engineering aspects have received scant attention when compared to the physico-chemical and biological aspects. For example, mathematical modeling which is very important for the prediction of distribution/solubilization of biomolecules in RMs has not been given its due importance. This review, besides briefly considering important physico-chemical and biological aspects, highlights the engineering aspects including mathematical modeling and discusses the recent developments in RME. Special emphasis has been given to some recent applications of RME.

2 Reverse Micellar Systems

A RM is a nanometer size droplet of an aqueous solution stabilized in an apolar environment by the surfactant present at the interface. In these systems, the proteins are solubilized inside the polar core of surfactant shell that protects the biomaterials from denaturation by organic solvent. The RMs formed in ternary

surfactant-water-organic solvent mixtures have mostly spherical shape (in certain cases rods or prolate ellipsoids have also been observed) and are also called water-in-oil emulsions. The composition involved in RME include an organic medium (~80–90%), water (~1–10%), and a surfactant (<10%). In addition to the hydrophilic biomolecules such as proteins/enzymes [33, 34], microbial cells [35] can also be incorporated into the water core of RMs, facilitating their extraction. RMs are generally smaller than their hydrophilic counterparts (micelles), their aggregation number being mostly lower than 50 [36]. Characteristic properties of reverse micellar systems include (i) thermodynamic stability (no phase separation with time), (ii) spontaneous formation, (iii) low interfacial tension ($<10^{-2}$ mN m^{-1}), (iv) transparent nature (nanometer size, <100 nm, is responsible for transparent nature of microemulsions which is in contrast to the turbid appearance of normal emulsions), (v) large surface area (several hundred square meters per cubic centimeter), (vi) viscosity comparable with the pure organic solvents, and (vii) capability to dissolve polar substances.

Although RMs are thermodynamically stable, they are highly dynamic. The RMs constantly collide with each other and occasionally a collision results in the fusion of two RMs temporarily. During this fusion surfactant molecules and the contents residing inside RMs may be exchanged. In AOT reverse micellar system, this dynamic behavior exhibits second-order kinetics with rate constants in the order of 10^3 to 10^6 M^{-1} s^{-1} [37]. This dynamic nature not only influences the properties of the bulk system but also affects the enzymatic reaction rates [38].

The following section briefly summarizes the basic components of RME.

2.1 Surfactants

A special group of lipids that possess both hydrophilic and hydrophobic (lipophilic) parts are termed as amphiphiles or amphipathics and are also referred to as surfactants. They adsorb at surfaces or interfaces and change the interfacial free energy associated with the building of an interface. A surfactant molecule consists of two distinct chemical groups (i) the head which is hydrophilic (water-loving) and (ii) the tail which is hydrophobic (water-fearing).

The hydrophobic tail may consist of a single chain (alkyl chain in soaps) or up to four chains (quaternary ammonium salts). The hydrophilic head can be a simple charged group, such as the carboxylic group in soaps, or can have a complicated structure as in lecithins or can be an uncharged apolar group as the poly (oxyethylene) part in many nonionic surfactants. The complex nature of polar and apolar moieties are responsible for the abnormal behavior of amphiphiles in solution, namely formation of aggregates. The different types of aggregates are: monolayer, bilayer, lamellar (liquid crystalline phase), liposomes (vesicles), micelles (in aqueous solutions), and reverse micelles (in apolor/organic solvents) (Fig. 1). Micelles are the most well known and extensively studied among these different types of aggregates.

Amphiphiles differ greatly in the relative balance between their hydrophilic and hydrophobic moieties which is reflected by their behavior in water and provides a basis for their classification. Depending on their solubility in water, am-

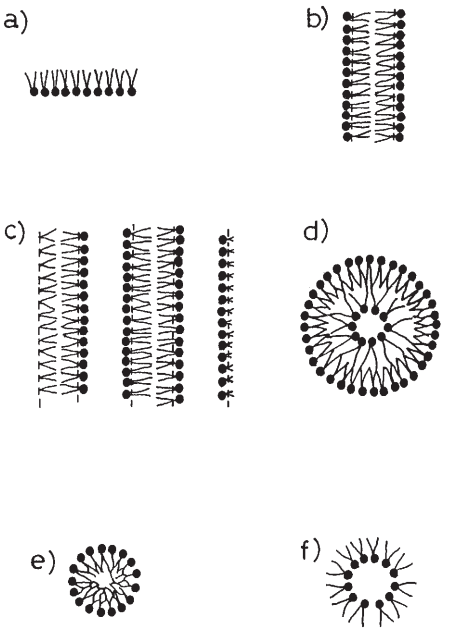

Fig. 1a–f. Various forms of surfactant aggregations in solution: **a** Monolayer; **b** bilayer; **c** liquid crystalline phase (lamellar); **d** vesicle (liposome); **e** micelle; **f** reverse micelle. (Reproduced from [39] with permission of PL Luisi)

phiphiles are classified into soluble and insoluble amphiphiles. Soluble amphiphiles are generally referred to as surfactants/detergents. Based on their nature and hydrophilic part they are further classified into nonionic, zwitterionic, anionic, and cationic surfactants. In addition, surfactants are also classified into two groups: (i) those which display lyotropic mesomorphism (i.e., they can form liquid crystals at high concentration) and (ii) those which do not display lyotropic mesomorphism due to the presence of bulky and complicated cyclic/aromatic hydrocarbons. Table 1 gives various surfactants commonly used in RME. Most of the studies on enzyme solubilization in RMs have been carried out using aerosol-OT (AOT), mainly because it can form RMs without the need of a cosurfactant and when compared to most other surfactants it has the ability to solubilize large amounts of water. For instance per AOT molecule up to 65 water molecules can be solubilized in *n*-heptane [40].

Commercial surfactants are, in general, chemically impure and may contain varying amounts of water and additives. After prolonged storage of liquid nonionic surfactants the composition tend to change. It should be observed that even trace impurities might sometimes produce a bottleneck in carrying out spectroscopic studies of proteins/nucleic acids in RMs. In addition, the impurities may interfere with the behavior of biomolecules and also cause problems of reproducibility. To achieve reproducible results, it is advisable to purify the surfactants to be used whenever possible [12].

2.2 Solvents

Organic phase occupies about 80–90% of the reverse micellar systems. Water solubilization capacity of the RMs, for a given surfactant, is strongly dependent on the type of solvent used. It was showed that in case of AOT-RMs, maximum water solubilization can be obtained with *n*-heptane as solvent (water content of RM, $W_0 = 65$). When *n*-heptane was replaced by a solvent of higher carbon number such as hexadecane, water solubilization capacity decreased significantly ($W_0 = 5$) [40]. Lang et al. [41] observed that micellar size decreased with an increase in the molecular size of the solvent. According to them, as the molecular size of the solvent increases their ability to penetrate into the interfacial surfactant layer decreases thereby increasing the intermicellar attractions between the surfactant tails, and the micelles get sticky. In other words, increase in solvent molecular size reduces the contribution of the entropy of dispersion favoring the formation of smaller micelles. Various organic solvents and surfactants used in RME are listed in Table 1.

2.3 Co-Solvents

Co-solvent is a type of solvent (also termed as co-surfactant) which can help surfactants dissolve in the organic solvent and form RMs thereafter. Although the

Table 1. Commonly used surfactants, solvents, and cosolvents

Surfactants	Anionic Sodium bis(2-ethyl-1-hexyl) sulfosuccinate (Aerosol OT, AOT); sodium dodecylbenzene sulfonate (SDBS); sodium di-2-ethyl hexyl phosphate (NaDEHP); dioleyl phosphoric acid (DOLPA); di(tridecyl) phosphoric acid (DTDPA); sodium dodecyl sulfate (SDS); 1,3-dilauroyl glycerol-2-disodium phosphate (2-modified 1,3-diacyl glycerol)
	Cationic Cetyltrimethyl ammonium bromide (CTAB); dodecyltrimethyl ammonium bromide (DTAB); tetradecyltrimethyl ammonium bromide (TTAB); trioctylmethyl ammonium chloride (TOMAC); *N*-benzyl-*N*-dodecyl-*N*-bis(2-hydroxy ethyl) ammonium chloride (BDBAC); cetyl pyridinium chloride (CPC); quaternary ammonium salt with carbon atoms of R ranging from 8–10 ($CH_3\ R_3\ N^+\ Cl^-$) (Aliquat 336)
	Nonionic Polyoxyethylene sorbitan trioleate (Tween 85); sugar ester (DK-F-110); tetraoxyethylene monodecyl ether ($C_{10}E_4$); polyoxyethylene-*p*-*t*-octyl phenol (Triton X-100); pentaethylene glycol dodecyl ether
	Zwitterionic
	Soybean lecithin
Solvents	C_7–C_{15} *n*-alkanes; Isooctane; *n*-decane; carbon tetrachloride; cyclohexane; octane; *n*-heptane; *n*-hexane; hexadecane
Cosolvents	Isopropanol; butanol; hexanol; octanol; decanol; Rewopal HV5; (nonylphenoxy) pentaethylene oxide

exact mechanism of the co-solvent is still not clear, it has been suggested that co-solvent molecules might be inserted between the surfactant molecules [42]. The co-surfactant seems to buffer the strong repulsive ion-ion interaction between the surfactant head groups, thereby allowing their close packing in order to form the inner core of a RM [43].

Formation of RMs by Aliquat-336 in isooctane can be achieved by addition of a co-solvent (straight chain alkyl alcohols) [42, 44]. Only those alcohols having low solubility in water can be used as co-solvents for formation of RMs [44]. Some of the general co-solvents (Table 1) employed are long chain alcohols, acetates, butyrates, etc. [43].

3 Protein Extraction Using Reverse Micelles

In order to be exploitable for extraction and purification of proteins/enzymes, RMs should exhibit two characteristic features. First, they should be capable of solubilizing proteins selectively. This protein uptake is referred to as forward extraction. Second, they should be able to release these proteins into aqueous phase so that a quantitative recovery of the purified protein can be obtained, which is referred to as back extraction. A schematic representation of protein solubilization in RMs from aqueous phase is shown in Fig. 2. In a number of recent publications, extraction and purification of proteins (both forward and back extraction) has been demonstrated using various reverse micellar systems [44, 46–48]. In Table 2, exclusively various enzymes/proteins that are extracted using RMs as well as the stability and conformational studies of various enzymes in RMs are summarized. The studies revealed that the extraction process is generally controlled by various factors such as concentration and type of surfactant, pH and ionic strength of the aqueous phase, concentration and type of co-surfactants, salts, charge of the protein, temperature, water content, size and shape of reverse micelles, etc. By manipulating these parameters selective sepa-

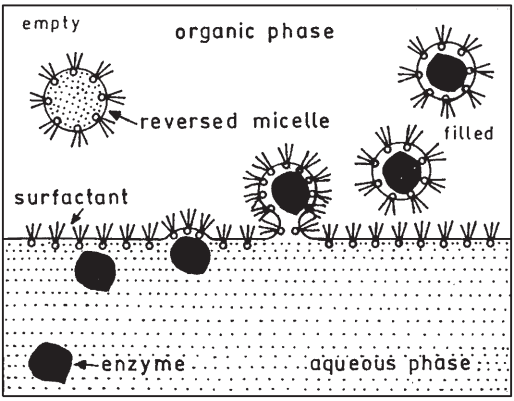

Fig. 2. Schematic representation of mechanism of protein solubilization into reverse micellar phase from aqueous phase. (Reproduced from [45] with permission of Elsevier Science)

Table 2. Enzymes/proteins studied in reverse micellar systems

Biomolecule	Source	Reverse micellar system	Nature of study	Reference
Horse radish peroxidase	*Armoracia rusticana* roots	AOT/C_7–C_{15} *n*-alcohols	Extraction and purification	[49]
		AOT/isooctane	Extraction	[50, 51]
Peroxidase		AOT/isooctane	Activity studies	[52]
α-Amylase	*Bacillus subtilis*	Aliquat 336/isooctane/*n*-alcohol	Extraction	[44, 48]
	Bacillus licheniformis	CTAB/isobutanol/hexanol/isooctane	Extraction and purification	[53]
Cutinase	*Fusarium solanipisi*	AOT/isooctane	Stability	[54]
Recombinant cutinase	*Fusarium solani* (expressed in *E. coli*)	AOT/isooctane	Catalytic properties	[55]
	Fusarium solani (expressed in *E. coli*)	AOT/hexanol/isooctane CTAB/hexanol/isooctane	Deactivation and conformation	[56]
Glucoamylase	*Aspergillus awamori* (expressed in *S. cerevisiae*)	TOMAC/Revopal HV5/*n*-octanol/ isooctane CTAB/hexanol/butanol/ isooctane	Extraction	[57, 58]
Lysozyme	Chicken egg white	AOT/isooctane	Extraction	[59, 60]
α-Chymotrypsin		AOT-DOLPA/isooctane	Extraction	[61]
		AOT/isooctane Tetradecyl trimethyl ammonium bromide (TTAB)/heptane/octanol	Thermal stability	[62]
		AOT-DOLPA mixed RMs	Extraction and activity	[63]
Trypsin	Porcine pancreas	Tetraoxyethylene monodecylether/ *n*-hexane	Extraction and purification	[64]
		CTAB/chloroform/isooctane	Activity studies	[65]
α-Chymotrypsin, trypsin		Lecithin/isooctane/alcohol	Enzyme characteristics	[66]
Cytochrome C		AOT/isooctane	Extraction	[67]

Table 2 (continued)

Biomolecule	Source	Reverse micellar system	Nature of study	Reference
Superoxide dismutase	Bovine red blood cells	AOT/heptane	Extraction and purification	[68]
Alcohol dehydrogenase	Yeast	AOT/isooctane	Kinetics	[69]
	Yeast	AOT/isooctane	Activity and stability	[70]
Ribonuclease A, soybean trypsin inhibitor, thaumatin, α-lactalbumin		AOT/isooctane	Solubilization	[71]
Ribonuclease A, cytochrome C, lysozyme	Bovine pancreas, Horse heart, Chicken egg	AOT/isooctane	Solubilization	[72]
Lysozyme, α-chymotrypsin, pepsin		AOT/isooctane	Extraction and purification	[73]
Pepsin, Chymosin	Porcine, Bovine	AOT/isooctane	Extraction and purification	[74]
Glutathione transferase	Octopus hepatopancreas	AOT/isooctane	Kinetics	[75]
Periplasmic hydrogenase	*Desulfovibrio gigas*	Cationic surfactant	Thermal and operational stability	[76]
Calcium ATPase	Sarcoplasmic reticulum	Triton X-100/phospholipids/toluene	Conformational studies	[77]
Rhus Laccase		AOT/*n*-octane	Solubilization and catalytic studies	[78]
Catalase	Bovine liver	AOT/isooctane	Activity and spectroscopic studies	[79]
Elastase	Porcine pancreas	AOT/isooctane	Solubilization and catalytic studies	[80]

Table 2 (continued)

Biomolecule	Source	Reverse micellar system	Nature of study	Reference
Urease	Soybean	AOT, CTAB, Triton X-100, mixed AOT-Triton X-100 & detergent free microemulsions (hexane/isopropanol/water)	Solubilization and catalytic studies	[81]
Polyphenol oxidase		Tetraethylene glycol dodecyl ether/dodecane	Solubilization and catalytic studies	[82]
Lipase	*Chromobacterium viscosum*	AOT/isooctane	Extraction	[83]
	Chromobacterium viscosum	AOT/Tween 85 mixed micellar system	Activity studies	[84]
	Penicillium citrinum	AOT/isooctane	Extraction and purification	[85]
	Rhizopus delemar	AOT/isooctane	Extraction and kinetics	[86]
Phospholipase D	Cabbage	Triton X-100/phosphotidyl choline/diethyl ether	Enzyme characteristics	[87]
Inulinase	*Candida kefyr*		Comparison of cross-flow filtration, RME, expanded-bed adsorption techniques for DSP	[88]
Invertase	Yeast		Stability studies	[89]
Cellulolytic enzymes (β-glucosidase, β-xylosidase, β-xylanase)	*Trichoderma reesei*	AOT/isooctane	Recovery of enzymes from broth after wheat straw hydrolysis	[90]
Lipoxygenase-1	Soybean	AOT/*n*-octane	Enzyme specificity studies	[91]
Lipoxygenase	Soybean	AOT/isooctane	Activity studies	[92]
D5–3-ketosteroid isomerase	*Pseudomonas testosteroni*	AOT/isooctane	Kinetics and stability studies	[93]
Penicillinase	*Bacillus cereus*	AOT/isoocatne	Activity and stability studies	[94]

Table 2 (continued)

Biomolecule	Source	Reverse micellar system	Nature of study	Reference
Myrosinase		AOT/isooctane	Kinetics	[95]
Alkaline phosphatase	Human placenta	AOT/isooctane	Kinetics	[96]
Acid Phosphatase	Potato	CTAB/isooctane/chloroform	Activity studies	[97]
RNase A	Bovine pancreas	DAB/cyclohexane	Activity studies	[98]
Large molecular weight proteins (catalase, β-galactosidase, BSA, hemoglobin)		AOT/isooctane	Extraction and purification	[99]
Arginase		Triton X-100/hexanol/hexane	Stability	[100]
Glucose oxidase	*Aspergillus niger*	AOT/*n*-octane	Solubilization	[101]
Triosphosphate isomerase	Rabbit muscle	CTAB/octane/hexanol	Conformational studies	[102]
Recombinant Cytochrome b_5	*E. coli*	CTAB/cyclohexane/decanol	Extraction	[103]
Recombinant Cytochrome C_{553}	*E. coli* periplasm	AOT/isoocatne	Extraction and purification	[104]
Alkaline protease	*Bacillus* sp.	AOT/isooctane	Extraction	[15]
Carbonic anhydrase	Bovine erythrocytes	TOMAC/Rewopal HV5/octanol/isooctane	Solubilization	[105]
Flavodoxin	*Megasphaera elsdenii*			
Hemoglobin	Bovine blood			
Hexokinase	Yeast			
Insulin	Bovine pancreas			
Rubredoxin	*M. elsdenii*			
Superoxide dismutase	Bovine erythrocytes			

ration of the desired protein from mixtures can be achieved. These parameters are discussed below.

3.1
Water Content and Water Pool

The water content of the RMs is defined as the ratio of the water molecules to that of the surfactant molecules per RM (W_0 = [H2O]/[surfactant]). W_0 strongly depends on the relative solubility of surfactant in the polar and nonpolar solvents, expressed as hydrophilic-lipophilic balance (HLB) of the surfactant and it increases with HLB [106, 107]. The HLB increases in the following manner for cationic surfactants: TOMAC < DDAB < BDBAC < CTAB ~ CPB [43]. W_0 has a major role in protein solubilization and function. Krei and Hustedt [43] have observed a significant influence of W_0 or size of the RM on the partitioning behavior of proteins (e. g., α-amylase) in various reverse micellar systems containing cationic surfactants. They found that below a certain critical value of W_0 (~ 40), the physico-chemical properties of the aqueous microphase strongly depends on the micellar size, thereby favoring the partition coefficient of the protein towards the excess aqueous phase. Hilhorst et al. [34] have concluded that W_0 of the TOMAC/octane system can be varied by exchanging surfactant counterions with ions in the aqueous bulk solution, and by changing the amount of alcohol or cosurfactant, or nature of cosurfactant. Further, they found that increasing W_0 (up to a certain value) facilitates transfer of α-amylase into the RMs and transfer is observed at a lower pH. In a recent study, it was reported that a high W_0 (~ 120) was required to achieve almost complete solubilization of inulinase into BDBAC/isooctane/hexanol RMs [108].

The nature of the water in the core of the reverse micelle is of great importance since proteins/enzymes and other biomaterials reside in this water pool. The water pool is generally regarded to be a composite of two different types, the bound water (lining the interior wall of the AOT micelles) and the (remaining) free water [109]. Further subdivisions of the water pool have also been proposed. Gierasch et al. [110] used IR spectra. It should be stressed that water entrapped in RMs is different from bulk water and is similar to water present in the vicinity of biological membranes or proteins in that it has restricted mobility, depressed freezing point, and characteristic spectroscopic properties. The unusual behavior of this water has been attributed to its strong interaction with the head groups of the surfactant as well as to an overall disruption of the three-dimensional hydrogen-bonded network usually present in bulk water [111].

3.2
Aqueous Phase pH

The aqueous phase pH determines the ionization state of the surface-charged groups on the protein molecule. Solubilization of the protein in RMs is found to be dominated by electrostatic interactions between the charged protein and the inner layer of the surfactant head groups [112]. Solubilization of protein is favored at pH values above the isoelectric point (pI) of the protein in the case of

cationic surfactants, while the opposite is true for anionic surfactants. Chang et al. [48] showed that the solubilization of α-amylase in Aliquat-336 could be achieved by increasing the pH above its pI (5.4). They observed a maximum solubilization (~85%) of the enzyme at pH 10. Many other studies also indicated dependence of protein solubility on pI [44, 46, 49, 83, 113]. It may be noted that for proteins with small molecular weight such as cytochrome C, lysozyme, and ribonuclease (MW range 12,000–14,500 Da), the (pH – pI) value required for optimum solubilization is much lower (< 2) when compared to that of larger proteins such as α-amylase (MW 48,000 Da) [36] and alkaline protease (MW 33,000 Da) [15] where (pH – pI) is around 5. This can be explained with the reasoning that as the protein size increases, size of the RM also has to increase in order to incorporate the protein molecule. To increase the size of RM, higher energy is required which can be provided by increasing the number of charged groups on the protein [34, 36]. This increase in charge density on the protein molecule can be accomplished by manipulating the pH of the aqueous solution (i.e., by increasing the pH much higher than the pI of the protein) [105]. For small proteins whose size is smaller than the size of the water pool inside an RM, solubilization occurs as soon as the net charge is opposite to that of the reverse micellar interface.

3.3 Ionic Strength

The influence of ionic strength (KCl/NaCl concentration) on the solubilization of proteins in RMs is explained purely as an electrostatic effect [114]. The electrostatic potential of a protein molecule in an electrolyte is inversely proportional to the ionic strength of the solution and is characterized by Debye length. In general, it was observed that as the ionic strength of the aqueous solution increases, the protein intake capacity of the RMs decreases [83, 115, 116]. Two reasons were given to explain this phenomenon. First, increasing the ionic strength decreases the Debye length thereby reducing the electrostatic interaction between the charged protein molecules and charged surfactant head groups of the RMs. Second, increasing the ionic strength reduces the electrostatic repulsion between the charged head groups of the surfactants in a RM, thereby decreasing the size of RM [36]. The smaller RMs will have larger curvature, which increases the density of the surfactant monolayer near the surfactant head groups, resulting in a gradual expulsion of the protein molecules residing inside the RMs. The process is termed as a squeezing-out effect [114]. Further, it has been observed that not only the concentration but also the type of the ions play a very important role in determining W_0 and partition behavior of proteins in RMs [46, 116]. It may be noted that although lower side of ionic strength favors the protein transfer, one cannot perform the experiments at very low ionic strengths (NaCl/KCl concentration ≤ 0.01 mol l^{-1}) because under these conditions the solution becomes cloudy [116]. Further, Marcozzi et al. [116] have stated that the type and concentration of salt used in the forward extraction process remarkably affect the percentage recovery and activity in the back extraction process.

3.4
Surfactant Type

The protein distribution is mainly dependent on the charge difference between the protein and the surfactant head groups. When other effects are insignificant, pH of the protein solution determines the distribution behavior of protein in RMs stabilized by charged surfactants. In addition to the charge, other surfactant-dependent parameters such as the size of RMs, the energy required to enlarge the RMs, and the charge density on the inner surface of the RMs may also influence the protein distribution.

Most of the work on RMs reported to date has been with AOT, which is an anionic surfactant [46, 74]. Cationic surfactants such as quaternary ammonium salts (TOMAC and CTAB) have also been used for protein solubilization [34, 42, 103, 117]. The studies with AOT RMs in many cases have shown a rapid degradation of the protein activity after their solubilization [83, 118, 119]. Protein denaturation was also observed in case of RMs having cationic surfactants. For instance, glucose-6-phosphate dehydrogenase was denatured in CTAB/hexanol/octane RMs [120]. Recently, many researchers have studied protein transfer using non-ionic surfactants such as Tween-85 [121–124]. It was demonstrated that a non-ionic surfactant has an apparent advantage over ionic surfactants [124] due to the absence of strong charges at the aqueous/organic interface, which provide a suitable environment for the protein. Further, Tween-85 is nontoxic [125]. Although, a few studies have been carried out using non-ionic surfactants and shown to alleviate significantly protein stability problems, there has been little understanding regarding the reason for enzyme stability (with respect to structure and function) and solubilization in these RMs [124]. In many cases the effect of temperature, pressure, and ionic strength were found to be opposite to those observed in ionic based mixtures [34, 126].

3.5
Surfactant Concentration

The concentration of surfactant has been shown to have a little effect on the structure and size or aggregation number of the RMs [127]. However, it causes changes in the number of RMs, which increases the protein solubilization capacity of the RMs. Enhanced amino acid [115] and protein solubilization [47, 128] were observed in RMs by increasing the TOMAC (up to 200 mmol l^{-1}) and BDBAC (up to 150 mmol l^{-1}) concentration respectively. However, further increase in the surfactant concentration decreased solubilization of biomolecules [108, 115]. At surfactant concentration above a certain value, the micellar interactions may occur leading to percolation and interfacial deformation, with a change in the micellar shape and micellar clustering. Goklen [129] suggested that at high surfactant concentrations, monodisperse spherical micelles might not be present predominantly in the solution. The micellar clustering decreases the interfacial area available to host the biomolecules causing a decrease in the solubilization capacity of the RMs. This is especially true for solutes with strong interfacial interactions, such as tryptophan [115]. Alexandridis et al. [130] and

Cardoso et al. [115] have shown that AOT concentration is related to percolation. The percolation phenomenon was followed by a steep increase in the micellar conductivity [115]. Huang and Lee [49] observed a drastic reduction in the recovery (around 40 %) of the horse radish peroxidase when AOT concentration was at 5 mmol l^{-1} and further increase in AOT concentration to 10 mmol l–^{1} produced no recovery at all.

3.6 Micelle Size

Micelle size is dependent on the ratio $W_0 = [H_2O]/[\text{Surfactant}]$ but not on $[H_2O]$ or [Surfactant] alone [131]. The monodisperse small sized RMs [132] can accommodate only proteins of certain dimensions. Hence, micelle size may be used to include or exclude certain proteins. However, it should be noted that several micelles can regroup to form larger micelles when certain operating conditions are altered. It was also hypothesized that a protein can create around itself a new larger micelle of a requisite size to facilitate solubilization. Wolf and Luisi [133] reported that a given protein induces the formation of large enough micelles for the protein to fit into. Besides water and surfactant concentration, it was also demonstrated that equilibrium micelle size can be controlled by ionic strength of the bulk aqueous phase [134]. As the ionic strength increases the micellar size decreases due to decrease in the electrostatic repulsion between the head groups of surfactants. This results in gradual expulsion of the protein molecule from the RMs, which is termed as a squeezing out effect [114]. Besides ionic strength, micelle size is also influenced by the type of the solvent (see Sect. 2.3). Therefore selection of a suitable solvent becomes an important task and several solvents should be tested. Goklen and Hatton [135] studied the effect of solvent structure on maximum RM size, W_0^{max}. Hexane, isooctane and octane were reported to have much higher W_0^{max} values (75 – 115) compared to dodecane, cyclohexane, xylenes, carbon tetrachloride, or chloroform (5 – 20).

3.7 Miscellaneous Factors

Other factors that may affect protein extraction are volume ratio of organic to aqueous phases (V_{org}/V_{aq}), cosurfactant, temperature, mass transfer efficiency, protein charge, electrostatic potential of the RMs, and presence of other ions such as Ca^{+2}, Mg^{+2}, Ba^{+2}, etc.

(V_{org}/V_{aq}) is a critical parameter in extraction and concentration of enzymes. For an ideal system, in general, this ratio should be low for extraction and high for stripping steps to achieve concentration. The use of a cosurfactant may enhance the solubilization kinetics, stability of a RM, and even selectivity. Medium-chain length alcohols like isopropanol and hexanol have been used for this purpose. Temperature is a factor to investigate within the range of enzyme stability and inactivation. It was reported that as temperature increases, water solubilization capacity increases in the organic phase in case of AOT-RMs [46], and the exactly opposite phenomenon occurs in the case of TOMAC-RMs [136].

The variation in the water uptake is due to a change in the aggregation number of the surfactants. It was also noted that to maintain a clear reverse micellar phase after forward extraction, temperature control (25 °C) was critical [46]. In contrast to these observations, Huang and Chang [137] have recently reported that, as temperature increases, AOT content in the organic phase reduces, resulting in a poor forward transfer efficiency. They also observed that back extraction of the enzyme α-chymotrypsin was favored at higher temperature (40 °C). Two postulates were made for this enhanced enzyme recovery: (i) the RMs will be disrupted at higher temperatures due to their high energy level and the relaxation time for enzyme transfer through oil-water interface will be decreased and (ii) the migration rate of the AOT-RMs through the oil-water interface toward the water phase will be higher at higher temperatures, which leads to enhanced recovery of the enzyme activity. Protein charge and electrostatic potential within the RMs are closely linked to factors such as pH and ionic strength. In addition to the chemical and biochemical factors, protein transfer also depends on physical aspects such as extent of mixing and contact surface between the two phases.

Presence of ions was also found to have an effect on protein solubilization. Misiorowski and Wells [138] studied the solubilization and the activity of phospholipase A_2 in RMs and found that incorporation of the enzyme into micelle was greatly dependent on the presence of divalent cations. Though Ca^{+2} was absolutely necessary for specific catalytic function, solubilization could also be achieved by Mg^{+2} and Ba^{+2}. Regalado et al. [51] have observed a poor solubility of horse radish peroxidase in AOT-RMs mainly due to the presence of high mineral content in the crude extract, which has reduced the W_0 value of RMs significantly. The ions caused an electrostatic screening of the surfactant head groups hindering their interactions with the protein molecule, leading to reduced W_0 values. Addition of calcium scavengers (citric acid-citrate and EDTA-disodium salt) improved the solubilization and recovery of the enzyme.

3.8
Mechanism and Methods of Protein Solubilization

Although many studies have been performed on the RME of proteins [15, 42, 105, 131, 139–142] and the catalytic properties of enzymes in RMs [143, 144], very little is known about the mechanism of protein solubilization in RMs and the major driving forces which affect the solubilization.

There are three commonly used methods [145] to incorporate enzymes in RMs: (i) injection of a concentrated aqueous solution, (ii) addition of dry lyophilized protein to a reverse micellar solution, and (iii) phase transfer between bulk aqueous and surfactant-containing organic phases. Figure 3 shows schematically the three enzyme solubilization methods. The injection and dry addition techniques are commonly used in biocatalytic applications, the latter being well suited to hydrophobic proteins [146]. The phase transfer technique is the basis for extraction of proteins from aqueous solutions.

Several experimental and theoretical studies have been reported on the solubilization of proteins in RMs. Experimental tools used to study protein solubi-

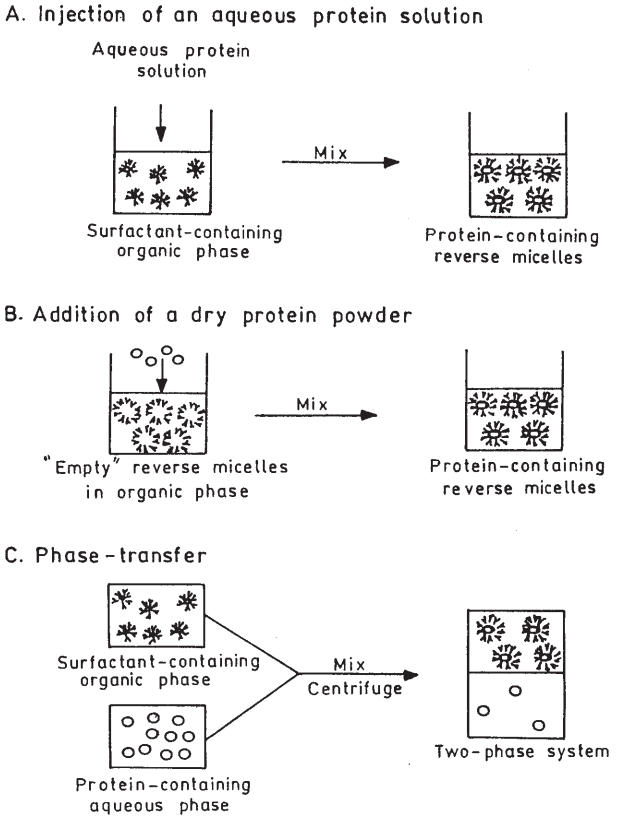

Fig. 3a–c. Various methods of protein solubilization in reverse micelles. (Reproduced from [145] with permission of Wiley)

lization include ultracentrifugation [147–149], quasi-elastic light scattering (QELS) [146], small-angle neutron scattering (SANS) [150–152], small-angle X-ray scattering (SAXS) [153, 154], and fluorescence recovery after fringe pattern photobleaching [155]. Protein structure in reverse micellar phase has been examined with ultraviolet (UV) and fluorescence spectroscopies as well as optical rotary dispersion and circular dichroism [132, 156]. High-pressure electron paramagnetic resonance spectroscopy was also used to assess protein mobility in RMs [125].

Blanch and coworkers [145] investigated in detail the solubilization properties of α-chymotrypsin and alcohol dehydrogenase (ADH) in RMs prepared by the above three techniques. Protein solubilization in RMs greatly depends on the method used for protein addition as well as on the size of the protein and of the RM. For the dry addition method protein solubilization is strongly dependent on micelle size whereas for the injection method it is less dependent. For smaller proteins like α-chymotrypsin (diameter of 44 Å), maximum solubilization occurred when the micelle diameter was 50–60 Å. For larger proteins like ADH

(dimensions of 45 × 60 ×110 Å), maximum solubilization occurred at a larger micelle size of 80–90 Å. Therefore, when a dry protein powder is added, the size of the RM must be approximately the same or larger than the protein molecule for efficient solubilization. It appears that the energy barrier for solubilization of a large protein in a small micelle is too large to overcome. For a larger micelle, since the micelle is not required to rearrange its contents to incorporate a protein, the energy barrier is lower and the protein is solubilized [145, 157]. Matzke et al. [145] also revealed that, at intermediate micelle diameters, the reverse micellar system enhances the solubility of ADH above a value that is attainable in bulk aqueous phase. This enhanced solubility suggests that ADH interacts with the reverse micellar interface. Vos et al. [158] reported electrostatic interactions between ADH and AOT interface, which was supported by Matzke et al. [145].

For the injection method, where a saturated protein solution is added directly to the surfactant-containing organic phase, the RMs are forced to form around the proteins already present in the solution. Thus, protein solubilization is not strongly dependent on micelle size in this technique.

The phase transfer method of protein solubilization is fundamentally different from the other two methods. In this method, there are two bulk phases (aqueous and organic) which are brought to equilibrium. Under certain conditions, the protein molecules are transferred from the aqueous phase to the surfactant-containing organic phase. Unlike the dry-addition and injection methods, it is difficult to obtain a value for the maximum solubilization using the phase-transfer method. Moreover, since this method is mainly used for protein extraction, it is desirable to use aqueous phase protein concentrations consistent with those in a typical fermentation broth. For the phase-transfer method, pH of the aqueous phase, the size and isoelectric point of the protein, and the surfactant type were shown to have a significant effect on protein solubilization [145].

Cardoso et al. [115] using the phase transfer technique studied the driving forces involved in the selective solubilization of three different amino acids having same pI, namely aspartic acid (hydrophilic), phenylalanine (slightly hydrophobic), and tryptophan (hydrophobic) in cationic TOMAC-RMs. The main driving forces involved were found to be hydrophobic and electrostatic interactions. Few other researchers have also identified that the major driving forces involved in the amino acid solubilization were hydrophobic interactions [114, 159] and amino acid structure as well as its ionization state [160, 161].

3.9 Back Extraction

Transfer of solubilized proteins from the reverse micellar phase back to an aqueous phase constitutes back extraction. A successful RME should include both forward and back extraction processes in their optimized conditions. In contrast to the extensive studies investigating the forward extraction process, back extraction has been addressed to a much lesser extent. Most of the earlier studies tacitly assume that conditions, which normally prevent protein uptake in the forward transfer, would promote their release in the back transfer. That is to select a pH and salt condition that had minimal forward transfer efficiency. This

assumption, however, is not true [74] and resulted in only a low protein recovery [42, 134]. As reviewed by Kelley et al. [162], overall recovery in RME is generally below 80%. Rahaman et al. [15] reported only 10–20% of alkaline protease recovery from AOT/isooctane RMs, which was attributed to kinetic limitations.

Recently, some alternative approaches for enhanced recovery of the proteins from RMs have been investigated. They include: (i) use of silica particles for the sorption of the proteins as well as surfactants and water directly from the protein-filled RMs [134, 163] and use of ion-exchange columns [164], (ii) addition of dewatering agents such as isopropyl alcohol [74] and dehydration of RM with molecular sieves to recover the protein [165], (iii) addition of large amount of a second organic solvent, such as ethyl acetate to destabilize the RM and hence to release the protein [105], (iv) formation of clathrate hydrates via pressurization [166], (v) use of temperature to dewater the RMs and hence to release the protein [136, 137], (vi) use of NaDEHP/isooctane/brine RMs which can easily be destabilized by adding divalent cations (such as Ca^{2+}) and subsequent release of the protein into aqueous media [167], (vii) addition of sucrose to enhance the protein recovery by reducing the protein-surfactant interactions [168], and (viii) back extraction with the aid of a counter-ionic surfactant [104] and through the gas hydrate formation [169].

3.10 Mass Transfer Kinetics

Rate of protein transfer to or from a reverse micellar phase and factors affecting the rate are important for the practical applications of RME for the extraction and purification of proteins/enzymes and for scale-up. The mechanism of protein exchange between two immiscible phases (Fig. 2) can be divided into three steps [36]: the diffusion of protein from bulk aqueous solution to the interface, the formation of a protein-containing micelle at the interface, and the diffusion of a protein-containing micelle in to the organic phase. The reverse steps are applicable for back transfer with the coalescence of protein-filled RM with the interface to release the protein. The overall mass transfer rate during an extraction processes will depend on which of these steps is rate limiting.

Dekker et al. [170] studied the extraction process of α-amylase in a TOMAC/isooctane reverse micellar system in terms of the distribution coefficients, mass transfer coefficient, inactivation rate constants, phase ratio, and residence time during the forward and backward extractions. They derived different equations for the concentration of active enzyme in all phases as a function of time. It was also shown that the inactivation took place predominantly in the first aqueous phase due to complex formation between enzyme and surfactant. In order to minimize the extent of enzyme inactivation, the steady state enzyme concentration should be kept as low as possible in the first aqueous phase. This can be achieved by a high mass transfer rate and a high distribution coefficient of the enzyme between reverse micellar and aqueous phases. The effect of mass transfer coefficient during forward extraction on the recovery of α-amylase was simulated for two values of the distribution coefficient. These model predictions were verified experimentally by changing the distribution coefficient (by adding

nonionic surfactant to the reverse micellar phase) and the mass transfer coefficient of the enzyme during the forward extraction (by increasing the stirrer speed). The experimental results correlated well with the model predictions. In this way the performance of the reverse micellar extraction of α-amylase was improved to give an 85% yield of active enzyme in the second aqueous phase and 17-fold concentration of the enzyme. The surfactant losses were also reduced to 2.5% per circulation of the reverse micellar phase. The model also predicted further improvement in the extraction efficiency by modifying the extraction techniques, e.g., by reducing the residence time during the extraction in combination with a further increase in the mass transfer rate. The use of centrifugal separators or extractors might be valuable in this respect.

4 Mathematical Modeling of Reverse Micellar Extraction

Mathematical modeling of the solubilization of biomaterials in RMs is essential for an in-depth understanding and for effective use of RME in downstream processing of biomolecules. However, the quantitative modeling of protein solubilization in RMs is a complex problem. Moreover, many parameters are unknown or difficult to quantify, which include hydrophobic interactions of ions with the protein and surfactant, the free energy changes associated with the change in size of the RMs on protein uptake, and the distribution of charged groups on the protein molecule [170]. Models presented in the literature for protein solubilization range from simple geometric models [147] to more rigorous molecular thermodynamic models [153, 171–173].

Bonner et al. [147] first proposed the shell and core model to determine the radii of protein-filled and unfilled RMs assuming that the protein was in the water pool of the RM. They used an analytical ultra-centrifugation technique to measure the molecular weight of the protein-containing RM as a function of the molar water-to-surfactant ratio, W_0, in the one-phase system. The water pool volume is the sum of the protein volume and the volume of the water of the contributing unfilled RMs. The water content of the protein-filled RM was assumed to be the same as the initial W_0. The protein-containing RMs were generally found to be larger than the unfilled ones, especially at low W_0. It was assumed in this model that the empty RMs combine to form a filled micelle in such a way that the net water-to-surfactant ratio, W_0, of the filled-RM is the same as that of the reverse micellar solution as a whole. However, it is now well recognized that this is not the case. Nonetheless, this pioneering effort has stimulated more detailed modeling studies.

An alternative description of protein-containing RMs was given by Levashov et al. [148] from ultra-centrifugation studies. Water-soluble dyes (picric acid) were used to determine the molecular weights and sedimentation behavior of the non-protein-containing and protein-containing RMs. The proposed model involved two regimes of W_0: (i) at low W_0 (where the inner reverse micellar diameter was less than the protein diameter), the protein 'created' a new RM around itself such that the volume of the inner cavity of the filled RM was essentially the volume of the solubilized protein and (ii) at water contents where

the reverse micellar inner diameter was greater than the protein diameter, the surfactant aggregation number and W_0 were assumed to be the same as in the initial, unfilled RMs. Thus, the model predicted that the diameter of the RM changed very little upon protein solubilization. This model has received stern opposition from Luisi's group [149] and Hatton's group [151] as the model violates the area and volume constraints imposed on the system by the predetermined water, protein and surfactant concentrations, and the results of the Soviet group were thought to be an artifact of the experimental and analytical procedures. This argument has been rebutted by the Soviet group who justified their assumption by ^{13}C nuclear magnetic resonance experiments [174]. They postulated that the reverse micellar water boundary shifted outward upon protein solubilization and contended that their proposed scenario is consistent with deeper penetration of the surfactant head group region by water, owing to the presence of the protein in the micelle core. Thus, no change in the outer diameter would be expected.

Zampieri et al. [149], in order to circumvent the inherent problems of the earlier sedimentation studies, employed two different dyes (one water soluble and the other strong interfacially active) to monitor the association of water and surfactant with empty and filled RMs independently. They were able to estimate the sizes of filled and empty RMs based on water, protein, and surfactant balances by determining the individual W_0 values for the two types of RMs. The conclusions arrived at were in sharp contrast to those of Levashov et al. [148], as it was shown that both the filled and empty RMs increased in size with the overall W_0 and that neither the filled nor the empty RM size was the same after protein uptake. An assumption made by Zampieri et al. [149] is that the two dyes distributed between the RMs in proportion to water and surfactant, respectively. Hatton's group [152] suggested that this assumption may not be true based on their analyses of the substrate distribution effects and suggested that the statistical distribution of solutes over the micelle population may be skewed to one or the other of two types of RMs.

Other molecular thermodynamic models for protein-reverse micelle complexes have also emerged. Bratko et al. [171] presented a model for phase transfer of proteins in RMs. The shell and core model was combined with the Poisson-Boltzmann approximation for the protein-RM complex and for the protein-free RM. The increase in entropy of counterions released from RMs on solubilization of a protein was the main contribution to the decrease in free energy of complexation. Good agreement was found with SANS results of Sheu et al. [151] for cytochrome C solubilization and the effect of electrolytes on it. However, this model assumes that filled and empty RMs are of the same size, independent of salt strength and pH, which is not true according to experimental evidence available since then.

Woll and Hatton [175] have developed a phenomenological thermodynamic model for the partitioning of proteins between aqueous and reverse micellar phases. A simple expression for the protein partition coefficient was derived as a function of pH and surfactant concentration and the partitioning of ribonuclease A and concanavalin A were shown to correlate well with the model. However, this model was a correlative one but not predictive.

Caselli et al. [172] presented a simplified thermodynamic model for protein solubilization. Electrostatic interactions between the protein and reverse micellar inner surface were included. The model was found to have good agreement with the ultra-centrifugation data of Zampieri et al. [149]. Rahaman and Hatton [152] developed a thermodynamic model to predict the sizes of protein-filled and unfilled RMs made by both the injection and phase transfer techniques. This model assumed a bidisperse population of RMs consisting of empty and filled micelles. These results differ from those of Caselli et al. [172], who found that the sizes of both filled and unfilled RMs varied with variation in water content. This model was also used to test the SANS data of Sheu et al. [151] with good agreement for cytochrome C solubilization at low protein concentrations [172]. However, poor agreement was found at higher cytochrome C concentrations, which may be due to protein-interface interactions [154].

The distribution behavior of proteins between a bulk aqueous phase and a reverse micellar phase has been modeled based mainly on electrostatic interactions between the charges on the protein molecules and the charges on the ionic head groups of the RMs [175–177]. In addition to the free energy change resulting directly from this interaction, an additional contribution arising from the redistribution of surfactant and protein counter-ions, of other free ions, of water, and of surfactant on phase transfer must be considered. Although calculations were made of the total free energy change on the uptake of a hypothetical small protein in RMs [176], no comparisons have been shown with experimentally determined distribution data. Fraaije et al. [177] analyzed the distribution behavior of cytochrome C between an aqueous phase and a reverse micellar phase of TOMAC in isooctane, in a more phenomenological approach, with respect to the aqueous phase pH and ionic strength. From the experimental data, calculations were made on the copartitioning of protons and other small ions accompanying protein uptake in RMs. Around the optimal pH for protein transfer to the reverse micellar phase, both protons and surfactant counter-ions (chloride) were found to be redistributed.

Protein partitioning and ion co-partitioning in the two-phase system was also modeled by Fraaije et al. [177]. Experiments performed on the partitioning of cytochrome C in TOMAC-octanol-isooctane provided good agreement with the model. At the pH of maximum solubilization, no co-partitioning of ions occurred. At pH values below and above the maximum solubilization pH, there was exclusion and inclusion, respectively of electrolytes.

All these models are useful in analyzing experimental data of protein partitioning and in identifying the most important system parameters affecting the value of the distribution coefficient. The neglected parameter in all the above models was the distribution of charged groups on the protein molecules. In all the approaches, an equal distribution of surface charge on a globular protein molecule was assumed. At present, however, the models are yet to be shaped to perfection to give accurate predictions of the distribution coefficient of a protein.

4.1
Model for Protein Inclusion

There have been relatively few studies on the modeling of protein-containing reverse micellar systems. Bonner et al. [147] were the first to address this problem based on a simple hypothesis that the RM expands by a volume equal to that of protein when a protein is encapsulated within it. However, no account was taken of the physico-chemical interactions occurring in the system that might be responsible for the formation of a protein-micelle complex. Woll and Hatton [175] extended this idea to relate the complex size to protein size and charge, and surfactant concentration. They developed a phenomenological model which adequately correlated experimental results on the partitioning of the proteins (ribonuclease A and concanavalin A) between bulk aqueous and reverse micellar solutions. This model was only correlative and not predictive in nature and does not provide insight into the fundamentals of the protein-containing reverse micellar systems. The simplified thermodynamic model of Caselli et al. [172] for the prediction of the sizes of filled and empty RMs come closer to the goal. The authors based their model on the minimization of an approximate expression for the system free energy incorporating contributions from the electrostatic interactions between the protein and charged reverse micellar head groups. Further, Caselli et al. [173] extended this model for protein inclusion in RMs utilizing SANS measurements as a control test. The radii of the protein-filled and empty RMs (Fig. 4) following the Sheu convention which includes the polar heads [151], can be obtained, once the polar head volume V_{sh} (Å^3) has been assigned:

$$R_e = \left\{ \frac{3}{4\pi} \left(N_e^w V_w + N_e^s V_{sh} \right) \right\}^{\frac{1}{3}} \tag{1}$$

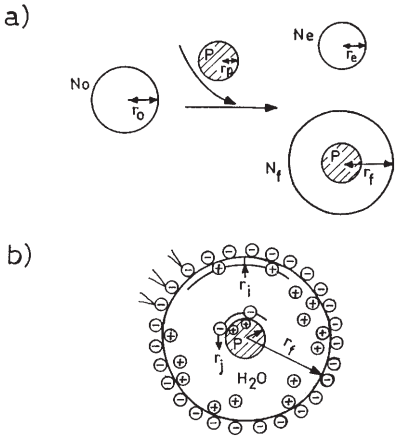

Fig. 4. **a** Schematic representation of protein solubilization in reverse micelles indicating the main geometrical parameters. **b** The protein-filled reverse micelle seen as a system of two interacting concentric microcapacitors. (Reproduced from [172] with permission of American Chemical Society)

$$R_F = \left\{ \frac{3}{4\pi} \left(N_F^w V_w + N_F^s V_{sh} + V_p \right) \right\}^{\frac{1}{3}} \tag{2}$$

where R_e is the radius of the empty RMs including the polar heads, R_F is the radius of protein filled RMs including the polar heads, N_e^w and N_e^s are the water aggregation number and the surfactant aggregation number of empty RMs, N_F^w and N_F^s are the water aggregation number and the surfactant aggregation number of filled RMs, V_w is water molecule volume (Å^3), and V_p is protein volume (Å^3).

Taking the free energy variation into account, the authors have also derived a thermodynamic equilibrium condition:

$$\frac{d\Delta\xi}{dz} = \frac{\partial\Delta\xi}{\partial z} + \frac{\partial y}{\partial z} = \frac{\partial\Delta\xi}{\partial y} = 0 \tag{3}$$

In this equation $\Delta\xi = \Delta\xi_{Eel} + \Delta\xi_{Sel} + \Delta\xi_{id} + \Delta\xi_{mix}$ and $\Delta\xi$ was a reduced quantity utilized in place of ΔG, the insertion free energy and given by

$$\Delta\xi = \frac{\Delta G}{NkTC_p} \tag{4}$$

where N is Avagadro number, k is Boltzmann constant, T is absolute temperature, and C_p is protein concentration. $\Delta\xi_{Eel}$ (reduced form of the electrostatic energy contribution to the free energy), $\Delta\xi_{Sel}$ (reduced form of the electrostatic entropy contribution to the free energy), $\Delta\xi_{id}$ (reduced form of the counter-ions mixing contribution to the free energy), and $\Delta\xi_{mix}$ (reduced form of the RMs partition contribution to the free energy) are described thoroughly by Caselli et al. [172, 173].

Equations (1–3) provide the complete formalization of the simplified thermodynamic model. The model was found to show good agreement for cytochrome C concentrations up to 40 µmol l^{-1}, but not at higher concentration (160 µmol l^{-1}). With all its merits, this model was thought to be inconsistent in the limits of occupancy of RMs, where the radius of filled RMs is the same as that of the unfilled ones. The assumption made by the authors about constant surfactant head group coverage implies that there is the same number of filled RMs as there were empty RMs initially. This was argued to result in a violation of the constraint of constant water volume in the system.

4.2 Model for Protein Extraction Using Hollow Fibers

Dahuron and Cussler [178] calculated overall mass transfer coefficients for seven proteins in RMs and in ATPS in hollow fibers from the equations given by Zhang and Cussler [179] and Dahuron [180] for the estimation of concentrations.

For co-current flow:

$$\ln \frac{\Delta C}{\Delta C^0} = -t \left\{ \left(\frac{1/V_{in} + 1/HV_{out}}{1/Q_{in} + 1/HQ_{out}} \right) \left[1 - e^{-4K_{in}\ell/\nu_{in}d(1 + Q_{in}/HQ_{out})} \right] \right\} \tag{5}$$

For counter-current flow:

$$\ln\frac{\Delta C}{\Delta C^0} = -t\left\{\left[Q_{in}\left(\frac{1}{V_{in}}+\frac{1}{HV_{out}}\right)\right]\left[\frac{1-e^{-4K_{in}\ell/v_{in}d(1-Q_{in}/HQ_{out})}}{1-\frac{Q_{in}}{HQ_{out}}e^{-4K_{in}\ell/v_{in}d(1-Q_{in}/HQ_{out})}}\right]\right\} \tag{6}$$

For both co-current and counter-current flows, the concentration differences on the left- hand sides are given by

$$\ln\frac{\Delta C}{\Delta C^0} = \ln\left[\frac{C_{in}\left(1+\frac{V_{in}}{HV_{out}}\right)-\frac{C^0_{in}V_{in}}{HV_{out}}-\frac{C^0_{out}}{H}}{C^0_{in}-\frac{C^0_{out}}{H}}\right] \tag{7}$$

where C is solute concentration, C^0 is initial solute concentration, d is fiber diameter, H is partition coefficient, K_{in} is overall mass transfer coefficient, t is time, ℓ is fiber length, Q_{in} and Q_{out} are volumetric flows of inner and outer fluids, V_{in} and V_{out} are reservoir volumes of inner and outer fluids, and v_{in} is the inlet velocity.

The mass transfer coefficient K_{in} can be calculated from the slope of the line obtained by plotting the solute concentration ratio (ln $[\Delta C/\Delta C^0]$) from Eq. (7) vs time. This K_{in} is related to Eqs. (5) and (6). However, the parameters in the above Eqs. (5) – (7) are quite complicated functions. Hence, the gas absorption equations developed by Yang and Cussler [181] in hollow fiber contactors have been extended for liquid-liquid systems. The overall mass transfer resistance in hollow fiber modules is given by [2, 182]:

$$\frac{1}{K_{in}} = \frac{1}{k_{in}} + \frac{1}{k_{mem}} + \frac{1}{k_{out}H} \tag{8}$$

where k_{in}, k_{mem}, and k_{out} are the individual mass transfer coefficients inside the fiber, across the fiber wall, and outside the fibers, and H is the partition coefficient. Equation (8) differs from the conventional mass transfer equation by the inclusion of the membrane resistance term, $1/k_{mem}$ [179]. k_{mem} can be given by

$$k_{mem} = \frac{D}{\delta} \tag{9}$$

where D is the diffusion coefficient in the membrane and δ is the effective membrane thickness, which includes both the void fraction and the pore tortuosity of the particular membrane. The effective thickness, δ, cannot be estimated theoretically, but must be found experimentally. Equation (9) holds good only if the membrane is wet by the inner solution. If the membrane is wet by the outer solution, then

$$k_{mem} = \frac{DH}{\delta} \tag{10}$$

While Eq. (10) is mathematically similar to Eq. (9), it is dramatically different when H is significantly different from unity. It is evident from Eqs. (9) and (10) that k_{mem} does depend on the diffusion coefficient of the solute in the solvent within the pores and effective thickness, δ, which is a membrane property. It does not depend on flow properties of the adjacent solutions. The flow properties affect only k_{in} and k_{out}.

For proteins in RMs, k_{in} is given by the empirical correlation [178]:

$$\frac{k_{in}d}{D} = 1.5\left(\frac{d^2 v_s}{\ell D}\right)^{\frac{1}{3}} \tag{11}$$

Similarly k_{out} can be given by [178]

$$\frac{k_{out}d_e}{D} = 8.8\left(\frac{d_e^2 v_s}{\ell v_s}\right)\left(\frac{v_s}{D}\right)^{\frac{1}{3}} \tag{12}$$

where v_s is the velocity, and d is the fiber diameter.

Very good agreement was observed between the experimental and calculated results of mass transfer coefficient for proteins in RMs using Eqs. (11) and (12).

4.3 Enzyme Distribution in Relation to Water Content

In RMs, enzyme properties will depend on essentially three factors: the structure of RMs, the dynamics of RMs, and the distribution of enzyme in RMs. Based on an understanding of these aspects, Bru et al. [183] have developed a model, as summarized below, which simulates the dependence of enzyme activity on water content.

Reverse micelles are microheterogenous media where solubilized enzyme molecules are subject to the partitioning between different phases. The enzyme distribution between the phases is given by [183]

$$K_E^1 = \frac{[E]_b}{[E]_f} \tag{13}$$

$$K_E^2 = \frac{[E]_s}{[E]_b} \tag{14}$$

where K_E^1 and K_E^2 are enzyme partition coefficients between domains, and $[E]_i$ is the enzyme concentration in each domain. The total number of moles of enzyme is given by

$$[E]_{total} = [E]_f V_f + [E]_b V_b + [E]_s V_s \tag{15}$$

where V_i is the volume of each domain. Thus

$$[E]_f = \frac{[E]_{total}}{V_f + K_E^1 V_b + K_E^1 K_E^2 V_s} \tag{16}$$

The enzyme shows different catalytic activities when solubilized in the free water, bound water, and the surfactant types (defined as K_f, K_b, and K_s, respectively).

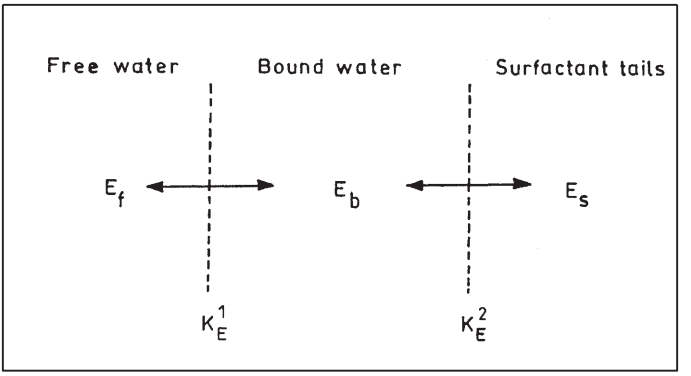

Fig. 5. Scheme showing enzyme distribution in reverse micellar microenvironment. (Reproduced from [183] with permission of The Biochemical Society)

Assuming [S]»K_m, the enzyme activity in a specific phase with respect to the overall volume can be expressed [184] as

$$v_i = \frac{K_i [E]_i V_i}{V} \tag{17}$$

and the observed activity or overall reaction rate is:

$$v = \sum_{i = f,b,s} v_i \tag{18}$$

The scheme showing enzyme distribution in micellar microenvironments [183] is given in Fig. 5.

4.4
Modeling of Forward and Back Extractions

In order to describe and optimize the reverse micellar extraction process, Dekker et al. [170] have proposed a mathematical model, which satisfactorily describes the time dependency of the concentration of active enzyme in all the phases, based on the flow, mass transfer, and first-order inactivation kinetics. For each phase, a differential equation is derived. For forward extraction:

$$\frac{dC_{w1}}{dt} = \frac{C_{w1,in} - C_{w1}}{\tau_1} - \frac{k_{01}A_1}{1 - \varepsilon_1}(C_{w1} - C^*_{w1}) - k_{iw1}C_{w1} \tag{19}$$

$$\frac{dC_{RM1}}{dt} = \frac{C_{RM2} - C_{RM1}}{\tau_1} + \frac{k_{01}A_1}{\varepsilon_1}(C_{w1} - C^*_{w1}) - k_{iRM}C_{RM1} \tag{20}$$

For back extraction:

$$\frac{dC_{w2}}{dt} = \frac{0 - C_{w2}}{\tau_2} - \frac{k_{02}A_2}{\varepsilon_2}(C_{RM2} - C^*_{RM2}) - k_{iw2}C_{w2} \tag{21}$$

$$\frac{dC_{RM2}}{dt} = \frac{C_{RM1} - C_{RM2}}{\tau_2} - \frac{k_{02}A_2}{1-\varepsilon_2}(C_{RM2} - C^*_{RM2}) - k_{iRM}C_{RM2} \tag{22}$$

where A_j is specific surface area in mixer j ($m^2\,m^{-3}$), C_j is concentration of active enzyme in phase j ($kg\,m^{-3}$), k_{ij} is inactivation rate constant in phase j (s^{-1}), k_{oj} is individual mass transfer coefficient in mixer j ($m\,s^{-1}$), t is time (s), ε_j is hold-up of dispersed phase in mixer j, and τ_j is residence time in mixer j (s).

Dekker et al. [170] have also shown that the steady state experimental data of the extraction and the observed dynamic behavior of the extraction are in good agreement with the model predictions. This model offers the opportunity to predict the effect of changes, both in the process conditions (effect of residence time and mass transfer coefficient) and in the composition of the aqueous and reverse micellar phase (effect of inactivation rate constant and distribution coefficient) on the extraction efficiency. A shorter residence time in the extractors, in combination with an increase in mass transfer rate, will give improvement in the yield of active enzyme in the second aqueous phase and will further reduce the surfactant loss. They have suggested that the use of centrifugal separators or extractors might be valuable in this respect.

4.5 Thermodynamic Model for Protein Partitioning

Fraaije et al. [177] reported a thermodynamic model for protein partitioning and the copartitioning of electrolytes in an aqueous-organic two-phase system. The model predictions were found to be in good agreement with experimental results. The main objective of this model was to derive a relation between the dependency of the protein partition coefficient on electrolyte concentrations in the aqueous phase, and the copartition ratios. The relation between the protein partition and the copartition of the ionic species is fully determined through their chemical potentials only in the water phase. The method assumed three conditions: (i) the surfactant and co-surfactant reside exclusively in the organic phase, (ii) the apolar solvent is ideally immiscible with water, and (iii) the volumes of the two phases are not affected by the protein partition. Further, it was assumed that the water phase is dilute in solutes so that the molar fraction of water is approximately unity and that the temperature and pressure are constant. The principal equation, which relates the copartition ratios to the protein partition and the chemical potentials, is given by

$$\Delta r_i = \frac{1}{C_P^{org}} \int_0^{\Pi} \left(\frac{\partial (C_P^{org}/C_P^{aq})}{\partial \mu_i} \right)_{\Pi,\, \mu_{j\neq i}} d\Pi \tag{23}$$

where Π is the osmotic pressure, Δr_i is copartition ratio, μ_i is the chemical potential of the species i, and C_P^{aq} and C_P^{org} are concentrations of protein in aqueous and organic phases respectively. Equation (23) was further simplified by assuming that the partition coefficient does not depend on the aqueous phase protein concentration and by employing Van't Hoff's law for the osmotic pressure owing to the low protein concentrations in the aqueous phase (< 5 μmol l^{-1}):

$$\Delta r_i^0 = RT\left(\frac{\partial \ln H}{\partial \mu_i}\right)_{\mu_{j\neq i}} \tag{24}$$

where H, the partition coefficient, is given by

$$H \equiv \lim_{C_P^{aq}\to 0}\left(\frac{C_P^{org}}{C_P^{aq}}\right) \tag{25}$$

4.6 Thermodynamic Modeling for the Size of RMs

The shell and core model combined with Poisson-Boltzmann approximation developed by Bratko et al. [171] which describes the thermodynamics of protein solubilization in RMs, assuming the electrostatic interactions and the ideal mixing of the proteins into the micellar solution as the important model components. The predictions of the model showed good agreement with the known salting out effect of cytochrome C in AOT-RMs. However, they assumed that filled and empty micelles are of the same size, independent of pH and salt concentration, while the experimental evidence [185] suggests that the RM size changes with a change in pH and salt concentration.

Rahaman and Hatton [152] developed a thermodynamic model for the prediction of the sizes of the protein filled and unfilled RMs as a function of system parameters such as ionic strength, protein charge, and size, W_0 and protein concentration for both phase transfer and injection techniques. The important assumptions considered include: (i) reverse micellar population is bidisperse, (ii) charge distribution is uniform, (iii) electrostatic interactions within a micelle and between a protein and micellar interface are represented by nonlinear Poisson-Boltzmann equation, (iv) the equilibrium micellar radii are assumed to be those that minimize the system free energy, and (v) water transferred between the two phases is too small to change chemical potential.

Thus the system total free energy can be given as

$$G_{tot} = G_{el} + G_{mix} + G_{tails} \tag{26}$$

where G_{el} represents the contributions from electrostatic interactions both between protein-surfactant and surfactant-surfactant, G_{mix} represents the contributions from the ideal mixing of the two classes of RMs into the organic medium, and G_{tail} represents the contributions from the steric interactions between the adjacent surfactant tails.

G_{el} can be given by

$$G_{el} = 4\pi N_F\{R_P^2\sigma_P\int_0^1 \psi(R_P;\lambda_c)\,d\lambda_c + R_F^2\sigma_m\int_0^1 \psi(R_F;\lambda_c)\,d\lambda_c\} + 4\pi N_e R_e^2\sigma_m\int_0^1 \psi(R_e;\lambda_c)\,d\lambda_c \tag{27}$$

where λ_c is the charging parameter and represents the fraction of the final charge attained on the protein and micellar surfaces at any stage in the charging process, ψ is the electrostatic potential at the radial position r within the

micelle, N_e and N_F are the reference salt concentration in the bulk aqueous phase for the empty and filled micelles, R_P, R_e and R_F are the radii of the protein, empty, and filled micelle, and σ_m and σ_P are the surface charge densities of micelle and protein.

G_{mix} can be given by

$$G_{mix} = k\,T \sum_i x_i \ln x_i \tag{28}$$

where the summation extends over the components i, i.e., over filled micelles, empty micelles, and solvent molecules, k is the Boltzmann constant, T is absolute temperature, and x is the mole fraction.

G_{tail} can be given by

$$G_{tails} = \beta \times \sum_i c_{si} \left\{ 1 - \frac{v}{\left[1 + \frac{1}{R_i} + \frac{1}{3}\left(\frac{1}{R_i}\right)^2 \right] - \frac{a}{l}\left[1 + \frac{a}{R_i} + \frac{1}{3}\left(\frac{a}{R_i}\right)^2 \right]} \right\}^2 \tag{29}$$

where c_{si} is the concentration of surfactant forming micelles of type i, β is the empirical model parameter, v is the surfactant packing parameter, and a is the thickness of surfactant head-group region.

This model provided an excellent agreement with SANS data for α-chymotrypsin in AOT-isooctane reverse micellar systems. As the water content increased in reverse micellar systems formed by the injection technique, the size of the protein-filled RMs remained approximately constant while the size of the unfilled RMs increased. Protein transfer was strongly dependent on salt concentration. Changes in protein concentration had no effect on reverse micellar radii, while an increase in salt concentration decreased the radius of unfilled RMs to a greater degree than that of protein-filled RMs. It was concluded that an optimum size of protein-filled RMs existed for a given pH and ionic strength. As W_0 was varied, only the size of the unfilled RMs varied in order to satisfy the material balance. Though the results were consistent, they are restricted to the solubilization of α-chymotrypsin which is known to reside in the water pool of the RM. This model, however, may not be extendable to proteins that are associated with the surfactant interface.

4.7 Interfacial Mass Transfer Model

Dungan et al. [186] have measured the interfacial mass transfer coefficients for the transfer of proteins (α-chymotrypsin and cytochrome C) between a bulk aqueous phase and a reverse micellar phase using a stirred diffusion cell and showed that charge interactions play a dominant role in the interfacial forward transport kinetics. The flux of protein across the bulk interface separating an aqueous buffered solution and a reverse micellar phase was measured for the purpose. Kinetic parameters for the transfer of proteins to or from a reverse micellar solution were determined at a given salt concentration, pH, and stirring

speed by measuring the bulk protein concentration as a function of time, the rates being determined for short-time data for which the flux was constant. This initial flux J is related to the mass transfer coefficient through the relation:

$$\begin{aligned} J &= \frac{V}{A}\frac{dc_{\text{meas}}}{dt} \\ &= k_{\text{f}}\left(c_{\text{aq}} - \frac{1}{H}c_{\text{org}}\right) \quad \text{for forward transfer} \\ &= k_{\text{r}}\left(c_{\text{org}} - Hc_{\text{aq}}\right) \quad \text{for back transfer} \end{aligned} \tag{30}$$

where k_{f} and k_{r} are the mass transfer coefficients for forward and back transfer, c_{aq} and c_{org} are the concentrations of the aqueous and organic phases, V is the volume of each phase, A is the interfacial area, and H is the partition coefficient ($H = c_{\text{org}}/c_{\text{aq}}$) relating equilibrium concentrations in each phase. Considering that for most forward transfer conditions studied $c_{\text{org}}/H < c_{\text{aq}}$, Eq. (30) can be integrated to give

$$\ln\left(1 - \frac{c_{\text{org}}}{c^0}\right) = -\frac{A}{V}k_{\text{f}}t \tag{31}$$

where c^0 is the initial concentration in the aqueous phase. Equation (31) represents forward transfer and there is a corresponding expression for back transfer. Thus, the mass transfer coefficient can be evaluated from the slope of the left-hand side value plotted as a function of time.

There also exists a linear relation between the bulk resistance ($R_{\text{f,b}}$) and the inverse of the stirring speed (N_{s}), i. e.,

$$R_{\text{f,b}} \alpha N_{\text{s}}^{-1} \tag{32}$$

Total resistance (R_{f}) is evaluated by adding two contributions, that is $R_{\text{f}} = R_{\text{f,b}} + R_{\text{f,i}}$, where $R_{\text{f,i}}$ is the interfacial resistance to forward transfer, which suggests that the total observable resistance is equivalent to that of the interfacial step. In practice, however, high stirring speeds will emulsify the two phases, so that there is an upper limit that dictates how fast the system may be stirred.

Considering $k_{\text{f}} = 1/R_{\text{f}}$ and Eq. (32), forward mass transfer coefficients can be expressed by the relation

$$k_{\text{f}} = \frac{\alpha' N_{\text{s}} k_{\text{f,i}}}{\alpha' N_{\text{s}} + k_{\text{f,i}}} \tag{33}$$

where α' is a prefactor dependent upon the diffusion coefficient of the species being transferred.

Electrostatic interactions between a spherical charged protein particle and an oppositely charged, deformable interface can be estimated by evaluating the electrostatic force on a small segment of the interface as that produced by an adjacent 'flat' section on the protein surface. The strength of this interaction is dependent on the separation distance (b) between those two segments, and so will be a function of the position of the interfacial segment:

$$b = f(F_{\text{e}}, q^1, q^{\text{P}}, K) \tag{34}$$

The function on the right hand side of Eq. (34) consists of a series of elliptic integrals, which depend not only on the unknown electrostatic force but also on the surface charge densities, q^{I} and q^{P} on the interface and protein surface, respectively, and on the inverse Debye screening length (1/K).

This definition for K holds only for monovalent ions and depends on the aqueous dielectric constant (ε), Boltzmann's energy ($k_B T$), and the electronic charge (e). The Debye length varies inversely with the ionic strength of the solution and thus measures the ability of the ions to screen the protein/interface interactions.

The electrostatic force (F_e) between two charged plates separated by an electrolyte solution can be determined from an existing implicit solution to the nonlinear Poisson-Boltzmann equation and can be expressed in the form [187]

$$F_e = \Delta\Pi - \frac{1}{2}\varepsilon E^2 \tag{35}$$

The second term in Eq. (35), which depends on the electric field E between the surfaces, represents the attractive interaction caused by the opposite charges on the surfaces, while the first term is the osmotic pressure contribution which results in a repulsive interaction. Equation (35) predicts that the net electrostatic force between two surfaces can be either positive or negative, depending on how far apart they are from each other. If the surfaces are far apart, the second term that arises from the interaction of opposite charges will cause the surfaces to attract each other. At very close separations, electroneutrality requirements lead to a very high concentration of counter ions being squeezed between the plates. This high concentrations results in a strong osmotic pressure which pushes the plates apart. The interplay between repulsive and attractive interactions creates a situation in the protein/interfacial system whereby some portions of the deformable interface are pulled toward the protein surface and other portions are pushed away, depending upon how far the interfacial section is from the protein surface.

4.8 Modeling of Affinity Based RME

A simplified equilibrium extraction model (Fig. 6) was presented by Dordick and colleagues [188] to explain the resolution behavior of glycoproteins in affinity based reverse micellar extraction and separation (ARMES). Their system for the study includes soybean peroxidase (SBP, MW 37 KDa, pI 4.1) and α_1-acid glycoprotein (AGP, MW 43 KDa, pI 3.7) as glycoprotein solutes, concanavalin A (ConA) as the affinity ligand in AOT/isooctane RMs. The separation factor (α) for the separation of SBP from AGP can be given by

$$\alpha = \frac{[\mathrm{SBP}]_{org}}{[\mathrm{AGP}]_{org}} = \frac{H_{p,SBP}}{H_{p,AGP}} \times \frac{K_{d,AGP}}{K_{d,SBP}} \times \frac{[\mathrm{SBP}]_{aq}}{[\mathrm{AGP}]_{aq}} \tag{36}$$

where H_{pi} and K_{di} are the partition and distribution coefficients of protein i, respectively. The ratios of partition coefficients and the concentrations of the free glycoproteins in the aqueous phase can be obtained by simultaneous solution of the mass balance expressions.

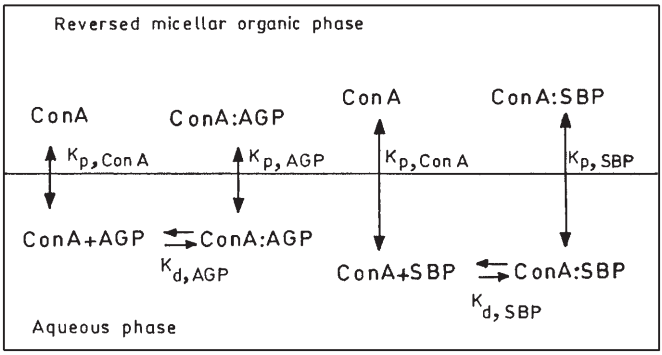

Fig. 6. Equilibrium extraction model involved in the ARMES process. (Reproduced from [188] with permission of AIChE)

The ratios of lectin-glycoprotein dissociation constants were measured by microtiter plate binding assay method. At pH≥7.5, α values reached a maximum of about 50, indicating an extremely efficient separation between SBP and AGP.

4.9 Molecular Thermodynamic Model for Osmotic Pressures

Very recently, Li et al. [189] have developed a simple and a new equation of state to correlate the osmotic pressures in micelles at various temperatures and in microemulsions at 25.5°C considering the deformation, van der Waals, and long range electrostatic interactions between the droplets. Osmotic pressure in a dispersed system has a direct influence on the interactions between the particles/liquid droplets and their sizes. The major contributions considered for the development of the model were: (i) repulsion term from the force between the hard spheres with surface bending energy from the deformation of droplets described with the improved Carnahan-Starling equation by Petsev and Linse [190], (ii) van der Waals interaction contribution term obtained from the Hamaker energy equation [191], and (iii) long range electrostatic contribution based on mean spherical approximations given by Blum and Hoye [192]. The general expression for the total osmotic pressure was given by:

$$\Pi = \Pi^{i-CS} + \Pi^{vdW} + \Pi^{MSA} \tag{37}$$

where Π^{i-CS} is the repulsion term with droplet deformation, Π^{vdW} is the van der Waals term, and Π^{MSA} is the long range electrostatic term.

Li et al. [189] assumed that a pair of deformable droplets has the shape of truncated sphere separated by a planar film and used the improved Carnahan-Starling equation to describe the repulsion term as:

$$\Pi^{i-CS} = \frac{\rho k T (1 + \Phi^{eff} + \Phi^{eff2} - \Phi^{eff3})}{(1 - \Phi^{eff})^3} \tag{38}$$

where Φ^{eff} is the effective volume fraction, ϱ is the density number, k is the Boltzmann constant, and T is the absolute temperature. The van der Waals term is given by

$$\Pi^{\text{vdW}} = -\frac{Z A_{\text{eff}} \varrho \Phi^3}{36 (\Phi_{\text{cp}} - \Phi_{\text{cp}}^{1/3} \Phi^{2/3})^2} \tag{39}$$

where Z is the coordination number, A_{eff} is the effective Hamaker constant, Φ_{cp} is the hexagonally close packed volume fraction, and Φ is the volume fraction of the droplets.

The long-range electrostatic term is expressed by mean spherical approximations which is a very promising method for describing the thermodynamic properties of electrolyte solutions [192, 193]:

$$\Pi^{\text{MSA}} = k T \xi_0 \Delta \phi \tag{40}$$

where $\Delta\phi$ is the excess osmotic coefficient of the charged particles.

From Eqs. (37–40), the total osmotic pressure of the system can be obtained. The model has showed not only good correlation ability but also good prediction capabilities at other conditions.

4.10 Remarks on Modeling

Although a considerable amount of effort has gone into modeling, still many aspects remain to be addressed in order to improve the understanding in this area. A theoretical understanding of how and why micellar sizes change with system conditions could provide information about micellar structure, address issues such as size exclusion of proteins from RMs, and contribute to an understanding of the partitioning behavior of proteins between bulk aqueous and reverse micellar solutions. Moreover, a better understanding of the nature of the protein-micelle complex, and how the sizes of empty and protein-filled RMs change with overall water content, could provide some insight into the reasons for the accompanying changes in reaction rates frequently observed in reverse micellar biocatalysis studies [198, 199].

The existing models provide some new insights into the process of protein solubilization in RMs and into the nature of the protein/RM complex. For instance, the model calculations by Rahaman and Hatton [152] indicate that it is the balance between electrostatic interactions and tail bending stresses that determines the variation of the total free energy, and hence the level of protein solubilization, in the reverse micellar system. This model identifies free energy associated with simple charge interactions within micelles and between proteins and micelles as the major electrostatic driving force for changes in protein solubilization behavior with the salt concentration.

Although the thermodynamic model for protein solubilization in – and water distribution over – the reverse micellar solutions presented here is consistent with the experimental results, it must be recognized that significant improvements can be made in the model formulation. Obvious extensions include a

more realistic description of the tail bending terms to account for solvent penetration and the presence of co-surfactants, etc. The entropy of mixing contribution may be better represented by other formulations, accounting for attractive intermicellar interactions and hard sphere repulsions. The effect of charge distribution over the protein surface, and of the location of the protein in the micelles, should be included to extend the generality of the model. Finally, as all ions are treated simply as point charges, the thermodynamic model cannot account for specific ion effects on protein transfer. To do this it may be necessary to invoke the more detailed model of the electrical double layer in the description of selective ion partitioning between the bulk aqueous and reverse micellar solutions [152, 200].

Recently, a simple solubilization theory has been developed to predict the equilibrium distribution of zwitterionic amino acids from information of the initial conditions of the system. This theory is based on the chemical and electrostatic interactions between the amino acids and active reverse micellar interface. The predictions of the model are in excellent agreement with the experimental results [201].

Similarly, further development of ARMES for the resolution of glycoforms will require better understanding of the mechanism of extraction and the role of other parameters on separation, such as charge-shielding and hydrophobic interactions [188].

5 Technology Development Aspects of Reverse Micellar Extraction

Reverse micellar extraction combines the steps of concentration and purification of the desired enzyme in a single process and has several interesting advantages over existing processes. A total process development involves first reaching a stage where the technical feasibility as well as a well-balanced economic evaluation can be made. Second one must define the degree of uncertainty, as far as possible a priori, so as to enable implementation of the process. Third one should furnish the required guidelines for basic engineering and design and, last, provide a liaison between development and implementation [131, 202].

The various steps involved, in general, which need to be considered for the development of a process for the extraction and purification of proteins by RME are:

1. Selection of the reverse micellar system
2. Optimization of forward and back extraction processes
3. Selection of extraction equipment
4. Recovery and recycling of the system components such as surfactants and solvents

Selection of a suitable reverse micellar system is mainly based on the nature and charge of the protein to be extracted. The optimization of forward and back extraction processes is carried out by studying the effect of various parameters (Sect. 3) on the extraction/stripping of proteins experimentally using full or

fractional factorial designs to develop a meaningful system description. Other statistical designs can also be used. The steps involved, in general, are [131]: (i) specification of separation desired, (ii) identification of transfer required, (iii) selection of mode of separation, (iv) choice of solvent type, and (v) test of biochemical/microbial feasibility.

An organic phase can be used several times provided the sample feed (fermentation broth) does contain cells or cell debris. Presence of such contaminants may render it necessary to regenerate the organic phase for its prolonged use. A literature survey suggests that the knowledge available on the recovery and reuse of surfactants is very little. However, the removal of surfactants from the stripping aqueous solution can be achieved by filtration and then can be recycled [10]. Use of ultrafiltration was also shown to be a successful technique for the separation of surfactants from reverse micellar solution [203].

The RME processes can be performed by using four basic types of extractors, namely mixer/settler, agitated column extractor, centrifugal, and membrane extractors. The mixer/settler and centrifugal extractors seem to be more appropriate for solvent extraction using RMs [33]. For some RME, mixer/settler and agitated column extractors cannot be used due to the formation of stable emulsions between the aqueous phase and reverse micellar phase as the presence of surfactants stabilizes these emulsions. In such cases, centrifugal extractors may be applied to reduce the settling time. Additionally, membrane extraction techniques may be adapted for use with these types of systems, the membrane serving to stabilize the reverse micellar/aqueous phase interface. For systems where short residence times are required, centrifugal extractors might be very useful. Reissinger and Schroter [204] provided a good guide for selecting suitable equipment for LLE. At present, process development has centered exclusively on the use of mixer/settlers [139, 205, 206] and membrane extractors [178, 207].

Dekker et al. [139] reported promising results for the continuous extraction of α-amylase using mixer/settler units. Figure 7 shows the flow sheet for the combined forward and back extraction processes. The enzyme was concentrated to eightfold involving about 30% and 15% loss of enzyme activity and surfactant respectively owing to the complex formation between inactivated protein and surfactant at the aqueous and reverse micellar phase. To maintain the system balance and to restore the extraction efficiency, surfactant was replenished to the reverse micellar phase. The investigations on the optimum conditions for the enzyme distribution behavior was carried out at a 4-ml scale and were extended to the continuous mode of extraction wherein the operating volumes of two settlers employed were 900 and 650 ml.

Efficient extraction of proteins has been reported with reverse micellar liquid membrane systems, where the pores of the membrane are filled with the reverse micellar phase and the enzyme is extracted from the aqueous phase on one side of membrane while the back extraction into a second aqueous phase takes place at the other side. By this, both the forward and back extractions can be performed using one membrane module [132, 208]. Armstrong and Li [209] confirmed the general trends observed in phase transfer using a glass diffusion cell with a reverse micellar liquid membrane. Electrostatic interactions and surfactant concentration affected the protein transfer into the organic membrane and

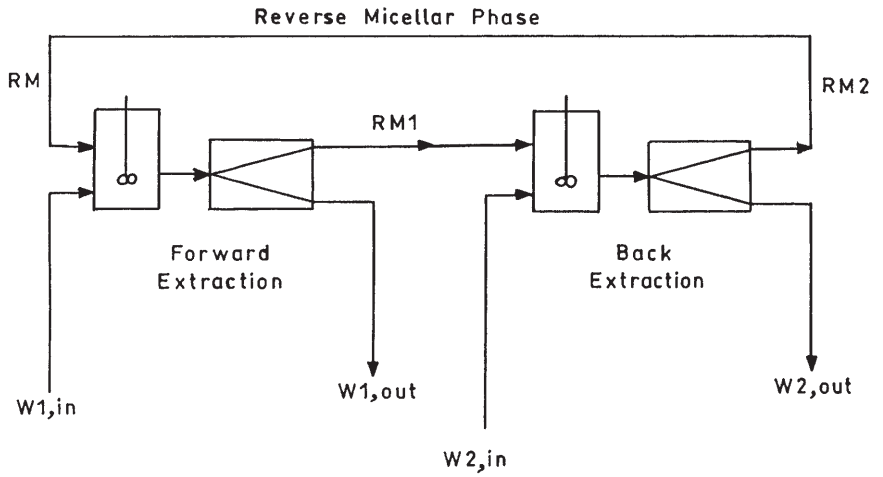

Fig. 7. Flow sheet of combined forward and back extraction processes in continuous mode using two mixer/settler units with reverse micellar phase recirculation. W1: feed (first) aqueous solution, W2: stripping (second) aqueous phase, RM: reverse micellar phase. (Reproduced from [139] with permission of Elsevier Science)

the back transfer increased with the salt gradient across the membrane. No significant denaturation of proteins (cytochrome C, lysozyme, myoglobin, and bovine serum albumin) was observed on either side of the membrane. Further, the development of compatible synthetic membranes, optimal configuration of membranes, and membrane support matrices will have significant impact in minimizing the adsorption effects and in improving the feasibility of the process.

Asenjo and coworkers [210] studied the kinetics of protein extraction using RMs in a well-mixed system and a liquid-liquid spray column. The authors have shown that pH and ionic strength control the equilibrium distribution of proteins whereas the partitioning kinetics was influenced by the operating conditions of the contacting device (volume ratio, rate of mixing, dispersed phase flow rate, etc.). In both the systems studied, it was reported that the forward transfer is limited by diffusion in the aqueous boundary layer film while back transfer is limited by an interfacially controlled mechanism. It was suggested that for the design of RME equipment, kinetic considerations must be evaluated. In the same year Han et al. [211] demonstrated the utility of a simple spray column for the RME of intracellular proteins from *Candida utilis*. The optimal forward transfer was observed after two circulations at a flow rate of 0.2 ml s^{-1}, while the optimal back transfer occurred after 7–9 circulations.

Very recently, Lazarova and Tonova [53] reported an integrated process for extraction and stripping of α-amylase using RMs in a stirred cell with separated compartments for each process. A comparison between the classical process and the integrated process indicated a 1.27-fold enhancement in the enzyme purification by the latter. This integrated process was operated with 100 ml volume in

each compartment, which suggests that relatively large volumes can be processed by this technique.

6
Recent Developments in Reverse Micellar Systems

Most proteins must be folded into a specific three-dimensional conformation to express their specificity and activities, which complicates the DSP [212]. Researchers in the area of RME of proteins/enzymes have realized this and directed more efforts in developing novel and imaginative techniques in RME as well as coupling the existing techniques such as chromatography, electrophoresis, and membrane extractions with RME. Such promising techniques developed in the recent past have been discussed in this section. Apart from these techniques, use of novel surfactants in the RME and surfactant based separation processes (e.g., cloud-point extraction) are also considered.

6.1
Affinity Based Reverse Micellar Extraction and Separation (ARMES)

High selectivity for protein extraction in RME has been achieved in a limited number of cases by using affinity partitioning. This technique involves the affinity interaction between a protein and its ligand coupled with incorporation and stripping of these complexes into and out of RMs, respectively. Three steps are commonly involved in any affinity-based separation process [213]. Initially, a reversible ligand-ligate complex followed by its selective removal from other mixture components, and subsequently, its dissociation resulting in the isolation of pure ligate. The affinity ligand is regenerated for further reuse. Coughlin [214] proposed the possibility of incorporating certain affinity molecules that strongly bind the proteins into micelles. Hatton and coworkers [215] demonstrated the practical application of ARMES for the first time in 1989 wherein selective extraction of conconavalin A (con A) into AOT-isooctane RMs was achieved by employing *n*-octyl-β-D-glucopyranoside as affinity cosurfactant. The amount of con A transferred to RMs was substantially high with no influence on the transfer of ribonuclease A. The increased transfer was observed around pI of con A and was attributed to the affinity interaction between con A and the glycosyl moiety of the cosurfactant.

Later, Coughlin and Baclaski [216] synthesized the affinity surfactant *N*-lauryl biotinamide. They showed a significant enhancement in the transfer of the protein avidin from aqueous solution into AOT-isooctane RMs. Glucose- or mannose-containing glycoproteins have been purified from non-glycosylated proteins and other cellular material by using glucose/mannose-specific lectin-con A [217]. Choe et al. [188] resolved structurally similar glycoproteins (soyabean peroxidase and α_1-acid glycoprotein) from each other using ARMES and con A as affinity ligand. A schematic representation of this ARMES process is depicted in Fig. 8. Although both proteins have affinity towards con A, soyabean peroxidase was exclusively extracted at pH 8, with a separation factor greater than 50, which was more than 25-fold higher than that observed in the conven-

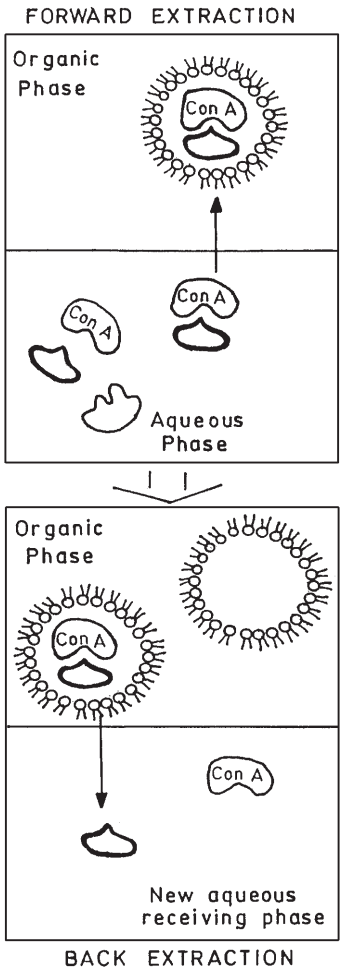

Fig. 8. The ARMES process with the forward extraction involving affinity interaction between a lectin (Con A) and a glycoprotein to separate from a mixture of glycoproteins and back extraction involving recovery of glycoprotein into an aqueous stripping phase. (Reproduced from [188] with permission of AIChE)

tional con A affinity chromatography. The high resolution was ascribed to the hydrophobic interactions and/or charge shielding effects at the lectin-glycoprotein complex. Based on these results, it was suggested that ARMES depends on weak monomeric interactions, unlike other commonly used affinity techniques.

Affinity-based separations are divided into two fundamentally distinct methodologies: (i) individualized and (ii) group-specific. In the former case, the affinity ligand has a very narrow specificity for a single compound (or a limited number of related compounds) and involves the use of a small molecule as a ligand to bind selectively to larger molecules that are of interest to separate. Conversely, the group-specific interactions invariably involve high molecular

weight, bio-ligands [218]. This second methodology can be used to separate entire classes of compounds, including high molecular weight ligates.

Other aspects such as the effects of ligand concentration and free ligand addition to aqueous phase [162, 215], the effect of pH and/or ionic strength [162, 215, 216], and the extraction mechanism and the effect of the tail length of affinity cosurfactant [219, 220] are also of interest.

Recently, Poppenborg and Flaschel [221] have extracted proteins by means of ARMES containing a metal chelating surfactant. Sun et al. [222, 223] have developed a novel reverse micellar system with crude soybean lecithin as a weak ionic surfactant. An affinity ligand, cibacron blue F-3GA (CBF), was immobilized by reacting with the amino groups of the phosphotidyl ethanolamine contained in the crude lecithin. The extraction capacity and selectivity of lysozyme were shown to improve significantly. Similarly, lysozyme was also selectively solubilized and hence separated from BSA. Although BSA has little affinity towards CBF, it was not extracted because of its high molecular weight causing a significant steric hindrance [222]. Addition of Tween-85 to CBF-lecithin RMs increased the W_0 and thereby enhanced their lysozyme solubilization capacity. However, higher W_0 did not affect the size exclusion to extract BSA [223].

Macromolecular ligands (e. g., proteins) [224], polysaccharides [225], small ligands (e. g., triazine dyes) [226], metal chelates [227], and inhibitors [228] can provide unparalleled selectivity in forming ligand-ligate affinity complexes.

6.2 Reverse Micellar Extraction in Hollow Fibers

Extraction of proteins using RME in hollow fibers was found to be substantially faster than the protein extractions with conventional equipment. Dahuron and Cussler [178] performed continuous liquid membrane extraction of protein solutions employing RMs in hollow fibers. The advantages of hollow fibers center on their large surface area per volume, '*a*'. In particular, these systems routinely have surface areas of 30 $cm^2\ cm^{-3}$ (1000 $ft^2\ ft^{-3}$) and values ten times larger have also been claimed [229]. While the mass transfer coefficient, *K*, is not unusually high in fibers, the product '*Ka*' is often 10 – 50 times larger than in conventional extraction towers [178]. Moreover, in hollow fibers the two fluid flows are almost completely independent. As a result, there is no constraint due to flooding, loading, or channeling. Hollow fibers appear to be a superior way to achieve rapid mass transfer. The overall mass transfer coefficients can be calculated from the solute concentration measurements.

6.3 Some New Surfactants for Reverse Micellar Systems

In spite of the many advantages of ionic surfactants, they were reported to cause protein denaturation in some of the extraction processes due to the strong electrostatic interactions that exist between their head group and protein [60, 230]. This problem could be overcome by employing nonionic surfactants such as Tween 85 [231, 232]. Further, AOT-RMs, despite their popularity as a research

model system, have some serious limitations such as poor ability to release the proteins into aqueous medium during back extraction and slow phase separation [233]. These problems could be avoided by using some new RMs employing novel surfactants.

6.3.1 *Nonionic Surfactants*

Tween 85 is used extensively for RME [84]. Russell and coworkers [234] used Tween 85/isopropanol microemulsions in hexane to solubilize proteins and not only showed > 80 % solubilization of cytochrome C at optimum conditions, but also proved that Tween 85 does not have a detrimental effect on the structure, function, and stability of subtilisin and cytochrome C. There are other reports available on the extraction and purification of proteins using Tween 85-RMs and also on the stability of protein activity in these systems [234]. It has also been shown that Tween 85-RMs can solubilize larger amounts of protein and water than AOT. Tween 85 has an HLB of 11, which indicates that it is soluble in organic solvents. In addition, it is biodegradable and can be successfully used as an additive in fertilizers [235, 236]. Pfammatter et al. [35] have demonstrated that RMs made of Tween 85 and Span 80 can be successfully used for the solubilization and growth of whole cells. Recently, Hossain et al. [84] showed an enhanced enzymatic activity of *Chromobacterium viscosum* lipase in AOT/Tween 85 mixed reverse micellar systems when compared to that in classical AOT-RMs. This is due to the modification of the interface in AOT-RMs caused by the co-adsorption of Tween 85, and increased availability of the olive oil molecules (substrate) to the enzyme.

6.3.2 *Di(tridecyl) Phosphoric Acids as Surfactants*

Goto et al. [237] synthesized di(tridecyl) phosphoric acid (DTDPA), a new surfactant, and used it for the formation of RMs that could extract many proteins. In particular, hemoglobin, which is difficult to extract using AOT-RMs, was successfully extracted using this system. DTDPA was found to form stable RMs in the concentration range above 1 mmol l^{-1}. Under the same conditions the size of a DTDPA-RM was found to be smaller than that of AOT. The formation of DTDPA-RMs can be controlled by aqueous phase pH adjustment unlike AOT-RMs, which is independent of aqueous phase pH. Phase separation rate of DTDPA-RMs was found to be very high even at a high concentration of the surfactant, unlike that of AOT-RMs. These authors [238] synthesized another organophosphorus type surfactant called dioleyl phosphoric acid (DOLPA) applicable for extraction of proteins. However, the DOLPA-RMs posed a problem with respect to phase separation at high surfactant concentration (0.1 mol l^{-1}), wherein a stable emulsion was observed at the oil-water interface necessitating centrifugation. Employing DTDPA-RMs, complete extraction of cytochrome C and lysozyme, ~80% extraction of hemoglobin, and about 50 % extraction of α-chymotrypsin was achieved under optimum conditions (pH = 6.8, C_{KCl} = 100 mol m^{-3} and C_{surf} = 10 – 100 mol m^{-3}) [237].

6.3.3
Sugar Ester as Surfactant

Naoe et al. [239] used the sugar ester DK-F-110, a mixture of sucrose esters of fatty acids, as a nonionic surfactant along with isopropyl alcohol and hexane in a reverse micellar system to extract cytochrome C. This surfactant has a critical micellar concentration of 0.5 g/l and HLB of 11. Aqueous phase pH was found to have a major role in the forward extraction and optimum extraction was achieved at pH 8.0. However, for optimum back extraction, addition of isopropyl alcohol at 20 vol.% was found to be very essential. Further, the esterification reaction rate of *Rhizopus delemar* lipase was found to be maximum in DK-F-110 systems and also higher than those obtained in AOT and lecithin-RMs at a water concentration of 0.25 mol l^{-1}.

6.3.4
Sodium Bis(2-ethyl hexyl) Phosphate (NaDEHP) as a Novel Anionic Surfactant

Sodium bis(2-ethyl hexyl) phosphate (NaDEHP) is an anionic surfactant which has the same hydrocarbon tail as AOT, but a different polar head [167]. Its advantages over AOT are (1) its RMs can be easily broken by converting the sodium salt to non-surface-active divalent metal salt, $M(DEHP)_2$ and (2) the phase separation rate is faster than AOT-RMs. In addition, this surfactant can be readily recycled. The ability of this surfactant to form RMs has been shown by many researchers [240, 241]. Yu and Neuman [242] reported that the NaDEHP-RMs attain giant rod-like shapes with a radius of gyration ≤ 53 nm which is in contrast to the literature view that large micelles can only be formed in aqueous media and average micellar aggregation numbers in organic media are much smaller (seldom >10 nm). The primary driving force for the growth of rod-like RMs is proposed to be a long range electrostatic interactions among surfactant head groups and their counter-ions.

Hu and Gulari [167] were the first to show the effective utility of these RMs for protein extraction. They investigated the forward and back extraction of model proteins α-chymotrypsin and cytochrome C in this system and showed high forward transfer at low ionic strength and neutral pH. Maximum recovery was obtained by contacting the reverse micellar solution with a divalent cationic (e.g., Ca^{2+}) aqueous solution at neutral pH. Further, Hu and Gulari [243] utilized NaDEHP-RMs efficiently for the extraction and recovery of aminoglucoside antibiotics such as neomycin and gentamicin.

6.4
Enzymatic Reactions in RMs Coupled with Membrane Processes

As enzymes could be used to carry out synthetic reactions in organic solvents [244–246] only under certain specific conditions, the application of RMs as enzyme hosts to perform biotransformations has attracted a great deal of research attention in the recent past. The reverse micellar environment represents a medium where the aqueous/organic interface is very large (~100 m^2 ml^{-1}) [247].

Various enzymatic reactions in RMs have been reported in the literature which include the production of triglycerides [248], steroid conversions [249], peptide synthesis [250, 251], and amino acid synthesis [252]. Very recently Stamatis et al. [144] have presented an exhaustive review comprising the bioorganic reactions involved in microemulsions, taking lipase catalyzed reactions as the case study. This enzymatic catalysis inside the RMs with all its advantages over the conventional enzymatic catalysis has some drawbacks associated with separation and purification of products as well as the recovery of enzymes. Use of membrane extractors in combination with RMs could solve this problem. The principle is that the membranes can be used to retain the enzymes and their hosting RMs in the reactors while the products can be recovered in a stripping solution on the other side of the membrane.

Cabral and coworkers [253] have investigated the batch mode synthesis of a dipeptide acetyl phenylalanine leucinamide (AcPhe-Leu-NH_2) catalyzed by α-chymotrypsin in a ceramic ultrafiltration membrane reactor using a TTAB/octanol/heptane reverse micellar system. Separation of the dipeptide was achieved by selective precipitation. Later on the same group successfully synthesized the same dipeptide in the same reactor system in a continuous mode [254] with high yields (70–80%) and recovery (75–90%). The volumetric production was as high as 4.3 mmol peptide/l/day with a purity of 92%. The reactor was operated for seven days continuously without any loss of enzyme activity. Hakoda et al. [255] proposed an electro-ultrafiltration bioreactor for separation of RMs containing enzyme from the product stream. A ceramic membrane module was used to separate AOT-RMs containing lipase from isooctane. Application of an electric field enhanced the ultrafiltration efficiency (flux) and it further improved when the anode and cathode were placed in the permeate and the retentate side respectively.

6.5 Micellar Enhanced Ultrafiltration (MEUF)

Micellar enhanced ultrafiltration (MEUF) is a recently proposed technique to separate dissolved organic compounds from aqueous streams [256–258]. In this process, surfactant is added to an aqueous stream containing organic solute for forming micelles in order to solubilize the target compound. The subsequent concentration and purification of the target compound is achieved by ultrafiltration by optimizing the process parameters [259–261].

This technique of MEUF has also been successfully employed for the recovery of thuringiensin [258], removal of cresols [262], extraction of chromate anion [257], removal of dissolved organic pollutants [256], removal of *n*-alcohols [263], preconcentration and removal of iron [260], and preconcentration of aniline derivatives [261]. Kandori and Schechter [264] have given a detailed account of selecting surfactants for MEUF. The design characteristics of micellar enhanced utrafilters and cross-flow ultrafiltration of micellar surfactant solutions have been described by Markels et al. [265].

6.6
Micellar Electrokinetic Capillary Chromatography (MECC)

Micellar electrokinetic capillary chromatography (MECC), in contrast to capillary electrophoresis (CE) and capillary zone electrophoresis (CZE), is useful for the separation of neutral and partially charged species [266, 267]. In MECC, a surfactant, usually sodium dodecyl sulfate (SDS), is added to the buffer solution above its critical micellar concentration to form micelles. Although SDS is certainly the most popular anionic surfactant in MECC, other surfactants such as bile salts have proved to be very effective in separating nonpolar analytes that could not be resolved using SDS [268].

MECC has also been reported to be an effective method for the separation of enantiomers [269, 270]. Tsai et al. [271] reported γ-cyclodextrin-modified micellar capillary electrophoresis technique for the separation of dansylated-DL-amino acids.

Extraction and separation of plant phenolics [272], corticosteroids [268], verapamil [273], hydrophobic molecules [274], and ingredients of a medicine for common cold [275] were recently performed using this technique. Seifar et al. [276] gave the mechanisms involved in such separations.

6.7
Cloud-Point Extractions (CPE)

Aqueous micellar solutions of many nonionic surfactants, with an increase in temperature, become turbid over a narrow temperature range, which is referred to as their cloud-point [17, 277]. Above the cloud-point temperature, such solutions separate into two isotropic phases. Cloud-point extraction (CPE) is also referred to as a particular case of ATPE [278, 279] and more specifically as aqueous micellar two-phase systems [10, 277]. Very recently, in an extensive review, Quina and Hinze [280] have discussed in detail the emergence of CPE as an environmentally benign separation process, highlighting the basic features, experimental protocols, recent applications, and future trends in this area.

Though CPE has many advantages [10], some problems remain to be solved such as (1) limited number of surfactants, (2) high cloud-point, and (3) strong hydrophobic nature. In an attempt to overcome some of these limitations, Tani et al. [281] proposed a new method that involves solubilization of hydrophobic membrane proteins into aqueous micellar solutions of alkylglucosides, followed by phase separation induced by the addition of a water-soluble polymer such as poly(ethylene)glycol (PEG) and dextran T-500. Using this approach they could carry out the whole procedure from solubilization to phase separation at 0 °C.

7
Some Recent Applications

In this section, several recent applications of reverse micellar systems reported in the last decade are discussed. In addition, a comprehensive table containing only salient features of many other recent applications of RMs is presented

(Table 3). Improved methods of extracting some of the enzymes/proteins are also presented in this table.

7.1 Protein Refolding

The production of proteins via genetic engineering often encounters the problem of formation of precipitating inclusion bodies owing to incorrect folding of the proteins. Thus, a protein refolding step is essential to regain the biological activity of these proteins during DSP. Conventionally it is achieved by unfolding of proteins by denaturants and reducing agents followed by their refolding at very low protein concentrations (< 1 mg l^{-1}) to avoid intermolecular interactions [301] and subsequent recovery from dilute mixtures. This results in a severe decrease in the yield during the recovery. Reverse micelles were shown to isolate the denatured protein molecules from each other during refolding, thus reducing the intermolecular interactions which lead to protein aggregation. Protein interactions can be controlled by the fact that by optimizing the parameters one protein molecule can be solubilized in one RM. Hagen et al. [302] were the first to demonstrate the feasibility of this process using RNase as model protein. Later on, the same group [303] expanded their study to investigate the general mechanisms involved and the possible biotechnological applications of the process. The refolding of γ-interferon, a hydrophobic protein, was not successful. This uncovers a limitation of this process, namely the strong interactions between unfolded proteins and surfactant or organic solvent. However, an attractive feature of this method is that protein concentration in the range of 1–10 g l^{-1} can be processed which is at least 1000-fold higher than the concentrations employed in the conventional refolding processes. Various steps involved in the refolding process using RMs are schematically represented in Fig. 9. With the advent of this technique, refolding of several proteins in RMs has been investigated: reversible thermal unfolding of ribonuclease T1 in

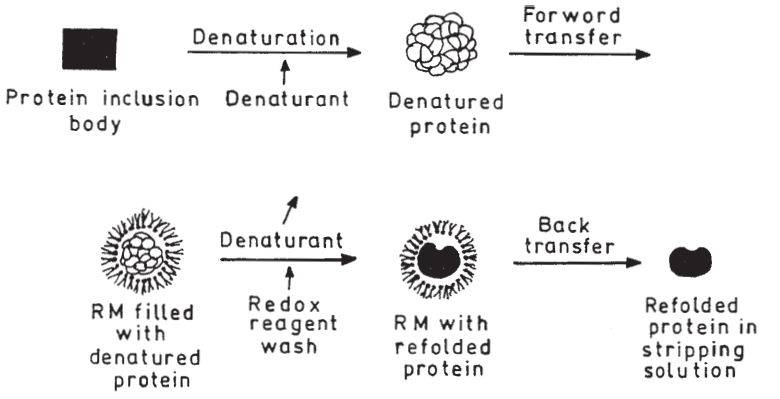

Fig. 9. Schematic representation of protein folding in reverse micelles

Table 3. Some recent applications of reverse micellar systems

Reverse micellar system	Biomolecules	Salient features	Ref.
AOT/several organic solvents (C_7 – C_{15} *n*-alcohols)	Horse radish peroxidase (HRP) from *Armoracia rusticana* roots	Enzyme purified 20-fold in one step by retaining the enzyme in bulk aqueous phase and solubilizing the contaminants in RMs, eliminating back extraction step	[49]
Aliquat 336/ isooctane/ *n*-alcohol	α-Amylase	Effect of cosolvent type on extraction was studied and *n*-butanol was found most suitable based on CD probe analysis	[48]
TOMAC/Revopal HV5/*n*-octanol/ isooctane CTAB/hexanol/ butanol/ isooctane	Glucoamylase from *Saccharomyces cerevisiae*	Extraction of charged fusion glucoamylase (with short peptides) was carried out and maximal recovery (95 %) was observed in CTAB system. Charged fusion process was shown to be advantageous and useful for extraction of proteins in RMs having small size	[58]
AOT/isooctane	Lysozyme from chicken egg white	Low concentrations of guanidine HCl suppressed gel formation and hence improved extraction of lysozyme by RMs. CD spectra confirmed the presence of GuHCl (0.06 M in 25 mM AOT-RMs) preserved structure and specific activity well	[59]
AOT-DOLPA/ isooctane	α-chymotrypsin	AOT–DOLPA–RMs showed a high degree of selectivity for native enzyme, suggesting that RMs can be tailored to recognize an active protein selectively but not the denatured one	[61]
AOT/isooctane			
AOT/isooctane	Cytochrome C	Protein extraction in relation to the amount of water present in organic phase was studied and a 100 % solubilization was noticed at a constant molar ratio of water to protein extracted (3500) at constant KCl concentration. At this stage, 2200 water molecules accompanied each protein inside RM. The ratio increased with ionic strength	[67]
AOT/heptane	Superoxide dismutase (SOD) from bovine red blood cells	SOD was extracted by RME in single step to electrophoretic purity. Contaminants solubilized in RM while retaining SOD in aqueous phase	[68]
AOT/isooctane	HRP	Response surface methodology RSM) was used for efficient enzyme extraction	[51]

Table 3 (continued)

Reverse micellar system	Biomolecules	Salient features	Ref.
AOT/isooctane	Recombinant Cutinase	Fluorescence study of cutinase in RMs to evaluate its structure and protein unfolding	[54]
Sodium lauryl sulfate/benzene	*Rhodopseudomonas sphaeroides*	Hydrogen production by cells entrapped in RMs was 25-fold higher	[282]
AOT/isooctane/ buffer	Horse liver alcohol dehydrogenase	Microemulsion system that is temperature sensitive to phase separate was used for recovery of proteins and enzymes	[283]
C_2H_5/heptane/ buffer AOT/isooctane	Ribonuclease A, cytochrome C, lysozyme	Fisher's polarity ratio (*P*) linearly related to hydrophilic surroundings at minimal AOT concentration for 100 % forward extraction. A procedure to estimate the AOT levels required for protein extraction was proposed	[72]
Marlipal O 13/60/ cyclohexane	Alcohol and formate dehydrogenases (ADH & FDH)	A 12-fold increase in ADH catalyzed reduction rates of 2-heptanone to *S*-2-heptanol was demonstrated in RMs. The NADH consumed in the reaction was regenerated by another enzyme FDH	[23]
Cetylpyridinium chloride (CPC)/ hexane	α-Amylase from brewers' yeast and invertase from bakers' yeast	Enzyme activities in cells entrapped in RMs were high compared to free cells	[284]
AOT/isooctane	Trypsin, α-chymotrypsinogen A	Investigation on protein-protein interactions in RMs. Trypsin showed superactivity by a factor of 21.3 during activation of α-chymotrypsinogen A to α-chymotrypsin	[285]
AOT/isooctane	Protamines from sperm head nucleoproteins of fish	Conformational studies on model polypeptides with amino acid sequences similar to clupeine and salmine were carried out in RMs	[286]
AOT/octane	Oligomeric enzymes (ketoglutarate dehydrogenase, alkaline phosphaatase, lactate dehydrogenase, glyceraldehyde phosphate dehydrogenase)	Use of RMs as microreactors for the design of supramacromolecular complexes of proteins and separation of oligomers was demonstrated	[287]
AOT/isooctane	Pig liver ribosomes	Solubilization and possible applications of ribosomes in RMs were discussed	[288]
AOT/octane	Recombinant cytochrome b_5	Forward and back extractions were performed and the efficiency of back extraction was found to decrease at low temperature and high salt concentration	[289]

Table 3 (continued)

Reverse micellar system	Biomolecules	Salient features	Ref.
AOT/*n*-hexane	Bovine liver catalase and penicillinase	Encapsulation of enzymes by polyacrylamide matrices in RMs was studied as nanoreactors	[290]
Tetraethylene glycol dodecyl-ether (TEGDE)/ *n*-decane	Merocyanin	The spiropyran derivative incorporated RMs showed good photo-controlled extraction of zwitter-ionic amino acid under UV irradiation and release under visible irradiation	[291]
AOT/octane	Native and artificially glycosylated α-chymo-trypsin	Unlike native enzyme, the modified counterpart tended to form reversible oligomeric structures in RMs, which allowed in realizing the role of carbo-hydrate moieties in the functioning of glycoproteins	[292]
AOT/isooctane	Melanocyte stimulating hormone (α and δ forms)	Localization of peptidal hormones inside RMs was investigated	[293]
	Endoproteinase with trypsin like activity (*Ostrinia nubilalis*) was extracted	The enzyme isolated from freeze-dried powder of a larvae of corn borer into RMs. The inhibition of this enzyme in RMs were studied using commercial and isolated trypsin inhibitors	[294]
AOT/isooctane	Melittin	The peptide (melittin) was found associated to RMs in a single state as opposed to involvement of at least two forms of melittin with lipid in phospholipid vesicles. Folding and dynamics of this peptide in RMs were also investigated	[295]
AOT/isooctane	Microbial lipase, α-chymotrypsin	In RMs, activity of α-chymotrypsin was unaffected by pressurization while lipase lost its activity at low pressures and regained on depressurization. The use of pressure as a switch for lipase catalysis is discussed	[296]
AOT/isooctane	Amino acids and peptides	Partition coefficients for 11 amino acids, 17 dipeptides and 5 longer peptides in RMs were determined. The effect of amino acid sequence on peptide partitioning was discussed	[297]
Dioctyl dimethyl ammonium chloride (DODMAC)/ isooctane/decanol	Aspartic acid, glutamic acid, threonine	The mechanism for the observed selective separation of amino acids at higher molar ratios of decanol to DODMAC was studied	[298]

Table 3 (continued)

Reverse micellar system	Biomolecules	Salient features	Ref.
AOT/isooctane	Periplasmic cytochrome C_{553} (recombinant protein)	Back extraction was performed using a counter-ionic surfactant (TOMAC). Yield and purity were comparable to column chromatography	[104]
AOT/isooctane	Chymotrypsin	Presence of RMs is shown to be not a prerequisite for protein extraction. A new mechanism for protein solubilization has been proposed	[299]
CTAB/chloroform/*n*-octanol	Penicillin G	>90% extraction was achieved at pH 5–8 and the mechanism of extraction was realized to be ion-pairing electrostatic interactions	[300]

AOT/isooctane [304], refolding of recombinant proteins such as lysozyme [305], and refolding studies on triosephosphate isomerase using fluorescence resonance energy transfer [306].

7.2 Self Replicating RMs

Recently, there has been a significant research interest in studying self replicating process of RMs. Luisi and colleagues [307] carried out LiOH catalyzed hydrolysis of octyl octanoate at the interface of sodium octanoate/isooctane-RMs and octanoic acid formed via hydrolysis was found to assemble spontaneously into new RMs reflecting the reaction as a self replicating process. Kinetics and spectroscopic studies of this self replicating process were also reported. Nucleotide coupling was also shown to be possible in RMs and the same was discussed at length by Boehler et al. [308] in connection with a micellar self replication program. The self replication was found to occur either under very alkaline conditions or in the presence of permanganate [309, 310]. Hammouda and Pileni [311] synthesized nanosized latexes by UV-irradiation mediated polymerization of the RMs prepared by polymerizable surfactant (didecyl dimethyl ammonium methacrylate).

7.3 Antigen-Antibody Interactions

Quenching fluoroimmunoassay (QFIA), a new method, for performing homogeneous fluoroimmunoassay in apolar organic media, was proposed by Metveeva et al. [312]. The conjugate of atrazine with fluorescein was employed for fluorescence detection of antigen-antibody interactions in RMs. The binding

of this conjugate with antibodies solubilized in RMs resulted in fluorescence quenching. The authors also discussed the potential of this method as an excellent tool for analysis of compounds with low water solubility.

7.4 Other Applications of RMs

In recent years, RMs were reported to be applicable in diverse areas other than proteins and enzymes, which deserve a note here. These include extraction and determination of metals and metal ions, photoinduced electron transfer, RMs in supercritical liquids, extraction of antibiotics/drugs, synthesis of nanoparticles, etc.

Slepnev et al. [313] presented a simple method for protein radio-labeling with Bolten-Hunter reagent (*N*-hydroxy succinimide ester of 3-(*p*-hydroxy ([^{125}I] diiodophenyl)) propionic acid) in AOT/octane-RMs using mouse IgG, human transferrin, protein A, and α_2-interferon as labeling examples. The yield of radio-labeling in RMs was found to be higher than that achieved in homogeneous aqueous solution.

Evans and Farr [314] patented a process for preparation of aerosol inhalants containing proteins and peptides (with particular reference to insulin) solubilized in RMs.

The results from the study of the picosecond time resolved Stoke's shift of the laser dye coumarin 480 in AOT/heptane-RMs [315] indicated that the water molecules in the water pool undergo slow relaxation on the nanosecond time scale.

Recently, the controlled growth of microporous crystals in RMs has attracted many researchers. Microporous crystals with sodalite structures (zincophosphate) were prepared in RMs by Dutta et al. [316] and Reddy et al. [317] by introducing zinc and phosphate ions into separate micelles to control the crystallization by collision and exchange kinetics. The reverse micellar interface provided the site for crystal nucleation. The growth process automatically gets interrupted by sedimentation when the crystals grow large enough. This approach provided a means of controlling the morphology as well as the size of growing crystals. Sangregorio et al. [318] synthesized nanometer diameter gold (Au) and Cu-Au by controlled chemical reduction of metal cations at different W_0 values in RMs. It was possible to obtain a uniform particle size distribution and compound metal nanoparticles (Cu_3Au) were also prepared by this technique. The formation of several other metal nanoparticles reported using this technique, includes: copper metallic particles employing functionalized surfactants [319], silver sulfide semiconductors [320], composite CdS-ZnS nanoparticles [321], and titania nanoparticles [322]. Further, few more studies indicated that RMs constitute an excellent medium for the nanoparticle synthesis of various metals [323, 324].

Berthod et al. [325] employed countercurrent chromatography with diethylhexyl phosphoric acid (DEHPA) reverse micelles in heptane as a stationary phase to extract metallic cations such as La^{3+}, Ce^{3+}, Pr^{3+}, and Nd^{3+} (lanthanide series). This technique was suggested for the application of ion filtering and concentration or for deionization of aqueous phases. Ashrafizadeh et al. [326] re-

ported experimental and modeling studies on the extraction of K^+, Mg^{2+}, and H^+ using dinonylnaphthalene sulfonic acid-RMs and the selectivity was found to be in the order of $Mg^{2+} > H^+ > K^+$. The system exhibited behavior similar to that of conventional ion-exchange resins. Concentration of metals by RMs was also reported by Bulavchenko et al. [327].

Desfosses et al. [328] measured binding of oxyphenyl betazone to the *N*-terminal peptic fragment of human serum albumin (HSA) in aqueous buffer and AOT/isooctane-RMs. The peptide affinity for the drug did not decrease in RMs. The interactions of HSA at membrane mimetic interface and its subsequent unfolding was suggested to constitute a drug release facilitating mechanism.

Reverse micelles can also act as a convenient membrane mimetic medium for studying membrane interactions of bioactive peptides [329, 330]. Fluorescence behavior of piroxicam in AOT-RMs and Triton X-100 microemulsions was investigated by Andrade and Costa [331]. Dutta et al. [332] studied the interactions of an antileprotic drug dapson in dipalmitoyl phosphotidyl choline (DPPC)-RMs in chloroform. The DPPC was found to form RMs just beyond 6 mmol l^{-1} concentration, which is relatively low compared to conventional AOT concentration.

Pirchanont et al. [333] proposed the use of RMs as a novel method for production of chiral epoxides. *Mycobacterium* sp. containing monooxygenase was employed as a biocatalyst and the potential of this method for chiral biotransformation was realized as superior to the conventional method. Another example for enantioselective reaction performed in RMs was provided by Buriak and Osborn [334].

Photoinduced electron transfer from eosin and ethyl eosin to $Fe(CN)_6^{3-}$ in AOT/heptane-RMs was studied and the life time of the redox products in reverse micellar system was found to increase by about 300-fold compared to conventional photosystem [335]. The authors have presented a kinetic model for overall photochemical process. Kang et al. [336] reported photoinduced electron transfer from (alkoxyphenyl) triphenylporphyrines to water pool in RMs. Sarkar et al. [337] demonstrated the intramolecular excited state proton transfer and dual luminescence behavior of 3-hydroxyflavone in RMs. In combination with chemiluminescence, RMs were employed to determine gold in aqueous solutions of industrial samples containing silver alloy [338, 339]. Xie et al. [340] studied the α-naphthyl acetic acid sensitized room temperature phosphorescence of biacetyl in AOT-RMs. The intensity of phosphorescence was observed to be about 13 times higher than that seen in aqueous SDS micelles.

Reverse micellar systems were shown to be useful for obtaining sulfur-free coal. Chloroperoxidase in AOT/isooctane-RMs was demonstrated as a versatile catalyst for sulfoxidation of aliphatic and aromatic sulfur-containing model coal compounds [341].

High pressure liquids and supercritical fluids were also served as solvent systems for the formation of RMs [342, 343]. Franco et al. [344] implemented RMs in supercritical CO_2 for protein solubilization.

8 Concluding Remarks

One of the critical factors for downstream processing of enzymes/proteins using RMs is the selection of appropriate reverse micellar system. Most of the systems reported in the literature used either anionic surfactant AOT or cationic surfactants TOMAC, BDBAC, or CTAB. These systems have some desirable characteristics such as suitable physical properties, ease of formation of RMs, etc. However, as the solubilization of proteins by these systems involves strong electrostatic interactions between protein and surfactant head groups, there is a possibility of loss in enzyme activity and further, a stripping process is quite difficult to achieve, resulting in lower recovery of proteins. Although a few alternative methods such as use of silica, addition of isopropyl alcohol and ethyl acetate have been proposed for enhanced recovery of proteins, these methods may not look attractive as far as simplicity and economics of the process are concerned. In this context a reverse micellar system containing NaDEHP, an anionic surfactant, extensively studied by Gulari and coworkers [167, 243] appears to be more attractive than the conventional AOT reverse micellar system for the extraction of proteins. NaDEHP-RMs can be easily broken by the addition of a divalent metal salt solution which can be used as an aqueous stripping media. In addition, few other new reverse micellar systems pointed out in Sect. 6.3 could be potential economical alternatives to the widely studied conventional systems.

In contrast to the extensively studied ATPE, RME appears to be more economical due to the relatively low cost of surfactants compared to polyethylene glycol (PEG), the most commonly used polymer in ATPE. Further, the concentration of surfactants used in RME is always less than 10% as opposed to the concentration of PEG used in ATPE, which is more than 10% in the majority of the cases. This factor has a very high impact as far as economy of the process is concerned in the industrial scale extractions. In addition, surfactants used in RME can easily be recovered and reused several times, whereas lack of cost-effective methods for the recovery and reuse of PEG is still a notable drawback in ATPE. Despite the fact that the cost of the organic solvents used in RME is high, they can be easily recovered and reused several times, which automatically brings down the overall cost of the process.

Extraction and purification of proteins by employing RMs have been extensively studied using model systems (proteins from commercial suppliers) such as cytochrome C, ribonuclease, α-chymotrypsin, etc. However, very few reports are available on the extraction studies of proteins from the real systems of fermentation broths using RMs [15, 43]. As we know that fermentation broths containing proteins are very much more complicated media compared to model proteins and mixture of model proteins, there is a need to investigate extraction behavior of proteins present in these real systems.

On the laboratory scale, RME for downstream processing of proteins is well established. To the best of our knowledge, there are no reports available on the larger-scale extraction of proteins using this technique, at levels above the 1-l scale. The same is true with regard to continuous operation of RME, which was

reported using mixer/settler units by Dekker et al. [139] wherein the operating volumes of the two settlers were 900 and 650 ml for forward and back extractions, respectively. Therefore, there is a need to investigate large scale extractive recovery of proteins from the fermentative media of real systems using industrial equipment to prove the process feasibility. In particular there is a need for the applicability of RME for successful recovery of genetically engineered proteins to be investigated in detail, as very few reports [345] are available in this area at the present time.

The rate of phase separation after extraction in AOT-RMs is slow [167]. Keeping this in view, there is a need to study in detail the phase separation kinetics of this reverse micellar system in order to evolve means to enhance the phase separation rate. This is a very important aspect as far as industrial adaptability of RME is concerned, since the slower separation rate may become a bottleneck as in the case of ATPE. One possible approach to enhance phase separation is the application of external fields such as electric, acoustic, and microwave to reverse micellar systems. These are shown to enhance the phase separation rate in the case of ATPE [346–348]. Employing reverse micellar systems which phase separate quickly without the need for any external effort could also be a plausible solution. Some examples of such systems are DTDPA-RMs [237], sugar esters DK-F-110 RMs [239], and NaDEHP-RMs [167, 243].

In conclusion, in the context of downstream processing accounting for a large share of the final product cost in many biotechnological processes, RME appears to be an efficient and promising bioseparation technique. The envisaged applications of the RME are in the recovery of extracellular enzymes and other biomolecules from fermentation broths and tissue cultures, and possibly to separate intracellular products after cell lysis or from whole cells. Products from both natural and genetically engineered cells could be recovered. However, scale-up and engineering aspects appear to have received scant attention and mathematical modeling is to be given its due importance.

Although this review highlights proteins/enzymes, they are not the only biological entities that can be extracted using RMs. Nucleic acids have been successfully solubilized in RMs by Imre and Luisi [349]. The potential of RME for a variety of other biomolecules is in the process of establishment.

ATPE of proteins/enzymes was reported several years ago [350] while only recently this concept has been developed as a pilot scale by Kula and coworkers [351]. We envisage that RME, despite the fact that industrial or pilot scale studies are not reported, has the potential to develop into a new bioseparation tool for biotechnology.

Acknowledgements. The authors wish to thank Dr. V. Prakash, Director, CFTRI for the encouragement. SHK and NDS are grateful to Council of Scientific and Industrial Research (CSIR), New Delhi for the award of Senior Research Fellowships.

References

1. Ohlson S, Hansson L, Glad M, Mosbach K, Larrson PO (1989) Trends Biotechnol 7:179
2. Treybal RE (1980) Mass transfer operations, 3rd edn. McGraw Hill, New York
3. Albertsson PA (1986) Partition of cell particles and macromolecules, 3rd edn. Wiley, New York
4. Walter H, Brooks DE, Fischer D (eds) (1985) Partitioning in aqueous two-phase systems: theory, methods, uses and applications to biotechnology. Academic Press, Orlando, FL
5. Diamond AD, Hsu JT (1992) Adv Biochem Eng Biotechnol 47:89
6. Zaslavsky BY (1995) Aqueous two-phase partitioning: physical chemistry and bioanalytical applications. Marcel Dekker, New York
7. Raghavarao KSMS, Guinn MR, Todd P (1998) Sep Purif Methods 27:1
8. Raghavarao KSMS, Rastogi NK, Gowthaman MK, Karanth NG (1995) Adv Appl Microbiol 41:97
9. Srinivas ND, Rashmi KR, Raghavarao KSMS (1999) Process Biochem 35:43
10. Liu CL, Nikas YJ, Blankschtein D (1996) Biotechnol Bioeng 52:185
11. Berggren K, Veide A, Nygren PA, Tjerneld F (1999) Biotechnol Bioeng 62:135
12. Luisi PL, Magid LJ (1986) Crit Rev Biochem 20:409
13. Hatton TA (1987) ACS Symp Ser 342:170
14. Hatton TA (1989) In: Scamehorn JF, Harwell JH (eds) Surfactant based separations. Marcel Dekker, New York, p 55
15. Rahaman RS, Chee JY, Cabral JMS, Hatton TA (1988) Biotechnol Prog 4:218
16. Ramelmeier RA, Terstappen GC, Kula MR (1991) Bioseparation 2:315
17. Saitoh T, Hinze WL (1991) Anal Chem 63:2520
18. Nikas YJ, Liu CL, Srivatsava T, Abbott NL, Blankschetin D (1992) Macromolecules 25:4794
19. Terstappen GC, Ramelmeier RA, Kula MR (1993) J Biotechnol 28:263
20. Sanchez-Ferrer A, Bru R, Garcia-Carmona F (1994) Crit Rev Biochem Mol Biol 29:275
21. Hayes DG, Gulari E (1990) Biotechnol Bioeng 35:793
22. Holmberg K (1994) Adv Colloid Interface Sci 51:137
23. Orlich B, Schomaecker R (1999) Biotechnol Bioeng 65:357
24. Martinek K, Levashov AV, Klyachko NL, Khmelnitsky YL, Berezin IV (1977) Dokl Akad Nauk SSSR 236:920
25. Langevin D (1984) In: Luisi PL, Straube BE (eds) Reverse micelles: biological and technological relevance of amphiphilic structure in a polar media. Plenum, New York, p 287
26. Tondre C, Xenaksis A (1984) In: Mittal KL, Lindaman R (eds) Surfactants in solutions. Plenum, New York, vol 3, p 1881
27. Speiser P (1984) In: Luisi PL, Straube BE (eds) Reverse micelles: biological and technological relevance of amphiphilic structure in a polar media. Plenum, New York, p 339
28. Scheper T, Likidis Z, Makryaleas K, Nowottny C, Schugerl K (1987) Enzyme Microb Technol 9:625
29. Scheper T, Makryaleas K, Nowottny C, Likidis Z, Tsikas D, Schugerl K (1987) Ann NY Acad Sci 501:165
30. Scheper T (1990) Adv Drug Dev Rev 4:209
31. Barenschee T, Scheper T, Schugerl K (1992) J Biotechnol 26:143
32. Bornscheuer UT, Padmanabhan P, Scheper T (1999) In: Arshady R (ed) The MML Series: Microspheres, microcapsules and liposomes. Citus Books, London, vol 1, p 541
33. Cabral JMS, Aires-Barros MR (1993) In: Kennedy JF, Cabral JMS (eds) Recovery processes for biological materials. Wiley, New York, p 254
34. Hilhorst R, Sergeeva M, Heering D, Rietveld P, Fijneman P, Wolbert RBG, Dekker M, Bijsterbosch BH (1995) Biotechnol Bioeng 46:375
35. Pfammatter N, Hochkoppler A, Luisi PL (1992) Biotechnol Bioeng 40:167
36. Dekker M, Leser ME (1994) In: Street G (ed) Highly selective separations in biotechnology. Blackie, Glasgow, p 86
37. Lye GJ, Asenjo JA, Pyle DL (1995) Biotechnol Bioeng 47:509

38. Fletcher PDI, Robinson BH (1981) Ber Bunsen-Ges Phys Chem 85:863
39. Wolf R (1982) PhD thesis, ETH No 7027. Swiss Federal Institute of Technology, Zurich
40. Hou MJ, Shah DO (1987) Langmuir 3:1086
41. Lang J, Jada A, Milliaris A (1988) J Phys Chem 92:1946
42. Jolivalt C, Minier M, Renon H (1990) J Colloid Interface Sci 135:85
43. Krei GA, Hustedt H (1992) Chem Eng Sci 47:99
44. Chang QL, Chen JY (1995) Biotechnol Bioeng 48:745
45. Dekker M, Van't Riet K, Bijsterbosch BH, Fijneman P, Hilhorst R (1990) Chem Eng Sci 45:2949
46. Regalado C, Asenjo JA, Pyle DL (1994) Biotechnol Bioeng 44:674
47. Krei GA, Meyer U, Borner B, Hustedt H (1995) Bioseparation 5:175
48. Chang QL, Chen JY, Zhang XF, Zhao NM (1997) Enzyme Microb Technol 20:87
49. Huang SY, Lee YC (1994) Bioseparation 4:1
50. Regalado C, Asenjo JA, Pyle DL, Trinck LA, Gilmour S (1994) Food Bioprod Process 72:123
51. Regalado C, Asenjo JA, Pyle DL (1996) Enzyme Microb Technol 18:332
52. Arsene ML, Niculescu S, Dumitru IF (1995) Prog Catal 4:79
53. Lazarova Z, Tonova K (1999) Biotechnol Bioeng 63:583
54. Carvalho CML, Cabral JMS, Aires-Barros MR (1999) Enzyme Microb Technol 24:569
55. Melo EP, Aires-Barros MR, Cabral JMS (1995) Appl Biochem Biotechnol 50:45
56. Melo EP, Carvalho CML, Aires-Barros MR, Costa SMB, Cabral JMS (1998) Biotechnol Bioeng 58:380
57. Forney CE, Glatz CE (1994) Biotechnol Prog 10:499
58. Forney CE, Glatz CE (1995) Biotechnol Prog 11:260
59. Naoe K, Shintaku Y, Mawatari Y, Kawagoe M, Imai M (1995) Biotechnol Bioeng 48:333
60. Naoe K, Imai M, Shimizu M (1996) Trans Inst Chem Eng C 74:163
61. Goto M, Ono T, Nakashio F, Hatton TA (1996) Biotechnol Techn 10:141
62. Serralheiro MLM, Cabral JMS (1999) Biocatal Biotrans 17:3
63. Goto M, Ishikawa Y, Ono T, Nakashio F, Hatton TA (1998) Biotechnol Prog 14:729
64. Adachi M, Shibata K, Shioi A, Harada M, Katoh S (1998) Biotechnol Bioeng 58:649
65. Fadnavis NW, Babu RL, Deshpande A (1998) Biochimie 80:1025
66. Peng Q, Luisi PL (1990) Eur J Biochem 188:471
67. Ichikawa S, Imai M, Shimizu M (1992) Biotechnol Bioeng 39:20
68. Eremin AN, Metelitsa DI (1996) Prikl Biokhim Mikrobiol 32:284
69. Chen DH, Chen HH, Huang TC (1995) J Chem Technol Biotechnol 64:217
70. Sarcar S, Jain TK, Maitra A (1992) Biotechnol Bioeng 39:474
71. Andrews BA, Pyle DL, Asenjo JA (1994) Biotechnol Bioeng 43:1052
72. Imai M, Natsume T, Naoe K, Shimizu M, Ichikawa S, Furusaki S (1997) Bioseparation 6:325
73. Chang QL, Liu HZ, Chen JY (1994) Enzyme Microb Technol 16:970
74. Carlson A, Nagarajan R (1992) Biotechnol Prog 8:85
75. Tang SS, Chang GG (1996) Biochem J 315:599
76. Pires MJ, Cabral JMS (1994) Appl Biochem Biotechnol 48:137
77. Barrabin H, Scofano HM, de-Gomez-Puyou MT, Gomez-Puyou A (1993) Eur J Biochem 213:757
78. Du YM, Zhang JM (1995) Gaodeng Xuexiao Huaxue Xuebao 16:715
79. Haber J, Maslakiewicz P, Rodakiewicz-Nowak J, Walde P (1993) Eur J Biochem 217:567
80. Bru R, Walde P (1993) Biochem Mol Biol Int 31:685
81. Puchkaev AV, Metelitsa DI (1994) Biokhimiya (Moscow) 59:45
82. Sanchez-Ferrer A, Perez-Gilabert M, Garcia-Carmona F (1992) Prog Biotechnol 8:755
83. Aires-Barros MR, Cabral JMS (1991) Biotechnol Bioeng 38:1302
84. Hossain MJ, Takeyama T, Hayashi Y, Kawanishi T, Shimizu N, Nakamura R (1999) J Chem Technol Biotechnol 74:423
85. Krieger N, Taipa MA, Aires-Barros MR, Melo EHM, Lima-Filho JL, Cabral JMS (1997) J Chem Technol Biotechnol 69:77

86. Nagayama K, Nishimura R, Doi T, Imai M (1999) J Chem Technol Biotechnol 74:227
87. Subramani S, Dittrich N, Hirche F, Ulbrich-Hosmann R (1996) Biotechnol Lett 18:815
88. Pessoa A Jr, Vitolo M (1998) Appl Biochem Biotechnol 70/72:505
89. Sellappan S, Shah C, Datta M (1996) Appl Biochem Biotechnol 60:33
90. Zamarro MT, Domingo MJ, Ortega F, Estrada P (1996) 23:117
91. Shkarina TN, Kuehn H, Schewe T (1992) Lipids 27:690
92. Rodakiewicz-Nowak J, Maslakiewicz P, Haber J (1996) Eur J Biochem 238:549
93. Levashov AV, Khettal B, De Lauzon S, Waks M, Cittanova N (1992) Biochimie 74:561
94. Chakravarty K, Varshney M, Maitra A (1995) Indian J Biochem Biophys 32:100
95. Hochkoeppler A, Palmieri S (1992) Biotechnol Prog 8:91
96. Chang GG, Shiao SL (1994) Eur J Biochem 220:861
97. Lalitha L, Mulimani VH (1996) Biochem Mol Biol Int 40:571
98. Huang W, Li XF, Zhou JM, Gu TR (1996) Colloid Surf B 7:23
99. Shiomori K, Kawano Y, Kuboi R, Komasawa I (1995) J Chem Eng Jpn 28:803
100. Subramani S, Madamwar D (1995) Biotechnol Techn 9:45
101. Raabe E, Croh L, Vogel J (1994) J Biochem Biophys Methods 29:207
102. Garza-Ramos G, de Gomez-Puyou MT, Gomez-Puyou A, Gracy RW (1992) Eur J Biochem 208:389
103. Pires MJ, Cabral JMS (1993) Biotechnol Prog 9:647
104. Jarudilokkul S, Poppenborg LH, Valetti F, Gilardi G, Stuckey DC (1999) Biotechnol Techn 13:159
105. Wolbert RBG, Hilhorst R, Voskuilen G, Nachtegaal H, Dekker M, Van't Riet K, Bijsterbosch BH (1989) Eur J Biochem 184:627
106. Griffin WC (1949) J Soc Cosmet Chem 1:311
107. Griffin WC (1954) J Soc Cosmet Chem 5:249
108. Pessoa A Jr, Vitolo M (1998) Process Biochem 33:291
109. Luisi PL, Meier P, Imre VE, Oande A (1984) In: Luisi PL, Straub BE (eds) Reverse micelles. Plenum, New York, p 323
110. Gierasch LM, Thompson KF, Lacy JE, Rockwell AL (1984) In: Luisi PL, Straub BE (eds) Reverse micelles. Plenum, New York, p 265
111. Thompson KF, Gierasch LM (1984) J Am Chem Soc 106:3648
112. Sadana A (1994) Bioseparation 4:39
113. Jolivalt C, Minier M, Renon H (1993) Biotechnol Prog 9:456
114. Leodidis EB, Hatton TA (1990) J Phys Chem 94:6400
115. Cardoso MM, Barradas MJ, Kroner KH, Crespo JG (1999) J Chem Technol Biotechnol 74:801
116. Marcozzi G, Correa N, Luisi PL, Caselli M (1991) Biotechnol Bioeng 38:1239
117. Laane C, Luisi PL (1986) Trends Biotechnol 4:153
118. Larson H, Adlercreutz J, Mattiasson B (1987) Eur J Biochem 166:157
119. Samana JP, Lee KM (1987) Eur J Biochem 163:609
120. Giovenco S, Verheggen F (1987) Enzyme Microb Technol 9:470
121. Lee KM, Biellman JF (1987) FEBS Lett 223:33
122. Sanchez-Ferrer A, Bru R, Garcia-Carmona F (1988) FEBS Lett 233:363
123. Dekker M, Hilhorst R, Laane C (1989) Anal Biochem 178:217
124. Ayala GA, Kamat S, Beckman EJ, Russell AJ (1992) Biotechnol Bioeng 39:806
125. Affleck R, Clark DS, Kamat S, Russell AJ (1994) Biotechnol Bioeng 43:342
126. Kahlweit M, Strey R, Schomacker R, Haase D (1989) Langmuir 5:305
127. Battistel E, Luisi PL (1989) J Colloid Interface Sci 128:7
128. Krei GA (1993) PhD thesis. Technical Unviersity Braunschweig, Germany
129. Göklen KE (1986) PhD thesis. MIT, Cambridge
130. Alexandridis P, Holzwarth JF, Hatton TA (1995) J Phys Chem 99:8222
131. Kadam KL (1986) Enzyme Microb Technol 8:266
132. Luisi PL, Bonner FJ, Pellegrini A, Wiget P, Wolf R (1979) Helv Chim Acta 62:740
133. Wolf R, Luisi PL (1979) Biochem Biophys Res Commun 89:209
134. Leser ME, Luisi PL (1990) Chimia 44:270

135. Göklen KE, Hatton TA (1984) AIChE Annual Meeting, San Fransisco, California, Paper 5a
136. Dekker M, Van't Riet K, Van der Pol JJ, Baltussen JWA, Hilhorst R, Bijsterbosch BH (1991) Chem Eng J 46:B69
137. Huang SY, Chang HL (1995) Bioseparation 5:225
138. Misiorowsky RL, Wells MA (1974) Biochemistry 13:4928
139. Dekker M, Van't Riet K, Weijers SR, Baltussen JWA, Laane C, Bijsterbosch BH (1986) Chem Eng J 33:B27
140. Göklen KE, Hatton TA (1987) Sep Sci Technol 22:831
141. Woll JM, Dillon AS, Rahaman RS, Hatton TA (1987) In: Burgess R (ed) Protein purification: micro to macro. Liss, New York, p 117
142. Fletcher PDI, Parrot D (1988) J Chem Soc Faraday Trans 84:1131
143. Luisi PL, Giomini M, Pileni MP, Robinson BH (1988) Biochim Biophys Acta 947:209
144. Stamatis H, Xenakis A, Kolisis FN (1999) Biotechnol Adv 17:293
145. Matzke SF, Creagh AL, Haynes CA, Prausnitz JM, Blanch HW (1992) Biotechnol Bioeng 40:91
146. Chetanay D, Urbach W, Cazabat AM, Vacher M, Waks M (1985) Biophys J 48:893
147. Bonner FJ, Wolf R, Luisi PL (1980) J Solid-Phase Biochem 5:255
148. Levashov AV, Khmelnitsky YL, Klyachko NL, Chernyak VY, Martinek K (1982) J Colloid Interface Sci 88:444
149. Zampieri GG, Jäckle H, Luisi PL (1986) J Phys Chem 90:1849
150. Fletcher PDI, Howe AM, Perrins NM, Robinson BH, Toprakcioglu C, Dore JC (1984) In: Mittal KL, Lindman B (eds) Surfactants in solution. Plenum, New York, vol 3, p 1745
151. Sheu E, Göklen KE, Hatton TA, Chen SH (1986) Biotechnol Prog 2:175
152. Rahaman RS, Hatton TA (1991) J Phys Chem 95:1799
153. Pileni MP, Zemb T, Petit C (1985) Chem Phys Lett 118:414
154. Brochette P, Petit C, Pileni MP (1988) J Phys Chem 92:3505
155. Chatenay D, Wurbach W, Nicot C, Vacher M, Waks M (1987) J Phys Chem 91:2198
156. Luisi PL, Henninger F, Joppich M, Dossena A, Casnati G (1977) Biochem Biophys Res Commun 74:1384
157. Leser ME, Wei G, Luthi P, Haering G, Hochkoeppler A, Blochliger E, Luisi PL (1987) J Chem Phys Physicochim Biol 84:1113
158. Vos K, Laane C, Van Hoek A, Veeger C, Visser AJWG (1987) Eur J Biochem 169:275
159. Leodidis EB, Hatton TA (1990) J Phys Chem 94:6411
160. Adachi M, Harada M, Shioi A, Sato Y (1991) J Phys Chem 95:7925
161. Cardoso MM, Barradas MJ, Kroner KH, Carrondo MT, Crespo JG (1998) Bioseparation 7:65
162. Kelley BD, Wang DIC, Hatton TA (1993) Biotechnol Bioeng 42:1199
163. Leser ME, Mrkoci K, Luisi PL (1993) Biotechnol Bioeng 41:489
164. Choudhuri JB, Spirovska G (1994) Biotechnol Techn 8:909
165. Gupta RB, Han CJ, Johnston K (1994) Biotechnol Bioeng 44:830
166. Phillips JB, Nguyen H, John VT (1991) Biotechnol Prog 7:43
167. Hu Z, Gulari E (1996) Biotechnol Bioeng 50:203
168. Spirovska G, Choudhuri JB (1998) Biotechnol Bioeng 58:374
169. Noritomi H, Hidaka Y, Kato S, Nagahama K (1999) Biotechnol Techn 13:181
170. Dekker M, Van't Riet K, Bijsterbosch BH, Wolbert RBG, Hilhorst R (1989) AIChE J 35:321
171. Bratko D, Luzar A, Chen SH (1988) J Chem Phys 89:545–550
172. Caselli M, Luisi PL, Maestro M, Roselli R (1988) J Phys Chem 92:3899
173. Caselli M, Maestro M, Morea G (1988) Biotechnol Prog 4:102
174. Shapiro YE, Budanov NA, Levashov AV, Klyachko NL, Khmelnitsky YL, Martinek K (1989) Collect Czech Chem Commun 54:1126
175. Woll JM, Hatton TA (1989) Bioprocess Eng 4:193
176. Maestro M, Luisi PL (1986) In: Proceedings of 8th International Symposium on Surfactants in Solution, New Delhi, Aug 22–28
177. Fraaije JGEM, Rijnierse EJ, Hilhorst R, Lyklema J (1990) Colloid Polym Sci 268:855
178. Dahuron L, Cussler EL (1988) AIChE J 34:130

179. Zhang QI, Cussler EL (1985) J Membr Sci 31:1548
180. Dahuron L (1987) PhD thesis. University of Minnesota, Minneapolis
181. Yang MC, Cussler EL (1986) AIChE J 32:1910
182. Cussler EL (1984) Diffusion, Cambridge, London
183. Bru R, Sanchez-Ferrer A, Garcia-Carmona F (1989) Biochem J 259:355
184. Yang F, Russel AJ (1995) Biotechnol Bioeng 47:60
185. Kelley BD, Rahaman RS, Hatton TA (1990) In: Hinze WL (ed) Analytical chemistry in organized media:Reversed micelles. JAI Press, Greenwich, CT
186. Dungan SR, Bausch T, Hatton TA, Plucinski P, Niitsch W (1991) J Colloid Interface Sci 145:33
187. Bell GM, Peterson GC (1972) J Colloid Interface Sci 41:542
188. Choe J, VanderNoot A, Linhardt RJ, Dordick JS (1998) AIChE J 44:2542
189. Li XS, Lu JF, Li YG, Liu JC (1999) Ind Eng Chem Res 38:2817
190. Petsev DN, Linse P (1997) Phys Rev E 55:586
191. Jönsson AS, Jönsson B (1996) J Colloid Interface Sci 180:504
192. Blum L, Hoye JS (1977) J Phys Chem 81:1311
193. Loehe JR, Donohue MD (1997) AIChE J 43:180
194. Evans DF, Ninham BW (1983) J Phys Chem 87:5025
195. Chen SJ, Evans DF, Ninham BW, Mitchel DJ, Blum FD, Pickup S (1986) J Phys Chem 90:842
196. Fletcher PDI, Howe AM, Robinson BH (1987) J Chem Soc Faraday Trans 83:985
197. Pecora R (1964) J Chem Phys 40:1604
198. Luisi PL, Steinmann-Hofmann B (1987) Methods Enzymol 136:188
199. Martinek K, Levashov AV, Klyachko NL, Khmelnitsky YL, Berezin IV (1986) Eur J Biochem 155:453
200. Leodidis EB, Hatton TA (1989) In: Pileni MP (ed) Structure and reactivity in reversed micelles. Elsevier, Amsterdam, p 353
201. Rabie HR, Vera JH (1996) Ind Eng Chem Res 35:3665
202. Blumberg R (1983) Plenary lecture, International Solvent Extraction Conference, Denver, Colorado
203. Schomaecker R, Braun GA (1996) Langmuir 12:2362
204. Reissinger KH, Schroter J (1978) Chem Eng 85:109
205. Laane C, Dekker M (1986) In: Proceedings of 8th International Symposium on Surfactants in Solutions, New Delhi, Aug 22–28
206. Dekker M, Baltussen JWA, Van't Riet K, Bijsterbosch BH, Laane C, Hilhorst R (1987) In: Laane C, Tramper J, Lilly MD (eds) Biocatalysis in organic media. Elsevier, Amsterdam, p 285
207. Dekker M, Van't Riet K, Wijnans JMGM, Baltussen JWA, Bijsterbosch BH, Laane C (1987) In: Proceedings ICOM, Tokyo, p 793
208. Meier P, Imre VE, Fleschar M, Luisi PL (1984) In: Mittal KL, Lindman B (eds) Surfactants in solutions. Plenum, New York, vol 2, p 999
209. Armstrong DW, Li W (1988) Anal Chem 60:86
210. Lye GJ, Asenjo JA, Pyle DL (1994) Spec Publ – R Soc Chem 158:273
211. Han DH, Lee SY, Hong WH (1994) Biotechnol Techn 8:105
212. Sadana A, Raju RR (1990) BioPharm (May) 53
213. Senstad C, Mattiasson B (1989) Biotechnol Appl Biochem 11:41
214. Coughlin RW (1986) Engineering approaches to continuous affinity purification. Proposal submitted to National Science Foundation, USA
215. Woll JM, Hatton TA, Yarmush ML (1989) Biotechnol Prog 5:57
216. Coughlin RW, Baclaski JB (1990) Biotechnol Prog 6:307
217. Paradkar VM, Dordick JS (1991) Biotechnol Prog 7:330
218. Paradkar VM, Dordick JS (1993) Biotechnol Prog 9:199
219. Kelley BD, Wang DIC, Hatton TA (1993) Biotechnol Bioeng 42:1209
220. Chen JP, Jen JT (1994) Sep Sci Technol 29:1115
221. Poppenborg L, Flaschel E (1994) Biotechnol Techn 8:307
222. Sun Y, Ichikawa S, Sugiura S, Furusaki S (1998) Biotechnol Bioeng 58:58

223. Sun Y, Gu L, Tong XD, Bai S, Ichikawa S, Furusaki S (1999) Biotechnol Prog 15:506
224. Pommerening K, Mohr P (1985) In: Affinity chromatography: practical and theoretical aspects. Marcel Dekker, New York, p 75
225. Mattiasson B, Ling TG (1986) In: McGregor WC (ed) Membrane separations in biotechnology. Marcel Dekker, New York, p 270
226. Qadri F (1985) Trends Biotechnol 3:7
227. Arnold FH, Suh SS, VanDam ME, Wuenschell GE, Plunkett S (1990) ACS Symp Ser 427:139
228. Luong JHT, Male KB, Nguyen AL (1988) Biotechnol Bioeng 31:516
229. Matson SL, Lopez J, Quinn JA (1983) Chem Eng Sci 38:503
230. Ichikawa S, Imai M, Shimizu M (1992) Biotechnol Bioeng 39:20
231. Chang QL, Chen JY (1996) Process Biochem 31:371
232. Vasudevan M, Tahan K, Wiencek JM (1995) Biotechnol Bioeng 46:99
233. Kuboi R, Mori Y, Komasawa I (1990) Kogaku Kogaku Ronbunshu 16:1060
234. Ayala GA, Kamat S, Komives C, Beckman EJ, Russell AJ (1992) Bio/Technol 10:1584
235. Schoenfeldt N (1969) Surface active ethylene oxide adducts. Pergamon, London
236. Moroi Y (1992) Micelles: theoretical and applied aspects. Plenum, New York
237. Goto M, Kuroki M, Ono T, Nakashio F (1995) Sep Sci Technol 30:89
238. Goto M, Kondo K, Nakashio F (1990) J Chem Eng Japan 23:513
239. Naoe K, Nishino M, Ohsa T, Kawagoe M, Imai M (1999) J Chem Technol Biotechnol 74:221
240. Neuman RD, Jones MA, Zhou NF (1990) Colloid Surf 46:45
241. Shioi A, Harada M, Matsumoto K (1993) J Phys Chem 97:8281
242. Yu ZJ, Neuman RD (1994) Langmuir 10:2553
243. Hu Z, Gulari E (1996) J Chem Technol Biotechnol 65:45
244. Klibanov AM (1989) Trends Biochem Sci 14:141
245. Hari Krishna S, Manohar B, Divakar S, Karanth NG (1999) J Am Oil Chem Soc 76:1483
246. Hari Krishna S, Manohar B, Divakar S, Prapulla SG, Karanth NG (2000) Enzyme Microb Technol 26:131
247. Verhaert RMD, Hilhorst R (1991) Recl Trav Chim Pays-Bas 110:236
248. Morita S, Narita H, Matoba T, Kito M (1984) J Am Oil Chem Soc 61:1571
249. Hilhorst R, Laane C, Veeger C (1983) FEBS Lett 159:225
250. Luthi P, Luisi PL (1984) J Am Chem Soc 106:7285
251. Shield JW, Ferguson HD, Gleason KK, Hatton TA (1989) ACS Symp Ser 392:90
252. Eggers DK, Blanch HW (1988) Bioprocess Eng 3:83
253. Serralheiro MLM, Prazeres DMF, Cabral JMS (1994) Enzyme Microb Technol 16:1064
254. Serralheiro MLM, Prazeres DMF, Cabral JMS (1999) Enzyme Microb Technol 24:507
255. Hakoda M, Nakamura K, Enomoto A, Hoshino T (1996) J Chem Eng Jpn 29:300
256. Dunn RO Jr., Scamehorn JF, Christian SD (1985) Sep Sci Technol 20:257
257. Christian SD, Bhat SN, Tucker EE, Scamehorn JF, El-Sayed DA (1988) AIChE J 34:189
258. Tzeng YM, Tsun HY, Chang YN (1999) Biotechnol Prog 15:580
259. Dunn RO Jr., Scamehorn JF, Christian SD (1987) Sep Sci Technol 22:763
260. Pramauro E, Bianco A, Barni E, Viscardi G, Hinze WL (1992) Colloid Surf 63:291
261. Pramauro E, Prevot AB, Savorino P, Viscardi G, de la Guardia M, Cardells EP (1993) Analyst 118:23
262. Bhat SN, Smith GA, Tucker EE, Christian SD, Scamehorn JF, Smith W (1987) Ind Eng Chem Res 26:1217
263. Gibbs LL, Scamehorn JF, Christian SD (1987) J Memb Sci 30:67
264. Kandori K, Schechter RS (1990) Sep Sci Technol 25:83
265. Markels JH, Lynn S, Radke CJ (1985) AIChE J 41:2058
266. Tangen A, Lund W, Frederiksen R (1997) J Chromatogr 767:311
267. Cartoni G, Coccioli F, Jasionowsk R (1995) J Chromatogr 709:209
268. Bumgarner J, Khaledi M (1996) J Chromatogr 738:275
269. Gassmann I, Kuo JE, Zare RN (1985) Science 230:813
270. Ozaki H, Ichihara Y, Terabe S (1995) J Chromatogr 709:3

271. Tsai CF, Li CF, Chang HM (1998) J Agric Food Chem 46:979
272. Boyce M, Bennett I (1996) Anal Lett 29:1805
273. Clothier J, Tomellini S (1996) J Chromatogr 723:179
274. Cole R, Sepaniak M, Hinze W, Gorse J, Oldiges K (1991) J Chromatogr 557:113
275. Nishi H, Fukuyama T, Matsuo M (1990) J Chromatogr 498:313
276. Seifar R, Kraak J, Kok W (1997) Anal Chem 69:2772
277. Tani H, Saitoh T, Kamidate T, Kamataki T, Watanabe H (1997) Biotechnol Bioeng 56:311
278. Walter H, Johansson G (eds) (1994) Aqueous two-phase systems. Methods Enzymol, vol 228
279. Cabezas H (1996) J Chromatogr 680:3
280. Quina FH, Hinze WL (1999) Ind Eng Chem Res 38:4150
281. Tani H, Kamidate T, Watanabe H (1998) Anal Sci 14:875
282. Singh A, Pandey KD, Dubey RS (1999) World J Microbiol Biotechnol 15:243
283. Larsson KM, Adlercreutz P, Mattiasson B (1990) Biotechnol Bioeng 36:135
284. Gajjar L, Singh A, Dubey RS, Srivastava RC (1997) Appl Biochem Biotechnol 66:159
285. Fadnavis NW, Chandraprakash Y, Deshpande A (1993) Biochimie 75:995
286. Ebert G, Nishi N, Zoelzer U (1992) Colloid Surf 67:157
287. Kabanov AV, Klyachko NL, Nametkin SN, Merker S, Zaroza AV, Bunik VI, Ivanov MV, Levashov AV (1991) Protein Eng 4:1009
288. Palazzo G, Luisi PL (1992) Biochem Biophys Res Commun 186:1546
289. Pires MJ, Cabral JMS (1994) J Chem Technol Biotechnol 61:219
290. Munsi N, Chakraborty K, De TK, Maitra AN (1995) Colloid Polym Sci 273:464
291. Ino M, Tanaka H, Otsuki J, Araki K, Seno M (1994) Colloid Polym Sci 272:151
292. Levashov AV, Rariy RV, Martinek K, Klyachko NL (1993) FEBS Lett 336:385
293. Bhattacharyya K, Basak S (1993) Biophys Chem 47:21
294. Bernardi R, Palmieri S (1996) Biotechnol Lett 18:663
295. Bismuto E, Sirangelo I, Irace G (1993) Biochim Biophys Acta 1146:213
296. Rao AM, Kommareddi N, John VT (1992) Biotechnol Prog 8:514
297. Chen WY, Wang YH, Wang LK (1994) J Chem Eng Jpn 27:685
298. Wang W, Weber ME, Vera JH (1995) Biotechnol Bioeng 46:343
299. Paradkar VM, Dordick JS (1994) Biotechnol Bioeng 43:529
300. Wu Z, Jia Y, Chu Y, Wang Y, Liu P, Ma Z (1993) Gaodeng Xuexiao Huaxue Xuebao 14:1427
301. Weir MP, Sparks J (1987) Biochem J 245:85
302. Hagen AJ, Hatton TA, Wang DIC (1990) Biotechnol Bioeng 35:955
303. Hagen AJ, Hatton TA, Wang DIC (1990) Biotechnol Bioeng 35:966
304. Shastry MCR, Eftink MR (1996) Biochemistry 35:4094
305. Mall S, Spirovska G, Chaudhuri JB, Thatcher D (1994) IChemE Res Event Two-Day Symp, Inst Chem Eng:Rugby, UK, vol 1, p 180
306. Sepulveda-Becerra MA, Ferreira ST, Strasser RJ, Garzon-Rodriguez W, Beltran C, Gomez-Puyou A, Darszon A (1996) Biochemistry 35:15,915
307. Bachmann PA, Luisi PL, Lang J (1991) Chimia 45:266
308. Boehler C, Bannwarth W, Luisi PL, Giustini M (1993) Helv Chim Acta 76:1341
309. Boehler C, Bannwarth W, Luisi PL (1993) Helv Chim Acta 76:2313
310. Boehler C, Bannwarth W, Luisi PL (1994) NATO ASI Ser, Ser C 446:249
311. Hammouda A, Pileni MP (1994) Prog Colloid Polym Sci 97:229
312. Metveeva EG, Nelil-Nubarov NS, Miethe P, Levashov AV (1996) Anal Biochem 234:13
313. Slepnev VI, Melik-Nubarov NS, Kabanov AV (1992) Bioconjugate Chem 3:273
314. Evans RM, Farr SJ (1993) US Pat 5 230 884A
315. Sarkar N, Das K, Datta A, Das S, Bhattacharyya K (1996) J Phys Chem 100:10,523
316. Dutta PK, Jakupca M, Reddy KSN, Salvati LM (1995) Nature 374:44
317. Reddy KSN, Salvati LM, Dutta PK, Abel PB, Suh KI, Ansari RR (1996) J Phys Chem 100:9870
318. Sangregorio C, Galeotti M, Bardi U, Baglioni P (1996) Langmuir 12:5800
319. Lisiecki I, Boulanger L, Lixon P, Pileni MP (1992) Prog Colloid Polym Sci 89:103
320. Motte L, Billoudet F, Cizeron J, Pileni MP (1995) Prog Colloid Polym Sci 98:189

321. Sato H, Hirai T, Komasawa I (1995) Ind Eng Chem Res 34:2493
322. Moran PD, Barlett JR, Woolfrey JL, Bowmaker GA, Cooney RP (1995) Ceram Trans 51:27
323. Natarajan U, Handique K, Mehra A, Bellare JR, Khilar KC (1996) Langmuir 12:2670
324. Petit C, Lixon P, Pileni MP (1993) J Phys Chem 97:12,974
325. Berthod A, Xiang J, Alex S, Gonnet-Collet C (1996) Can J Chem 74:277
326. Ashrafizadeh SN, Weber ME, Vera JH (1993) Ind Eng Chem Res 32:125
327. Bulavchenko AI, Batishcheva EK, Podlipskaya TY, Torgov VG (1996) Colloid J 58:153
328. Desfosses B, Nicot C, Waks M (1992) Biochem Int 26:257
329. Bhattacharyya K, Basak S (1995) Photochem Photobiol 62:17
330. Quarzago D, Moroder L (1995) Lett Pept Sci 1:171
331. Andrade SM, Costa SMB (1996) Prog Colloid Polym Sci 100:195
332. Dutta G, Parvathanathan PS, Rao URK, Deniz KU (1992) Physiol Chem Phys Med NMR 24:51
333. Pirchanont S, Stucky DC, Leak DJ (1994) IChemE Res Event, Two Day Symposium Inst Chem Eng, Rugby, UK, vol 1, p 238
334. Buriak JM, Osborn JA (1996) Organometallics 15:3161
335. Joselevich E, Willner I (1995) J Phys Chem 99:6903
336. Kang YS, McManus HJD, Liang K, Kevan L (1994) J Phys Chem 98:1044
337. Sarkar M, Ray JG, Sengupta PK (1996) Spectrochim Acta 52:A275
338. Imdadullah, Fujiwara T, Kumamaru T (1991) Anal Sci 7:1399
339. Imdadullah, Fujiwara T, Kumamaru T (1993) Anal Chem 65:421
340. Xie JW, Xu JG, Chen GZ (1995) Huaxue Xuebao 53:952
341. Walsh CT (1993) NTIS Energy Res Abstracts 18:18664
342. Zhang J, Bright F (1992) J Phys Chem 96:5633
343. Giddings LD, Olesik SV (1994) Langmuir 10:2877
344. Franco TT, Marty A, Condoret JS (1994) Cienc Tecnol Aliment 14(suppl):17
345. Pires MJ, Aires-Barros MR, Cabral JMS (1996) Biotechnol Prog 12:290
346. Raghavarao KSMS, Stewart RM, Todd P (1990) Sep Sci Technol 25:985
347. Raghavarao KSMS, Stewart RM, Todd P (1991) Sep Sci Technol 26:257
348. Srinivas ND, Barhate RS, Raghavarao KSMS, Todd P (2001) Appl Microbiol Biotechnol 53:650
349. Imre VE, Luisi PL (1982) Biochem Biophys Res Commun 107:538
350. Albertsson PA (1958) Nature 182:709
351. Hustedt H, Kroner KH, Menge U, Kula MR (1985) Trends Biotechnol 3:139

Received: March 2001

Enzyme Catalysis in Reverse Micelles

Bernhard Orlich[1], Reinhard Schomäcker[2]

[1] Henkel KGaA, WEV, Henkelstrasse 67, 40191 Düsseldorf, Germany,
e-mail: Bernhard.Orlich@denotes.henkel.de
[2] Institut für Technische Chemie, Technische Universität Berlin, Strasse des 17. Juni 135,
10623 Berlin, Germany, e-mail: Schomaecker@tu-berlin.de

Water in oil microemulsions with reverse micelles provide an interesting alternative to normal organic solvents in enzyme catalysis with hydrophobic substrates. Reverse micelles are useful microreactors because they can host proteins like enzymes. Catalytic reactions with water insoluble substrates can occur at the large internal water-oil interface inside the microemulsion. The activity and stability of biomolecules can be controlled, mainly by the concentration of water in these media. With the exact knowledge of the phase behaviour and the corresponding activity of enzymes the application of these media can lead to favourable effects compared to aqueous systems, like hyperactivity or increased stability of the enzymes.

Keywords. Reverse micelles, Microemulsion, Enzymes, Immobilisation

1 Introduction 186

2 The Properties of Microemulsions 191

3 Enzyme Catalysis in W/O-Microemulsions 194

3.1 General Aspects of Enzyme Activity in Microemulsions 194
3.2 Influence of Microemulsion Composition on Enzyme Activity . . . 195
3.2.1 Influence of the Oil 196
3.2.2 Influence of the Surfactant 197
3.2.3 Influence of the Water Concentration 198
3.3 Stability of Enzymes in Microemulsions 200

4 Immobilisation Methods 201

4.1 Phase Separation 201
4.2 Microemulsion-Based Gels 201
4.3 Centrifuge Reactor 202
4.4 Filtration Systems 202

5 Synthesis Reactions 203

6 Outlook 205

References 205

Advances in Biochemical Engineering/
Biotechnology, Vol. 75
Managing Editor: Th. Scheper
© Springer-Verlag Berlin Heidelberg 2002

List of Abbreviations and Symbols

µE	microemulsion
a	mass ratio of the oil in the mixture of water and oil (–)
A_1, A_2	preexponential factors
$A_{surfactant}$	surface of a surfactant headgroup at an interface (m^2)
ADH	alcohol dehydrogenase
AOT	aerosol OT, Bis ethylhexyl sulfosuccinate
BSA	bovine serum albumin
CPCR	*Candida parapsylosis* carbonyl reductase
CRL	*Candida rugosa* lipase
CT	chymotrypsine
CVL	*Chromobacterium viscosum* lipase
cµc	critical microemulsion concentration
CiEOj	nonionic surfactant with hydrocarbon chain of i carbonation and j ethylene oxide unit as head group
D	deactivated enzyme
E	enzyme
f	surfactant headgroup dependent factor (m)
γ	surfactant mass fraction (–)
η	viscosity of dispersion (Pa s)
η_0	viscosity of solvent (Pa s)
η_{rel}	relative viscosity (–)
HLADH	horse liver alcohol dehydrogenase
k	reaction rate constant, deactivation rate constant
l_c	length of hydrocarbon chain in surfactants (m)
m	mass (kg)
n	molar amount (mol)
P	distribution coefficient between water and octanol (–)
PPL	pig pancreas lipase
$r_{rev.mic.}$	radius of a reverse micelle (m)
r(t)	enzyme activity (U/mg)
Sp	packing parameter (–)
t	time (s)
ttn	total turn-over number (–)
V	volume (m^3)
w_0, w_1	molar ratio of water to surfactant (–)
HLB	hydrophilic-lipophilic-balance
YADH	yeast alcohol dehydrogenase
Φ	volume fraction of dispersed phase

1 Introduction

During the past years a variety of stereoselective syntheses have been developed in enzyme technology. There is great interest in finding suitable organic media for less water soluble substrates in order to increase the substrate concentration

and, therefore, the reaction rates. Phase transfer catalysts, like crown ethers or quaternary ammonia salts, are often not applicable to biomolecules because they were developed to transfer inorganic salts or small guest molecules into an organic phase. Furthermore, phase transfer catalysts are often toxic and inhibit or denature enzymes. By now there exist various methods for biotransformations in organic media [1, 2] which improve the solubility of the reactants, particularly that of non-polar substrates, and the volumetric productivity of the reaction system [3]. Some strategies for incubating hydrophobic substrates with enzymes are shown schematically in Fig. 1.

The reaction in a homogeneous solution with a polar organic solvent in which the enzymes and substrates are both soluble, occurs often at the expense of the enzyme stability [4, 5]. Besides immobilised enzymes in organic solvents [6], emulsion reactors, especially enzyme-membrane-reactors coupled with a product separation by membrane based extractive processes [7–9] and two-phase membrane reactors [10–12], are already established on a production scale.

The reverse micelles, found in most w/o-microemulsions, are useful microreactors for enzymatic reactions. The self aggregation of amphiphilic molecules dissolved in organic solvents is a well understood phenomenon. Reverse micelles (RM) or w/o-microemulsions, structurally inverse analogues to normal micelles, are capable of hosting proteins in their so-called water pool. Reverse micelles usually have low aggregation numbers of the surfactant molecules, but this aggregation number is greatly increased upon addition of water which is solubilised between the polar head groups of the surfactant, forming water-swollen reverse micelles or w/o-microemulsion. In this paper no distinction is made between reverse micelles, water swollen reverse micelles and the water droplets of w/o-microemulsions.

Since the beginning of enzyme catalysis in organic solvents (introduced by A. M. Klibanov) and microemulsions (introduced by P. P. Luisi), several reactions

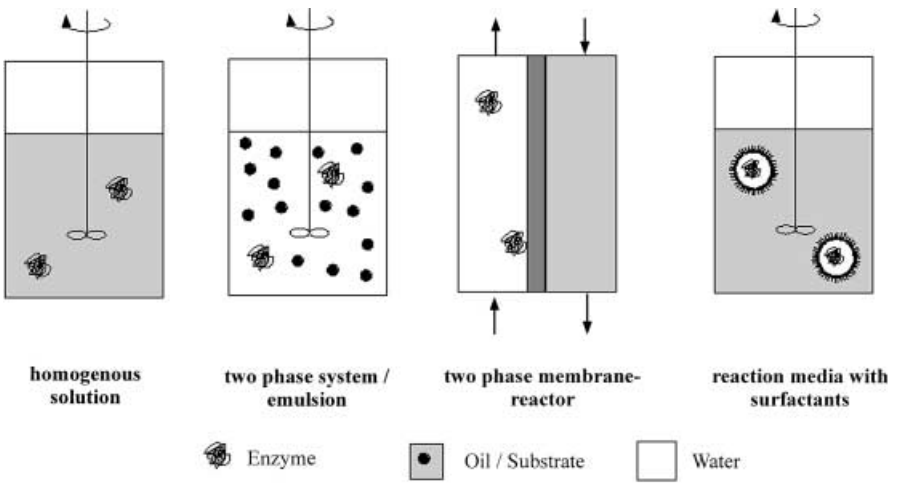

Fig. 1. Approaches for biotransformations with hydrophobic substrates

with less water soluble substrates became feasible. Beside the research groups of Klibanov at the MIT in Boston (USA) and Luisi (ETH-Zuerich, Switzerland), the groups of Laane (Netherland), Martinek (Soviet Union), Robinson (UK) and Holmberg (Sweden) founded the basic knowledge about enzyme catalysis in reverse micelles in the early 1980s. Besides catalysis, the nanostructures within a microemulsion enables some effects, which are favourable for specific investigations in enzymology:

- Overcoming solubility limitations of hydrophobic and hydrophilic reactants
- Shifts of thermodynamic equilibrium in enzyme catalysed condensation and hydrolysis reactions due to a controllable water concentration
- Possibility of suppressing product inhibition
- Possibility of enhanced stereo selectivity, activity and stability of enzymes
- Possibility of cryoenzymology (the melting point of water in reverse micelles can be lower than –20 °C)
- Possibility of investigations under conditions that mimic biological environments in optically transparent solutions

The most often investigated enzymes in microemulsions are lipases, because these enzymes are very stable and active in this medium [14]. Until now, most of the relevant interactions between the biomolecules and the reaction medium have been investigated. Many enzymes which are well investigated in aqueous reaction media can be solubilised in w/o-microemulsion, retaining their activity and stability, as shown in Table 1.

Table 1. Enzyme catalysis in w/o-microemulsion

Enzyme	w/o – micro-emulsion (surfactant-oil)	Investigations/results	Ref.
Lipoxygenase	AOT-isooctane	Influence of the water concentration (w_0) on the activity	[15]
Lipoxygenase	AOT-isooctane	Influence of the pH-value inside the RM on the activity (concentration)	[16]
Five different lipases (e.g. CRL and PPL)	AOT-toluene AOT-heptane	Esterification of Diterpenes: enhancement of activity, influence of acid chain length	[17]
α-CT	AOT-octane	Covalently binding of a fluorescence marker= enhancement of stability [f(w_o) – several month]	[18]
Several lipases	AOT-isooctane	*p*-Nitrophenyl ester hydrolysis as an activity sensor	[19, 20]
CRL-*Y*ADH	P40 (with Triton X35); Tween 85 (with ethylene glycol); AOT; Brij56 – cyclohexane; heptane	Combination of lipase and ADH; cofactor regeneration; activity in different µE - compositions	[21, 22]

Table 1 (continued)

Enzyme	w/o – micro-emulsion (surfactant-oil)	Investigations/results	Ref.
Cutinase	AOT-isooctane	Spin-label at the active site; activity and stability measurements (w_0)	[23]
CRL	AOT-lecithin/ isooctane	Conversion dependent kinetics	[24]
Urease	SDS-hexane	Potentiometric urea sensor	[25]
α-CT, several Lipases, Lipo-xygenase, Lysozyme	AOT-heptane AOT + sodium taurocholate – heptane	Solubilisation and protein folding in reverse micelles (time dependent), activity	[26, 27]
Lipase	potassium dodecanoate – several oils	Effect of oil chain length on the trigliceride synthesis	[28]
CVL	AOT-heptane; CTAB -heptane	Influence of the water concentration on the product distribution of the esterification of glycerine	[26]
PPL	AOT-octane	Kinetic and modelling of the triglyceride hydrolysation	[30]
α-CT	AOT-isooctane	Theory of the "hyperactivity" of hydrolases in reverse micelles (influence of water concentration)	[31]
CRL, HLL	AOT-isooctane	Regioselective esterification of butane-1,3-diol with oleic acid	[32]
BSA	PFPE-CO_2	First described proteins in water-CO_2- µE	[33]
*Y*ADH	AOT-isooctane	Theory of deactivation processes of enzymes in reverse micelles (for ADH)	[34]
α-CT, *HL*ADH, BSA, Lysozyme, Trypsine, γ-Globuline	AOT–octane	Comprehensive sedimentation analysis in reverse micelles	[35]
α-CT	AOT–isooctane, Na-dioleyl phos-phate (SDOLP)-isooctane	Comparison of the microemulsion proper-ties using AOT and SDOLP, influence on the the esterification kinetics	[36]
Phosphor-lipide, Hexokinase	Triton X100-propylbenzene, Triton X100-toluene	Comprehensive investigation of the phase behaviour and the influence on enzyme activity and stability [37, 38]	[37, 38]
α-CT, γ-CT	AOT–isooctane	Clarification of the deactivation process (location and bindings)	[39]
cytochrome c	Tween 85/ Span 85-hexane/ i-propanol	First phase transfer catalysis and activity investigation in using Tween surfactants	[40]

Older compilations about the state of the art can be found in several review articles [41 – 47]. It is surprising that most work is carried out with the surfactant bis-ethylhexyl-sulfosuccinate (tradename AOT or Aerosol OT). The reasons seem to be the variability of the obtained reverse micelles (from very low up to high water concentrations) and the well-known phase behaviour of AOT with water and several oils [48, 49]. AOT is approved for medical application, e. g. as an additive in suppositories, but not for food engineering.

In the majority of cases, the enzyme is transferred into the microemulsion by use of the so-called injection method, because this method ensures a high enzyme activity [50]. In the injection method an aqueous stock solution of the enzyme is injected into an already prepared solution of surfactant in oil. The microemulsion is obtained by shaking the solution until it is transparent. In contrast, if the water is added to a suspension of the enzyme in oil or by adding dry enzyme to an already prepared microemulsion, little or no activity is obtained [50, 51]. Beside the interactions of the enzymes with the oil, it is essential for their activity that the flexibility of the protein is ensured. Already some water molecules (less than a monolayer of water on the protein surface) can guarantee this flexibility in organic solvents [52]. The injection method works very fast, but has one disadvantage: the one-phase region predicted from the phase diagram of the ternary water-oil-surfactant mixture is often shifted by the addition of salts, buffers and enzymes to the aqueous part of the microemulsion. Therefore the obtained solution is not thermodynamically stable. The reason is that the components also have an influence on the behaviour of the surfactant at the water-oil interface. In case of macromolecules, like proteins, the phase boundary between a single phase microemulsion and a two-phase system is often shifted towards lower water concentrations, as shown in Fig. 2.

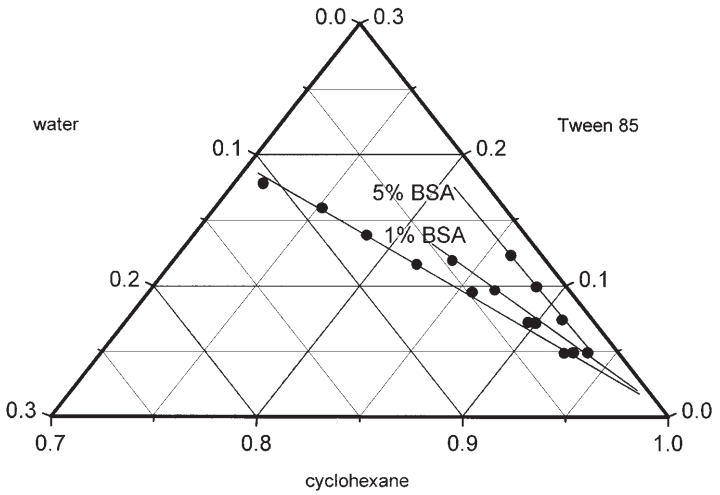

Fig. 2. Oil-rich region of the Gibbs phase triangle of the ternary mixture Tween 85, cyclohexane and water

In order to obtain a thermodynamically stable microemulsion, the analysis of the phase behaviour is indispensable. With bovine serum albumin instead of an enzyme (because of the cost of the bio-catalyst) phase behaviour studies are shown in Fig. 2. A strong shift of the phase boundary is observed, yielding a system that solubilises much less water in the presence of the protein. In case of hydrophobic enzymes, the addition of dry lyophilised protein to an already prepared reverse micellar solution can also work well [53].

An alternative to the injection method for importing enzymes into a microemulsion is the phase transfer method. In this method, a layer of an aqueous enzyme solution is located under a mixture of surfactant and oil. Upon gentle shaking, the enzyme is transferred into the reverse micelles of the hydrocarbon phase. Finally, the excess of water is removed and the hydrophobic substrates can be added. The main advantage of this method is that it ensures thermodynamically stable microemulsions with maximum water concentrations. However, the method is very time consuming. The method is often applied in order to purify, concentrate or renaturate enzymes in the reverse micellar extraction process [54–58].

In case of lipases, one of the simplest methods to combine an enzyme with an organic solvent is to coat the lipase with a lipid or surfactant layer before lyophilisation. It is estimated that about 150 surfactant molecules are sufficient for encapsulating one lipase molecule. Following this route the surfactant coated lipase forms reverse micelles with a minimum of water concentration. The modified lipases are soluble in most organic solvents, and the reaction rates are increased compared to the suspended lipases due to the interfacial activation [59, 60].

2 The Properties of Microemulsions

The most important properties of reverse micellar systems, which are of significance for enzyme activity and stability, will be described in this section. Some of the properties are illustrated schematically and reduced to the major aspects of their influence in enzymology.

Microemulsions are optically transparent, thermodynamically stable mixtures. These macroscopic homogeneous mixtures are heterogeneous on a nanometer scale. Depending on the composition and temperature, small droplets of oil are dispersed in water, or, in case of an oil rich microemulsion, reverse micelles of water are dispersed in oil. The water and oil in a one-phase microemulsion are separated by a surfactant monolayer at the large internal interface [61, 62]. The droplet contents exchange rapidly because of the droplet collisions caused by their thermal energy [63]. The composition of w/o-microemulsions are characterised by the weight fraction α of the oil in the mixture of water and oil, the weight fraction of the surfactant γ in the ternary mixture, and the molar ratio of water to surfactant w_0:

$$\gamma = \frac{m_{\text{Surfactant}}}{m_{\text{Surfactant}} + m_{\text{Water}} + m_{\text{Oil}}} \tag{1}$$

$$\alpha = \frac{m_{\text{Oil}}}{m_{\text{Water}} + m_{\text{Oil}}} \tag{2}$$

$$w_0 = \frac{m_{\text{Water}}}{m_{\text{Surfactant}}} \tag{3}$$

The parameter w_1 which takes the concentration of the non-aggregated surfactant in the oil into account – the cμc – is directly proportional to the radius of the reverse micelles $r_{\text{rev. mic.}}$ because of the volume to surface ratio of spherical droplets [64–66]:

$$w_1 = \frac{n_{\text{Water}}}{n_{\text{Surfactant, total}} - n_{\text{Surfactant, solution}}} = \frac{n_{\text{Water}}}{n_{\text{Surfactant, interfacial layer}}} \tag{4}$$

$$\frac{V_{\text{rev.mic.}}}{A_{\text{rev.mic.}}} = \frac{n_{\text{H}_2\text{O}} V_{\text{H}_2\text{O}}}{n_{\text{Surfactant, interfacial layer}} A_{\text{Surfactant}}} = \frac{r_{\text{rev.mic.}}}{3} \tag{5}$$

$$r_{\text{rev.mic.}} = w_1 \frac{9 \cdot 10^{-29}\ \text{m}^3}{A_{\text{Surfactant}}} \tag{6}$$

$$r_{\text{rev.mic.}} = f \cdot w_1 \tag{7}$$

The factor f in Eq. (7) is mainly dependent on the surface area of the surfactant head group. Nevertheless, taking into account that the surface area of surfactants is in the range of less than 1 nm^2, Eq. (8) is a useful approximation for calculations of the droplet radii in microemulsions:

$$f = (1{,}5 \ldots 2{,}5) \cdot 10^{-10}\ \text{m} \tag{8}$$

Regarding the phase behaviour of ternary mixtures of water, oil and a nonionic surfactant, Fig. 3 shows schematically the so-called one-phase channel. This sec-

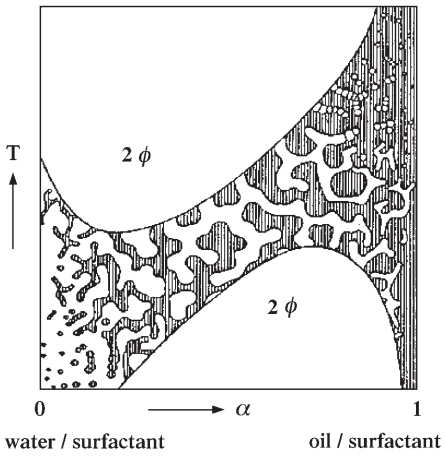

Fig. 3. Schematic one-phase channel

tion of the phase prism with the temperature as ordinate is obtained by keeping the amount of surfactant, γ, constant while varying the water to oil ration.

At a constant surfactant concentration, a region of isotropic single-phase solutions is observed extending from the water-rich region to the oil-rich side of the phase prism. The single phase region is surrounded by two two-phase regions in which the surfactant is dissolved either in the aqueous phase (low temperature) or in the organic phase (high temperature). The hatching in the single phase region in Fig. 3 illustrates the microstructures of the solutions.

Different surfactants are usually characterised by the solubility behaviour of their hydrophilic and hydrophobic molecule fraction in polar solvents, expressed by the HLB-value (hydrophilic-lipophilic-balance) of the surfactant. The HLB-value of a specific surfactant is often listed by the producer or can be easily calculated from listed increments [67]. If the water in a microemulsion contains electrolytes, the solubility of the surfactant in the water changes. It can be increased or decreased, depending on the kind of electrolyte [68, 69]. The effect of electrolytes is explained by the HSAB principle (hard-soft-acid-base). For example, salts of hard acids and hard bases reduce the solubility of the surfactant in water. The solubility is increased by salts of soft acids and hard bases or by salts of hard acids and soft bases. Correspondingly, the solubility of the surfactant in water is increased by sodium alkyl sulfonates and decreased by sodium chloride or sodium sulfate. In the meantime, the physical interactions of the surfactant molecules and other components in microemulsions is well understood and the HSAB-principle was verified. The salts in water mainly influence the curvature of the surfactant film in a microemulsion. The curvature of the surfactant film can be expressed, analogous to the HLB-value, by the packing parameter *Sp*. The packing parameter is the ratio between the hydrophilic and lipophilic surfactant molecule part [70]:

$$\mathrm{Sp} = \frac{V}{A_{\mathrm{Surfactant}} \cdot l_{\mathrm{c}}} \tag{9}$$

with the volume of the hydrophobic alkane chain V, its length l_c, and the surface requirement of the hydrophilic molecule part in the interface a_0. With *Sp*-values around one (corresponding to HLB = 8 – 10) the formation of bicontinuous microemulsions with little film curvature is preferred. Higher *Sp*-values (corresponding to HLB = 4 – 6) favour the formation of reverse micelles with negative film curvature. The more *Sp* differs from one, the higher is the solubility of the surfactant in one of the dispersed fluids, expressed in a high cmc (high solubility in water) or cμc (high solubility in oil). Regarding the enzyme catalysis in microemulsions, the influence of salts or macromolecules on the phase behaviour should not be neglected. The influence of additives on the *Sp*-value is described in Table 2 [71].

Microemulsions with different structures, like micelles, reverse micelles or bicontinuous networks, can be used for several inorganic, organic [72] or catalytic reactions which require a large contact area between oil and water. Besides enzyme catalysis, this can be the formation of nanoparticles [54, 73, 74], hydroformylation reactions [75] or polymerisations [76 – 78].

Table 2. Influence of different additives on the surfactant curvature (curvature viewed from the water)

Additives	Effect on the curvature	Reason
Salt	Negative with increasing salt concentration	Effective shielding of the hydrophilic surfactant part reduces a_0
Chain length of the oil	Positive with increasing chain length	Integration of the oil in the interfacial layer (solvation), decreasing with increasing chain length
Alcohol (co-surfactant)	Negative until $l_{alcohol} < l_c$, otherwise positive	influence of the hydrophilic (a_0) and hydrophobic (l_c) part of the co-surfactant on the resulting main curvature
Temperature (ionic surfactant)	Positive with increasing temperature	Surfactant–counter ion dissociation increases
Temperature (nonionic surfactant)	Negative with increasing temperature	Surfactant head area decreases with increasing dehydratisation

The different microstructures, shown in Fig. 3, are highly dynamic aggregates. They can be detected by well established scattering techniques, like X-ray, light or neutron scattering [13]. Beside scattering techniques, the transitions between the microstructures can be detected from the changes of the viscosity of w/o-microemulsion. For a diluted dispersion of spherical droplets without interactions, the relative viscosity η_{rel} is expected to obey the Einstein-relation:

$$\eta_{rel} = \frac{\eta}{\eta_0} = 1 + \frac{5}{2}\varphi \tag{10}$$

with η_0 being the viscosity of the solvent, Φ the volume fraction of droplets and η the viscosity of the dispersion. For droplet volume fractions up to 0.2, a maximum relative viscosity η_{rel} of 1.5 is expected. A higher η_{rel} indicates structural changes of the microemulsion [54]. The structural changes are of great importance for understanding the highly different enzyme activity depending on the composition of the microemulsion. In contrast to pure ionic surfactant systems or monodisperse C_iEO_j systems, which may regarded as well understood [68, 79], the phase behaviour of polydisperse surfactants of technical grade has not been examined systematically so far. Therefore, there is great interest in knowing the behaviour of microemulsions with such surfactant mixtures [80, 81].

3 Enzyme Catalysis in W/O-Microemulsions

This section will give an overview on the catalysis of several biocatalysts in microemulsions. Several general features of enzyme behaviour in microemulsions

will be described by using the observations with lipases and ADHs as examples. In order to develop suitable synthesis processes, the activity and stability of the biocatalysts in these media is of great interest. Therefore, the interactions between the enzymes and reverse micelles, which depend on the composition of the microemulsion, have to be investigated in very great detail.

3.1 General Aspects of Enzyme Activity in Microemulsions

Enzyme activity is highly dependent on the composition, and as a consequence on different microstructures of the microemulsion. Up to the present, no suitable theory exists to explain the correlation between the reaction media properties and their effects on enzymatic reactions in microemulsions. All experimental results on enzymatic reactions show that the activity is greatly affected by the structure of the microemulsion.

Low γ and w_1 values correspond to small spherical reversed micelles. In these structures the enzymes are forced into the interfacial film between the oil and the water. In contrast to lipases which are activated by interfaces, alcohol dehydrogenases show much lower activity under these circumstances. With increasing water concentration (increasing w_1) the reversed micelles grow. As a result, the influence of the interface on the enzyme decreases, enhancing the activity of an ADH, as shown in Fig. 4.

With even higher water concentrations in the microemulsion the activity of the ADH decreases again. In this composition range a increasing viscosity is also observed, which indicates the beginning of the phase separation into a surfactant-rich aqueous phase and a w/o-microemulsion. As a consequence, the

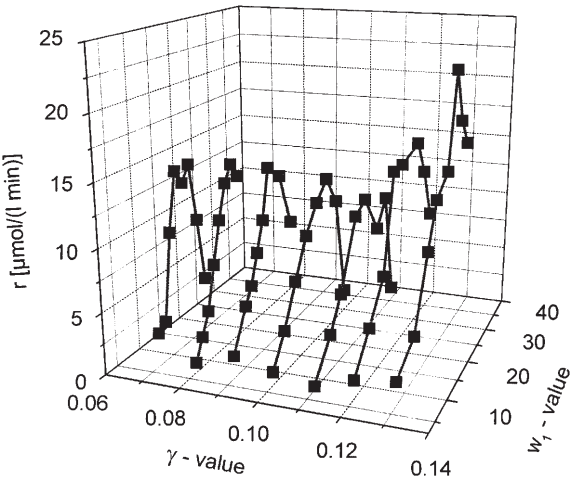

Fig. 4. Activity of an alcohol dehydrogenase (carbonyl reductase from *Candida parapsilosis* 0.13 mg/ml) reducing 2-butanone (0.67 mol/l) depending on the composition (γ/w_1) of the microemulsion (Marlipal O13–60/Water/Cyclohexane) at pH 7. The cofactor concentration is c_{NADH} = 115 µmol/l

substrate is unequally distributed between the w/o-microemulsion and the aqueous phase. Therefore, the beginning phase separation effects the enzyme activity, because the access of the hydrophobic substrates to the enzyme, which is dissolved mainly in the aqueous phase, is suppressed.

The determination of the enzyme activity as a function of the composition of the reaction medium is very important in order to find the optimal reaction conditions of an enzyme catalysed synthesis. In case of lipases, the hydrolysis of *p*-nitrophenyl esters in w/o-microemulsions is often used as a model reaction [19, 20]. The auto-hydrolysis of these esters in w/o-microemulsions is negligible. Because of the microstructure of the reaction media itself and the changing solvent properties of the water within the reverse micelles, the absorbance maximum of the *p*-nitrophenol varies in the microemulsion from that in bulk water, a fact that has to be considered [82]. Because of this, the water- and surfactant concentrations of the applied microemulsions have to be well adjusted.

3.2
Influence of Microemulsion Composition on Enzyme Activity

The kinetics of an enzyme catalysed reactions in a w/o-microemulsions is dependent on several parameters. For example, the substrates and enzymes distribute within the different parts of a one-phase microemulsion with different concentrations. The enzymes are located in the water and hydrophobic substrates are mainly dissolved in the oil. Additionally, the choice of oil and surfactant, the water concentration, and the structure of the interfacial layer can influence the activity and stability of biocatalysts. The influences of the main parameters on the kinetics will be discussed in this chapter.

The basic kinetic model for enzyme catalysed conversions in water and in w/o-microemulsions is based on the theory of Michaelis and Menten [83]. Although the Michaelis-Menten-model is often sufficient to describe the kinetics, the bi-bi-models (e. g. random bi-bi, ordered bi-bi or ping-pong bi-bi), which describe the sequences of substrate bindings to the enzyme are the more accurate kinetic models [84].

3.2.1
Influence of the Oil

The used oils in microemulsion systems are, with rare exception, non-polar and hydrophobic. The hydrophobicity of the oil has a strong influence on the resulting enzyme activity. This was first explained as being due to the interactions of the oil with the surfactants [85]. By now the studies of Laane and co-workers have shown that the solubility of the oil in the water pool has more influence on the enzyme activity independent of the choice of surfactant [4, 46]. They established the so called "log P"-concept to describe the correlation between the hydrophobicity of the oil and the resulting enzyme activity. P is the distribution coefficient of the oil in the mixture of water and 1-octanol. In general, very hydrophilic oils ($\log P < 2$) are not suitable for the enzyme catalysis in microemulsion because the activity and stability of the biocatalysts in these mixtures is

very low. In contrast, the usage of hydrophobic oils (log P > 4) or aliphatic alkanes (log P > 7) results in higher activities and stabilities because the enzymes are located in the water pool and do not contact the hydrophobic compartments within the microemulsion [86].

A major goal of enzyme catalysis in w/o-microemulsion is the replacement of the oil by pure hydrophobic substrates, in cases where the substrates are liquids. These reactions in so-called "super saturated" or "solvent free" solutions are becoming more and more established in enzyme catalysis, especially for poorly water soluble substrates. The enzyme activity and stability in pure substrate is highly dependent on the water concentration of these solutions. Pepin and Lortie investigated the initial reaction rates of the lipase catalysed enantioselective esterification in racemic Ibuprofen. Their results indicate a significant impact of the water concentration on the activity and enantioselectivity [87]. As substantial progress, Vulfson and co-workers could determine high conversions of several glycosidases catalysed reactions in supersaturated substrate solutions consisting of glucose, water and poly (ethylene glycol) [88, 89]. Meanwhile, the enzyme catalysis in pure substrates is used for several syntheses, such as lipase catalysed esterifications of sugars or lipase catalysed ring-opening polymerisations, on the kilogram scale [90].

A new approach in enzyme catalysis is the usage of supercritical carbon dioxide instead of hydrocarbons in microemulsion technology. Johnston et al. introduced this method in 1996 and proved that the water droplets in these microemulsions are able to host proteins at mild conditions (high pressures but low temperatures) [33]. The enzyme activity in supercritical carbon dioxide is highly dependent on the water concentration in the solution and often the resulting activities are quite low. Nevertheless, after removing the solvent the enzymes are still active, and sometimes more active than before they were tried in carbon dioxide [91, 92]. As an example, it was shown that the activity of a lipase catalysed acetylation could be increased in carbon dioxide compared to several other solvents due to the low viscosity and surface pressure resulting in a high diffusivity of the hydrophobic substrates [93].

3.2.2 *Influence of the Surfactant*

The influence of surfactant on the catalytic activity of lipases in water is well known. The addition of surfactants can enhance the activity and enantioselectivity of these enzymes in aqueous solutions [94] due to the interfacial activation and due to the emulsification of hydrophobic substrates.

The surfactant mass fraction in a microemulsion defines the size of the interfacial area between the water and oil. The reaction rate of organic reactions in microemulsions can be dramatically enhanced by increasing the specific interfacial area [95]. Enzyme catalysis in microemulsions is usually not influenced by the size of the interfacial area because only a small fraction of the reverse micelles are hosting a bio-molecule. Most investigations published so far were made with low enzyme concentrations resulting in a low population of enzymes per reverse micelle.

The choice of surfactant, which is mostly constrained by the choice of the oil and the resulting phase behaviour of the microemulsion, can have different effects on the enzyme stability and activity. In general we have to differentiate between ionic and nonionic surfactant types:

- The nonionic surfactants are often ethoxylated fatty alcohols. The characteristics of the interfacial film (between the water core and the oil) are mainly controlled by the length of the ethoxy chain. Especially with very long ethoxy chains (EO $\gg$ 10) the lipase-catalysed triglyceride hydrolysis can be inhibited because the enzymes cannot contact the substrates through the thick interfacial film. The ethoxy chains stretching out from the interface into the water core of the reverse micelles can prevent the enzyme from entering the interfacial region [45, 81]. In such cases, the choice of a less ethoxylated fatty alcohol or an ionic surfactant is useful. The usage of ethoxylated nonylphenols in surfactant technology is becoming less important against the background of the pseudo hormonal behaviour of the nonylphenols [96]. Nevertheless, the surfactant choice has to match the oil in order to obtain a microemulsion.
- In contrast to nonionic surfactants, ionic surfactants build up a high zeta-potential at the water-oil interface which can also can influence the enzyme activity. Most investigated systems used AOT as the surfactant because its phase behaviour is well understood. However, AOT is often not very suitable, because it can totally inhibit enzymes (e.g. the formate dehydrogenase from *Candida bodinii*). The usage of lipases in AOT-based microemulsions is generally unfavourable as AOT is an ester that is hydrolysed itself.

3.2.3
Influence of the Water Concentration

Many investigations have been undertaken regarding the effect of the water concentration in the microemulsion on the catalytic behaviour of enzymes. The surfactant concentration of the microemulsion defines the size of the internal interface but it often has no measurable influence on the enzyme kinetics. On the other hand, the physical properties of the water located inside the reverse micelles differ from those of bulk water, and the difference becomes progressively smaller as the water concentration, expressed in the w_1-value, increases.

The hyperactivity of, for example, lipases at low w_1-values (shown in Fig. 5) is explained by the water-shell-model [2]. The activity of the enzyme at w_1-values higher than 5 corresponds to its activity in bulk aqueous solutions. There exist two aqueous regions within a reverse micelle, schematically shown in Fig. 6. One is located in the inner part of the reverse micelle and has the same physical properties as bulk water; the other is attached to the polar head groups of the surfactant and differs in its physical properties strongly from bulk water.

These differences are, e.g. a lowered melting point and a lowered dielectric constant [97]. If lipases are forced into this structured layer of water at the interface between water and oil by reducing the size of the reverse micelles ($w_1 < 5$), a lipase catalysed hydrolysis can be accelerated. On the other hand, the activity of oxidoreductases and their stabilities can decrease dramatically inside such small reverse micelles.

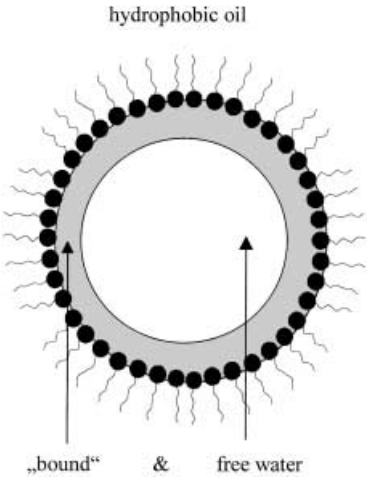

Fig. 5. Water-shell-model: schematically drafted location of two water parts in a reverse micelle. One is located in the inner part of the reverse micelle and has the same physical properties as bulk water, the other is attached to the polar headgroups of the surfactant

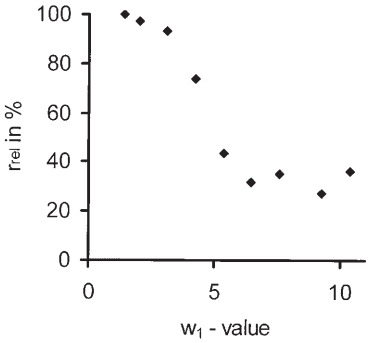

Fig. 6. Relative CRL-activity using different water concentrations

The water-shell-model, strictly speaking, will only apply to very hydrophilic enzymes which do not contain hydrophobic parts. Many enzymes, like lipases, are surface active and interact with the internal interface of a microemulsion. In fact, lipases need a hydrophobic surface in order to give the substrate access to the active site of the enzyme. Nevertheless, Zaks and Klibanov found out that it is often not necessary to have a monolayer of water on the enzyme surface in order to perform a catalytic reaction in an organic solvent [98].

The size of reverse micelles can change when they are filled with an enzyme. This effect again is highly dependent on the water content of the system. It can be predicted that the sizes do not differ significantly if the cavity of the empty reverse micelles is equal or exceed the size of the protein. Very little is known about the exact localisation of proteins inside reverse micelles. For example, the

protein may be hosted in the interfacial layer, in the inner cavity of the water or outside a reverse micelle (completely in the oil or in between two reverse micelles [99]).

3.3
Stability of Enzymes in Microemulsions

The deactivation process of enzymes can be classified generally into first-order and non-first-order processes. The first-order model is often sufficient for describing the deactivation, especially in case of highly stable enzymes in microemulsions, like lipases. For a lot of enzymes the activity decay in microemulsions has to be fitted to the deactivation model which involves an active intermediate in order to describe the deactivation processes qualitatively [34, 100–102]:

$$E \overset{k_1}{\rightarrow} E^* \overset{k_2}{\rightarrow} D \tag{11}$$

In the case of this two-state model the activity of the enzyme, related to the initial activity, can be described with an exponential equation:

$$\frac{r(t)}{r(t=0)} = A_1 e^{k_1 \cdot t} + A_2 e^{k_2 \cdot t} \tag{12}$$

with the preexponential factors $A_1 + A_2 = 1$, the measured activities r(t) and the initial activity r(t = 0). The one-state model, which involves no active intermediate of the enzyme, does not explain two characteristic properties of measured deactivation curves: a steep decay in the beginning and a long tailing where the one-state model already predicts a decrease of the activity below the limit of detection as shown in Fig. 7.

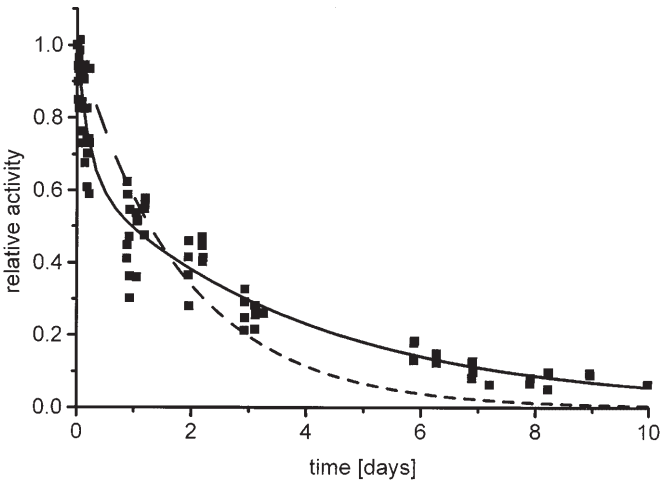

Fig. 7. Deactivation of CPCR in microemulsion Marlipal O13–60/Water/Cyclohexane at γ = 0.1 and w_0 = 5 following the two-step-model (*solid line*). The one-step-model (*dotted line*) does not fit the experimental results appropriately

Nevertheless, the one-state model can be handled as a special case with either $A_2 = 0$ or $k_1 = k_2$. While, e. g. lipases show good stabilities in several organic reaction media [14], alcohol dehydrogenases are less stable, having half-lifetimes in microemulsions of only a few hours [34, 103, 104] or even only minutes [105]. The stability depends on the microemulsion composition and additionally on the components of the reaction mixture, like salts, buffers or impurities of the surfactant.

4 Immobilisation Methods

Major problems that need to be solved before application of microemulsion systems in industrial processes are the isolation of the products from the reaction mixture and the recovery of the enzyme. Therefore, suitable immobilisation methods and product separation strategies have to be developed.

4.1 Phase Separation

A common technique for separating the water and the oil in a microemulsion is a temperature-induced phase separation, yielding an excess water phase (increasing the temperature) or an excess oil phase (decreasing the temperature). It is the simplest way to separate the oil and the water. Nevertheless this method is quite time consuming and often not complete. In case of enzymatic reaction, a change in temperature can lead to a loss of enzyme stability.

Larsson et al. [106] exploited the temperature sensitivity of the phase behaviour of the microemulsion in order to split it into an oil-rich phase and a water-rich phase. The enzyme reuse and product recovery were investigated using horse liver alcohol dehydrogenase (HLADH) catalysing a coupled substrate-coenzyme regenerating cycle. A small change in temperature induced a shift into a two-phase system: an oil-rich phase containing the products and a water-rich phase containing the surfactant and the enzyme. The oil-rich phase could be replaced by a new solution of substrate and oil, and then the temperature was changed back to the temperature where the one-phase microemulsion was stable. In this way, the reaction and the separation procedure were repeated up to ten times.

4.2 Microemulsion-Based Gels

The addition of small amounts of water to soybean-lecithin reverse micelles can causes a dramatic increase in viscosity and the formation of a rigid, optically transparent gel matrix [107]. Viscosity and light scattering experiments suggest that the gelation process is caused by the self aggregation of lecithin molecules into polymer-like cylindrical reverse micelles. This gel may be used for the immobilisation of enzymes located inside the water droplets. Another interesting immobilisation method is the gelation of the microemulsions using gelatine as

a gelling component resulting in so-called microemulsion-based gels (MBG) [108–113]. The MBG is usually prepared by mixing a one-phase microemulsion containing the enzymes with a hot aqueous gelatine solution. Due to the decrease of the temperature, the transparent mixtures forms a gel. In this way, the enzymes which are located in the reverse micelles are surrounded by gelatine and may be used for catalysis in organic reaction media. MBG structures have been described on the basis of several models but until now the exact internal structure of MBGs has not been proved. These models predict a robust three-dimensional network of the hydrophilic gelatine in the oil which stabilises the reverse micelles [101] or bicontinuous water and oil structures [97, 98].

Analogous to the MBG-method, Boy and Voss introduced the enzyme catalysis in liquid crystalline surfactant phases [114, 115]. The enzymes, e.g. alcoholdehydrogenase, were entrapped in a liquid crystalline surfactant rich phase, and this phase was rinsed with an organic phase containing the substrate. In this way, they can perform the reaction continuously using a packed reactor module without apparent loss of activity.

4.3
Centrifuge Reactor

A completely different approach in order to immobilise enzymes in reverse micelles and to develop a continuous process, is the centrifugation of microemulsions proposed by Russel and Komives [116]. They used a pesticide containing organic phase which was bubbled slowly through a heavier w/o-microemulsion phase containing detoxifying enzymes: the biocatalysts were immobilised together with the microemulsion droplets by centrifugal force in a continuous flow reactor included in a centrifuge, and the wash out of enzyme by the light phase could be neglected. In contrast to membrane-based immobilisation methods, this alternative encompasses the advantage of a stable and low cost continuous process because no fouling occurs and the continuous phase does not have to be further processed.

4.4
Filtration Systems

The ultrafiltration of the microemulsion is a very useful operation for separating water and oil in these mixtures [117–120]. Because of the limited availability of solvent stable membranes, most of the work published so far was performed using ceramic membranes, which show a high adsorption of surfactant at the membrane surface and comparably low rejection rates of reverse micelles. Using electro ultrafiltration, where the concentration polarisation phenomenon of the reverse micelles (using the ionic surfactant AOT) at the membrane surface is depressed by asymmetric high voltage electrical fields, the rejection rates can be increased, but not to economical values [121, 122].

The change of flux velocity with transmembrane pressure can be explained by the concentration polarisation phenomenon. The physical processes at the membrane surface during the filtration procedure may be described by theo-

retical models which were developed for the ultrafiltration of macromolecules, like the gel layer model, the model of osmotic pressure or the friction force model [65, 66, 123]. A characteristic unfavourable feature of continuous filtration processes, the fouling of the membrane surface with biomolecules, is often not observed with microemulsions. Because of the surfactant adsorption no adsorption of enzymes to the membrane surface occurs. Unfortunately the adsorption of the surfactant at the membrane surface and in the pores often leads to a closure of the pores and a reduction of the permeate fluxes. New pervaporation techniques in membrane technology could overcome this restriction [124].

In both media water and w/o-microemulsions the enzymes denaturate with time. The complete immobilisation of the enzyme system in a continuous process leads to a limitation caused by the denaturation of the enzymes only. In order to obtain a complete immobilisation of the enzyme the transmembrane pressure of the ultrafiltration unit should often not exceed 1 bar [120].

5 Synthesis Reactions

The majority of the published investigations are concentrated onto the reaction conditions of enzymes in reverse micelles at low substrate concentrations, because high substrate concentrations in microemulsions influence their phase behaviour. Additionally, high substrate and enzyme concentrations often lower the enzyme stability to uneconomical values. At high enzyme concentrations the activity can be lowered due to the formation of protein aggregates.

A lot of enzymes, like oxidoreductases, require a cofactor like NADH. Only little is published about NAD^+/NADH regenerating systems in microemulsions: Beside the established strategy that uses an alcohol which is oxidised during the reduction of a target ketone experiments with whole cells [125], formate dehydrogenase [104] or multi enzyme systems [126] in microemulsions were the subjects of publications. Cofactors requiring enzymatic reactions are often uneconomical because of the high cofactor costs. These costs may be drastically reduced if a high total turn-over number (ttn) for the cofactor can be achieved. The ttn is defined as the molar amount of synthesised product in relation to the molar amount of the applied cofactor:

$$ttn = \frac{c_{\text{product}}}{c_{\text{cofactor}}} \tag{13}$$

The usage of formate dehydrogenase for the regeneration of NADH can lead to ttn of more than 2000 [104] which is a great improvement because values higher than 100 can, depending on the reaction product, be economical. Yang and Russel have shown that the regeneration of NADH by the oxidation of an alcohol using yeast alcohol dehydrogenase can be very effective when it is coupled to a ketone reduction [22].

Comparing the published synthesis reactions in reverse micelles, lipases seem to be the most stable enzymes in the microemulsion as reaction media and

suitable for a lot of synthesis. Beside the hydrolysis of triglycerides to free fatty acids and glycerol, lipases also catalyse transformations with hydrophobic synthetic substrates. Hayes and Gulari published the synthesis of glycerides in reverse micelles (AOT/isooctane) catalysed by *Rhizopus delemar* lipase at conversions of about 60 %, with results showing that the rate of conversion is highly dependent on temperature, substrate, product and water concentration of the microemulsion [129].

On the basis of the lipases numerous applications, also on an industrial scale, have been shown using an enzyme from this family. Table 3 summarises some applications of a popular lipase, often used in reverse micellar media, the *Candida rugosa* lipase.

In particular, substrates like terpene alcohols are often used with *Candida rugosa* with very high enantiomeric excesses and at high yields. Lee et al. could increase significantly the maximum reaction velocity of this lipase in AOT-based reverse micelles and obtained conversions up to 70 % during the esterification of diterpenes alcohols (geraniol, menthol, citronellol) [130].

Table 3. *Candida rugosa* Lipase in unusual reaction media

Reaction medium	Investigation	Ref.
Supercritical CO_2	Racemic resolution of menthol	[86, 87]
Vinyl acetate	Stereoselective synthesis of an insecticide-esters	[127]
Hexane	Enantioselective esterification of Menthol with several anhydrides	[128]
AOT/ isooctane	Esterification of different triglicerides Trigliceriden	[129]
AOT/ isooctane	Esterification of several terpenes alcohols	[130]
Isopropylether	Influence of temperature on the enantioselectivity during the esterification of Ibuprofen	[131]
Supercritical CO_2 and 15 different solvents	Esterification of racemic 1-phenylcyclohexanol	[93]
Isooctane (glucose based surfactant; synthesis of surfactant coated lipase)	Enantioselective esterification of 2-Octanol and Phenylethanol with Lauric acid	[59] [59]
Isooctane	Racemic resolution of several Naproxen analogues combined with the re-racemisation of the second enantiomer	[132, 133]
Butanol (supersaturated substrate solution)	Enhanced enantioselectivity due to the addition of alkali metals	[134]
Toluene, hexane, diisopropylether, trichloroethane	Evaluation of the ping-pong kinetics	[135]
Two phase system (substrate)	Comparison: transesterification, hydrolysis, esterification (synthesis of enantiomeric pure 2-Butanol)	[136]

6 Outlook

Microemulsions are a promising tool in enzyme technology for biotransformations with hydrophobic substrates, although there is still the disadvantage that enzyme samples with very high concentrations are needed. Such samples are not available for all enzymes. As a consequence, the productivity of enzyme catalysed synthesis in microemulsions is often quite low compared to enzyme catalysed reactions in aqueous reaction media. The major advantage of the application of microemulsions is the increased stability of the enzymes in comparison to other non-polar solvent. The search for methods that make hydrophobic substrates accessible to enzyme catalysis will yield in an interesting competition between different approaches over the next few years. One new approach in enzyme technology is the synthesis of cross-linked enzyme crystals, CLEC [137–139]. Cross-linked enzyme crystals of 1–100 mm diameter are of pure enzymes that are cross-linked with bifunctional reagents, like glutar dialdehyde. The CLEC are also very stable in organic solvents and have a high activity in these media. Additionally they are more stable at higher temperatures [140]. If they could be applied in reverse micelles or as surfactant coated biocatalysts the problem of low productivities in enzyme catalysis in organic solvents would decrease.

An auspicious new strategy, in order to perform biocatalysis with hydrophobic substrates in w/o-microemulsion, is the usage of whole cells instead of purified enzymes [3, 124, 141]. There exist only a few surfactant-oil systems, in which whole cells are stable and suitable for a segmentation. Mainly the biodegradable surfactant based on sorbitan (Tween and Span) seems to be well suited for the solubilisation of whole cells in organic reaction media [142, 143].

References

1. Wong CH (1989) Science 244:1145
2. Klibanov AM (1986) Chemtech 16:354
3. Cabral JMS, Aires-Barros MR, Pinheiro H, Prazeres DMF (1997) J Biotechnol 59:133
4. Laane C, Boeren S, Vos K, Veeger C (1987) Biotechnol Bioeng 30:81
5. Rodakiewicz-Nowak J, Kasture SM, Dudek B, Haber J (2000) J Mol Cat B Enzymatic 11:1
6. Buchholz K, Kasche V (1997) Biokatalysatoren und Enzymtechnologie. VCH Verlagsgesellschaft mbH, Weinheim
7. Liese A, Karutz M, Kamphuis J, Wandrey C, Kragl U (1996) Biotechnol Bioeng 51:544
8. Liese A, Zelinski T, Kula MR, Kierkels H, Karutz M, Kragl U, Wandrey C (1998) J Mol Cat B Enzymatic 4:91
9. Kruse W, Hummel W, Kragl U (1996) Recl Trav Chim Pays-Bas 115:239
10. Giorno L, Drioli E (1997) J Chem Tech Biotechnol 69:11
11. Giorno L, Molinari R, Drioli E, Bianchi D, Cesti P (1995) J Chem Tech Biotechnol 64:345
12. Giorno L, Molinari R, Natoli M, Drioli E (1997) J Memb Sci 125:177
13. Sjöblom J, Lindberg R, Friberg SE (1996) Adv Colloid Interface Sci 95:125
14. Stamatis H, Xenakis A, Kolisis FN (1999) Biotechnol Adv 17:293
15. Perez-Gilabert M, Bru R, Sanchez-Ferrer A, Garcia-Carmona F (1998) J Biotechnol 60:137
16. Rodakiewiecz-Nowak J, Maslakiewicz P, Haber J (1996) Eur J Biochem 238:549

17. Gonzales-Navarro H, Braco L (1998) Biotechnol Bioeng 59:122
18. Dorovska-Taran VN, Veeger C, Visser JWG (1993) Eur J Biochem 211:47
19. Manoj KM, Swaminathan T (1997) Bioproc Eng 17:185
20. Schomäcker R, Robinson BH, Fletcher PDI (1988) J Chem Soc Faraday Trans I 84(12): 4203
21. Yang F, Russel AL (1995) Biotechnol Bioeng 47:60
22. Yang F, Russel AL (1994) Biotechnol Bioeng 43:232
23. Papadimitriou V, Xenakis A, Cazianis CT, Kolisis FN (1997) Colloid Polym Sci 275:609
24. Knezevic ZD, Siler-Marinkovic SS, Mojovic LV (1998) Appl Microbiol Biotechnol 49:267
25. Das N, Prabhakar P, Kayastha AM (1997) Biotechnol Bioeng 54:329
26. Lee SS, Kiserow DJ, McGown LB (1997) J Coll Interface Sci 193:32
27. Freeman KS, Lee SS, Kiserow DJ, McGrown LB (1998) J Coll Interface Sci 207:344
28. Oh SG, Holmberg K, Ninham BW (1996) J Coll Interface Sci 181:341
29. Fletcher PDI, Freedman RB, Robinson BH, Rees GD, Schomäcker R (1987) Biochim Biophys Acta 912:278
30. Malakhova EA, Kurganov BI, Levashov AV, Berezin IV, Martinek K (1983) Dokl Akad Nauk SSSR (Eng) 270:182
31. Ruckenstein E, Karpe P (1990) Biotechnol Let 12:241
32. Macris JB, Stamatis H, Kolisis FN (1996) Appl Microbiol Biotechnol 46:521
33. Johnston KP, Harrison KL, Clarke MJ, Howdle SM, Heitz MP, Bright FV, Carlier C, Randolph TW (1996) Science 271:624
34. Chen DW, Chen HH, Huang TC (1995) J Chem Eng Jap 28:551
35. Levashov AV, Khmelnitsky YL, Klyachko NL, Chernyak VY, Martinek K (1982) J Coll Interface Sci 88:444
36. Iskandar L, Ono T, Kamiya N, Goto M, Nakashio F, Furusaki S (1998) Biochem Eng J 2:29
37. Rodriguez R, Vargas S, Fernandez-Velasko DA (1998) J Coll Interface Sci 197:21
38. Fernandez-Velasko DA, Rodriguez R, Vargas S, de Gomez-Puyou MT, Gomez-Puyou A (1998) J Coll Interface Sci 197:29
39. Almeida FCL, Valente AP, Chaimovich H (1998) Biotechnol Bioeng 59:360
40. Ayala GA, Kamat S, Beckman EJ, Russel AJ (1991) Biotechnol Bioeng 39:806
41. Luisi PL (1985) Angew Chem Int Ed 24:439
42. Luisi PL, Giomini M, Pileni MP, Robinson BH (1988) Biochim Biophys Acta 947:209
43. Martinek K, Levashov AV, Klyachko N, Khmelnitski YL, Berezin IV (1986) Eur J Biochem 155:453
44. Holmberg K (1997) Microemulsions in biotechnology. In: Solans C, Kunieda H (eds) Industrial applications of microemulsions. Marcel Dekker, NY, p 69
45. Holmberg K (1994) Adv J Coll Int Sci 51:137
46. Laane C, Tramper J, Lilly MD (1987) Biocatalysis in organic media. Proceedings of an International Symposium held at Wageningen, The Netherlands, 7–12. December 1986. Elsevier, Amsterdam
47. Oldfield C (1994) Biotech Genetic Eng Rev 12:255
48. Tamura K, Schelly ZA (1979) J Am Chem Soc 101:7643
49. Tamura K, Schelly ZA (1981) J Am Chem Soc 103:1013
50. Ke T, Klibanov AM (1998) Biotechnol Bioeng 57:746
51. Dai L, Klibanov AM (1999) Proc Natl Acad Sci USA 96:9475
52. Zaks A, Klibanov AM (1988) J Biol Chem 263:8017
53. Chetanay D, Urbach W, Cazabat AM, Vacher M, Waks M (1985) Biophys J 48:893
54. Hagen AJ, Hatton TA, Wang DIC (1990) Biotechnol Bioeng 35:955
55. Hayes DG (1997) Biotechnol Bioeng 53:583
56. Hashimoto Y, Ono T, Goto M, Hatton TA (1998) Biotechnol Bioeng 57:620
57. Adachi M, Shibata K, Shioi A, Harada M, Katoh S (1998) Biotechnol Bioeng 58:649
58. Adachi M, Yamazaki M, Harada M, Shioi A, Katch S (1997) Biotechnol Bioeng 53:406
59. Kamiya N, Kasagi H, Inoue M, Kusunoki K, Goto M (1999) Biotechnol Bioeng 65:227
60. Kamiya N, Goto M (1997) Biotechnol Prog 13:448
61. Schwuger MJ, Stickdorn K, Schomäcker R (1995) Chem Rev 95:894

62. Moulik SP, Paul BK (1998) Adv Colloid Interf Sci 78:99
63. Fletcher PDI, Howe AM, Robinson BH (1987) J Chem Soc Faraday Trans 1 83:985
64. Lade M, Mays H, Schmidt J, Willumeit R, Schomäcker R (2000) Coll Surf A Physicochem Eng Aspects 163:3
65. Schomäcker R, Braun G (1996) Langmuir 12:2362
66. Schomäcker R, Orlich B, Braun G (1997) Ber Bunsenges Phys Chem 101:1695
67. Pfüller U (1986) Mizellen-Vesikel-Mikroemulsionen. Springer, Berlin Heidelberg New York
68. Kahlweit M, Strey R (1985) Angew Chem 97:655
69. Kahlweit M (1995) J Phys Chem 99:1281
70. Mitchell J, Ninham BW (1981) J Chem Soc Faraday Transactions 77:601
71. Fletcher PDI, Parrot D (1989) Protein-partitioning between water-in-oil microemulsions and conjugate aqueous phases. In: Pileni MP (ed) Structure and reactivity in reverse micelles. Elsevier, Amsterdam, p 303
72. Tjandra D, Lade M, Wagner O, Schomäcker R (1998) Chem Eng Technol 21:666
73. Fendler JH (1987) Chem Rev 87:877
74. Schmidt J, Guesdon C, Schomäcker R (1999) J Nanopart Res 1:267
75. Van Vyve F, Renken A (1999) Catalysis Today 48:237
76. Morgan JD, Kaler EW (1998) Macromolecules 31:3197
77. Co CC, Kaler EW (1998) Macromolecules 31:3203
78. Chew CH, Li TD, Gan LH, Quek CH, Gan LM (1998) Langmuir 14:6068
79. Schubert KV, Kaler EW (1996) Ber Bunsenges Phys Chem 100:190
80. Ryan LD, Kaler EW (1999) Langmuir 15:92
81. Ryan LD, Kaler EW (1998) J Phys Chem B 102:7549
82. Orlich B, Schomäcker R (2001) Enz Microbial Technol 28:164
83. Michaelis L, Menten ML (1913) Biochem Zeitschrift 49:333
84. Biselli M, Kragl U, Wandrey C (1995) Reaction engineering for enzyme-catalyzed biotransformations. In: Drauz K, Waldmann H (eds) Enzyme catalysis in organic synthesis. VCH-Weinheim
85. Han D, Rhee JS (1986) Biotechnol Bioeng 28:1250
86. Huang SY, Chang HL, Goto M (1998) Enz Microbial Technol 22:552
87. Pepin P, Lortie R (1999) Biotechnol Bioeng 63:502
88. Millqvist-Fureby A, Gill IS, Vulfson EN (1998) Biotechnol Bioeng 60:190
89. Millqvist-Fureby A, MacManus DA, Davies S, Vulfson EN (1998) Biotechnol Bioeng 60:197
90. Metzger JO (1998) Angew Chem 110:3145
91. Michor H, Marr R, Gamse T, Schilling T, Klingsbichel E, Schwab H (1996) Biotechnol Letters 18:79
92. Michor H, Gamse T, Marr R (1997) Chem Ing Tech 69:690
93. Celia EC, Cernia E, D'Acquarica I, Palocci C, Soro S (1999) J Mol Cat B Enzymatic 6:495
94. Liu YY, Xu J, Hu Y (2000) J Mol Cat B Enzymatic 10:523
95. Bode G, Lade M, Schomäcker R (1999) Chem Ing Tech 71:877
96. Bolt HM, Degen GH (2000) Chem Unserer Zeit 34:30
97. Schomäcker R (1991) J Phys Chem 95:451
98. Zaks A, Klibanov AM (1988) J Biol Chem 263:3194
99. Ramakrishnan VR, Darszon A, Montall M (1983) J Biol Chem 258:4857
100. Larsson KM, Adlercreutz P, Mattiasson B (1987) Study of horse liver alcoholdehydrogenase (HLADH) in AOT-cyclohexane reverse micelles. In: Laane C, Tramper J, Lilly MD (eds.) Biocatalysis in organic media. Elsevier, Amsterdam, p 355
101. Skrika-Alexopoulos E, Muir J, Freedman RB (1993) Biotechnol Bioeng 41:894
102. Carvalho CML, Cabral JMS, Aires-Barros MR (1999) Enz Microb Technol 24:569
103. Lee KM, Biellmann JF (1987) FEBS Letter 223:33
104. Orlich B, Schomäcker R (1999) Biotechnol Bioeng 65:357
105. Samara JP, Lee KM, Biellmann JF (1987) Eur J Biochem 163:609
106. Larsson KM, Adlercreutz P, Mattiasson B, Olsson U (1990) Biotechnol Bioeng 36:135

107. Scartazzini R, Luisi PL (1988) J Phys Chem 92:829
108. Backlund S, Eriksson F, Kanerva LT, Rantala M (1995) Coll Surf B Biointerfaces 4:121
109. Backlund S, Eriksson F, Hedström G, Laine A, Rantala M (1996) Colloid Polym Sci 274:540
110. De Jesus PC, Rezende MC, Nascimento MG (1995) Tetrahedron Asymmetry 6:63
111. Fadnavis NW, Koteshwar K (1999) Biotechnol Prog 15:98
112. Jenta TRJ, Batts G, Rees GD, Robinson BH (1997) Biotechnol Bioeng 54:416
113. Nagayama K, Karaiwa K, Doi T, Imai M (1998) Biochem Eng J 2:121
114. Boy M, Voss H (1998) J Mol Cat B Enzymatic 5:355
115. Boy M, Voss H (1996) Chem Ing Tech 68:831
116. Russel AJ, Komives C (1994) Chemtech 1:26
117. Nakamura K, Hakado M (1995) J Chem Eng Japan 28:14
118. Luethi P, Luisi PL (1984) J Am Chem Soc 106:7285
119. Prazeres DMF, Garcia FAP, Cabral JMS (1994) Bioprocess Eng 10:21
120. Orlich B, Schomäcker R (1999) Chem Eng Technol 22:753
121. Hakoda M, Enomoto A, Hoshino T, Shiragami N (1996) J Ferm Bioeng 82:361
122. Hakoda M, Nakamura K, Enomoto A, Hoshino T (1996) J Chem Eng Japan 29:300
123. Jönsson AS, Jönsson B (1996) J Coll Interf Sci 180:504
124. Aouak T, Moulay S, Hadj-Ziane A (2000) J Membr Sci 173:149
125. Andersson M, Holmberg H, Adlercreutz P (1998) Biotechnol Bioeng 57:79
126. Hilhorst R, Laane C, Veeger C (1983) FEBS Letters 159:225
127. Costa VEU, Alifantes J, Martins JED (1998) Tetrahedron Asym 9:2579
128. Wu WH, Akoh CC, Phillips RS (1996) Enz Microbial Technol 18:536
129. Hayes DG, Gulari E (1990) Biotechnol Bioeng 35:793
130. Lee KKB, Poppenburg LH, Stuckey DC (1998) Enz Microbial Technol 23:253
131. Yasufuku Y, Ueji AI (1997) Bioorg Chem 25:88
132. Chang CS, Tsai SW, Kuo J (1999) Biotechnol Bioeng 64:120
133. Chang CS, Tsai SW (1999) Biochem Eng J 3:239
134. Okamoto T, Ueji S (1999) Chem Commun 9:939
135. Janssen AEM, Sjursnes BJ, Vakurov AV, Hallig PJ (1999) Enz Microbial Technol 24:463
136. Cambou B, Klibanov AM (1984) Biotechnol Bioeng 26:1449
137. Zelinski T, Waldmann H (1997) Angew Chem 109:746
138. Kalaf N, Govardhan PC, Lalonde JJ, Persichetti RA, Wang YF, Margolin AL (1996) J Am Chem Soc 118:5494
139. Persichetti RA, Lalonde JJ, Govardhan CP, Khalaf NK, Margolin AL (1996) Tetrahedron Lett 37:6507
140. Clair NS, Wang YF, Margolin AL (2000) Angew Chem 112:388
141. Famiglietti M, Hochköppler A, Wehrli E, Luisi PL (1992) Biotechnol Bioeng 40:173
142. Komives CF, Lilley E, Russel AJ (1994) Biotechnol Bioeng 43:946
143. Komives CF, Osborne DE, Russel AJ (1994) J Phys Chem 98:369

Received: April 2001

Perspectives in Liquid Membrane Extraction of Cephalosporin Antibiotics

G. C. Sahoo, N. N. Dutta

Chemical Engineering Division, Regional Research Laboratory, Jorhat, 785 006, India,
e-mail: chemengg@hq.csir.res.in; Fax: 0376 370011

In this paper an overview of the developments in liquid membrane extraction of cephalosporin antibiotics has been presented. The principle of reactive extraction via the so-called liquid-liquid ion exchange extraction mechanism can be exploited to develop liquid membrane processes for extraction of cephalosporin antibiotics. The mathematical models that have been used to simulate experimental data have been discussed. Emulsion liquid membrane and supported liquid membrane could provide high extraction flux for cephalosporins, but stability problems need to be fully resolved for process application. Non-dispersive extraction in hollow fiber membrane is likely to offer an attractive alternative in this respect. The applicability of the liquid membrane process has been discussed from process engineering and design considerations.

Keywords. Cephalosporin antibiotics, Liquid membrane, Reactive extraction, Liquid-liquid ion extraction, Aliquat-336, Hollow-fiber membrane

1 Introduction 211

2 Theoretical Aspects 212

2.1 Bulk Liquid Membrane 214
2.2 Emulsion Liquid Membrane 215
2.3 Supported Liquid Membrane 215
2.4 Dispersion Free Extraction in Hollow Fiber Membrane 216

3 Current Literature 217

3.1 Bulk Liquid Membrane 218
3.2 Emulsion Liquid Membrane 219
3.3 Supported Liquid Membrane 220
3.4 Dispersion Free Extraction 221

4 Mathematical Modeling 222

4.1 Bulk Liquid Membrane 222
4.2 Emulsion Liquid Membrane 223
4.3 Supported Liquid Membrane 230
4.4 Dispersion Free Extraction in Hollow Fiber Membrane 233

5 Process Consideration 235

5.1 Chemical Driving Force 235
5.2 Stability Problems 236

Advances in Biochemical Engineering/
Biotechnology, Vol. 75
Managing Editor: Th. Scheper
© Springer-Verlag Berlin Heidelberg 2002

5.3 Membrane Recoverability and Reuse 237
5.4 Process Economics 238

6 Research Needs of Pragmatic Importance 239

7 Conclusion 240

References 240

List of Abbreviations and Symbols

μ	viscosity of emulsion [cp]
A	amine carriers
B^-	dissociated buffer anion in stripping solution
C	concentration [mol/m^3]
C*	interfacial concentration [mol/m^3]
C^d	dimensionless concentration
d	diameter of emulsion globule [cm]
D	diffusivity [cm/s^2]
δ	thickness of mass transfer boundary layer [cm]
D_{eff}	effective diffusivity [cm/s^2]
δ_f, δ_r	thickness of mass transfer boundary layer in feed and receiving phases of a SLM [cm]
d_{if}	diameter of a hollow fiber at the location of the immobilized phase interface [cm]
ε	porosity of microporous membrane
H	height of hollow fiber module [cm]
k_{-1}	backward reaction rate constant [m^4/mol/s]
k_1	forward reaction rate constant [m^4/mol/s]
k_a	boundary layer mass transfer coefficient for aqueous phase [cm/s]
K_a	dissociation constant of buffer acid
K_{a2}	upper dissociation constant of solute
K_d	distribution of constant buffer ion between organic and aqueous phases
K_{eq}, K_A	equilibrium constant of the reaction given by Eqs. (4) and (27) respectively
k_f, k_m, k_r	mass transfer coefficients in feed, receiving, membrane and the interfaces of BLM
k_{II}, k_{III}	internal and external phase mass transfer coefficient in ELM [cm/s]
K_L	overall mass transfer coefficient [cm/s]
k_{mf}, k_{mr}	and SLM [cm/s]
k_{or}	mass transfer coefficient for organic phase [cm/s]
L	thickness of SLM [cm]
m	distribution coefficient
M_2	molecular weight of solvent
N	number of hollow fibers in a MHF module
N_m	number of emulsion globules
n_s	stirring speed, rev/s

P^-	cephalosporin anion
Q	flow rate in HF membrane [m^3/s]
QCl	Aliquat-336 carrier
QP	solute-carrier complex
ϱ	density of emulsion [g/cm^3]
r	radial coordinate [cm]
R	radius of emulsion globule [cm]
S	surface or interfacial area [m^2]
T	temperature, K
t	time [s]
τ	tortuosity of microporous membrane
V	volume [m^3]
Z	length of MHF module [m]

Superscript

0	initial value
d	dimensionless

Subscripts

0	position at $\delta_f = 0$ or at h = 0
a	aqueous phase
em	emulsion
eq	equilibrium value
ext	external phase
f	feed phase
fm	feed-membrane phase interface
g	overall
I, II, III	phase I, phase II, and phase III
if	phase interface of SLM
L	position at $\delta_r = L$
m	membrane phase
mf	membrane-feed phase interface
mr	membrane-receiving phase interface
or	organic phase
P^-	cephalosporin anion
rm	receiving-membrane phase interface
t	time

1 Introduction

Cephalosporins, a common class in the β-lactam family of antibiotics, are therapeutically important/advantageous for their broad antibacterial activity. Out of a total worldwide production of around 5×10^7 kg/annum, the β-lactam group constitutes an amount of the order of 3×10^7 kg/annum. Penicillins and cephalosporins are the main constituents of commercially important β-lactams and they are mainly produced by biosynthetic routes, the mechanism of which is now fairly well understood [1].

Since the discovery of cephalosporin-C (CPC) in 1955 [2], the process for production of natural and semisynthetic cephalosporins have undergone various modifications. The biosynthetic route for production of cephalosporin antibiotics has several advantages over chemical synthesis in which toxic organic solvent is involved. In view of this, the enzymatic process has gained much attention during recent years [3]. There are about 13 therapeutically important semisynthetic cephalosporins, but only limited species of natural cephalosporins are known so far. Consequent to development of high yielding strain of *Cephalosporium acremonium*, the understanding of the enzymes involved in the biosynthesis of CPC has considerably been improved. Microbial cells and their enzymes like penicillin-G acylase and CPC acylase can produce β-lactam nuclei of 7-aminodeacetoxy cephalosporanic acid (7-ADCA) and 7-amino cephalosporanic acid (7-ACA) which are in turn used for the production of semisynthetic cephalosporins [3–5]. Penicillin-G acylase from *Escherichia coli*, *Basillus magaterium*, and *Penicillium ruttqgeri* and penicillin-V acylase as well as intact cells of *Erwinia aroidae* hydrolyze 7-phenyl acetoamido-7-ADCA into 7-ADCA [6]. Acylase enzymes from *Acetobacter turbidians*, *Xanthomonas citri*, and *Achromobacter species* can produce cephalexin from 7-ADCA [6]. Direct enzymatic hydrolysis of CPC into 7-ACA with CPC-acylase of *Pseudomonas* strains is possible [7, 8]. 7-ACA, a versatile β-lactam for preparation of various semisynthetic cephalosporins, is usually obtained from CPC by chemical method [9]. During recent years, emphasis has been given on enzymatic production of 7-ACA using two types of cephalosporin acylases, i. e., glutaryl 7-ACA acylase and CPC acylase [10]. However the most important development is perhaps the two-step bioconversion of CPC to 7-ACA[11]. In the first step, aqueous solution of CPC reacts with O_2 in presence of D-aminoacid oxidase enzyme to produce 7β-(4-carboxybutanamido)-cephalosporanic acid (glutaryl 7-ACA) via 7β-(5-carboxy-5-oxopentamamido)-cephalosporanic acid (ketoadipoyl 7-ACA). In the second step, glutaryl-7ACA is converted to 7-ACA using glutaryl-7ACA acylase enzyme.

The growing interest in various β-lactam antibiotics, especially the cephalosporins, over the last decade has called upon improvement in their production methods via modification of either the basic process and the microbial strain or the downstream processing techniques. The product recovery may involve various methods of extraction and purification which play an important role in the overall process economics [12]. During recent years much attention has been given to the development of liquid membrane (LM) processes which usually exhibit high extraction rates and selectivity as compared to those achievable in conventional solvent extraction and adsorption processes.

The purpose of this article is to highlight briefly progress and prospects of the liquid membrane as a method for the extraction and purification of cephalosporin antibiotics in the context of the status of its current developments.

2 Theoretical Aspects

Cephalosporin antibiotics are unstable at high pH and their distribution coefficients in most of the known solvents are very low. Because of the presence of ion-

izable group(s) in their structure, they are hydrophilic in nature and therefore, conventional solvent extraction processes can seldom be effective for their separation and purification. In such cases, extraction accompanied by chemical reaction with an extractant, called 'reactive extraction' can provide an effective method for their separation. Two mechanisms in general can be suggested for reactive extraction of cephalosporins.

In the first, called "ion-pair extraction," the extractant, typically an amine, 'A', dissolves in an organic solvent and reacts with the anion, P^- of cephalosporin molecule and a proton in the aqueous phase:

$$A_{or} + H_a^+ \Leftrightarrow HA_o^+ \quad (1)$$

$$HA_{or}^+ + P_a^- \Leftrightarrow AHP_o \quad (2)$$

and the overall reaction is

$$A_{or} + H_a^+ + P_a^- \Leftrightarrow AHP_o \quad (3)$$

The first step is the activation, i.e., protonation of the carrier. The active protonated carrier can react with cephalosporin anion (P^-) to form a complex AHP which is soluble in organic phase. The transport of anion from one phase to another requires the co-transport of cation (H^+). The reaction is instantaneous and the mass transport of the ionic species controls the reaction rate.

The other mechanism, known as "liquid-liquid ion-exchange," involves water insoluble extractant such as Aliquat-336 (tri-caprylylmethyl ammonium chloride) and counter-transport of a second anion to provide electroneutrality. In a typical situation, the removal of cephalosporin anion, P^- from the aqueous phase by an ion exchange with the anion, Cl^- of the extractant (QCl) dissolved in the organic phase takes place according to

$$QCl_{or} + P_a^- \Leftrightarrow QP_{or} + Cl_a^- \quad (4)$$

The extraction efficiency depends on the nature of cephalosporin molecule (i.e., its dissociation constant), solvent, and extractant through equilibrium relationship. The extractant should be able to provide stripping of anion to another aqueous phase to affect the separation.

It is apparent that for the reactive extraction to be effective, the cephalosporins should be in dissociated form which is maintained by selecting appropriate pH values depending on the dissociation constant (pK_a) of the molecules. Table 1 gives the pK_a values for various cephalosporin molecules.

The theory of liquid membrane extraction of β-lactam relies broadly on reactive extraction. In the liquid membrane which comprises an organic phase containing the carrier, the solute is extracted from an aqueous phase called the "source" feed phase to the membrane phase from which the solute is re-extracted to another aqueous phase called the receiving phase. The aqueous phases are maintained at different pH values depending on the reactive extraction mechanism. In case of ion-pair extraction the feed phase pH is lower than the receiving phase pH and the transport of solute is augmented by a co-extraction of a cation (i.e., H^+). In case of ion-exchange extraction of β-lactam, the feed phase pH is higher than that of the receiving phase pH and the solute transport

Table 1. pK_a values of cephalosporins

Molecule	pK_{a1}	pK_{a2}	pK_{a3}
Cefalothin	2.22	–	–
CPC	2.60	3.10	9.80
Cefazolin	2.54	–	1.70
Cefotaxim	–	–	–
7-ACA	2.02	4.42	–
Cefadroxil	–	–	–
7-ADCA	2.95	4.87	–
Cefaloridin	1.67	–	–

in the membrane phase is augmented by counter-transport of an anion (i. e., anion of the quaternary ammonium salt). The configuration of the two aqueous and membrane phases depends on the type of liquid membrane system as discussed below under separate headings.

2.1 Bulk Liquid Membrane

Figure 1 shows several types of mass transfer or diffusion cells, which are of the simplest design for performing bulk liquid membrane (BLM) processes. Each of the devices is divided into two parts: a common part containing the membrane liquid, M and a second part in which the donor solution F and acceptor solution R are separated by a solid impermeable barrier. The liquid, M contacts with the two other liquids and affects the transfer between them. All three liquids are stirred with an appropriate intensity avoiding mixing of the donor and acceptor solutions. For a liquid-ion exchange in a BLM system, Fig. 2 shows the transfer mechanism of cephalosporin anions, P^-, from donor (F) to acceptor (R) solution

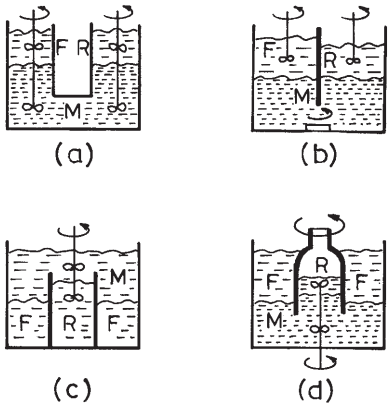

Fig. 1 a–d. Mass transfer (diffusion) cells: **a** U-type (Schulmann bridge); **b** with a flat vertical separating wall; **c** with a cylindrical wall (beaker-in-beaker type); **d** with a rotating inner cylinder

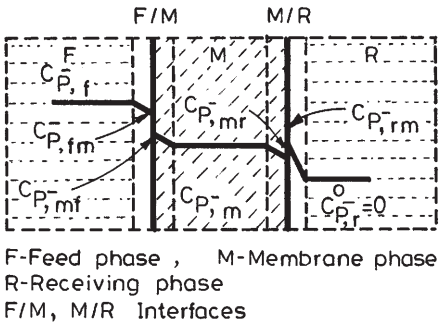

Fig. 2. Concentration profile of cephalosporin antibiotics in the liquid phases of BLM system

facilitated by the carrier, QCl_{or} taken in a solvent as the membrane phase (M). For transport to be effective, the pH of the aqueous feed phase should necessarily be maintained above the pK_{a2} value (amine dissociation constant) for adequate complexation with the carrier. The driving force for the process may be provided by the difference in chloride ion concentrations in the receiving and feed phases. At the F/M interface, the carrier binds with P^- to form a complex QP_{or} which is extracted by the membrane. The complex is transported due to concentration gradient to the M/R interface where another interfacial ion-exchange reaction takes place, thereby releasing cephalosporin anion into the receiving phase. The carrier returns to the F/M interface to recombine with the solute anion, the transport being accompanied by counter transport of an anion, Cl^- of the carrier. Alternately, buffer anion may also provide the driving force for the transport.

2.2
Emulsion Liquid Membrane

In the early 1970s Li [13] proposed a method that is now called "Emulsion (surfactant) Liquid Membrane (ELM)" or "Double Emulsion Membrane (DEM)" (Fig. 3). The name reveals that the three liquid system is stabilized by an emulsifier, the amount of which reaches as much as 5% or more with respect to the membrane liquid. The receiving phase R, which usually has a smaller volume than the donor solution, F of similar nature, is finally dispersed in the intermediate phase, M. In the next step the donor solution F is contacted with the emulsion. For this purpose, the emulsion is dispersed in the donor solution F by gentle mixing typically in a mixer-settler device. After this step, the emulsion is separated and broken. The enriched acceptor solution is further processed and the membrane liquid M is fed back for reuse.

2.3
Supported Liquid Membrane

The term "Supported Liquid Membranes" (SLM) usually defines solid (polymer or ceramic) porous membranes, the open pores of which are soaked with the

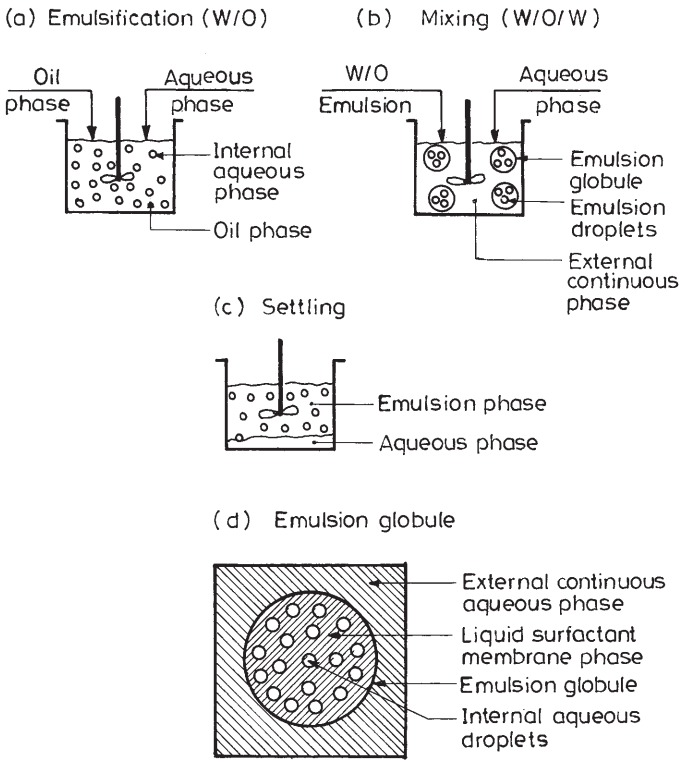

Fig. 3 a–d. Schematic diagram of emulsion liquid membrane

membrane liquid, as shown in Fig. 4 a. In a broader sense, this term also refers to much thicker "membranes," supported on both sides by porous solid membranes (Fig. 4 b). These homogeneous liquid films supported on both sides, may also be termed as a bulk liquid membrane.

The method of impregnating liquid membranes has become more and more popular. By impregnating fine-pore polymer films with a suitable membrane liquid, relatively stable heterogeneous solid-liquid membranes are obtained. These membranes are shaped as thin, flat barriers or hollow fibers. Usually they are manufactured from oleophilic polymers, wettable by membrane liquid. The two interfaces, F/M and M/R, have equal or close areas which can be made very large by employing modules of spirally wounded flat membrane or bundles of hollow fibers.

2.4 Dispersion Free Extraction in Hollow Fiber Membrane

Dispersion free extraction in hollow fiber (HF) membrane utilizes immobilized liquid-liquid interface at the pore mouth of a microporous membrane to effect phase to phase contact and the mass transfer process. HF module can be con-

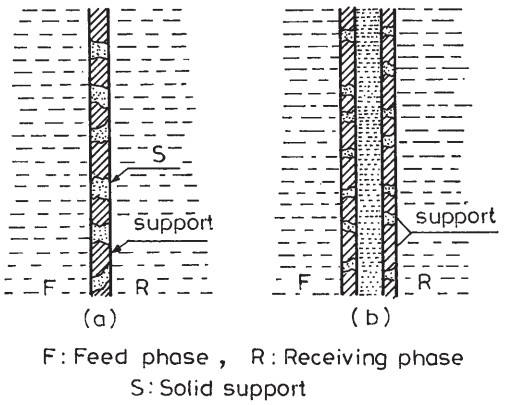

Fig. 4a, b. Supported liquid membranes: **a** membrane liquid fills the open pores of a solid support; **b** membrane liquid is supported on both sides by two porous solid membranes

figured with different packing fraction, surface area, and membrane type, providing flexibility in its selection and sizing for commercial application. The technique is amenable for reactive extraction and re-extraction for systems which are sensitive to the aqueous environment (i.e., pH). A pH swing process utilizing a two HF modules configuration has been suggested for separation and concentration of phenoxyacetic acid [14] based on the principle of reactive extraction with Amberlite LA2.

3 Current Literature

Schugerl [15] has recently furnished a detail analysis of the reactive extraction of penicillin-G and V and precursors like phenyl and phenoxy acetic acids. Thirty different amines have been studied for reactive extraction of penicillins [16] in various solvents such as butyl acetate, chloroform, di-isopropyl ether, kerosene, dioctyl ether, etc. Tertiary amines in *n*-butyl acetate were found to be advantageous because of their low reactivity with solvent but the distribution coefficients of their complexes are significantly lower than those of secondary amines. While using quaternary ammonium salts for ion-exchange extraction, re-extraction is difficult and very large amounts of anion (e.g., Cl^-) are needed to recover penicillins. The basic relationship for distribution coefficient and extraction kinetics have now been fairly developed for amine-penicillin systems.

Amine extraction of penicillins has been examined in a pilot scale extractor and its performance has been analyzed through suitable mathematical models [17–19]. Extraction efficiency as high as 90% was achieved under suitable conditions. The procedure for selection of volume ratios of the aqueous to organic phase and concentration ratio of carrier (Amberlite LA-2) to penicillin-G at a desired degree of extraction and enrichment has recently been described [20]. Ion-pair extraction of penicillin-V and phenoxy acetic acid with Amberlite LA-2 hydrochloride and tetrabutyl ammonium hydrogen sulfate can be effective in

various solvents such as hexane, amyl acetate, octanol, and chloromethane, the later being the preferred choice of solvent [21]. Olivanic and clavulanic acids are more effectively extracted by anion exchange with Aliquat-336 in butyl acetate and dichloromethane as solvents [21]. Anion exchange extraction is effective also for CPC which could be extracted from a carbonate buffer solution using Aliquat-336 in *n*-butyl acetate and re-extracted into citrate buffer solution without any decomposition [22]. Investigations recently carried out in the authors' laboratory revealed that the same carrier is effective for reactive extraction of 7-ACA, cephalexin, cephalothin, cefazolin, cephaloridine, cefadroxil, etc. from model medium as well as fermentation broth by using different liquid membrane systems [23–27].

3.1 Bulk Liquid Membrane

In order to develop the liquid membrane techniques, i. e., emulsion liquid membrane (ELM), supported liquid membrane (SLM), non-dispersive extraction in hollow fiber membrane (HFM), etc., for practical processes, it is necessary to generate data on equilibrium and kinetics of reactive extraction. Furthermore, a prior demonstration of the phenomena of facilitated transport in a simple liquid membrane system, the so-called bulk liquid membrane (BLM), is thought to be effective. Since discovery by Li [28], the liquid membrane technique has been extensively studied for the separation of metal ion, amino acid, and carboxylic acid, etc., from dilute aqueous solutions [29].

Some of the studies on metal ions resulted in active transport, while others exhibited passive transport. Mutihac et al. [30–32] has reported separation of amino acids using macrocyclic crown ether type (18-crown-6) using 1,2 dichloroethane as the organic phase. Applying BLM techniques, lactic acid separation using Aliquat-336 in *n*-octane has been studied using Cl^- ion in the receiving phase to achieve higher recovery and faster kinetics as compared to the transport of CO_3^{-2} and SO_4^{-2} [33]. Separation of amino acids using traditional extracting agents, e.g., amines [34], quaternary ammonium salt [35], and organic phosphoric acid extractant such as di-(2-ethylhexyl) phosphoric acid (D2EHPA) were also studied with promising results [36]. Boronic acids were used as carrier for facilitated transport of a range of hydrophilic sugars through lipophilic membranes [37–39]. The extraction and transport of penicillin-V through liquid membrane containing 1,2 dichloroethane between two aqueous phases having different pH values have been studied using Amberlite LA-2 as the carrier [40].

Our studies on BLM system for separation of 7-ACA [23], cephalexin [24], CPC [26] using Aliquat-336 as an anion exchange carrier revealed that pH gradient between the feed and stripping aqueous phases controlled the transport rate and separation efficiency. In some cases, uphill transport occurred with more than 90% recovery of cephalosporin molecules. BLM permeation study was also conducted for cephalothin, cefadroxil, cefazolin, cefotaxim, cefaloridin, and 7-ACA for evaluation of initial flux. The initial permeation fluxes for various cephalosporins were well correlated with hydrophobicity [41] and the extraction equilibrium constants. This seems to be in agreement with the idea that

higher hydrophobic nature of the solute should allow faster transport through the liquid membrane.

3.2 Emulsion Liquid Membrane

For practical application, an ELM system is expected to be advantageous because of the small volume of extractant required, high selectivity, and flux and larger interfacial area for solute transport. There is sufficient literature on ELM extraction of metal ion, amino acid, and carboxylic acid [42, 43]. Phenylalanine was extracted in an ELM system using Aliquat-336 and Paranox 100 as quaternary amine salt carrier and emulsion stabilizing nonionic surfactant, respectively and decyl alcohol as the co-surfactant [44, 45]. Effect of counter-ion lyotropy on ELM extraction was also discussed and it was shown that Cl^- was a better internal stripping agent compared to Br^- and I^-. A strong correlation exists between initial flux and hydrophobicity of amino acids in ELM systems [45]. Reisinger and Marr [46] described lactic acid (using Amberlite LA-2) and L-leucine (using quaternary ammonium salt, i.e., Aliquat-336) permeation in ELM systems. The concentration of L-phenylalanine in an ELM system was studied by using cation exchange carrier, D2EHPA [47]. The internal phase pH and acid concentration in the external phase were optimized with respect to concentration performance and membrane stability. Batch extraction of lactic acid using an ELM system was studied to address the effects of surfactant (span-80) and carrier (Alamine-336) on system stability, kinetics and swelling [48].

There is limited information on ELM extraction of cephalosporin antibiotics. Current studies at the authors' laboratory revealed evidence of facilitated transport of CPC and cephalexin in a suitably designed ELM system [25, 26]. CPC was extracted from a model medium as well as fermentation broth of *Cephalosporium acremonium*. Since the fermentation broth contains structurally similar CPC and deacetyl-CPC in appreciable proportions, selective separation is complicated from the practical point of view [49]. In a suitably formulated ELM system using Aliquat-336 as anion exchange carrier, CPC was selectively extracted from feed phase [26]. By maintaining an appropriate pH gradient in the feed and receiving phases, facilitated uphill transport could also be achieved in the ELM system. A simple mass transfer model predicts the permeation rate in the ELM system. An experimental study on batch extraction of cephalexin using an ELM system has also been reported by the authors [25]. The effects of surfactant, carrier and solutes concentrations, phase volume ratio, stirring, and counter-ion concentration on the extraction rate were examined. Aliquat-336, Span-80, and *n*-heptane-kerosene (1:1 v/v) were used as the carrier, surfactant, and diluent, respectively. Under optimized experimental conditions, emulsion swelling was found to be marginal. By maintaining an appropriate pH gradient in the feed and receiving phases, facilitated transport could be realized. Selective separation of cephalexin from a mixture of 7-ADCA was demonstrated in the ELM system [25].

Reactive extraction studied for cephalosporins and penicillins using different carriers and solvents can now be applied in LM for their separation from practical point of view [50–52]. In a typical membrane formulation of an oil phase

with a nonionic polyamine (ECA 4360J) as the surfactant and di-*n*-octylamine as the carrier in the mixture of *n*-butyl acetate-kerosene as the solvent, nearly complete extraction and re-extraction of penicillin-G can be achieved by an optimal adjustment of the pH of both the internal and external phases [50]. In fact, physical extraction processes are widely adopted for extractive separation of penicillin-G. But in situations where phenoxy acetic or phenyl acetic acid-penicillin-G/V mixtures are involved, reactive extraction in ELM would discriminate selectivity favoring extraction of penicillin [21]. The effect of carrier type for extraction of penicillin-G from a simulated feed stream has been extensively studied in a batch system [43, 53]. The most successful carrier is perhaps tri-*n*-octyl amine because it exhibits lowest activity towards solvents. At the early stages of extraction, penicillin-G is subjected to those pH values at which it is extremely unstable. It is necessary to have faster extraction rate and less membrane swelling so that the degree of decomposition may below. Decomposition was less than 1% in 40 min provided that the initial sodium carbonate concentration in the internal phase was correctly maintained [54], which apparently proved the applicability of the ELM process. The optimum extraction conditions were found to be 20% (v/v) of span-80 in ECA 4360J as a surfactant, kerosene as diluent, and Amberlite LA-2 as the carrier [55].

3.3 Supported Liquid Membrane

The mechanism of transport of CPC using SLM has been studied at the authors' laboratory [56]. CPC could be permeated from alkaline feed of carbonate buffer into an acidic stripping solution of acetate buffer across the membrane comprising Aliquat-336 in *n*-butyl acetate immobilized in a polypropylene (Celgard 2400) support. The transport mechanism is a case of counter transport exhibiting overall rate dependence on solute diffusion in the membrane phase as well as the mass transfer across the aqueous boundary films.

Facilitated transport of penicillin-G in a SLM system using tetrabutyl ammonium hydrogen sulfate and various amines as carriers and dichloromethane, butyl acetate, etc., as the solvents has been reported [57, 58]. Tertiary and secondary amines were found to be more efficient carriers in view of their easy accessibility for back extraction, the extraction being facilitated by co-transport of a proton. The effects of flow rates, carrier concentrations, initial penicillin-G concentration, and pH of feed and stripping phases on transport rate of penicillin-G was investigated. Under optimized pH conditions, i. e., extraction at pH 6.0 – 6.5 and re-extraction at pH 7.0, no decomposition of penicillin-G occurred. The same SLM system has been applied for selective separation of penicillin-G from a mixture containing phenyl acetic acid with a maximum separation factor of 1.8 under a liquid membrane diffusion controlled mechanism [59]. Tsikas et al. [60] studied the combined extraction of penicillin-G and enzymatic hydrolysis of 6-aminopenicillanic acid (6-APA) in a hollow fiber carrier (Amberlite LA-2) mediated SLM system.

However, the SLM system suffers from the drawback of high mass transfer resistance across the liquid membrane as well low membrane stability. In order to

eliminate the instability problem a new hybrid technique, the so-called "hollow fiber contained liquid membrane (HFCLM)", was developed first by Basu and Sirkar [61] and studied for separation of carboxylic acids. In this technique, the extractant forms a thin liquid phase situated or flowing between the polymeric membrane fiber rather than being immobilized. In HF modules, the feed solution flows through the bore of some of the fibers, the stripping solution through the bore of the others, and the membrane solution containing the carrier is kept at the shell side so that extraction and stripping take place in the same device. Separation of penicillin-G has been studied in an HFCLM system utilizing Amberlite LA-2 in tri-*n*-butyl phosphate as the membrane phase and liqui-cell TME 400/110 hollow fiber membrane module [62]. Due to facilitated transport of penicillin-G from an aqueous feed of citrate buffer to an alkaline stripping solution, over 90 % recovery was obtained.

3.4 Dispersion Free Extraction

Dispersion free extraction in HF membranes has been studied for separation of various pharmaceutical products [63] and carboxylic acids [64]. Protein and enzyme extractions have been explored using biphasic and reverse micelle systems with hydrophobic microporous hollow fibers [65, 66]. Prasad and Sirkar [67] have developed a comprehensive criterion for characterization of mass transfer rate in microporous hollow fiber (MHF) modules with either hydrophilic or hydrophobic fibers. The technique utilizes immobilized liquid-liquid interface at the pore mouth of the microporous membrane to effect phase to phase contact and a mass transfer process. HF modules can be configured with different packing fraction, surface area, and membrane type, thus providing flexibility in its selection and sizing for commercial application. They can offer a height of transfer unit comparable to a conventional extractor. Process design and scale-up appears to be much simpler than dispersion-based devices conventionally used for extractive separation processes. The technique is amenable for reactive extraction and re-extraction for systems which are selective to the aqueous environment, i. e., pH of the aqueous feed and stripping phases. A pH swing process utilizing a two-HF module configuration has been suggested for separation and concentration of phenoxy acetic acid [14] based on the reactive extraction principle with Amberlite LA-2 as the carrier. Solute distribution coefficient (m) and the membrane type which determine the overall mass transfer coefficient (K_L) control the separation efficiency. For an $m > 1$ system, an organic in-pore hydrophobic membrane has higher K_L value of extraction than an aqueous in-pore filled hydrophilic membrane. Similarly, for back extraction with $m < 1$, an aqueous in-pore hydrophilic membrane has higher K_L value than an organic in-pore hydrophobic membrane. Practically, there is no report on separation of cephalosporins using an HF membrane, except on the work done at the authors' laboratory [26]. Extraction as well as stripping has been studied using a pH swing procedure from a model medium of cephalexin and CPC, and fermentation product of *Cephalosporium acremonium*. An organic phase comprising *n*-heptane and Aliquat-336 as the diluent and anion exchange carrier, respectively,

was used to extract cephalosporin molecules from an aqueous solution of cephalosporin having a pH above pK_{a2} (amine dissociation constant) to the organic phase. The solute was stripped from the loaded organic phase to another aqueous phase of pH maintained well below the pK_{a2} value of the cephalosporin. Mass transfer performance of a single module has been evaluated and an experimentally observed low value of height of transfer unit (HTU) indicates good prospects for hollow fiber membrane for the extraction duty.

4 Mathematical Modeling

There have been more than 12 mathematical models proposed in the last 15 years but only a limited number have been applied practically to describe liquid membrane phenomena. This aspect has been discussed in detail in the current literature [29, 68, 69] and therefore this paper will highlight the models which have actually been used for simulation of the results on liquid membrane permeation of β-lactam antibiotics and related biomolecules.

4.1 Bulk Liquid Membrane

Due to the ionic nature of cephalosporin molecules, the interfacial chemical reaction may in general be assumed to be much faster than the mass transfer rate in the carrier facilitated transport process. Furthermore, the rate controlling mass transfer steps can be assumed to be the transfer of cephalosporin anion or its complex, but not that of the carrier. The distribution of the solute anion at the F/M and M/R interfaces can provide the equilibrium relationship [36, 69]. The equilibrium may be presumably expressed by the distribution coefficients, m_f and m_r, at the F/M and M/R interfaces, respectively and these are defined as

$$m_f = \frac{C_{P^-,mf}}{C_{P^-,fm}} \tag{5}$$

$$m_r = \frac{C_{P^-,mr}}{C_{P^-,rm}} \tag{6}$$

Based on the cephalosporins concentration profiles in the BLM system (Fig. 2), the following mass transfer models describe the change in solute concentration in the respective phases:

$$\frac{dC_{P^-,f}}{dt} = \frac{a_r k_{mf} k_f m_f}{V_f(k_f + k_{mf} m_f)} \left(C_{P^-,f} - \frac{C_{P^-,m}}{m_f} \right) \tag{7}$$

$$\frac{dC_{P^-,r}}{dt} = \frac{a_r k_{mf} k_r m_r}{V_r(k_r + k_{mr} m_r)} \left(\frac{C_{P^-,r^-}}{m_r} - C_{P^-,r} \right) \tag{8}$$

$$\frac{dC_{P^-,m}}{dt} = \frac{1}{V_m}\left[\frac{a_f k_{mr} k_f m_f}{(k_f + k_{mf} m_r)}\right](C_{P^-,f} - C_{P^-,m}/m_f) - \\ - \frac{a_r k_{mr} k_r m_r}{k_r + k_{mr} m_r}(C_{P^-,m}/m_r - C_{P^-,r}) \tag{9}$$

$$C_{P^-,m} = V_f/V_m\,(C^0_{P^-,f} - C_{P^-,f}) - V_r\,C_{P^-,r}/V_m \tag{10}$$

when $t = 0$; $C_{P^-,f} = C^0_{P^-,f}$, $C_{P^-,r} = C_{P^-,m} = 0$

The membrane phase concentrations are generally calculated from a mass balance equation given as

$$V_f\,C^0_{P^-,f} = V_f\,C_{P^-,f} + V_m\,C_{P^-,m} + V_r\,C_{P^-,r} \tag{11}$$

The equation for the equilibrium concentrations in the three phases can be deduced from Eqs. (5) – (11) as

$$\frac{C_{P^-,f,eq}}{C^0_{P^-,f}} = \frac{1}{\{1 + (m_f V_m/V_r) + (V_r/V_f)\,(m_f/m_r)\}} \tag{12}$$

$$\frac{C_{P^-,m,eq}}{C^0_{P^-,f}} = \frac{1}{\{(1/m_f) + (V_m/V_r) + (V_r/V_f m_f)\}} \tag{13}$$

$$\frac{C_{P^-,r,eq}}{C^0_{P^-,f}} = \frac{1}{\{(m_r/m_f) + (m_r V_m/V_r) + (V_r/V_f)\}} \tag{14}$$

This simplified mass transfer model was successfully used to simulate the experimental results for BLM transport of eicosapentanoic acid methyl ester using silver nitrate carrier taken in aqueous solution as the membrane phase [24]. On the basis of such a model, experimental data on permeation of amino acid (L-lysine) in BLM containing a cation exchange carrier (D2EHPA) in an organic membrane phase could be well simulated [36]. The partial mass transfer coefficients determined as the model parameter were correlated well with the liquid phase hydrodynamic conditions implying the validity of the model. In the authors' laboratory; such a model has been extended to describe the BLM transport behavior of 7-ACA, cephalexin, 7-ADCA, and CPC [23, 24, 26]. On the basis of the experimental data obtained for $C_{P^-,f}$, $C_{P^-,m}$, and $C_{P^-,r}$ and the suggested mass transfer model presented by Eqs. (7) – (10), the unknown partial mass transfer coefficients k_f, k_r, k_{mf}, and k_{mr} were calculated and theoretical P^- vs t profiles of solutes in all the phases were computed. The computed and calculated data were in reasonably good agreement.

4.2 Emulsion Liquid Membrane

The emulsion liquid membrane for cephalosporins relies essentially on "facilitated transport." There are basically, however, two types of facilitated transport in emulsion liquid membrane system, i. e., Type I and Type II facilitation. In the first type, the concentration gradient of the membrane soluble solute/permeate

is maximized by irreversibly reacting the solute with the reagent into an impermeable form in the receiving phase (usually internal phase) thereby maintaining the permeate concentration at effectively zero in this phase. In Type II facilitation, a carrier is incorporated in the membrane phase and it carries the diffusing solute across the membrane to the receiving phase, a mechanism commonly known as "carrier-mediated" facilitated transport.

Emulsion liquid membrane extraction of cephalosporins conform to the type II facilitated transport. Here the solute transport is either associated with a co-transport or counter-transport of an anionic species depending on whether ion-pair or ion-exchange extraction is exploited in the ELM system.

Various models have been proposed to describe the facilitated mass transfer phenomena, although five basic categories of models have mostly been reported in the literature [29]. The same models can essentially be applicable for Type II facilitated transport.

The mathematical model essentially involves rate equations capable of describing these phenomena. Although there are number of models for unfacilitated transport [42], there exist only a few quantitative models for facilitated transport in emulsion liquid membrane. In addition to mass transfer in emulsion liquid membrane, the chemical reaction between the solute, carrier, and the internal reagent should be considered. In such a system there are three possible rate controlling steps: mass transfer through the external phase, chemical reaction(s), and diffusion through the membrane phase. The aim of the modeling study is to simulate experimental data and identify which, if any, of these three steps controls the extraction rate. Table 2 shows the reported modeling studies for β-lactams and related biomolecules. Phenomenologically the models include mass transfer in the external phase, the solute-carrier chemical reaction, diffusion in the emulsion globule as described by a shrinking core model, and the stripping reaction [70, 71].

The following steps are considered for the transport process in developing such model which has been adopted for cephalosporins permeation study at the authors' laboratory [25]:

1. Diffusion of cephalosporin anion (P^-) from the bulk feed phase (III) to feed-membrane (III–II) interface of the emulsion globule
2. Reaction of P^- ion with the carrier QCl at the external interface releasing the counter-ion Cl^-
3. Diffusion of the solute-carrier complex, QP into the emulsion globule
4. Stripping of the complex at the internal interface between the membrane (II) and internal (I) phase
5. Back diffusion of the carrier to the feed (III) and membrane (II) phase interface

The following assumptions are inherent in the above process:

1. The extraction and stripping reactions are located at the interfaces and the amount of carrier dissolved in the aqueous phases is negligible.
2. Negligible transport resistance exists in the internal phase (I) because the phase I droplets are very small ($r_1 < 5$ μm): a quasi-homogeneous state.

Table 2. Reported studies on facilitated transport in liquid membrane for β-lactam antibiotics and related biomolecules

Species/Solute	Carrier	Internal reagent	Co/Counter transport of ion	LM type	Mathematical model	Inference	Reference
Lactic acid	Secondary amine LA-2 Tertiary amine Alamine-336	Sodium carbonate -do-	Co transport of H^+ -do-	ELM ELM ELM	Not done Not done Shrinking core model	Selectivity studies in relation to acetic, malic, gluconic acid, etc. Effect of convective transport and swelling accounted for modeling and model verification	[46] [70]
Lactic acid and Leucine	Amberlite LA-2 and Aliquat-336	Na_2CO_3 and NaCl	Co-transport of OH^- counter-transport of Cl^-	ELM	Simplified reaction-diffusion model	Reaction controlled transport mechanism	[46] and references cited therein
Lactic acid	Secondary amine	Na_2CO_3 and NaOH	Co-transport of OH^-	ELM	Model of mass transfer in external layer and internal diffusion in globule	pH variation occurred	[71]
Lactic acid	Aliquat-336	NaCl, Na_2CO_3, Na_2SO_4	Counter-transport of Cl^-	BLM	Not done	NaCl provides highest recovery and fastest kinetics of lactic acid pre-concentrated in the aqueous solution containing 0.5 mol/L of NaCl	[33]
Amino acid	-do-	–	Counter-transport of OH^-	ELM	–	Chiroselective transport	[93]
Mendalic acid	Optically active benzyl derivative	–	Counter-transport of H^+	BLM BLM	–	–	[94]
L-Phenyl-alanine	Di-2-ethylhexyl phosphoric acid (D2EHPA)	H_2SO_4	Counter-transport of H^+	ELM	–	Concentration as cation	[47]

Table 2 (continued)

Species/Solute	Carrier	Internal reagent	Co/Counter transport of ion	LM type	Mathematical model	Inference	Reference
L-phenyl-alanine and various other amino acids	Aliquat-336	KCl and KOH	Counter-transport of Cl^-	ELM	–	Concentration as anion carrier specificity for various aminoacids depends on hydrophobicity scale	[45, 95]
Phenylalanine and Lysine	D2EHPA	KCl in receiving phase	Counter-transport of K^+	BLM (RFP)	–	Continuous extraction and concentration	[96]
Di- and tri-peptides	D2EHPA	HCl	Counter-transport of H^+	ELM	–	Concentration and permeation depends on hydrophobicity scale	[97]
Amino acids in general	Crown ether and open chain polymer of transtetrahydro furan, 2,5-bis acetylene unit	–	–	SLM	–	Highly selective separation and enantiomeric resolution	[98, 99]
Dipeptide and phosphono dipeptide and several amino acids	Kryptafix2 (crown ether)	HCl in receiving phase	Counter-transport of Cl^-	SLM in HF	–	Stereoselective permeation of 1–1 dipeptide	[100]
Penicillin-G	Amberlite LA-2 and dioctylamine	Na_2CO_3	Co-transport of H^+	ELM ELM	Simple model of permeation rate accounting for product decomposition	Optimum extraction condition and procedure for determining the internal reagent worked out. DOA is a better carrier	[50, 53, 54, 100]

Table 2 (continued)

	Amberlite LA-2	-do-	-do-	SLM	Simple flux equation based on film theory considering aqueous boundary layer resistance and membrane diffusion	Optimal condition determined with respect to pH of the aqueous phase	[57, 58]
7-ACA, cephalexin, CPC	Aliquat-336	NaCl	Counter-transport of Cl^-	BLM	Simple mass transfer model	pH gradient or Cl^- counter trans port can provide the driving force	[23, 24, 26]
CPC	Aliquat-336	NaCl	-do-	SLM (polypropylene flat sheet)	Analysis of permeation controlling steps from mass transfer model	Membrane diffusion controlling	[56]
			-do-	HF extraction	Mass transfer model	Simultaneous extraction and stripping possible in two HF modules	[27] [25, 26]
Cepalexin with 7-ADCA and CPC including broth	-do-	-do	-do	ELM	Model incorporating external mass transfer and diffusion in globule	Selective separation of cephalexin from mixture with 7-ADCA and of CPC from deacetylCPC of broth	

3. Resistance in the oil layer (surfactant monolayer) at the external interface is negligible.
4. The stripping reaction is very fast due to large surface area of the phase I.

Figure 5 shows the concentration profile of cephalosporin anion, P^- in the emulsion globule. Applying two film theory, the mass transfer rate of P^- from bulk of phase III through the boundary layer of phase III to the III – II interface is given by

$$\frac{dC_{P^-}}{dt} = -\frac{1}{V_m} k_m S_{em} (C_{P^-} - C^*_{P^-}) \tag{15}$$

where C_{P^-} is the solute concentration in the external phase, $C^*_{P^-}$ is the concentration at the phase III–II interface, k_{III} is the external phase mass transfer coefficient, S_{em} is the total surface area of the emulsion globules, and V_{III} is the external phase volume.

Considering interfacial chemical reaction at III–II interfaces, the following equation holds:

$$\frac{dC_{P^-}}{dt} = -\frac{S_{em}}{V_{III}} k_1 C^*_{P^-} C^*_{QCl} \tag{16}$$

$= R_F$ = extraction reaction rate per unit area of III – II interface, where k_1 is the forward reaction rate constant for the extraction reaction.

The diffusion of the solute-carrier complex in the emulsion is described by Fick's second law and is given by the following equation:

$$\frac{V_{II}}{V_I + V_{III}} \frac{\delta C_{QP}}{dt} = D_{eff} \frac{\delta}{r^2 \delta r} \left(r^2 \frac{\delta C_{QP}}{\delta r} \right) - \frac{S_1}{V_I + V_{II}} k_{-1} C_{QP} C_{Cl^-} \tag{17}$$

where S_1 is the total surface area of the internal phase droplets (phase I), D_{eff} is the effective diffusivity of the complex, k_{-1} is the rate constant for the backward

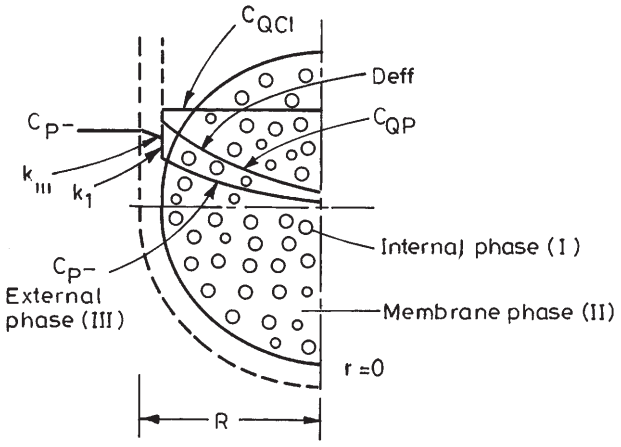

Fig. 5. Concentration profile of cephalosporin in an emulsion liquid membrane

reaction, and V_I and V_{II} are the phase volumes of the internal aqueous and membrane phases, respectively.

The equilibrium constant, K_{eq} for the complexation reaction (Eq. 4) can be expressed as

$$K_{cq} = \frac{C_{QP} C_{Cl^-}}{C_{QCl} C^*_{P^-}} \tag{18}$$

where

$$C_{QCl} = C^0_{QCl} - C_{QP} \tag{19}$$

and from Eqs. (18) and (19)

$$C^*_{P^-} = \frac{C_{Cl^-}}{K_{eq}} \left[\frac{C^0_{QCl}}{C_{QCl}} - 1 \right] \tag{20a}$$

or

$$C^*_{P^-} = \frac{C_{Cl^-} C_{QP}}{K_{eq} (C^0_{QCl} - C_{QP})} \tag{20b}$$

The initial and boundary conditions are given by:

$$t = 0, C_{P^-} = C^0_{P^-}, C_{QP} = 0, (0 \le r \le R) \tag{21}$$

Boundary conditions at the center of globule to have no flux is

$$r = 0, \frac{\delta C_{QP}}{\delta r} = 0, \ (t \ge 0) \tag{22}$$

At the feed-membrane interface

$$r = R, D_{eff} \frac{\delta C_{QP}}{\delta r} = k_m (C_{P^-} - C^*_{P^-}) \tag{23}$$

The following relationships may be used for the solution of the above model equations:

1. The number of emulsion globules, N_m is given by

$$N_m = \frac{V_I + V_{II}}{(4/3)\pi R^3} \tag{24}$$

where R is the mean globule radius, $D_{32}/2$
with $D_{32} = \sum n_I d_i^3 / \sum n_i d_i^2$ (Sauter mean diameter)
where 'n' is the number of globules of diameter of 'd'

2. Surface area of emulsion globule, S_{em} is given by

$$S_{em} = \frac{3 (V_I + V_{II})}{R} \tag{25}$$

3. The total surface area of internal droplets of phase I

$$S_I = \frac{3 V_I}{r_I} \tag{26}$$

In order to solve the mathematical model for the emulsion liquid membrane, the model parameters, i. e., external mass transfer coefficient (K_{III}), effective diffusivity (D_{eff}), and rate constant of the forward reaction (k_1) can be estimated by well known procedures reported in the literature [72 – 74]. The external phase mass transfer coefficient can be calculated by the correlation of Calderback and Moo-Young [72] with reasonable accuracy. The value of the solute diffusivity (D_a) required in the correlation can be calculated by the well-known Wilke-Chang correlation [73]. The value of the diffusivity of the complex involved in the procedure can also be estimated by Wilke-Chang correlation [73] and the internal phase mass transfer co-efficient (surfactant resistance) by the method developed by Gu et al. [75].

The kinetic constant, k_1 can be calculated from Lewis cell experiments [46] under the condition of higher carrier concentration compared to that of solute in aqueous phase, so that the mass transfer rate is controlled by the transport of the solute to the interface and the rate of reaction at the interface.

Equations (15) – (23) can be solved numerically using a combination of IMSL and NAG library subroutines. The DIVPAG subroutine of IMSL for ordinary differential equations and the D03PAF subroutine of NAG library for partial differential equations may serve the purpose and we applied this method for simulating the results for ELM extraction of CPC [26] and cephalexin [25]. The agreement between model prediction and experimental data was found to be quite reasonable.

4.3
Supported Liquid Membrane

The permeation of cephalosporin antibiotics in an SLM system under reactive extraction condition can be considered a coupled transport phenomenon which can describe metal ion permeation behavior. Various steps are involved in the coupled transport in the SLM system:

- Step 1: the P^- ion, after diffusing to the feed-SLM interface, reacts with QCl (Eq. 4) forming a solute-carrier complex, QP: Cl^- ions are simultaneously released into the feed solution (coupled transport).
- Step 2: QP diffuses across the membrane because of negative concentration gradient.
- Step 3: at the SLM-stripping interface, QP releases P^- ions into the aqueous phase, Cl^- ions replace P^- ions in the membrane (coupled transport).
- Step 4: the uncomplexed carrier, QCl returns across the membrane, the uncomplexed solute P^- cannot diffuse back because of low ionic solubility in the membrane phase.
  Since the ion exchange reactions are fast, decomposition of CPC does not occur at the pH range used [50]. In the stripping side, the presence of buffer anion (B^-) of the buffer acid (BH) is likely to cause another ion exchange reaction according to

$$B^- + QCl \Leftrightarrow QB + Cl^- \tag{27}$$

This reaction is suppressed by using a large excess of Cl^- ion in the stripping phase. Furthermore, the extraction equilibrium constant of the above reaction is much lower than that of reaction given by Eq. (4). The overall distribution coefficient of CPC, 'm_g' (defined as C_{QP}/C_{P^-}) is given by [50]

$$m_g = \frac{[K_{eq} C^0 BH - \{(1 - K_d) C_H/K_a + 1\} C_{B^-}]}{K_A C_{B^-}} \tag{28}$$

with

$$\log (m_g) = \log (K_{eq}) + \log (C_{QCl}/C_{Cl^-}) \tag{29}$$

where K_{eq} and K_A are the extraction equilibrium constants of the reaction given by Eqs. (4) and (27), respectively and K_d and K_a are the distribution equilibrium constant (between organic and aqueous phases) and dissociation constant, respectively, for the buffer acid.

The CPC present in the aqueous phase is distributed between the aqueous and organic phases at the SLM-liquid interface. By maintaining low Cl^- ion concentration in the feed phase and high Cl^- ion concentration in the stripping phase, the distribution ratio of CPC (P^- ion form) at the aqueous feed-SLM interface can be made much higher than that at the aqueous strip-SLM interface. Under this condition, the steady-sate overall CPC flux across the membrane can be obtained from Fick's distribution law applied to aqueous diffusion film as well as the membrane itself and from interfacial reaction kinetics which describe the interfacial flux.

The typical concentration profile of solute in an SLM system with quaternary ammonium salt as carrier is schematically shown in Fig. 6. To model the facilitated transport within a supported liquid membrane [58, 59], the following assumptions are usually made:

- Isothermal process.
- Carrier and solute-carrier complex dissolve in organic phase only.
- The concentration gradient in liquid membrane and aqueous film are linear.
- The mass transfer resistance of chloride ion in feed and stripping solution may be neglected.

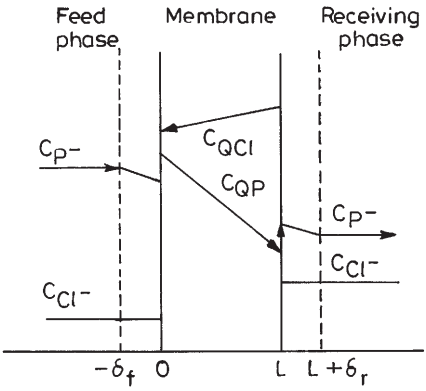

Fig. 6. Typical concentration profile in a supported liquid membrane system

- The concentration of solute-carrier complex on the M/R interface is much lower than on F/M interface.
- The decomposition of cephalosporins is negligible.

Thus, the mass transfer flux of solute in feed, liquid membrane, and stripping phases can be expressed by the following equations:

$$J_f = \frac{D_f}{\delta_f}(C_{P^-,f} - C_{P^-,0}) = k_f(C_{P^-,f} - C_{P^-,0}) \tag{30}$$

$$J_m = \frac{\varepsilon D_m}{\tau L}(C_{QP,0} - C_{QP,L}) = k_m(C_{QP,0} - C_{QP,L}) \tag{31}$$

$$J_r = \frac{D_r}{\delta_r}(C_{P^-,L} - C_{P^-,r}) = k_r(C_{P^-,L} - C_{P^-,r}) \tag{32}$$

where k_f, k_m, and k_r are the mass transfer coefficients in feed, membrane, and receiving phases, respectively; D_f and D_r represent the diffusivity of solute in feed and in stripping phase; D_m is diffusivity of the formed complex in liquid membrane phase; L is the thickness of liquid membrane; and ε and τ are the porosity and tortuosity of the microporous membrane, respectively.

By introducing the distribution coefficients at the two interfaces, i. e., m_f and m_r,

$$J_f = k_f(C_{P^-,f} - C_{QP,0}/m_f) \tag{33}$$

$$J_r = k_r(C_{QP,L}/m_r - C_{P^-,r}) \tag{34}$$

Under pseudo steady-state condition, the total or overall flux (J) is equal to the flux in each phase, i. e., $J = J_r = J_f = J_m$.

By eliminating the undetermined carrier concentrations ($C_{QP,O}$ and $C_{QP,L}$) at the boundaries of the SLM and under the usually valid condition of $m_r \ll m_f$, the mass transfer rate of the solute can be deduced as [54]

$$JS = -V_a\frac{dc_{P^-,f}}{dt} = K_L S C_{P^-,f} \tag{35}$$

where S represents the cross-sectional area of the membrane and K_L is an overall mass transfer coefficient defined as

$$\frac{1}{K_L} = \frac{1}{k_f} + \frac{1}{k_f}\frac{m_r}{m_f} + \frac{1}{m_f k_m} \tag{36}$$

The distribution coefficient is a function of solute concentration and Eq. (35) cannot be solved easily. However, solution exists for the following two limiting cases:

- Case 1: $C_{QCl} \gg C_{P^-,g}$

In case of very low solute concentration, the complex concentration in the liquid membrane is almost equal to zero. Thus, the transport process is mainly controlled by aqueous film resistance, and K_L is equal to k_f, which is independent of time. By integrating Eq. (35), the concentration variation of solute in feed phase

at any time ($C_{p^-,t}$) can be obtained as

$$\ln\left[\frac{C_{p^-,t}}{C_{p^-,g}}\right] = -(S/V)\,K_L t \tag{37}$$

The permeation or the mass transfer rate in aqueous film can be obtained from the slope of time course of solute concentration in the feed phase.

– Case 2: $C_{QCl} \ll C_{P^-,g}$

In this case, the solute concentration in feed phase is so high that all of the carrier in the liquid membrane are in a complex form and the complex concentration is equal to the overall carrier concentration. So, m_f and m_r become

$$m_{f,} = \frac{C_{QCL}}{C_{p^-}} \tag{38}$$

Because m_r is much smaller than m_f and the second term in the denominator of Eq. (36) is neglected, K_L is expressed by the following relation:

$$K_L = \frac{J}{C_{p^-}} = \frac{m_{f,}}{\frac{m_{f,}}{k_f} + \frac{1}{k_m}} = \frac{C_{QCL}}{\frac{C_{QCl}}{C_{P^-}k_f} + \frac{1}{k_m}} \tag{39}$$

and when C_{P^-} is large enough the flux can be expressed as

$$JS = -V\frac{dc_{P^-,f}}{dt} = C_{QCl}k_m S = \text{constant} \tag{40}$$

Integrating Eq. (40), the concentration of solute in feed phase at any time ($C_{P-,t}$) can be shown as

$$\frac{C_{P^-,t}}{C_{P^-,g}} = 1 - \frac{(C_{QCl}k_m)}{C_{P^-,g}}\frac{S}{V}\,t \tag{41}$$

The mass transfer coefficient in liquid membrane, k_m can be obtained from the plot of concentration vs. time.

This simple mass transfer model based on simplified film theory has been proposed to describe the process of facilitated transport of penicillin-G across a SLM system [53]. In the authors' laboratory, CPC transport using Aliquat-336 as the carrier was studied [56] using microporous hydrophobic polypropylene membrane (Celgard 2400) support and the permeation rate was found to be controlled by diffusion across the membrane.

4.4
Dispersion Free Extraction in Hollow Fiber Membrane

In the case of non-dispersive extraction of cephalosporins by reversible chemical complexation taking place across hydrophobic microporous hollow fiber (MHF) modules and co-current flow of the two phases, the solute in the aqueous

feed phase diffuses through the aqueous boundary layer to the phase interface at the membrane pore mouth, whereas the carrier diffuses through the organic boundary layer at the organic-filled hydrophobic membrane pores to reach the phase interface. Cephalosporin anion and the carrier react at the phase interface where reaction equilibrium exists. The complexation reaction product is insoluble in the aqueous phase and diffuses back to bulk of the organic phase through the organic-filled hydrophobic membrane pores and organic boundary layer. At steady state, the following system of algebraic and differential equations hold for axial variation of the species concentration for co-current flow with Z being the mean flow direction in the hollow fibers [63]:

$$\frac{dC^{d}_{P^-}}{dZ^*} = -\left(N \pi d_{if} k_a H/Q_a\right)\left(C^{d}_{P^-} - C^{d}_{P^-} - C^{d}_{P^-,if}\right) \tag{42}$$

$$\frac{dC^{*}_{QCl}}{dZ^{d}} = -\left(N \pi d_{if} k_{or} H/Q_{or}\right)\left(C^{d}_{QCl} - C^{d}_{QCl,if}\right) \tag{43}$$

$$\frac{dC^{d}_{QP}}{dZ} = -\left(N \pi d_{if} k_{or} H/Q_{or}\right)\left(C^{d}_{QP} - C^{d}_{QCl,if}\right) \tag{44}$$

The mass fluxes of species P^-, QCl, and QP at the interface are equal, and at the phase interface the following relations are valid:

$$K^{d}_{eq} = \frac{C^{e}_{QP,if}\, C^{d}_{Cl^-,if}}{C^{d}_{P^-,if}\, C^{d}_{Cl,if}} \tag{45}$$

where

$$K^{d}_{eq} = K_{eq} \quad \text{and} \quad Z^{d} = Z/H,\ C^{d}_{P^-} = C_{P^-}/C^{0}_{P^-},\ C^{d}_{QCl} = C_{QCl}/C^{0}_{P^-},$$
$$C^{d}_{QP} = C_{QP}/C^{0}_{P^-} \tag{46}$$

The initial conditions for Eqs. (44)–(46) are given by

$$\text{at } Z = 0,\ C^{d}_{P^-} = 1,\ C^{d}_{QCl} = C^{0}_{QCl}/C^{0}_{P^-} \text{ and } C^{d}_{QP} = 0 \tag{47}$$

The mass transfer coefficients k_a and k_{or} in Eqs. (42) – (44) are important parameters and their values depend on the surface properties (hydrophobic or hydrophilic) of the hollow fiber membrane and whether the organic/aqueous phase flows in shell or tube side of the fiber. k_a and k_o can be estimated from well established correlations [29] which have been successfully used for simulation purposes.

The system of algebraic and differential equations, i. e., Eqs. (42) – (45) can be simplified with the initial condition given by Eq. (47), the procedure for which has been well demonstrated in the literature [63, 64, 67].

Analytical solution of the equations are not available, but these can be solved numerically by using IMSL subroutine IVPRK, which is a modified version of subroutine DVERK based on the Runge-Kutta method. The solution would provide exit concentration of the solute from which percent extraction can be obtained.

5
Process Consideration

Selectivity higher than those attainable by current separation methods, saving on energy cost for final concentration of separated products, higher fluxes, compact installation, and low capital and operation costs are the common attractive feature of liquid membrane separation processes. The adsorption chromatography proposed as a final purification step by Fuji et al. [76] on filtered broth of cephalosporins has the limitation of generating dilute solutions necessitating energy intensive concentration operations and thereby increasing the price per kg of the material by several hundreds of dollars. Up to 50% of the total cost of a chromatographic process is eluent related. It is necessary to purify and recycle the spent solvent. A proportion (typically 3–5%) of solvent is usually lost and, considering the huge volume handled, this amount can be substantial. The liquid membrane process can be competitive to adsorption chromatography, but the following issues should be addressed for process design and practical application.

5.1
Chemical Driving Force

In liquid membrane extraction, if external driving force is not introduced, then driving force for the transport of cephalosporin anions is the chemical potential and dilution is inevitable. Phase ratio, use of counter-current flow, number of transfer stages, and reversibility of the extractant determine the degree to which the concentration of solute in the product solution approaches that in the feed phase [77]. Extractant design faces the choice between higher recovery and higher loading (strong extractant) on the one hand and higher product concentration (weaker extractant of higher reversibility) on the other. External driving force enables the concentration and higher recovery with product concentration to above its level in the feed phase (uphill transport). Product dilution through water co-transport should be avoided, e.g., by addition of salts to the feed phase, design of an acid/water selective membrane, or application of pressure on the stripping solution (in the case of HFM). Chemical and thermal energy can be used as driving forces in analogy to process in liquid-liquid extraction (electric energy in an electrodialysis resembling arrangement should also be considered).

Neutralization of the extracted molecule provides chemical energy. Thus, a NaOH-containing stripping phase was used by Li to provide the driving force for phenol separation and concentration through an ELM system [78]. Similar results were obtained by Friensen et al. [79] and by Basu and Sirkar [61], who showed up to three times higher transport rate and higher concentrations in the stripping phase. This type of chemical driving force can be applied for LM separation of cephalosporin antibiotics. A less prohibitive use of chemical energy for product concentration is the dilution of another compound. Such a process will be economic if the compound to be diluted is of relatively low cost and if there is a sink for its solution. Some examples of uphill pumping of the solute through dilution of another compound is as follows:

1. Water transport from product solution into a concentrated electrolyte solution (the membrane should transfer water and block the electrolyte and the solute).
2. Applying the common ion effect or salting out effect, the solute can be concentrated. The membrane should be designed to transfer the solute and block the additives and the impurities.
3. Simultaneous transport of solute with a transport of another solute in the same direction (syntrop) or in the opposite direction (antitrop).

5.2 Stability Problems

Membrane instability results in partial mixing of feed and stripping phases, which deteriorates the selectivity. In addition, raffinate and product are contaminated by the extractant, leading also to extractant losses. Economy of separation and hence industrial application of LM for separation of cephalosporins are strongly dependent on membrane stabilization.

Factors affecting ELM stability have been studied extensively [47, 80–83]. Usually the internal phase of ELM is much more concentrated than the external phase. Osmotic pressure driven water transport into the internal phase causes its swelling, sometimes to breaking point. The degree of swelling is affected by viscosity of the W/O emulsion, W/O/W dispersion, extractant composition, and surfactant and internal reagent compositions. Use of viscous paraffinic oils in the membrane phase and increasing surfactant concentration were proposed for decreasing ELM breakage. A tracer technique has been used to quantify emulsion break-up which is a time-dependent phenomena and can be expressed in terms of a measurable rate constant. However, in case of beta-lactam extraction in ELM, the emulsion swelling and break-up under specific experimental condition were found to be negligible [25, 26].

Although the emulsions were expected to be stabilized with increasing surfactant concentration, the degree of stability beyond a critical surfactant concentration becomes approximately constant due to the saturation of the surfactants at the oil-water interface. Again, higher concentration of surfactant will hinder demulsification after extraction. So a critical surfactant concentration value should be used for practical purposes.

In some cases, swelling due to water transport caused by surfactant, e. g., Span-80 destabilized the emulsion droplets. Use of a surfactant with low value of hydrophilic-lipophilic balance is essential for reducing the swelling. The surfactant should carry virtually no water during operation so as to alleviate osmotic swelling [83]. Span-80 as an emulsifier exhibits poor stability due to hydrolysis, especially when NaOH is incorporated into the internal phase. In such cases, PX-100 and ECA4360, polyamine surfactants may be used or Span-80 may be used by replacing NaOH with Na_2CO_3. Membrane with ECA4360 alone exhibits low osmotic swelling but high resistance to mass transfer. In contrast, membrane with Span-80 shows high swelling but low mass transfer resistance. By adding 2 % Span-80 to the membrane with ECA4360, the mass transfer resistance was substantially lowered while the swelling was still kept to a low tolerable level [82].

Extractant leakage from the pores of the polymeric membrane in SLM is due to osmotic flow of massive quantities of water through the membrane. Membrane stability decreases with increasing osmotic pressure gradient and depends upon composition of the SLM system. A high tendency to solubilize water, low extractant/aqueous interfacial tension, and high wettability of polymeric membrane leads to less stable SLMs. The following measures have been proposed for improvement of stability:

- Maintaining an interface immobilizing pressure difference across the porous membrane in a direction and of a magnitude effective to oppose the tendency of leakage [83, 84].
- Modification of extractant and the aqueous phases for achieving lower surface activity and lower miscibility [85].
- Modification of polymeric membrane for better adhesion of the extractant or designing it so that interface between the phases is immobilized at the porous membrane [84, 85].
- Blocking leakage by applying a thin gel layer, preferably by a gel network with a low mesh size built with chemically stable crosslinking. [86].
- Various degrees of binding the extractant to the polymeric membrane [87].

5.3 Membrane Recoverability and Reuse

Generally, an emulsion prepared with a high energy density input (such as by an electrostatic method) will have very small droplets. This will enhance membrane stability if the surfactant concentration is high enough. Meanwhile, the small droplet size gives a very large interfacial area for mass transfer, but an ultrastable emulsion should be avoided because of possible difficulties later during the demulsification step. Usually, a membrane leakage rate of about 0.1 % is allowable for a practical process [47].

Two principal approaches for the demulsification of the loaded emulsion are chemical and physical treatments. Chemical treatment involves the addition of a demulsifier to the emulsion. This method seems to be very effective. However, the added demulsifier will change the properties of the membrane phase and thus inhibits its reuse. In addition, the recovery of the demulsifier by distillation is rather expensive. Therefore, chemical treatment is usually not suitable for breaking emulsion liquid membrane, although few examples of chemical demulsification have been reported for certain liquid membrane systems [88].

Physical treatment methods including heating, centrifugation, ultrasonics, solvent dissolution, high shear, and use of high voltage electrostatic fields. Liquid membrane emulsion (both W/O and O/W type) can be effectively broken by the use of a specially formulated solvent mixture and high shear. The solvent mixture breaks the emulsion without damaging the surfactant. The solvents used are low boiling compound and they can be easily recovered later by evaporation. The method of demulsification by high shear includes the use of centrifugation as the first step, followed by pumping the half-broken emulsion through a high shear device [89].

Demulsification with electrostatic fields appears to be the most effective and economic way for breaking of W/O emulsion in ELM processes [90, 91]. Electrostatic coalescence is a technique widely used to separate dispersed aqueous droplets from nonconducting oils. Since this type of technique is strictly a physical process, it is most suitable for breaking emulsion liquid membranes to recover the oil membrane phase for reuse.

5.4 Process Economics

Beta-lactam antibiotics are generally costly and marketed at a price of around $100 to $165/kg. Thus, even 1% increase in yield via improvement in separation efficiency would offer substantial cost benefit in β-lactam production. For a typical production plant of capacity 5×10^4 kg/annum, a gross annual benefit of $50,000–250,000 can be expected [92]. The capital investment in LM process, a typical process, the flow design of which is shown in Fig. 7, is also likely to be low

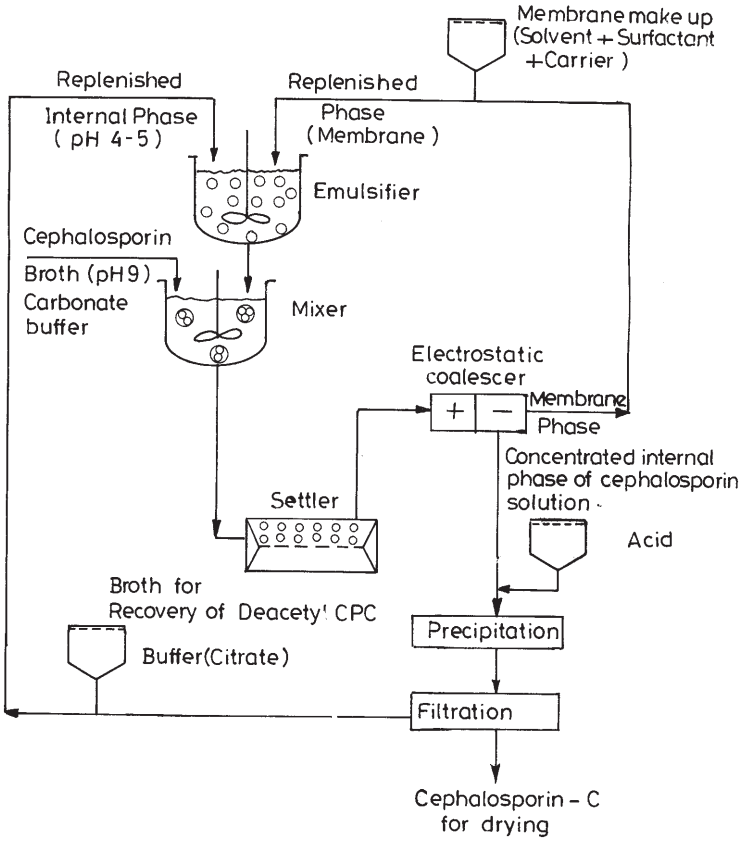

Fig. 7. Schematic diagram of a proposed CPC purification process using ELM system

because of reduced equipment volume and the low cost required for a particular duty. In an LM process, the external driving force allows high product recovery with product concentration well above its level in the feed (uphill pumping). Extractor design can be based on the choice between high recovery and high loading (strong extractant) on the one hand and high product concentration (weaker extractant of higher reversibility) on the other.

Except for the demulsification step, the process design principles of ELM process is fairly well understood. In the case of cephalosporins, membrane formulations as regards the extractant, stripping agent, surfactant, etc., can be based on thermodynamic and kinetic considerations identical to those applied for penicillins. Modeling and simulation of the reaction diffusion phenomena and validation from experimental results with independently measured model parameters may be required to understand the process design principles of the LM extraction of cephalosporins. For large scale application, the column extractor used for a conventional solvent extraction process can be effective for ELM processes. The well-understood design principle available for conventional extractors can be easily extended to ELM extractors [29].

The process design principles of SLM, non-dispersive extraction, and hybrid liquid membrane systems need to be understood through bench scale experiments using feed solution of practical relevance. While the economic analysis of an ELM process can be performed from small scale experiments, such an analysis is difficult for other LM systems. In particular, availability and cost of hollow fiber membranes for commercial application are not known apriori. A simple rule of thumb for cost scale-up may not be applicable in the case of an HF membrane. Yet we feel that the pilot plant tests would be adequate to make realistic cost benefit analysis of a liquid membrane process, since the volume of production in β-lactam antibiotic industries is usually low.

6 Research Needs of Pragmatic Importance

The liquid membrane (LM) technique for extraction of cephalosporin antibiotics appears to be the future generation technology of promise. The LM can perhaps function best for natural cephalosporins, which are usually present at considerably low concentration in the fermentation broth. The capital investment of the LM process is likely to be low because of reduced equipment volume required for a particular duty. In an LM process, the external driving force allows a high product recovery with product concentration well above its level in feed (uphill pumping). The importance of the LM process for cephalosporin separation will be more pronounced if the same is applied for direct extraction from culture broth. Since enzyme/microbial cell activity is likely to be effected under the reactive extraction condition, it is necessary to address this aspect from experiments using culture broth. Toxic effects of the extractants should be related to the membrane stability and enzyme/cell activity. As far as process application is concerned, it is not clear where an LM should belong in the downstream processing train. If LM is to be used early in the downstream processing for crude separation and concentration, it must be demonstrated that LM application can

compete commercially with well proven commercial processes like adsorption chromatography. If LM is to be used later in the downstream processing train, it must be shown that adequate, specific separation can be achieved, and product loss would be acceptable. It is apparent that scale-up studies on LM extraction of cephalosporin antibiotics will be highly useful as the economic incentives for such a process are expected to be very attractive.

7 Conclusion

Developments in liquid membrane separation of cephalosporin antibiotics are rather meager, but will be quite rewarding. In particular, ELM has great potential to be practically utilized for separation and concentration from dilute solution such as that encountered in fermentation broth. The most probable application of ELM appears to be the recovery and concentration of CPC, 7-ACA, and cephalhexin in downstream operation of biochemical processes. The integrated product formation and recovery by liquid membrane extraction will gain impetus in the future. Reactive extraction in liquid membrane and non-dispersive reactive extraction in hollow fiber membrane need extensive investigation leading to generation of process design information for practical exploitation in technological perspectives.

References

1. Martin JF, Liras P (1989) Enzymes involved in penicillin, cephalosporin and cephamycin biosynthesis. In: Fiechter A (ed) Adv in Biochem Eng Biotech. Springer, Berlin Heidelberg New York
2. Newton GGF, Abraham EP (1955) Nature 24:443
3. Lancini G, Lorenzetti R (1993) Biotechnology of antibiotics and other bioactive microbial metabolites, 2nd edn. Plenum Press, New York
4. Vandamme EJ (1990) Recent advances in the biotechnology of β-lactam and microbial bioactive peptides. In: Klein Kauf H, Von Dohren H (eds) Biochemistry of peptides antibiotics. Watter De Gruyter, Berlin
5. Hyun CK, Kim JK, Ruy DDY (1993) Biotech Bioeng 42:800
6. Schewale JG, Sivaraman H (1998) Proc Biochem 8X:148
7. Leinn JJ (1988) Eur Pat 0,293,218
8. Aramori I, Fukugawa M, Tsumara M, Iwami M, Ono H, Ishitani Y, Kojo H, Kohsaka M, Ueda Y, Iomanak H (1992) J Ferment Bioeng 73:185
9. Abraham EP, Loder HP (1972) In: Flynn HE (ed) Cephalosporins and penicillins: chemistry and biology. Academic Press, New York
10. Binder R, Brown J, Romanick G (1994) Appl Environ Microbiol 60:1805
11. Parmer A, Kumar H, Marwaha SS, Kenedy JF (1998) Crit Rev Biotech 18:1
12. Ghosh AC, Mathur RK, Dutta NN (1997) Extraction and purification of cephalosporin antibiotics. In: Scheper T (ed) Adv Biochem Eng Biotech 56:111–145
13. Li NN (1971) Ind Eng Chem (Proc Des Devel) 10:215
14. Wald AS, Leysez LJ, Matson LS (1989) Paper presented at the 3rd Annual meeting of the North American Membrane Society, 19 May, Texas, USA
15. Schugerl K (1994) Solvent extraction in biotechnology: recovery of primary and secondary metabolites, 1st edn. Springer, Berlin Heidelberg New York
16. Likidis Z, Schugerl K (1987) J Biotechnol 5:293

17. Reschke N, Schugerl K (1986) Chem Eng Biochem Eng J 32:B1–B5
18. Muller B, Schlichting E, Schugerl K (1988) Appl Microbiol. Biotechnol, 27:484
19. Likidis Z, Schlichting E, Bishoff E, Schugerl K (1989) Biotech Bioeng 33:1385
20. Lee KH, Lee WK (1994) Sep Sci. Technol 29:602
21. Harris TAJ, Khan S, Reuban GB, Shokoya T (1990) In: Pyle DL (ed) Separations for biotechnology. Elsevier, London, pp 172–180
22. Hano T, Matsumoto M, Ohtake T, Hori F (1992) J Chem Eng Jpn 25:293
23. Sahoo GC, Ghosh AC, Dutta NN, Mathur RK (1996) J Membr Sci 112:147
24. Sahoo GC, Ghosh AC, Dutta NN (1997) Process Biochem 32:265
25. Sahoo GC, Dutta NN (1998) J Membr Sci 145:15
26. Sahoo GC, Dass NN, Dutta NN (1999) J Membr Sci 157:251
27. Sahoo GC, Borthakur S, Dass NN, Dutta NN (1999) Bioprocess Eng 20:117
28. Li NN (1968) US Pat 3,410,794
29. Ho WSW, Li NN (1992) In: Ho WSW, Sirkar KK (eds) Membrane handbook, 1st edn. Van Nostrand Reinhold, New York
30. Mutihac L, Mutihac RZ, Nocolace LC, Constantinescu T (1992) Rev Roum Chim 37:91
31. Mutihac L, Luca C (1991) Rev Roum Chim 36:85
32. Mutihac L, Mutihac R (1992) Acta Chim Hung 129:573
33. Lazarova Z, Peeva L (1994) Biotechnol Bioeng 43:907
34. Roberts J, Caserio M (1964) Basic principles of organic chemistry, 1st edn. Benjamin Inc, New York, 2:247
35. Scheper T, Likidis Z, Makryaleas K, Nowottry C, Schugerl K (1987) Enz Microb Technol 9:625
36. Boayadzhiev L, Attanassova I (1991) Biotech Bioeng 38:1059
37. Smith BD (1996) In: Bartsch RA, Way JD (eds) Chemical separation with liquid membrane. ACS Symposium Series: 642. American Chemical Society, Washington, DC, pp 194–205
38. Smith BD (1996) Supramol Chem 7:55
39. Smith BD, Gardiner SJ (1998) Adv Supramol Chem 5:157
40. Cascaval D, Oniscu C, Cascaval C, Romanic M (1997) Roum Biotechnol Lett 2:407
41. Sahoo GC, Dutta NN, Dass NN (2000) Chem Eng Comm (in press)
42. Habaki H, Isobe S, Ega-Shiva R, Kawasaki J (1998) J Chem Eng Jpn 31:47
43. Tsikas D, Scheper T, Schugerl K (1989) Chem Ing Tech 61:418
44. Chan CC, Yang JF (1995) Sep Sci Technol 30(15):3001
45. Thien MP, Hatton TA, Wang DIC (1988) Biotechnol Bioeng 32:604
46. Reisinger H, Marr R (1993) J Membr Sci 80:85
47. Hong S-A, Choi H-J, Nam SW (1992) J Membr Sci 70:225
48. Chaudhuri JB, Pyle DL (1992) Chem Eng Sci 47:49
49. Wildfenur EM (1985) In: Leroith O, Schiloach J, Leaby JT (eds) ACS Symposium Series, ACS, Washington DC, 77:155–174
50. Hano T, Ohtake T, Matsumoto M, Ogawa SI, Hari F (1990) J Chem Eng Jpn 23:772
51. Bora MM, Dutta NN, Bhattacharya KG (1998) J Chem Eng Data 43:318
52. Bora MM, Ghosh AC, Dutta NN, Mathur RK (1997) Canad J Chem Eng 75:520
53. Lee SC, Lee WK (1992) J Chem Tech Biotechnol 53:251
54. Lee KH, Lee SC, Lee WK (1994) J Chem Tech Biotech 59:365
55. Lee KH, Lee SC, Lee WK (1994) J Chem Tech Biotech 59:371
56. Ghosh AC, Borthakur S, Roy MK, Dutta NN (1995) Sep Technol 5:121
57. Marchese J, Lopez L, Quin JA (1989) J Chem Tech Biotech 46:149
58. Lee JC, Yeh JH, Yang WJ, Kan RC (1993) Biotech Bioeng 42:527
59. Lee JC, Yeh JH, Kan RC (1994) Biotech Bioeng 43:309
60. Tsikas D, Kaltsidon SE, Brunner G (1992) Chem Ing Tech 64:545
61. Basu R, Sirkar KK (1991) AIChE J 37:383
62. Yang FZ, Rindfleisch D, Scheper T, Schuregl K (1993) 3rd International Conference on Effective Membrane Processes, New Perspectives, Bath, UK, 12–14 May
63. Prasad R, Sirkar KK (1989) J Membr Sci 47:235

64. Basu R, Sirkar KK (1992) Solvent Extr Ion Exch 10:119
65. Dahuron L, Cussler EL (1988) AIChE J 37:383
66. Dekker M, Riet K Van't, Wijmans JMGM, Baltussen JWA (1987) 1st International Congress Membrane and Membrane Processes, Tokyo
67. Prasad R, Sirkar KK (1990) J Membr Sci 50:153
68. Casamatta G, Boyadzhiev L, Angelio H (1994) Chem Eng Sci 29:2005
69. Teramoto M, Matsuyama H, Nakai K, Uesaka T, Ohnishi N (1994) J Membr Sci 91:203
70. Chaudhuri JB, Pyle DL (1992) Chem Eng Sci 47:41
71. Mok YS, Lee WK (1995) Membrane J 5:44
72. Calderback PH, Moo-Young MB (1961) Chem Eng Sci 16:39
73. Wilke CR, Chang P (1955) AIChEJ 264–266
74. Jefferson TB, Witzell OW, Libbit WL (1958) Ind Eng Chem 50:1518
75. Gu ZM, Wasan DT, Li NN (1985) Sep Sci Tech 20:599
76. Fuji T, Matsumoto K, Watanabe T (1976) Proc Biochem 11:12
77. Eyal AM, Bressler E (1993) Biotech Bioeng 41:287
78. Li NN (1973) US Pat. 3,779,907
79. Friensen DI, Babcock WC, Brose DJ, Chambers AR (1991) J Membr Sci 56:127
80. Bhakta A, Ruckenstein E (1995) Langmuir 11:4642
81. Szabo C (1992) Biotechnol Bioeng 4:247
82. Draxler J, Marr R (1986) Chem Eng Process 20:319
83. Li W, Dai X, Shi Y (1992) Proc Int. Solvent Extraction Conf., Kyoto, Japan, Part B, p 1655
84. Sirkar KK (1991) US Pat. 4,921,612
85. Sirkar KK (1991) US Pat. 4,997,569
86. Kemperman AJB, Bergeman D, Van Den BT, Strathmann H (1996) Sep Sci Technol 31(20):2733
87. Neplenbrock AM, Bergeman D, Smolders CA (1992) J Membr Sci 67:149
88. Zhang X-J, Huang P-Y, Chen X-J (1988) Proc First Sino-Jap Symp Liq Membr 24–27 Sept, Chona, pp 83–85
89. Kato S, Kawasaki J (1988) Proc First Sino-Jap Symp Liq Membr 24–27 September, Chona, pp 86–88
90. Lu G, Lu Q, Li P (1997) J Membr Sci 128:1
91. Sun D, Duan X, Yanling X, Zhang LT, Zhou D (1996) Harbin Gongye Daxue Xuebao 28:68
92. Ghosh AC, Bora MM, Dutta NN (1996) Bioseparation 6:91
93. Behr JP (1973) J Am Chem Soc 95:6108
94. Lehn JM (1975) J Am Chem Soc 97:2532
95. Itosh H, Thien MP, Hatton TA, Wang DIC (1990) Biotech Bioeng 35:853
96. Boydzhiev L, Atannossova I (1994) Proc Biochem 29:237
97. Hano T, Matsumoto M, Kawozu T, Ohtake T (1995) J Chem Tech Biotech 62:66
98. Yamaguchi T, Nishimura K, Shinbo T, Seigura M (1985) Chem Lett 10:1552
99. Bryjak M, Weiczorek P, Kafarski P, Leiczark B (1988) J Membr Sci 37:287
100. Wieczorek P, Kocorek A, Bryjak M, Kafarski P, Lejczak B (1993) J Membr Sci 78:83

Received: March 2000